Exploring oxytocin as a neuroprotectant for newborn brain injury: pre-clinical assessment in two mouse models of neonatal neuroinflammation

Knoop, Marit

UNIVERSITÉ DE GENÈVE

FACULTY OF MEDICINE

Exploring oxytocin as a neuroprotectant for newborn brain injury: pre-clinical assessment in two mouse models of neonatal neuroinflammation

Marit Knoop, PhD candidate

Faculty of Medicine

Université de Genève

Lemanic Neuroscience Doctoral School

Directors

Principal director: Prof. Olivier Baud

Deputy director: Prof. Stéphane Sizonenko

Jury

President: Prof. Rosa Paolicelli

Expert: Prof. Françoise Muscatelli

Expert: Dr. Julien Puyal

UNIVERSITÉ DE GENÈVE
FACULTÉ DE MÉDECINE

LEMANIC NEURO SCIENCE DOCTORAL SCHOOL

DOCTORAT EN NEUROSCIENCES
des Universités de Genève
et de Lausanne

UNIVERSITÉ DE GENÈVE
UNIL | Université de Lausanne

UNIVERSITÉ DE GENÈVE — FACULTÉ DE MÉDICINE

Professeur Olivier Baud, directeur de thèse
Professeur Stéphane Sizonenko, co-directeur de thèse

TITRE DE LA THÈSE

EXPLORING OXYTOCIN AS A NEUROPROTECTANT FOR NEWBORN BRAIN INJURY: PRE-CLINICAL ASSESSMENT IN TWO MOUSE MODELS OF NEONATAL NEUROINFLAMMATION

THESE
Présentée à la
Faculté de Médicine

de l'Université de Genève

pour obtenir le grade de
Docteure en Neurosciences

par

Marit KNOOP

d'Amersfoort, Pays-Bas

Thèse N° 463

Genève

Editeur ou imprimeur : Université de Genève

2025

UNIVERSITÉ DE GENÈVE
FACULTÉ DE MÉDECINE

DOCTORAT EN NEUROSCIENCES

des Universités de Genève et de Lausanne

Thèse de

Marit KNOOP
originaire des Pays-Bas

Intitulée

Exploring oxytocin as a neuroprotectant for newborn brain injury: pre-clinical assessment in two mouse models of neonatal neuroinflammation

Soutenue le : 7 novembre 2025

La Faculté de médecine, sur préavis du jury de thèse formé par :

Professeure Rosa Paolicelli, Faculté de médecine, Université de Lausanne, Présidente du jury
Professeur Olivier Baud, Faculté de médecine, Université de Genève, Directeur de thèse
Professeur Stéphane Sizonenko, Université de Genève, Co-directeur de thèse
Professeure Françoise Muscatelli, Université Aix-Marseille, Experte externe
Docteur Julien Puyal, Université de Lausanne, Expert

Autorise l'impression de la présente thèse, sans prétendre par là émettre d'opinion sur les propositions qui y sont énoncées.

Genève, le 7 novembre 2025

Thèse n° 463

Professeur Antoine Geissbühler

Doyen

N.B. *La thèse imprimée doit porter la déclaration précédente * et remplir les conditions énumérées dans les « Informations aux étudiants relatives aux thèses de doctorat à l'Université de Genève ».*

Abstract

Brain injury in newborns is a prominent health issue that can have a long-lasting detrimental impact throughout life. Encephalopathy of prematurity (EoP) and pediatric traumatic brain injury (TBI) are two of the most occurring types of newborn brain injury, that are characterized by a toxic neuroinflammatory response. As the driving force behind the neuroinflammatory response, microglia pose an attractive target for therapeutic modulation. However, there are currently no successful therapeutic targets for modulation of microglia or the neuroinflammatory response for newborns in the clinic. One potential target comes from the neonatal intensive care unit (NICU), where non-pharmacological interventions such as developmental care, skin-to-skin care, music exposure and environmental enrichment show positive effects on brain development. Notably, these interventions all induce elevations of endogenous oxytocin levels in the newborn. In parallel, pre-clinical studies in cell lines and other brain injury models support that oxytocin possesses anti-inflammatory properties, suggesting that oxytocin could be a potential therapeutic target for neuroinflammation related injury in the developing brain. However, the confirmation of this hypothesis and underlying mechanism in newborn brain injury remains elusive, as does its applicability to different types of inflammation models in the developing brain.

In this pre-clinical work, we investigated the neuroprotective potential of early-life oxytocin against the neural correlates of EoP and TBI in mice. We used a transgenic mouse line to conduct chemogenetic activation of oxytocinergic neurons, thereby simulating the natural oxytocin elevation witnessed in the clinic. We assessed the effects of increased oxytocin release on microglial cellular and transcriptomic functioning during the peak of inflammation, and we tracked the long-term effects of oxytocin on brain development using a cohesive battery of structural and functional brain imaging methods, immunohistochemistry, and behavioral tests.

Our studies found that oxytocin has anti-inflammatory effects on microglia in the acute phase after newborn brain injury, reducing the increase in cell density and amoeboid morphology. Oxytocin promoted microglial gene expression of key brain development support functions, including axon guidance and oligodendrocyte maturation. Oxytocin also suppressed expression of pro-inflammatory microglial functions, yet with different magnitudes for the different injury models – likely relating to the differences in inflammatory mechanisms between EoP and TBI. On the long-term, oxytocin-treated mice showed improved development of white matter microstructure, enhanced neurovascular recovery and correlation of neural connectivity between brain regions, and a rescue of social behavior. In further exploring this mechanism, we found support that the long-term effects of oxytocin are related to improved microglial support of oligodendrocyte development. We also discovered sex-specific effects of oxytocin in the EoP model, as well as distinct effects of oxytocin on the intricate microglia-astrocyte crosstalk in the TBI model.

Oxytocin has unique potential as a therapeutic target for neonates, as this neuropeptide is physiological, produced by the brain itself and released through non-invasive interventions in the neonatal intensive care. However, the scientific evidence of the benefits provided by oxytocin remained weak. Our translational study describes for the first time the biological mechanisms induced by the release of endogenous oxytocin and the enhancement of brain development, highlighting an important modulatory effect on microglia. A short treatment period was sufficient to exert lasting effects on the brain. As such, our results support a reinforced implementation of oxytocin-inducing practices in neonatal and pediatric units. Moreover, as neuroinflammation is a fairly constant feature of most perinatal injuries, this work could have a considerable impact on the care of all newborns at high risk of brain damage.

Résumé en français

Les lésions cérébrales chez les nouveau-nés constituent un problème de santé publique qui peut avoir des conséquences néfastes toute la vie durant. L'encéphalopathie du prématuré (EoP) et les traumatismes crâniens pédiatriques (TBI) sont deux des types de lésions cérébrales les plus fréquents chez les nouveau-nés, caractérisés par une réponse neuroinflammatoire. En tant que moteur de la réponse neuroinflammatoire, les microglies constituent une cible intéressante pour la modulation thérapeutique. Cependant, il n'existe actuellement aucune cible thérapeutique efficace pour la modulation des microglies ou de la réponse neuroinflammatoire chez les nouveau-nés en clinique. Une cible potentielle est suggérée par certaines interventions non pharmacologiques réalisées en unité de soins intensifs néonatals (USIN) comme les soins de développement, le peau à peau, l'exposition à la musique et l'enrichissement de l'environnement qui ont des effets positifs sur le développement cérébral. Il est à noter que ces interventions induisent une augmentation des niveaux d'ocytocine endogène chez le nouveau-né. Parallèlement, des études précliniques sur des lignées cellulaires et d'autres modèles de lésions cérébrales suggèrent que l'ocytocine possède des propriétés anti-inflammatoires, ce qui laisse penser qu'elle pourrait être une cible thérapeutique potentielle pour les atténuer ou prévenir les lésions liées à la neuroinflammation dans le cerveau en développement. Cependant, la confirmation de cette hypothèse et le mécanisme sous-jacent à cette association dans les lésions cérébrales chez les nouveau-nés restent à étudier, tout comme son applicabilité à différents types de modèles d'inflammation dans le cerveau en développement.

Dans le cadre de ces travaux précliniques, nous avons étudié le potentiel neuroprotecteur de l'ocytocine administrée tôt dans la vie contre les corrélats neuronaux de l'EoP et du TBI chez la souris. Nous avons utilisé une lignée de souris transgéniques pour procéder à l'activation chimio-génétique des neurones oxytocinergiques, simulant ainsi l'élévation naturelle de l'ocytocine observée en clinique. Nous avons évalué les effets de l'augmentation de la libération d'ocytocine sur le fonctionnement cellulaire et transcriptomique des microglies au pic de l'inflammation, et nous avons suivi les effets à long terme de l'ocytocine sur le développement cérébral à l'aide d'une batterie de méthodes de biologie moléculaire, d'imagerie cérébrale structurelle et fonctionnelle, d'immunohistochimie et de tests comportementaux.

Nos études ont montré que l'ocytocine a des effets anti-inflammatoires sur les microglies dans la phase aigüe après une lésion cérébrale, réduisant l'augmentation de la densité cellulaire et la morphologie amiboïde. L'ocytocine favorise l'expression génique des microglies pour des fonctions clés du développement cérébral, notamment le guidage des axones et la maturation des oligodendrocytes. L'ocytocine supprime également l'expression des fonctions microgliales pro-inflammatoires, mais avec des amplitudes différentes selon les modèles de lésion, ce qui est probablement lié aux différences entre les mécanismes inflammatoires de l'EoP et du TBI. À long terme, les souris traitées à l'ocytocine ont montré une amélioration du développement de la microstructure de la substance blanche, une meilleure récupération neurovasculaire et une corrélation de la connectivité neuronale entre les régions du cerveau, ainsi qu'une restauration du comportement social. En explorant plus en détail ce mécanisme, nos résultats suggèrent que les effets à long terme de l'ocytocine sont liés à une amélioration du soutien microglial au développement des oligodendrocytes. Nous avons enfin découvert des effets spécifiques au sexe de l'ocytocine dans le modèle EoP, ainsi que des effets distincts de l'ocytocine sur l'interaction complexe entre les microglies et les astrocytes dans le modèle TBI.

L'ocytocine présente un potentiel unique en tant que cible thérapeutique pour les nouveau-nés, car ce neuropeptide est physiologique, produit par le cerveau lui-même et relarguée dans certaines circonstances de prise en charge des nouveau-nés en unités de soins. Cependant, les preuves scientifiques concernant le fonctionnement de l'ocytocine restaient largement inconnues. Notre étude à visée translationnelle décrit les mécanismes biologiques induits par le relarguage de l'ocytocine

endogène et l'amélioration du développement cérébral, en soulignant un rôle modulateur important sur les microglies. Une courte période de traitement a suffi pour exercer des effets durables sur le cerveau. À ce titre, nos résultats soutiennent une mise en œuvre renforcée des pratiques induisant l'ocytocine dans les unités de néonatologie et pédiatriques. De plus, comme la neuroinflammation est une caractéristique assez constante de la plupart des lésions périnatales, ces travaux pourraient avoir un impact considérable sur les soins prodigués aux l'ensemble des nouveau-nés à haut risque de lésions cérébrales.

Nederlandse samenvatting

Wanneer een baby te wereld komt zijn zijn hersenen slechts een vierde de omvang van een volwassen brein. Het eerste levensjaar wordt gekenmerkt door enorme ontwikkeling: het brein verdubbelt in omvang, wat hand-in-hand gaat met de toenemende vaardigheden van het kind. Voor de meeste kinderen gaat dit zonder zorgen. Echter, sommige pasgeborenen worden slachtoffer van hersenschade. Dit gebeurt jaarlijks bij ongeveer 5 in 1000 pasgeboren, en kan veroorzaakt worden door processen zowel voor, tijdens, of na de geboorte. Schade aan de jonge hersenen kan kritische processen van ontwikkeling verstoren wat blijvende structurele en functionele verandering kan veroorzaken, evenals levenslange problemen op gedrags en cognitief vlak. De behandelingen na hersenschade die hedendaags beschikbaar zijn in pasgeborenen zijn veelal gericht op het verhelpen van de primaire oorzaak (de schade zelf of de oorzaak van de schade), en helpen minder tegen de problematische secundaire processen die de hersenschade veroorzaakt als imuunreactie. Ook zijn medische behandelingen vaak invasief en stressvol, iets wat – zeker in kinderen – problematisch is. Gegeven de emotionele en financiele last van hersenschade in pasgeborenen, is het een speerpunt van translationeel neurobiologisch onderzoek om nieuwe behandelingen te vinden voor dit medische probleem.

Het doel van wetenschappelijk onderzoek in de tak van neurobiologie is om inzichten te geven van de pathofysiologie van de hersenen, ofwel, het bestuderen hoe ziekte of verwonding de normale functies van de hersenen beïnvloedt. Inzichten in deze processen zorgt ervoor dat we therapiën kunnen ontwikkelen die de pathologische processen tegengaan. Deze inzichten in biologische processen kunnen met veel detail vernomen worden door ze na te bootsen en ze gedetailleerd te bestuderen in (knaag)dieren. Het is daarbij cruciaal dat de pathfysiologie in de dieren lijkt op wat er in de mens gebeurt. Op die manier vormt proefdieronderzoek een kans om therapiën te vinden die ook voor mensen werken. Dit is het grote doel van mijn tak van neurowetenschappen: het uitvoeren van translationeel neurowetenschappelijk onderzoek, waarbij onderzoek naar de hersenen in dieren therapeutische inzichten oplevert die uiteindelijk vertaald (= toegepast) kunnen worden naar de mens.

<u>Doel van het onderzoek</u>

In deze thesis heb ik translationeel onderzoek gedaan naar een therapie voor hersenschade in pasgeborenen. De therapie die ik heb onderzocht is oxytocine, een lichaamseigen stof die aangemaakt wordt door de hersenen in reactie op veel soorten van ontspanning, zoals bijvoorbeeld lichamelijk contact, knuffelen, massage, en borstvoeding. Het wordt ook wel gezien als de tegenhanger van stress. De wetenschappelijke interesse naar oxytocine als behandeling tegen hersenschade komt uit de kliniek, waar therapiën die op natuurlijke wijze oxytocine verhogen – zoals muziek of het horen van de stem van de ouders, of meer huid-op-huid contact tussen ouder en kind – een algehele positieve invloed hebben op hersenontwikkeling en het functioneren als de kindjes ouder zijn. Deze associatie is echter slechts indirect, en is tot heden nog niet gedetailleerd onderzocht op biologisch niveau: wat gebeurt er in de beschadigde hersenen als oxytocine wordt aangemaakt? Hoe zorgt dat uiteindelijk voor betere hersenontwikkeling?

In deze thesis heb ik de werkzaamheid van oxytocine onderzocht in twee soorten hersenschade die veel voorkomen bij pasgeborenen: traumatisch hersenletsel (“TBI”, dat ontstaat door fysieke impact met de schedel), en hersenschade geassocieerd met premature geboorte (die gebundeld zijn in de klinische term *encephalopathie van prematuriteit*; “EoP”). Wat deze twee soorten hersenschade verbindt is dat ze allebei een “koortsreactie” in de hersenen veroorzaken, ookwel neuroinflammatie genoemd. Neuroinflammatie is een process wat ook bij volwassenen plaatsvindt als gevolg van hersenschade, maar het jonge brein is minder bestand tegen deze immuunreactie. Het is aanvankelijk een positief proces – je lichaam schakelt het immuunsysteem in om de gevolgen van de hersenschade tegen te gaan – maar er is een groot risico dat de imuunreactie te heftig raakt, waarbij de cellen in een langdurige staat van

activatie komen en ook gezond hersenweefsel aan gaan vallen. Dit maakt neuroinflammatie specifiek schadelijk voor pasgeborenen, omdat het jonge brein nog niet ontwikkeld genoeg is om de immuunreactie goed te reguleren. Tegelijkertijd zijn de cellen die betrokken zijn bij deze neuro-inflammatie, genaamd glia cellen, cellen die eigenlijk bezig zouden moeten zijn om de hersenen te ondersteunen te groeien. Maar tijdens neuroinflammatie laten deze glia cellen hun normale functies links liggen en gaan ze andere functies uitvoeren: de hersenen bestrijden. Als gevolg kan deze reactie veel veranderingen teweegbrengen die het ontwikkelingsproces van de hersenen verstoren, en daarbij langdurige negatieve gevolgen kan veroorzaken. In mijn thesis heb ik een van deze glia celtypes specifiek onderzocht: microglia. Deze cellen zijn de *'first responders'* na hersenschade, die het neuro-inflammatie proces opstarten en vervolgens ook managen – waarbij ze veel andere celtypes en processen aansturen in de hersenen.

Om de potentie van oxytocin tegen hersenschade te kunnen onderzoeken, heb ik eerst TBI en EoP nagebootst ('gemodelleerd') in muizen. Vervolgens heb ik de muizen met hersenschade behandeld met het verhogen van hun oxytocine-aanmaak in de hersenen. De gevolgen van deze oxytocine behandeling heb ik op verschillende niveaus onderzocht: op cognitief niveau (met gedragsproefjes en het scannen van de hersenstructuren), op cel niveau (met de microscoop kijken welke cellen en eiwitten aanwezig zijn, in wat voor hoeveelheid, en op welke plekken), en op moleculair niveau (welke eiwitten worden aangemaakt door welke cellen, wat een inzicht geeft in hun functioneren).

<u>Resultaten van het onderzoek</u>

Mijn onderzoek laat zien dat oxytocine een dempend effect heeft op de microglia cellen die reactief zijn ter gevolg van de hersenschade van TBI en EoP. Ik heb gekeken op DNA/RNA niveau hoe oxytocine het functioneren van microglia verandert, wat liet zien dat oxytocine de gen-expressie vermindert van de productie van schadelijke stofjes van deze cellen. Tegelijkertijd herstelt oxytocine de gen-expressie van de ondersteunende functies van microglia voor belangrijke processen van hersenontwikkeling. Dit ging gepaard met een terugname in de verhoogde aanwezigheid van microglia in de hersenen, en een ommekeer van hun giftige vorm/structuur. Dit suggereert dat oxytocine de inflammatie-reactie van microglia cellen na hersenschade dempt, en het risico op over-activering en diens bijkomende schadelijke effecten vermindert.

Verhoogde oxytocine-aanmaak had ook op lange-termijn positieve effecten op de hersenontwikkeling na schade. Het verbeterde de kwaliteit en groei van witte stof – een belangrijke factor voor efficiënte communicatie binnen de hersenen. Dit heeft waarschijnlijk te maken met oxytocine's effect op de microglia: microglia cellen van muizen behandeld met oxytocine toonden meer gen-expressie betrokken bij de groei en ontwikkeling van de voorlopers van witte stof: oligodendrocyten. Andere lange-termijn effecten waren verbeterde coördinatie van activiteit tussen verschillende hersengedeeltes, het herstel van bloedsomloop in het gebied beschadigd door de fysieke impact van TBI, en het herstel van korte- en lange-termijn sociaal gedrag van de muizen. Deze effecten waren nog steeds aanwezig een maand na de laatste oxytocine verhoging– wat suggereert dat de korte periode van oxytocine behandeling structurele verandering teweegbrengt die de hersenontwikkeling na schade langdurig verbetert.

Het therapeutische effect van oxytocine was aanwezig in beide modellen van hersenschade, maar toonde ook subtiele verschillen. Die verschillen zijn hoogstwaarschijnlijk verbonden met het verschil in type hersenschade (meer opbouwende/gespreide neuroinflammatie in EoP, tegenover meer een acute en heftige neuroinflammatie in TBI) en de leeftijd van de muizen ten tijde van schade en de oxytocine behandeling (1-5 dagen oud in het EoP model, en 7-10 dagen oud in the TBI model). Ook vonden we een verschillend effect in vrouwtjes en mannetjes muizen in het EoP model, waarbij vrouwtjes muizen betere genezing toonden in reactie op de oxytocine behandeling dan mannetjes. Deze details zijn erg interessant om verder te onderzoeken met toekomstie studies. Ze zullen namelijk belangrijk zijn om individuele verschillen in de ontvankelijkheid van oxytocine beter te begrijpen, wat waarschijnlijk de uitkomst van klinische behandeling zal verbeteren. Ondanks deze kleine verschillen, laten onze

onderzoeken zien dat oxytocine een sterke beschermende werking heeft in beide modellen van pasgeboren hersenschade.

Implicaties voor de kliniek

Met de translationele onderzoeken gepresenteerd in deze thesis hebben we een biologisch mechanisme gevonden wat de positieve effecten van oxytocine op hersenontwikkeling in de kliniek verklaart. Tegelijkertijd hebben we aangetoond dat lichaamseigen oxytocine therapeutische werkt in twee verschillende veelvoorkomende soorten van hersenschade in pasgeborenen. Waarbij een korte behandelingsperiode sterk genoeg was om verandering te brengen die ook op lange-termijn stand houdt. Deze thesis is daarbij belangrijk voor algemene biologische kennis over neuroinflammatie en de rol van microglia in dit proces, en suggereert zien dat klinische therapiën gericht op natuurlijke oxytocine verhoging veelbelovend zijn voor pasgeborenen.

De grote kracht van deze thesis zit in de methodes van de onderzoeken. Een groot probleem in translationele neurobiologie is dat de onderzoeken in dieren niet goed menselijke mechanismes modelleren, waardoor gevonden therapeutische effecten niet omgezet kunnen worden naar success in patiënten. Dit heet ook wel de “vallei des doods” tussen pre-klinisch onderzoek en de kliniek (slechts 5-10% van preklinische therapien is ook succesvol in mensen). De manier waarop oxytocine is onderzocht als therapie in deze thesis heeft een grote translationele potentie. Lichaamseigen en lichaamsvreende oxytocine hebben niet dezelfde werking, dus het was belangrijk om lichaamseigen aanmaak na te bootsen – want in de klinische onderzoeken wordt dat immers ook gedaan. Dit hebben we bereikt door genetisch gemodificeerde muizen te maken, wiens oxytocine-neuronen te activeren zijn door het toedienen van een bepaald chemisch stofje. Door het verhogen van lichaamseigen oxytocine als behandeling zijn de resultaten van deze studies hoogswaarschijnlijk beter te vertalen naar de kliniek, en tegelijkertijd identificeert het oxytocine als unieke veelbelovende non-pharmacologische, non-invasieve, non-stressvolle therapie voor pasgeborenen met hersenschade.

Contents

List of abbreviations

EoP	encephalopathy of prematurity
PVL	periventricular leukomalacia
MRI	magnetic resonance imaging
TBI	traumatic brain injury
USA	United States of America
CP	cerebral palsy
TH	therapeutic hypothermia
MSC	mesenchymal stem cell
PVN	periventricular nucleus
SON	supraoptic nucleus
NICU	neonatal intensive care unit
HPA-axis	hypothalamic-pituitary-adrenal axis
ASD	autism spectrum disorder
DREADD	designer receptors exclusively activated by designer drugs
ERK	extracellular signal-regulated kinase
OL	oligodendrocyte
OPC	oligodendrocyte progenitor cell
MBP	myelin base protein
EE	environmental enrichment
BDNF	brain-derived neurotrophic factor
OXTR	oxytocin receptor
RNA	ribonucleic acid
GFAP	glial fibrillary acidic protein
CNO	clozapine n-oxide
PICU	pediatric intensive care unit
USD	United States dollar
IUGR	intra-uterine growth restriction
CSF	cerebral spinal fluid
OT/OXT	oxytocin
AVP	vasopressin
GA	gestational age
GABA	gamma-aminobutyric acid
NDD	neurodevelopmental disorder
LPS	lipopolysaccharide
IL	interleukin
TNF	tumor necrosis factor
iNOS	inducible nitric oxide synthase
HI	hypoxic-ischemic insult
VPA	valproate
ISH	in-situ hybridization
aDG	anterior dentate gyrus
RT-qPCR	reverse transcription quantitative polymerase chain reaction
IP	intraperitoneal
SC	subcutaneous

WT	wild-type
CLCF1	cardiotrophin-like cytokine factor 1
HIF	hypoxia-inducable factor
TGF	transforming growth factor
FGF	firoblast growth factor
PKA	protein kinase A
PKC	protein kinase C
MAPK	mitogen-activated protein kinase
MEK	mitogen-activated protein kinase kinase
JNK	c-Jun N-terminal kinase
NF-κB	nuclear factor kappa-light-chain-enhancer of activated B cells
ER	endoplasmic reticulum
ATF	activating transcription factor
IRE	inositol-requiring enzyme
PERK	PRKR-like endoplasmic reticulum kinase
eIF	eukaryotic initiation factor
CHOP	C/EBP homologous protein
NO	nitric oxide
KO	knock-out
ATP	adenosine triphosphate
5-HT	5-hydroxytryptamine (also known as serotonin)
COX	cyclooxygenase
NADPH	nicotinamide adenine dinucleotide phosphate
NOX	NADPH oxidase
ROS	reactive oxygen species
WM	white matter
DTI	diffusion tensor imaging
NODDI	neurite orientation dispersion and density imaging
FA	fractional anisotropy
RD	radial diffusivity
AD	axial diffusivity
ODI	orientation dispersion index
NDI	neurite density index
CSF	cerebrospinal fluid
CC	corpus callosum
EC	external capsule
CG	cingulum
M1Cx	primary motor cortex
S1Cx	primary somatosensory cortex
ROI	region of interest
fUS	functional ultrasound
CBV	cerebrovascular blood volume
DEG	differentially expression genes
FDR	false discovery rate
PCA	principal component analysis
GSEA	gene set enrichment analysis
S1bf	primary somatosensory cortex, barrel field
S1Tr	primary somatosensory cortex, trunk region

RSV	ventral retrosplenial cortex
RSD	dorsal retrosplenial cortex
HIP	hippocampus
WD	weighted degree
EC	eigenvector centrality
TSPO	18 kDa translocator protein
SUV	standard uptake value
VOI	volume of interest
PET	positron emmission tomography
PBS	phosphate buffered saline
PFA	paraformaldehyde
EWCE	expression weighted cell-type enrichment
scCWM	supra-callosal cerebral white matter
CC aF	corpus callosum, anterior forceps region
CC eC	corpus callosum, external capsule region
USV	ultrasound vocalization

Chapter 1: Introduction

1. Newborn brain injury

Due to its immaturity and state of rapid development, the newborn brain is at increased risk for experiencing injury. Every year, about 5 in 1000 children experience brain injury in the early-life period[1]. The incidence varies with the age of the infant and type of injury. Around 2-3 in 1000 full-term aged children experience some form of brain damage at birth, which increases up to 25-26 in 1000 infants born preterm[1]. Brain damage can occur during birth – due to impaired blood circulation or oxygen to the fetal brain, increased pressure on the brain during delivery, or low birth weight – or after birth – due to infection, sepsis or in the form of physical injury to the brain[2–4]. The injury itself is harmful, but additionally harmful are the consequential impairments to brain development that can occur. At birth, the newborn brain is roughly one quarter the size of the adult brain, and it doubles in size during the first year of life[5]. When this important window of development gets disturbed by means of injury, it can lay groundwork that affects children for the rest of their lives. Concurrently, newborn brain injury is associated with structural and functional alterations to the brain, which can manifest into lifelong socio-cognitive behavioral issues. In addition to the effects on the child, it can impose caretakers with long-term financial burdens including frequent medical visits, ongoing therapies, specialized equipment, home modifications, long-term care needs that require a reduction of working hours and income, and severe emotional distress[6–8]. It goes without saying, the ethical, emotional and financial burden of newborn brain injury is immense.

There are different causes of brain injuries in newborns. We separate here injuries surrounding birth, and injuries in the first year of birth. Two of the most occurring types of newborn brain injury are prematurity, and pediatric traumatic brain injury.

1.1 Encephalopathy of prematurity

Globally, approximately one in every 10 live births is preterm (before 37 weeks of gestation) (World Health Organization, 2023). Preterm births can be medically induced due to complications of the fetus or mother, or occur naturally. The major cause of naturally occurring preterm births is histological chorioamnionitis – defined as acute inflammation of the chorion and amnion – accounting for up to 40% of natural preterm births occurring before 32 weeks of gestation, and as high as 70% for births before 25 weeks of gestation (reviewed in Gressens & Volpe 2015[3]). Then there are perinatal complications that often occur in preterm infants, attributable to their fragile state and underdeveloped organs and immune system (such as neonatal sepsis, mechanical ventilation to support breathing, necrotizing enterocolitis, and hypoxia/ischemia)[2]. Preterm birth is associated with a collection of neural and neurocognitive impairments, that are bundled under the clinical term *Encephalopathy of prematurity* (EoP). EoP is characterized by cystic and non-cystic periventricular leukomalacia (PVL), and the diffuse neuronal and axonal deficiencies that often accompany PVL[2]. Its neuropathology is mostly associated with white matter loss, which has become a hallmark for EoP since 1980 when MRI scanning was starting to be used. The neural changes of EoP create developmental changes of reduced brain volumes, impaired maturation of interneurons, abnormal microstructure of the cortex, and white matter deficiency[9], which, on a behavioral level, can cause a collection of cognitive, attentional and social behavioral deficits[2]. These changes can last up to adulthood, where they can even increase the vulnerability to psychotic illness[10]. The economic burden of preterm birth includes a median birth hospitalization cost of $269,974 per preterm patient[11], which is excluding follow-up care and ongoing

therapies. The total financial burden associated with preterm birth in the USA was 26.2 billion dollars in 2005[12].

1.2 Pediatric traumatic brain injury

Where preterm birth occurs around birth, pediatric traumatic brain injury (TBI) is predominantly a postnatal injury. It is the most frequent type of brain injury throughout infancy, affecting around 1 in 100 children up to 4 years of age in the USA[4]. There is a bimodal age distribution in pediatric TBI, where adolescents and very young children (between 0-2 years old) are more commonly injured[13]. In newborns and young infants, TBI is caused by falls, motor vehicle accidents, and physical abuse (shaken-baby syndrome, for example)[4]. As such, pediatric TBI is largely a closed-head injury – this in contrast to adults, where TBI also happens in the form of penetrating injury through sharp objects[4]. TBI is characterized by a sequential injury mechanism. The primary injury refers to the neural damage that is created by the impact of the external force to the skull, and includes mechanical damage from tearing, shearing and stretching of neurons, glia, axons, and blood vessels[14,15] The secondary injury relates to the consequential processes in the brain that further the primary injury, such as excitotoxicity, mitochondrial dysfunction, decreased blood-brain barrier integrity, increased oxidative stress and protein aggregation.[16] Finally, the tertiary injury includes the long-term cognitive-behavioral issues that arise from the structural and functional brain alterations caused by TBI[16,17]. The effects caused by TBI in the developing brain can have a long-lasting impact on a child's functioning in all facets of life[18,19]. This can be attributed to the chronic neuro-pathophysiology of TBI, which includes widespread white matter damage[20] and alterations to brain circuitry[21,22]. On a behavioral level, TBI can create generalized cognitive deficiencies, memory impairment and executive function problems[23], as well as problems with social behavior[24]. Increased risk of developing psychiatric disorders and possibly even criminality has also been reported[25]. Around 14% of children who sustained mild TBI suffer from long-term disability, which spikes up to 62% for children who suffered moderate to severe injuries[26]. In 2010, the financial costs of children from 0-4 years old suffering from abusive head trauma was 13.5 billion dollars in the USA[27].

1.3 Sexual dimorphism in newborn brain injury

There appears to be sexual dimorphism in the occurrence of brain injury in newborns, where boys are generally more affected. They are more susceptible to injury, and show worse outcomes compared to females[28,29]. The same is seen in preterm birth and its associated complications, which shows increased occurrence in boys compared to girls[30]. Similarly, boys are two times more likely than girls to sustain TBI, especially in the age between 0 and 4 years old[31]. Although it remains a challenge to fully map the mechanisms underlying these sex differences, there are multiple factors that likely contribute[28]. Boys and girls have a different developmental exposure to steroid hormones, which is associated with sex-specific differences in brain development, including neurogenesis, cell survival and synaptic patterning[32]. Additionally, boys and girls show differences in their immune systems[33], where the female brain could be more innately protected against injury[34]. These sex-specific effects on brain injury are especially important because they are associated with sex-specific responses to treatments (reviewed in Kelly et al., 2023[29]). As such, it is essential to include both males and females in studies of newborn brain injury.

2. Neuroinflammation in the newborn brain

Early-life is an important window of development, and when this development gets affected, it can lay groundwork that affects children for the rest of their lives. Not only is the injury itself harmful, but

additionally harmful are the consequential events that happen in the brain. One of those secondary effects is neuroinflammation, an immune reaction in the brain in response to injury[9,34,35]. Immune cells like microglia orchestrate an offense to the injury that is initially beneficial, but is at the risk that it becomes excessive and starts affecting healthy tissue as well. Importantly, the newborn brain is far less equipped to accommodate this immune response than the adult brain. The newborn immune system is not yet developed to limit the excessive effects, and, in parallel, its immune cells are highly needed for brain development support – which is abandoned in favor of the immune functions. Needless to say, this neuroinflammatory response is a source of developmental issues for the newborn brain.

2.1 Microglial cells: the brain's support system

Microglial cells are crucial for the developing brain[36]. They originate in the yolk sac where they develop from erythro-myeloid progenitors. This is different from the other brain cells, as neurons, astrocytes and oligodendrocytes all develop from neuroepithelial progenitor cells located in the neural tube. After migration through the embryo, microglia enter the immature brain around 4 to 5 weeks of gestation in humans[37], and around embryonic day 8/9 in mice[38]. They enter the mouse brain through ventricles and meninges, and form a strong presence at the time when neurons and other glial cells are just starting to be produced[39]. This places microglia in the brain when neurons and neural circuits start to develop and assemble (**Figure 1**). In contrast to their eventual uniform distribution in the adult brain, microglia show a highly uneven distribution throughout the developing brain[37]. They accumulate at regions in a spatiotemporal pattern that overlaps with key brain development processes taking place – such as the formation of axonal tracts and guiding migration of interneurons[39]. In addition to supporting the development of cells within the brain, new studies suggest they also support morphogenesis of the brain itself. Specifically, they are needed for the formation and maintenance of key morphological boundaries of the cortex, such as the boundary between the cortex, striatum and amygdala, and the boundary between the cortex and the septum[40]. Without microglia present, the morphogenetic stress of the growing brain causes local caveats in the tissue. After the blood-brain-barrier closes, new microglia proliferate and self-renew from the pool of existing microglia in the brain[41]

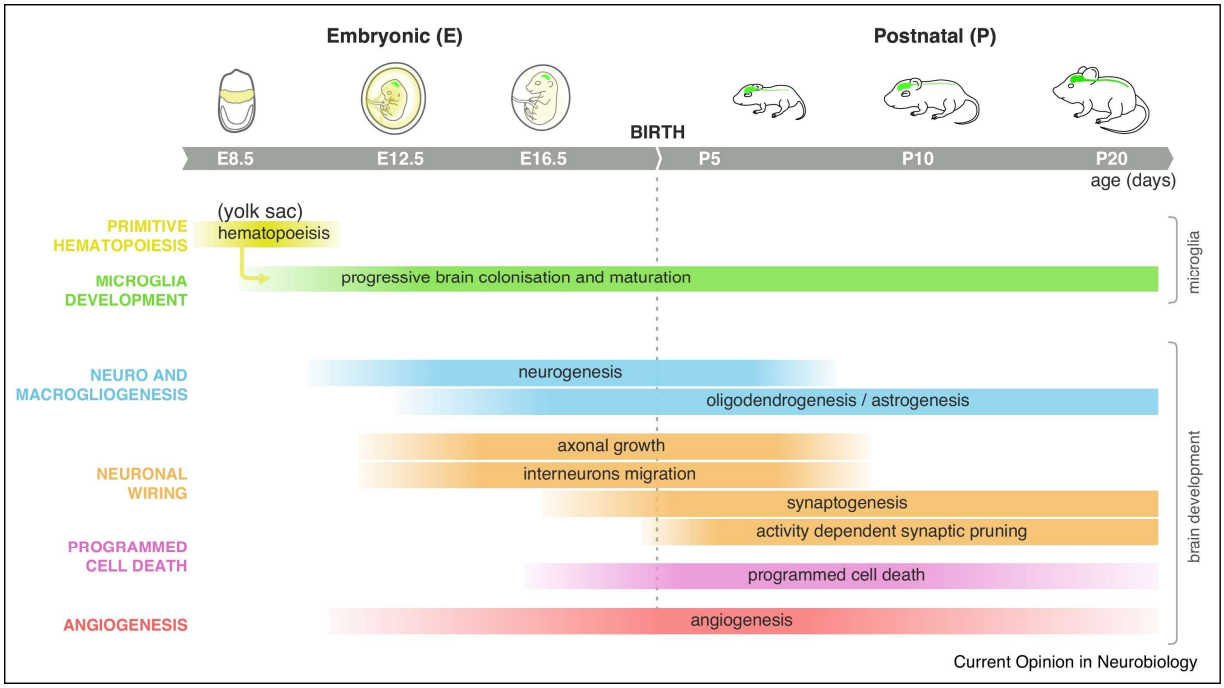

Figure 1: **Timeline of early-life microglia in relation to key brain development processes in mice**. Temporal overview of microglia development in relation to crucial brain development processes where microglia are implicated. Microglia colonization of the mouse brain depicted in green (top panel). Thion & Garel 2017.

A key characteristic of microglia cells is their highly dynamic nature. Although they make up only 5-15% of the brain cell population, microglia are in contact with many neural cells and through this, continuously sense the brain milieu[36,42]. This is enabled by the wide range of receptors that they express on their cell surface, which forms a true microglia 'sensome', and the ability to extend their process to contact many different cells. As such, they can quickly adapt their form and function to react to the changing neural environment and tweak their functions to provide what the brain needs. They do this in response to signaling of chemokines and cytokines, amino acids, purinergic molecules, inorganic substances, and changes in pH[43]. As such, they are involved in a myriad of different functions, including providing growth and proliferation of neurons, establishing and optimizing neural circuits via synaptic pruning, and they are key for the development of oligodendrocyte into fully functioning myelin sheaths (see **Figure 2**).

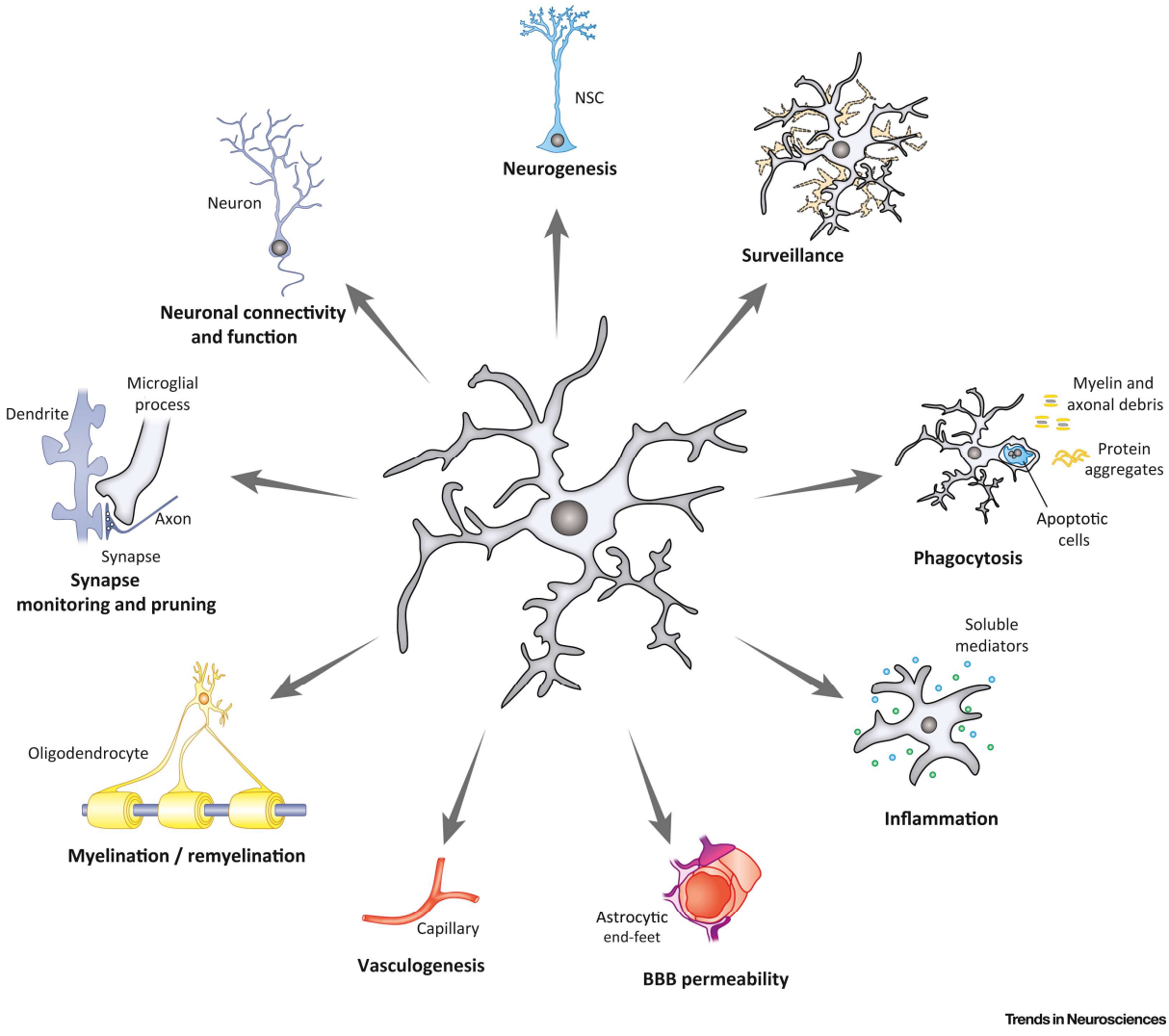

Figure 2: **Schematic representation of key physiological and pathological functions of microglia cells in the brain**. Microglia can shift between different functions as adaptations to the changing brain milieu. Sierra, Paolicelli & Kettenmann, 2019.

2.2 Microglia orchestrate the neuroinflammatory response to brain injury

The ability to respond quickly to changes in the brain milieu also makes microglia the first-responding immune cells after injury, infection, or another adverse stimulus that poses a threat to the brain. In response to such a stressor, microglia increase in cell density, largely discard their homeostatic functions and attain an aggressive immune-attacking form and function. This is traditionally termed the 'pro-inflammatory' phenotype, and is linked to a rounded, amoeboid morphology of the cells[44]. In this form, microglia – in highly increased numbers – recruit other cells of the immune system through the release of pro-inflammatory cytokines and chemokines, including IL-1β, IL-6, TNFα, IL-18, TGF-β, and IL-10[45]. One major cell type they recruit are astrocytes, who are specifically activated by microglia secretion of IL-1α, TNF-α and C1q[46]. Reactive astrocytes secrete soluble neurotoxins which induces neurotoxicity and apoptosis of mature neurons and oligodendrocytes[46]. Additionally, they amplify the inflammatory response by signaling and recruiting distant glial cells through calcium waves[47,48]. As a response, the brain increases its processes of cell clearance, through apoptosis and phagocytosis, directed towards eliminating the intruder, restricting the jury, and preserving the healthy tissue[45]. Microglia are able to be this adaptive in response to injury through the expression of many receptors. This includes the expression of pattern-recognition receptors, such as Toll-like receptor 4, that detect pathogen-associated- or damage-associated molecular patterns, the expression of chemokine receptors such as CX3CCR1, that enable migration towards the injury, and purinergic receptors for ATP, which drive phagocytic processes (reviewed in Colonna & Butovsky, 2017[49]). Microglia also express receptors for numerous neurotransmitters and neuropeptides, allowing them to respond to changes in neuronal activity[49].

Despite the beneficial effects, there are also risks associated with neuroinflammation. The disease-associated molecules produced by pro-inflammatory microglia, such as free radicals that generate reactive oxygen species and reactive nitrogen species, are highly toxic to neural cells[14]. Additionally, the neuroinflammatory phenotypic shift of microglia and astrocytes results in a neglect of their homeostatic duties[46]. This is especially problematic in the developing brain, where homeostatic glial functions are crucial, and where the immature immune system is not yet proficient at self-resolving the inflammatory response once the infection or injury has been eradicated[50,51]. As a result, neuroinflammation in the newborn brain can have a prolonged negative impact on brain development, and even develop into a chronic state of heightened microglia activity long after the initial injury or infection has been resolved[52,53].

One aspect of the developing brain that seems especially affected by newborn neuroinflammation is white matter. After birth, the young brain undergoes rapid development of oligodendrocyte cells to ultimately form myelinating sheaths to wrap axons and ensure signal transduction and the formation of neural circuits. Pre-myelinating, immature oligodendrocytes express many cytokine receptors, which makes them particularly sensitive to microglia signaling. In inflammation, when mostly toxic signaling molecules are secreted, oligodendrocytes largely die or their development gets severely hampered due to the lack of guidance they need from homeostatic microglia. Indeed, in vitro studies show that in an inflammatory milieu, microglia strongly reduce the release of tropic factors insulin-growth factor 1, and ciliary neurotrophic factor, both crucial for oligodendrocyte development and protection[54,55]. As a consequence, oligodendrocytes develop less into fully functioning myelinating cells, creating a substantial reduction in efficient neural transmission. Indeed, white matter damage is consistently found in newborns with brain injury, and it is likewise shown in preclinical animal models.

In summary, neuroinflammation associated with newborn brain injury is a temporal process with distinct phases, that can exert long-lasting changes on the structural and functional development of the brain,

which is associated with cognitive-behavioral issues such as attention deficits, language problems, social deficits, and in severe cases, even motor impairments such as cerebral palsy (**Figure 3**).

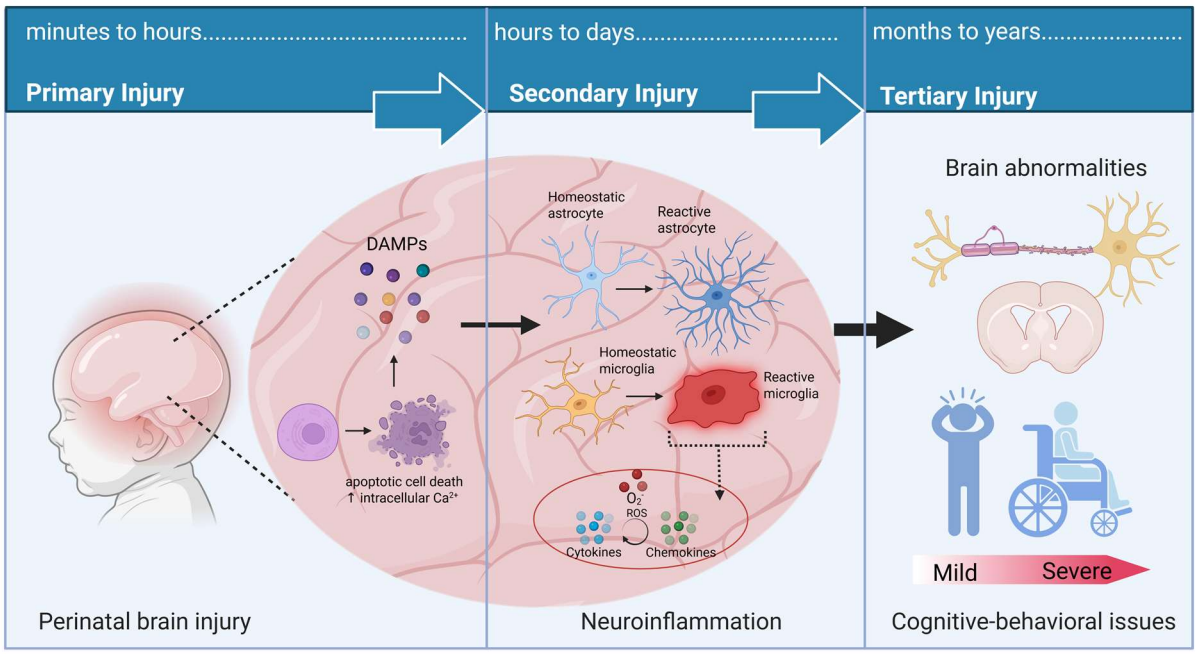

Figure 3: **Timeline of the acute, secondary and tertiary phases of inflammation associated with brain injury in newborns.** In the primary injury phase, the damage to the brain activates processes such as intrinsic and extrinsic apoptosis and neurotoxic increase in intracellular calcium, which causes cell death and the production of damage-associated molecular pattern molecules. As the secondary phase, these changes in brain milieu are sensed by microglia and astrocytes, who then undergo a phenotypic shift towards a reactive inflammatory phenotype. As a result, reactive microglia and astrocytes start producing toxic cytokines, chemokines and reactive oxygen species (ROS) that recruit additional glial cells, and instigate additional processes (such as phagocytosis). This inflammatory response in the newborn brain is at high risk to interfere with crucial brain development processes, causing abnormalities in brain structure and function, including dysmaturation of oligodendrocyte cells and myelination, which can manifest itself into long-lasting cognitive-behavioral issues in the child – which forms the tertiary phase of injury. Created with Biorender.com

2.3 Neuroinflammation mechanisms in EoP and pediatric TBI

Both EoP and TBI are highly associated with neuroinflammation, yet in slightly different matters. In preterm born infants, the cause of the premature birth is often associated with a complication[3]. Antenatal maternal immune affection, which creates inflammation in the fetus, or perinatal events such as hypoxia-ischemia[56], or postnatal complications such as sepsis or infection – because the immature immune system makes the child more susceptible to infection[9]. Inflammation can also be induced by interventions frequently accompanying prematurity, such as mechanical ventilation to help the child breathe[3]. This all induces systemic inflammation, where pro-inflammatory cytokines are released into the circulation, and reach the brain where it is converted into neuroinflammation by microglia: microglia react to the cytokines and chemokines from the periphery, and relay this with their own signaling response to instigate the neuroinflammatory response in the brain[57]. Accordingly, preterm infants show elevated levels of pro-inflammatory cytokines in the brain[58], and post-mortem studies likewise demonstrate increased density of microglial cells in brains of preterm infants[2,59,60]. The inflammatory

response in EoP is more directly associated with the primary injury, often causally contributing to the primary effects on the brain.

In pediatric TBI, the neuroinflammation mechanism is different. Rather than a systemic inflammation that gradually reaches the brain, the neuroinflammatory response to TBI is acute, and localized. Within minutes, microglia migrate to the injury site, and induce the inflammatory response[61]. The inflammatory response to TBI shows a strong hemispheric effect, mostly affecting the ipsilateral hemisphere[35]. With time, the local response gradually expands and affects distant tissue as well. In TBI, microglia further regulate the inflammatory response by close collaboration of other disease-associated mechanisms of TBI, including recruitment of peripheral macrophages through the damaged blood-brain barrier[61]. Compared to EoP, pediatric TBI has a more acute primary injury phase, associated with a relatively higher tissue damage. For this reason, in TBI we speak of a primary injury and secondary injury mechanism, where neuroinflammation is the secondary phase. This distinction between primary injury and neuroinflammation is less clear in EoP.

2.4 Modulation of microglia as therapeutic target for newborn brain injury

In response to brain injury, microglia have a natural counterpart to the pro-inflammatory phenotype, termed the anti-inflammatory phenotype. This form of microglia is focused on tissue repair and regeneration, and is generally attained as the "holy grail" of brain injury regeneration studies (See **Box 1** for the nomenclature of microglia phenotypes). The anti-inflammatory phase generally comes later in the injury timeline – although opposite temporal mechanisms have also been observed[62]. It is only beginning to be known what determines the microglial shift from the toxic to the regenerative phenotype. It has been attributed to certain signaling cytokines such as interleukin-10 (IL-10), IL-4, interferon growth factor 1, Arg1, Lgals3, and TGF-β[35,63,64]. Interestingly, these signaling molecules are also released by microglia and astrocytes themselves, in response to the altered brain milieu[47,65]. This self-regulating loop is further complicated by the high degree of cross-talk between microglia and astrocytes, who have the ability to both enhance and reduce each other's (inflammatory) functions[45,47,66].

Modulation of microglial cells in brain injury associated with neuroinflammation has been a target for biomedical research for many years[67–72]. Depletion of the cells after injury was initially presumed effective, but turned out to do more harm than good[40,73,74], emphasizing the importance of these cells for homeostatic brain processes. Rather, the focus shifted to modulating the phenotype of microglial cells during neuroinflammation. The aim of this therapeutic strategy is 3-fold: (1) shift microglia from a pro-inflammatory to an anti-

BOX 1: MICROGLIA NOMENCLATURE

Microglia cells have been traditionally categorized into either 'resting' or 'active', which is not accurate because also in their homeostatic states, they are actively surveilling the brain through their sensome. 'active' refers to the inflammatory phenotype they attain in response to injury, infection or other disturbances to the brain milieu. In this inflammatory state, microglial subtypes are likewise simplified and further differentiated into a toxic pro-inflammatory, or '*M1*', and regenerative anti-inflammatory, or '*M2*', phenotype. However, increasing evidence suggests that the same cell shifts between these two functions, and so the categorization of the *type* of cell more accurately refers to its *current state*. A recent consortium of microglia-experts pooled their efforts to advertise exactly this (Paolicelli et al., 2022). They rightfully plea for a more holistic consideration of these cells, taking into account their host-species, ontogeny, spatiotemporal characteristics, and experimental conditions. As such, in this thesis, 'resting' microglia will be termed *homeostatic microglia*. And 'active' microglia will be described as *reactive*, referring to their phenotypic change in reaction to brain injury.

inflammatory phenotype, (2) reduce post-injury inflammation, and (3) promote post-injury neuronal repair. This venture is especially challenging in the developing brain, where the homeostatic support functions of microglia are even more important than in the adult brain[75]. Additionally, the developing brain knows a substantially more heterogeneous microglia population[76,77], so its functioning in response to injury could have different dynamics from adult brain injury.

3. Oxytocin as a neuroprotective agent in the injured newborn brain

3.1 Current landscape of available treatments

Protecting the developing brain is a major focus for translational and clinical neuroscience. However, the clinical treatments that are currently available are not optimal. In pediatric TBI, current clinical treatments are focused on the primary injury phase. This includes therapies such as cerebrospinal fluid drainage or intravenous hypersmolar therapy to reduce intracranial hypertension and cerebral perfusion pressure, or treatment with prophylactics to reduce the risk of post-traumatic seizures[78]. Therapeutic hypothermia (TH) has also been explored to limit secondary injury given its functions to decrease metabolic demands, inflammation, excitotoxicity and cell death – as frequently used in brain injury associated with hypoxia-ischemia – but clinical trials report no effects on mortality or outcome in children with severe TBI[79,80]. There are currently no drugs proven to improve outcomes of pediatric TBI that are focused on reducing secondary injury mechanisms like neuroinflammation. Although research in animal models produced promising effects for anti-inflammatory agents such as glucocorticoids, hormonal and vitamin treatments and stem-cell therapies (reviewed in Jacquens et al., 2022[16]), they have not yet translated to clinical success.

Treatment to EoP is less defined, because EoP is less defined by clear neural injuries like TBI[2,3,81]. The pathology underlying EoP is multifactorial and so are its outcomes[82]. For example, motor dysfunction and cerebral palsy can be one of the outcomes of preterm birth – especially in preterm birth before 28 weeks of gestation, where the prevalence of CP is 16-21%[83]. Similarly, cognitive defects have been shown for 31% of children who were born preterm[84]. Delays in language development are also common[85]. Treatment of EoP is therefore focused on environmental enrichment and (physical) therapy that try and improve the outcomes of brain injury associated with EoP (provide stimulation and regain neuroplasticity). The acute biomedical therapies currently used include antenatal treatments – such as corticosteroids to facilitate fetal neurovascular development and magnesium sulfate treatment to reduce the risk of CP – and postnatal intervention such as seizure management, and TH to reduce metabolic rates (reviewed in Molloy et al., 2024[82]). Unlike term infants, however, the use of TH in preterm infants is not without risk and it can aggravate preterm-birth associated complications such as intracranial bleeding and respiratory issues[86]. There is a new line of research focused on anti-inflammatory and stem cell therapy against the diffuse white matter injury that characterizes EoP. This is focused on stimulation of endogenous brain repair mechanisms through the implementation of mesenchymal stem cells (MSCs) to the neonates[57,63]. Although promising, administration of genetically engineered MSCs to preterm infants has several methodological and safety challenges to overcome before becoming a real option in the clinic (such as optimizing delivery methods and efficacy, as well as managing side effects – see Chang et al., 2017 for a review[87]). Likewise, anti-inflammatory interventions focused on the reduction of the neuroinflammatory response and stimulation of white matter development have shown potential in animal models[63], but have not been developed into clinical options.

Although promising, the use of anti-inflammatory interventions for EoP and pediatric TBI has been, to date, primarily preclinical. This emphasizes the need for an effective anti-inflammatory treatment that is clinically successful. The translation to clinical success is challenging: around 95% of drugs that enter

clinical trials fail. This concept is known as the "valley of death" between preclinical and clinical research (reviewed in Seyhan, 2019[88]). The difficulty in translating success from preclinical studies to humans is in large aided by methodological challenges where animal milieus and animal disease models do not adequately simulate human conditions, and where therapies can be too complex to form a realistic option to the clinic[88]. An additional challenge for the development of successful clinical therapies specifically for newborns relates to stress. Neonatal stress and pain – measured for example as number of needle injections – is not beneficial for the brain development, and associates with altered neural connectivity and reduced white and gray matter volume at later age[89]. It is thus crucial to find clinical interventions that are minimally invasive and as comfortable as possible for newborns. One treatment that has potential to fulfill those requirements concerns a body-own substance with potentially innate protective effects on brain development: oxytocin.

3.2 Oxytocin and its importance in the neonatal period

Oxytocin is a neuropeptide produced in the hypothalamus, specifically by parvocellular and magnocellular neurons of the periventricular nucleus (PVN) and supraoptic nucleus (SON)[90]. After release, it follows two main trajectories. The peripheral route, where it goes through the posterior pituitary gland, and enters the peripheral bloodstream, where it acts on peripheral organs as a hormone[91]. The second path stays in the central nervous system, where oxytocin is spread as a neuropeptide via axonal projections to connecting synapses, via local somato-dendritic release in the PVN, or via volume transmission, where oxytocin can travel long distances in the brain via passive diffusion or bulk flow via cerebral spinal fluid in the ventricular system[92–95]. Via these different activation pathways, oxytocin can reach both neurons and surrounding glial cells and oligodendrocytes[95,96].

Oxytocin influences the brain via activation of the oxytocin receptor, a seven-transmembrane G-protein-coupled receptor. Oxytocin receptors are expressed on neurons throughout the brain, including cortex, hypothalamus, hippocampus and amygdala, emphasizing the vast size of the neural oxytocin system[97–99]. Through its dual coupling to Gq and Gi proteins, oxytocin receptors can enhance or suppress activation of its neurons[100–102]. The oxytocin system has many functions. It is most known for its role in the neonatal period where it stimulates lactation, parent-infant bonding, as well as for social behavior throughout life[103–105]. Oxytocin is also increasingly recognized for its additional functions, such as learning and memory, including modulation of synaptic transmission via effects on long-term potentiation and long-term depression[106–109]. One function that is increasingly investigated is oxytocin's role in brain development. It starts around birth, where oxytocin has important functions in flipping the GABA switch to protect from postnatal excitotoxic damage[110]. But also after birth, reports show that oxytocin is involved in structural brain development, and the establishment of functional brain circuitry[99,111,112]. This is supported by studies that have shown that the dynamic expression of oxytocin receptors in the brain overlaps with developmental windows of critical development. For example, there is a peak of oxytocin receptor expression in the motor and somatosensory cortices during the pediatric age in humans (0-12 years), which is an age that is characterized by substantial development in fine motor functioning and sensory exploration in children[113]. Similarly, the human brain shows a reduction in oxytocin receptor expression in the striatum and prefrontal cortex during the juvenile age. This can be associated with the risk-taking behavior that characterizes the juvenile age in humans, stimulated by a loss of limbic control over the response of the striatum to rewards[114]. This transient developmental pattern of oxytocin receptor expression is also seen in mice and rats (reviewed in Knoop et al., 2022[112]). In mice, oxytocin receptor expression in the neocortex peaks at P14, which overlaps with a local surge in development of synaptic pruning and wiring at that age[115]. The juvenile age is the start of sexual and aggressive behaviors that make up the majority of adult rodent behavior. In this age, oxytocin receptor

expression peaks in the ventromedial hypothalamus, which is the area causally associated with these adult social behaviors in mice[116].

3.3 Clinical studies associate oxytocin with improved brain development

The overlap between key developmental processes and the dynamic changes in oxytocin receptor expression suggest that oxytocin plays a role in brain development. However, the idea that oxytocin could be a potential neuroprotectant after brain injury comes from the clinic, specifically the neonatal intensive care unit (NICU), where preterm infants are hospitalized. Beyond medication and invasive procedures, daily caregiving that is provided in NICU has a positive impact on the development of the infants[82]. Clinical studies of non-pharmacological interventions like music therapy[117–120], Kangaroo Mother Care[121,121–126], skin-to-skin contact[127,128], and social environmental enrichment[129,130], show positive correlations with improved brain development in infants born preterm. The benefits are wide-ranging, from reduced pain and physiological response to stressors, to increased weight gain, and improved neural features such as increased brain volumes, organization of white matter, and altogether elevated neuro-behavioral functioning (**Table 1**). Strikingly, what these non-pharmacological interventions have in common is that they all induce natural elevations in oxytocin levels in the infant[131–137] (**Table 2**). This is thought to involve sensory and neuroendocrine mechanisms in the infant that stimulate the oxytocin system[135]. Concurrently, the stressful milieu that accompanies preterm birth and the NICU environment is associated with increased activation of the HPA axis and cortisol[105,138]. Cortisol can aggravate the young brain, and negatively impact brain developemt[139,140]. Oxytocin is a known natural counterpart to cortisol, that can reduce activity of the HPA axis[141]. In line with this, the oxytocin-associated clinical interventions are associated with reduced stress levels[124,126,132,142]. This suggests that oxytocin could be an important contributing factor to the observed neuroprotective effects in young infants.

Table 1: **Physiological effects and developmental outcomes of non-pharmacological clinical interventions associated with increased oxytocin levels in newborns**. Overview of existing literature.

Study	Patient population	Type of study	Type of intervention	Outcomes
Canadas et al., 2022a[122] *Int J Environ Res Public Health*	Preterm infants (n = 311)	Meta-analysis ; 12 studies included	Kangaroo Mother Care	Reduced physiological parameters of stress (respiratory rate)
Canadas et al., 2022b[123] *Int J Environ Res Public Health*	Preterm infants (n = 112)	Randomized controlled trial	Kangaroo Mother Care	Lower levels of cortisol, great weight gain and less need for supplementary nutrition, 12 days later
Zengin et al., 2023[124] *J Pediatr Nurs*	Preterm infants (n = 634)	Systematic review + meta-analysis ; 11 + 9 studies included	Kangaroo Mother Care	Reduced physiological parameters of stress (temperature and oxygen saturation) No effect on heart rate and respiratory rate
Charpak et al., 2022[125] *Acta Paediatr*	Adults who were born preterm (n = 178)	Randomized controlled trial	Kangaroo Mother Care	Improved volumes of total grey matter, basal nuclei and cerebellum Better organized white matter

				Regression analysis revealed a direct relation between duration of Kangaroo care and brain volumes
Nimbalkar et al., 2013[126] *Indian J Pediatr*	Preterm infants (n = 50)	Randomized controlled trial	Kangaroo Mother Care	Reduced pain response to heel sticks (less crying and smaller heart rate change)
Wang et al., 2021[121] *Breastfeed Med*	Preterm infants (n = 79)	Randomized controlled trial	Kangaroo Mother Care	Increased body weight and length at hospital discharge Improved neonatal behavioral neurological assessment scores at 40 weeks, 3 months and 6 months old
Arya et al., 2023[143] *EClinicalMedicine*	Neonates with low birth weight (n = 3136)	Randomized controlled trial	Kangaroo Mother Care	14%-24% decrease of sepsis (variable by birth weight) 37% decrease in sepsis-related mortality
Lillieskold et al., 2023[127] *JAMA Netw Open*	Very preterm infants (n= 71)	Randomized controlled trial	Skin-to-skin contact	Improved communicative and social skills with the mother at 4 month follow-up
Linner et al., 2022[128] *Acta Paediatr*	Very preterm infants (n = 91)	Randomized controlled trial	Skin-to-skin contact	Improved cardiorespiratory stabilization (heart rate, oxygen saturation and respiratory rate)
Loewy et al., 2013[117] *Pediatrics*	Preterm infants (n = 272)	Baseline-response trial	Music therapy	Reduced heart rate
Yue et al., 2021[118] *J Adv Nurs*	Preterm infants (n = 1093)	Meta analysis (13 studies)	Music therapy	Reduced respiratory rate Improved behavioral states
Ormston et al., 2022[119] *Brain Sci*	Neonates with brain injury (n = 3462)	Systematic review (11 studies)	Music therapy	Reduced pain scores during procedures and cardiorespiratory events Increased feeding rate and volume intake Larger amygdala volume
Yakobson et al., 2021[120] *Children (Basel)*	Preterm infants (n = 68)	Randomized controlled trial	Music therapy + skin-to-skin contact	Stabilization of autonomic nervous system: greater increase in high frequency heart rate variability
Yrjola et al., 2022[130] *Sci Transl Med*	Preterm infants (n = 109)	Randomized controlled trial	Family nurture intervention (= social environmental enrichment)	Improved connectivity of fronto-central cortical network
Welch et al, 2015[129] *J. Child Psychol. Psychiatry*	Preterm infants (n = 76)	Randomized controlled trial	Family nurture intervention (= social environmental enrichment)	Improved language and cognitive development Fewer attention problems

Table 2: **Effects of non-pharmacological clinical interventions used in newborns on natural oxytocin and cortisol levels**. Overview of existing literature.

Study	Patient population	Type of study	Type of intervention	Effect on oxytocin activity
Pavlyshyn et al., 2022[132] *Int J Dev Neurosc*	Preterm infants (n = 71)	Baseline-response trial	Skin-to-skin contact	Increase in urinary oxytocin levels
Vittner et al., 2018[134] *Biol Res Nurs*	Preterm infants (n = 28)	Randomized crossover study	Skin-to-skin contact	Increase in salivary oxytocin levels Reduced salivary cortisol levels
Seltzer, Ziegler & Pollak 2010[144] *Proc Biol Sci.*	Children aged 7-12 years (n = 61)	Randomized controlled study	Maternal speech	Increased urinary oxytocin release Reduced salivary cortisol levels 1h post-intervention
Ooishi et al., 2017[145] *PLoS One*	Adults (n = 26)	Baseline-response trial	Music exposure (slow tempo)	Increased salivary oxytocin concentration Increased heart rate variability Decreased heart rate

3.4 Oxytocin as anti-inflammatory agent

In addition to the general beneficial effects of oxytocin observed in the clinic, preclinical research has started exploring oxytocin as an anti-inflammatory agent. Brain injury models that are associated with neuroinflammation, like Alzheimer's disease or ischemic stroke, show general improvements after oxytocin treatment[146–149]. In these studies, oxytocin treatment reduces the neuroinflammatory response after injury[150], which is associated with improved neurocognitive recovery. Moreover, oxytocin is now being assessed with clinical trials as a treatment for autism spectrum disorder (ASD). This was initially based on oxytocin's pro-social functions to improve the social deficits of ASD[151], but the fact that microgliosis is also a hallmark of ASD[152,153], suggests that oxytocin's improvement of ASD symptomatology could be mediated by its effects on microglia. Cell culture studies further show that oxytocin can directly affect inflammatory microglia functioning in-vitro, demonstrating reduced secretion of cytokines IL-6, TNF-α, IL-1β, COX-2 and iNOS, and attenuation of cell proliferation[154,155]. This suggests that oxytocin could affect microglia in-vivo as well. However, the in-vivo expression of oxytocin receptors on microglia is debated. Single-cell sequencing assessments fail to consistently detect receptor expression[76,156,157]. The studies that do report oxytocin receptor expression, show that the expression is highly influenced by age (found in adults mostly[146,156]), experimental levels (demonstrated in-vitro mostly[154,155,158,159]), and experimental conditions (with contradicting reports of downregulated[156,158], upregulated[155], and unchanged[159] microglia oxytocin receptor expression during inflammation compared to basal conditions). The degree of oxytocin receptor expression in microglia in young mice – and thus the ability to directly influence microglia during neuroinflammation in newborn brain injury – remains to be clarified.

4. Gaps of knowledge

Despite the convincing evidence that oxytocin-associated clinical interventions contribute to improved neurodevelopmental outcomes in young children, the mechanisms underlying this effect remain largely

unknown. It is unclear how this effect happens, and which specific facets of brain development it affects. Some preclinical studies suggest that oxytocin is neuroprotective after brain injury[160–162]. However, these reports concern mostly assessment in adult rodents. The adult brain – including the adult *rodent* brain – is vitally different from the newborn brain. Important distinctive physiological characteristic of the developing brain include the immature developmental state of oligodendrocytes and myelination, of synaptogenesis, a higher oxygen consumption of cells, and increased cerebral blood flow[17]. Additionally, the state of the immune system and its microglial cells is vitally different. Research has already shown that age is an important determining factor for microglia functioning[76], including its neuroinflammatory response[163]. As such, the neurobiological workings of oxytocin in the injured *newborn* brain are largely unknown.

A specific challenge in the field of oxytocin research concerns the way of administration. Intravenous oxytocin injections are inefficient due to a short plasmic half-life (less than 2 minutes)[164] and proven difficulty to cross the blood brain barrier[165]. Many studies use intranasal administration, to increasing success[166–168], but this method can also have low efficacy in adequate distribution to target areas[169,170]. Importantly, these exogenous ways of treatment of oxytocin could have different workings from endogenous oxytocin[171]. This could be especially relevant in the developing brain, where exogenous oxytocin has shown to be less effective in protecting the fetal brain from hypoxia during childbirth, compared to endogenous oxytocin[171]. Previous work from our group demonstrated improved brain development when pups subjected to a double-hit model of intra-uterine growth restriction were treated with Carbetocin, a long-acting oxytocin receptor agonist[172]. However, agonists are also exogenous actors, and have their own challenges including uptake and receptor specificity[173]. The most optimal simulation of natural oxytocin elevations seen in the clinic is to similarly induce endogenous oxytocin elevations in the mouse. Preclinical modulation of endogenous oxytocin activity would not only optimally simulate the clinical interventions it wants to study, it concurrently would benefit from increased translational potential to the clinic, as a non-invasive, easy-to-implement therapy option. To optimize potential translation of findings to the clinic, oxytocin treatment should be investigated with high translational perspective.

5. Aim of this PhD

In this PhD project, we studied the neuroprotective potential of oxytocin in two mouse models of newborn brain injury: pediatric traumatic brain injury and Encephalopathy of Prematurity. We first developed the two injury models in the B6J mouse strain, after which we assessed the effects of oxytocin release on different levels of impaired brain development: white matter tracts, structural and functional brain connectivity, and behavior. Moreover, we assessed the effect of oxytocin on the neuroinflammatory response in the brain, specifically on microglia, by looking at microgliosis on a cell morphology and transcriptomic level. In doing so, we studied the separate contributions of microglia and astrocytes to the effect of oxytocin on neuroinflammation. In both disease models, oxytocin treatment was achieved by chemo-genetic activation of endogenous oxytocinergic neurons by use of the Cre-dependent DREADD construct in our transgenic mice, to ensure optimal simulation of clinical interventions in human neonates.

Chapter 2: Literary review

The role of oxytocin in abnormal brain development: effect on glial cells and neuroinflammation

Knoop M[1], Possovre ML[1], Jacquens A[2], Charlet A[3], Baud O[1,2,4,†], and Darbon P[3,†]. *Cells*. **2022**, *11*, 3899. doi: 10.3390/cells11233899. PMID: 36497156.

[1] Laboratory of Child Growth and Development, University of Geneva, 1205 Geneva, Switzerland
[2] Faculty of Medicine, Université Paris Cité, Inserm, NeuroDiderot, 75019 Paris, France
[3] Centre National de la Recherche Scientifique, Institute of Cellular and Integrative Neuroscience, University of Strasbourg, INCI UPR3212, 67000 Strasbourg, France
[4] Division of Neonatology and Pediatric Intensive Care, Children's University Hospital of Geneva, 1205 Geneva, Switzerland
[†] These authors contributed equally to this work.

Abstract: The neonatal period is critical for brain development and determinant for long-term brain trajectory. Yet, this time concurs with a sensitivity and risk for numerous brain injuries following perinatal complications such as preterm birth. Brain injury in premature infants leads to a complex amalgam of primary destructive diseases and secondary maturational and trophic disturbances and, as a consequence, to long-term neurocognitive and behavioral problems. Neuroinflammation is an important common factor in these complications, which contributes to the adverse effects on brain development. Mediating this inflammatory response forms a key therapeutic target in protecting the vulnerable developing brain when complications arise. The neuropeptide oxytocin (OT) plays an important role in the perinatal period, and its importance for lactation and social bonding in early life are well-recognized. Yet, novel functions of OT for the developing brain are increasingly emerging. In particular, OT seems able to modulate glial activity in neuroinflammatory states, but the exact mechanisms underlying this connection are largely unknown. The current review provides an overview of the oxytocinergic system and its early life development across rodent and human. Moreover, we cover the most up-to-date understanding of the role of OT in neonatal brain development and the potential neuroprotective effects it holds when adverse neural events arise in association with neuroinflammation. A detailed assessment of the underlying mechanisms between OT treatment and astrocyte and microglia reactivity is given, as well as a focus on the amygdala, a brain region of crucial importance for socio-emotional behavior, particularly in infants born preterm.

Full publication in Appendix A

My contributions as first author of this literary study include drafting the outline of the manuscript, searching and screening the literature, creating the figures and writing the manuscript.

Chapter 3: TBI study of acute neuro-inflammation

Oxytocin release modulates acute neuroinflammation and improves brain development after pediatric traumatic brain injury

Knoop M[1], Trak E[1], Possovre ML[1], Van de Looij Y[1,2], Schirmbeck G[1], Ceyzériat K[3], Pitetti JL[4], Sanches E[1], Musardo S[5], Millet P[6], Tsartsalis S[6], Tournier BB[6], Bellone C[5], Sizonenko S[1], Jacquens A[7,8,†], and Baud O[1,7,9,10,†]. bioRxiv 2025.06.02.652172; doi: https://doi.org/10.1101/2025.06.02.652172

[1] Laboratory of Child Growth and Development, University of Geneva, 1205 Geneva, Switzerland
[2] Center for Biomedical Imaging (CIBM), Animal Imaging Technology Section, Ecole Polytechnique Fédérale de Lausanne (EPFL), Lausanne, Switzerland
[3] Center for Biomedical Imaging (CIBM), University of Geneva, 1205 Geneva, Switzerland
[4] Laboratory animal facility, University of Geneva, 1205 Geneva, Switzerland
[5] Department of Basic Neuroscience, Faculty of Medicine, University of Geneva, 1205 Geneva, Switzerland
[6] Department of Psychiatry, University Hospital of Geneva and University of Geneva, 1205 Geneva, Switzerland
[7] Faculty of Medicine, Université Paris Cité, Inserm, NeuroDiderot, 75019 Paris, France
[8] Sorbonne University, GRC 29, AP-HP, DMU DREAM, Department of Anaesthesiology and Critical Care Medicine, Pitié-Salpêtrière Hospital, 75013 Paris, France
[9] Department of Neonatal Medicine of Port-Royal, Cochin Hospital, FHU Prem'IMPACT, AP-HP Centre - Université Paris Cité, 75014 Paris, France
[10] Epidemiology and Statistics Research Center/CRESS, Université Paris Cité, INSERM, INRAE, Paris, France
[†] These authors contributed equally to this work.

Abstract: Pediatric traumatic brain injury (TBI) is a leading cause of death and disability early in life in infants, and its neurodevelopmental consequences cannot currently be effectively treated. Since TBI is associated with neuroinflammation, modulation of the post-injury neuroinflammatory response is a promising strategy. Oxytocin is thought to have anti-inflammatory properties and appears to play a role in clinical interventions that improve brain development in neonates. However, the underlying mechanisms remain unclear, as does its applicability to acute brain injury. Here we investigate the effects of chemogenetic modulation of endogenous oxytocin on acute neuroinflammation and on long-term brain development after TBI in postnatal day 7 (P7) male mice. We show that oxytocin release attenuates the acute neuroinflammatory response to TBI 24 hours after injury, by reducing the expression of immune- and inflammation-related genes in astrocytes and promoting gene pathways for brain repair and development in microglia. In the long term, oxytocin exposure ameliorates subcortical and cortical white matter damage after TBI, prevents hyperactivity and loss of social behavior, and restores TBI-induced alterations in resting-state functional connectivity of the isocortex. These findings enhance our understanding of the modulation of neuroinflammation and its long-term effects and support intervention related to endogenous oxytocin release as a promising neuroprotective strategy in pediatric TBI.

Full study in Appendix B

My contributions as first author of this experimental study include optimizing the brain injury model, validating the chemogenetic DREADD tool, developing experimental paradigms, acquiring, analyzing and interpreting experimental data, creating the figures, and I wrote the manuscript.

Chapter 4: EoP study of systemic inflammation

Neonatal oxytocin release mitigates neuroinflammation and rescues neural correlates of encephalopathy of prematurity

Knoop M[1], Possovre ML[1], Trak E[1], Van de Looij Y[1,2], Sanches E[1], Tsartsalis S[3], Pansiot J[4], Schirmbeck G[1] and Baud O[1,4,5,6].

[1] Laboratory of Child Growth and Development, University of Geneva, 1205 Geneva, Switzerland
[2] Center for Biomedical Imaging (CIBM), Animal Imaging Technology Section, Ecole Polytechnique Fédérale de Lausanne (EPFL), Lausanne, Switzerland
[3] Department of Psychiatry, University Hospital of Geneva and University of Geneva, 1205 Geneva, Switzerland
[4] PROTECT, Inserm U1141, Université Paris Diderot, Paris, France
[5] Department of Neonatal Medicine of Port-Royal, Cochin Hospital, FHU Prem'IMPACT, AP-HP Centre - Université Paris Cité, 75014 Paris, France
[6] Epidemiology and Statistics Research Center/CRESS, Université Paris Cité, INSERM, INRAE, Paris, France

Abstract: Every year, 15 million babies are born preterm (< 37 weeks of gestation) which puts them at increased risk for encephalopathy of prematurity (EoP). EoP is characterized by neuroinflammation and microglial reactivity that can aggravate injury mechanisms. Effective therapies against inflammation in the preterm brain remain elusive. However, therapies such as Kangaroo care and music therapy have a positive impact in newborn brain development – yet the underlying mechanism is largely unknown. Here, we assess the neuroprotective effects of endogenous oxytocin modulation on the neural correlates of EoP. Using a well-established mouse model of systemic interleukin-1β to induce EoP, we show that neonatal chemogenetic activation of oxytocinergic neurons has anti-inflammatory effects on microglial gene expression, restoring brain development functions including axonal integrity and oligodendrocyte maturation. In the long-term, oxytocin release improved microstructural development of the corpus callosum and motor cortex, and rescued typical social behavior including ultrasound vocalization profiles. The neuroprotective effects of oxytocin were more prominent in females, showing enhanced reduction of microgliosis and improved rescue of social behavior compared to males. This study supports early clinical interventions and further explains how developmental care, that stimulate endogenous oxytocin release, can induce neuroprotective effect against brain injury associated with prematurity.

Full study in Appendix C

My contributions as first author of this experimental study include optimizing the injury model, developing experimental paradigms, acquiring, analyzing and interpreting experimental data, creating the figures, and I wrote the manuscript.

Chapter 5: Discussion

Our work demonstrates that oxytocin has neuroprotective effects on the neural correlates of brain injury associated with neuroinflammation induced either by traumatic brain injury (TBI) or Encephalopathy of Prematurity (EoP) in newborn mice. Chemogenetic activation of oxytocinergic neurons in the acute neuroinflammatory phase concomitantly or soon after the injury was found to be sufficient to improve multiple facets of brain development with effects lasting long after the treatment window ended, into adulthood. Compared to untreated controls, mice subjected to elevated oxytocin release after brain injury showed improved microstructure of white matter, restored functional connectivity of neural networks and rescued social and hyperactive behavior. These long-term effects were associated with changes to microglia phenotypes in the acute neuroinflammatory phase. Oxytocin reduced pro-inflammatory features of microglia cell density and morphology, and concurrently increased gene expression of microglia processes involved in brain development, including oligodendrocyte maturation. We also evidenced in vivo transcription of gene encoding for oxytocin receptors in microglia in young mice, suggesting that oxytocin has the ability to affect microglia directly in the developing mouse brain. We lastly assessed cross-talk between microglia and astrocytes, and found that oxytocin had distinct effects on microglia and astrocytes in neuroinflammation. Oxytocin mostly stimulated anti-inflammatory and brain development gene expression in microglia, and mostly reduced pro-inflammatory gene pathways in astrocytes, highlighting differential mechanisms of glia modulation in neuroinflammation-targeted therapy. Importantly, our work forms the first biological basis that explains the positive effects of early interventions and developmental care observed in brain-lesioned infants, and supports clinical interventions associated with endogenous oxytocin as a viable therapeutic target following neonatal brain insult.

1. Chemogenetic activation of oxytocinergic neurons reduces acute microgliosis in EoP and TBI

The vulnerable newborn brain is unprepared to optimally deal with damage or injury, as early-life microglia show much less transcriptional functions for immune processes compared to adult-age microglia[76]. This is problematic because the injury-induced immune response requires complex regulation, where the magnitude and duration of the inflammatory response have to be tailored to the severity and the nature of the injury[174]. If too low, reparative processes are insufficient. If set too high, inflammation-associated processes can induce collateral damage of healthy brain tissue[175]. In our models of EoP and TBI, we found a strong pro-inflammatory signature in microglia that was characterized by increased cell density, attainment of toxic amoeboid morphology, and increased transcriptomic signature of pro-inflammatory and immune functions including cytokine signaling, phagocytosis, response to lipopolysaccharide, glycolytic metabolic processes, and the production of TNF-a, IL-12, IL-8, IL-6 and type II interferon signaling molecules. Oxytocin had an overall anti-inflammatory effect on microglia. In both EoP and TBI, oxytocin reversed the increase in microglia cell density witnessed in response to injury, and morphological assessment in TBI showed that oxytocin also promotes ramified homeostatic-like cell shape. These findings are in line with existing studies on oxytocin or oxytocinergic analogs as anti-inflammatory molecules in brain injury. Previous work showed that oxytocin is protective against stroke in postpartum mice, showing decreased pro-inflammatory cytokines and decreased migration of blood leukocytes into the brain[176]. Similarly, intranasal oxytocin treatment improved recovery after intracerebral hemorrhage in adult mice[177]. But the current work extends these findings with strong data on chemogenetic activation of *endogenous* oxytocin, investigated for the first time in the injured

newborn brain. We performed detailed transcriptomic profiling of microglia, which revealed that oxytocin changes expression of many genes of inflammatory and immune pathways while restoring homeostatic support of brain development. One notable signaling mechanism that was upregulated by oxytocin after TBI was transcriptomic regulation of ERK1/ERK2 signaling, a known downstream target of the oxytocin receptor signaling pathway[178]. Previous studies similarly report ERK1/2 phosphorylation as a mechanism of anti-inflammatory effects of oxytocin on microglia in vitro[155]. Indeed, oxytocin was found to inhibit microglial reactivity by blockade of the ERK/p38 MAPK signaling pathway[179].

There were subtle differences in the effect of oxytocin on microglia functioning in EoP and TBI injury models. In EoP, oxytocin induced a strong reduction in pro-inflammatory and immune-associated gene expression in P3 microglia, which was more notable in females than in males (further discussed in section 5.5). In TBI, such a pro-inflammatory reversal was less evident, yet oxytocin still caused notable long-term improvements to brain recovery. This neuroprotective effect without affecting the pro-inflammatory phenotype as much in TBI could be explained by the different natures of the injury models. EoP is a subtle model where microglia reactivity is one of the causes of brain injury[9,34,63,180,181]. This is aided by the very immature state of immune system at P1-P5 (reviewed in Semple et al., 2013[182]), which explains how microglia reactivity can have such long-lasting impact on the brain in the EoP model. Excessive toxic microglial activity is not beneficial in EoP, which we saw reversed by oxytocin treatment. In TBI, microglia become reactive in response to external insult. TBI is a mechanical impact model of cell death that spreads to the white matter, and thus requires clearance of cell death, as well as demyelination and remyelination processes[53,62,183]. Pro-inflammatory microglial execution of phagocytosis and apoptosis are considered toxic processes in the absence of cell death. Yet in TBI, they are needed to facilitate regeneration and remyelination processes[184]. It was therefore interesting to see in the TBI model that oxytocin increased microglial anti-inflammatory functions (such as IL-10 expression) but also inflammatory processes in general, which could suggest that pro-inflammatory processes were sustained after treatment. Oxytocin also did not reduce $CD68^+$ phagocytic activity of microglia at the injury site and surrounding white matter – which was full of cleaved-caspase-3^+ cell death and thus required phagocytosis of dead cell debris (see Annex D). Rather, oxytocin improved additional microglia-functions after TBI such as cerebrovascular healing and nervous system development. This suggests that oxytocin increased anti-inflammatory microglial processes while not affecting much the pro-inflammatory processes. Potentially because the phagocytic processes associated with pro-inflammatory activity are still therapeutic at the acute timepoint we assessed (24h post-injury). Oxytocin did reduce microglia cell density after TBI, which suggests that the pro-inflammatory processes still would be kept in line to not become excessive. In line with this, oxytocin treatment after hypoxia in P5 pups showed to reduce excessive apoptosis through reduction of mitochondrial dysfunction[185]. It would be interesting to see the effect of oxytocin on microglia functioning at later stages of recovery. A previous study of brain injury timeline with regard to pro- versus anti-inflammatory microglia activity showed that the acute phase (3 days post injury; dpi) is more characterized by $iNOS^+$ pro-inflammatory activity, which shifted to an $Arg1^+$ anti-inflammatory predominance at 10 dpi that stayed 21 dpi[186]. This shift has been attributed to a demyelination to remyelination phase[184]. Our data suggest that oxytocin accelerates this shift after TBI, by stimulating anti-inflammatory functions. A previous study induced a shift from pro- to anti-inflammatory microglia by inhibition of NOX2 in the 3 first days after injury, which improved neuronal death 7 days later[187]. A practical distinction in neuroinflammation modulation research is whether to increase anti-inflammatory functions, or decrease pro-inflammatory microglial functions. Our studies suggest that oxytocin does both, and that its effects are tweaked to the nature of the injury and the needs of the brain milieu. It would be interesting for future research to go further into the respective importance of oxytocin's effect on pro-inflammatory versus anti-inflammatory microglia activity, knowledge that is likely useful for

other inflammation-disease models as well[64,188,189]. This could be explored with protocols where pro-inflammatory and anti-inflammatory microglia phenotypes are respectively depleted during oxytocin treatment after injury. This would be possible with the use of gadolinium chloride (anti pro-inflammatory microglia) and mannosylated clodronate liposomes (anti anti-inflammatory microglia)[63,186].

Another factor that likely influences the subtle differences we found between the two injury models is the difference in age and development stage of microglia at assessment (P3 in EoP *versus* P8 in TBI). Although some microglial states are present across development, some sub-clusters are more transitional, especially in the developing brain[76]. This heterogenous population of early-life microglia coincides with the distinct timeline of specific developmental processes in the brain[190]. As such, the timing of injury highly determines the precise effects on the brain[190]. The fetal brain shows different responses in cytokine expression after immune challenge in middle versus late gestation[191], associated with distinct long-term neuro-behavioral outcomes as well. Similarly, a previous study showed that the P1-P5 IL-1β model of EoP does not produce the same outcomes in pups injected with IL-1β between P6-P10[180]. Single cell RNA sequencing studies of early-life microglia help reveal the timeline of microglia development. Microglia from healthy P3, P6 and P9 mouse brains shows similar expression of microglial genes involved in transient development patterns[190]. However, in line with different phases of immune system development[182], early-life microglia show distinct inflammatory profiles in response to brain injury. Similarly, single cell RNA sequencing of the P1-P5 IL-1β model in OF1 mice showed a different inflammatory response to IL-1β injections in microglia from P3 compared to P5 brains, including altered gene expression of microglial pathways involved in the inflammatory response, TNF-α signaling and glycolysis[192]. Moreover, the P7 brain is characterized by a specific sub-cluster of microglia that has elevated phagocytic and proliferative activity, that resides almost exclusively in the developing corpus callosum and cerebellar white matter[77]. This overlaps with the peak of microglial engulfment of developing oligodendrocyte progenitor cells (OPCs) in the corpus callosum, also happening at P7[193]. This sub-cluster of $Spp1^{+}$ phagocytic microglia were also found in the developing corpus callosum in P4/P5 mice (termed axon-tract microglia; ATMs)[76], but the number of cells and engulfment of OPCs is significantly higher at P7 compared to P4[193]. This highlights important temporal differences between microglia of the EoP and TBI model influenced by the timepoint of their transcriptomic assessment at P3 and P8, respectively. This could have also influenced the respective effects of oxytocin on their functioning. For example, an increased phagocytic predisposition of microglia near the corpus callosum at time of injury and treatment in our TBI model could be more difficult to dampen with treatment. Indeed, oxytocin release after TBI showed more moderate anti-inflammatory effects on microglia in the corpus callosum compared to the cortex (concerning cell density and amoeboid shape), as well as more moderate protective effects on white matter damage compared to cortical damage at adult age.

In summary, oxytocin showed largely similar effects on microglia from EoP and TBI where it reversed the increases in microglia density and it promoted gene expression of anti-inflammatory, brain development and repair functions. Yet the effect of oxytocin on pro-inflammatory microglia gene expression was relatively dependent on the specific injury mechanism in EoP and TBI, and could be further mediated by the different developmental phase at time of injury between the two models.

2. Oligodendrocyte development as mediator between acute microglia functioning and long-term myelination improvement after chemogenetic oxytocin release

White matter damage is a prominent hallmark of EoP[85,194] and TBI[20,195], that is predictive of impaired cognitive functioning throughout a child's life[196,197]. Using diffusion tensor-MRI imaging and micro-scale analysis of MBP immunoreactivity, we found that mice exposed to oxytocin release had improved white matter microstructure after injury, including increased corpus callosum thickness, lower radial diffusivity and lower fractional anisotropy, and reduced neurite orientation dispersion, of corpus callosum sub-regions. That raises the question: How does increased oxytocin in the neonatal phase lead to improved white matter microstructure in adult age? Our data strongly suggest a mediating effect on developing oligodendrocytes (OLs). Myelinating OLs develop from neuroepithelial OL progenitor cells (OPCs; also known as oligodendrocyte *precursor* cells) that come from the ventral and dorsal ventricular zones. OPCs highly proliferate in the first neonatal week in mice, reaching their peak density around P7[198]. Their development into eventual mature myelinating cells is highly intertwined with activity of microglia cells: OPCs express a myriad of receptors for cytokines and chemokines excreted by microglia. In this, they respond to trophic factors released by microglia, for which the OPCs – generated in excess – compete[184]. Additionally, there is a subpopulation of amoeboid microglia ($Cd11c^+$) located around the developing corpus callosum that is in high contact with viable progenitor OLs, performing necessary pruning of excess cells as a homeostatic mechanism for proper myelin formation[193]. This population of OPC-pruning microglia peaks in density around P7[193]. Interestingly, under-pruning of OPCs by microglia is as detrimental for efficient myelin development as over-pruning: it causes excessive OPC to axon ratios, which ultimately leads to thinner myelin[193]. Due to their overlap with a critical window for oligodendrocyte development[182], preclinical models of P1-P7 perinatal brain injury strongly suggest an arrest/hamper in OL development due to reactive microglia and neuroinflammation. Indeed, previous studies of the P1-P5 EoP model showed elevated ratio of OPCs ($PDGFRa^+$) compared to mature OLs ($O4^+$) in male mice[180]. Similar effects of this model were found in the cerebellum, in addition to reduced local proliferation of OPCs[181]. This was associated with reduced MBP immunoreactivity at later age[63]. A study using a double-hit model of fetal inflammation and P4 hypoxia in rats similarly demonstrated reduced MBP production at P18 and P30, associated with a decrease in differentiating OLs ($CNPase^+$)[199]. In these studies of EoP, OL survival remained largely unaffected[63,180,181] – which is also seen post-mortem in preterm infants with periventricular leukomalacia (a severe form of EoP) who show myelination issues despite an available pool of OPCs[200]. This in contrast with preclinical pediatric TBI injury, which induces acute OPC ($PDGFRa^+$) cell death after the impact[35]. We similarly found an increase in cleaved caspase-3^+ apoptosis immunodensity in the corpus callosum 24h after TBI – strongly suggesting death of local developing OPCs which are known to accumulate in the CC around this age (P8)[193]. Demyelination/remyelination is likely more a characteristic of pediatric TBI than EoP, suggesting that there are 2 pathways impacting oligodendrocyte development in TBI: death of viable OPCs due to the consequences of primary injury, and, a hamper in OPC development due to toxic processes of reactive microglia as part of the post-injury inflammatory response. In line with this, the OPC cell death in pediatric TBI is associated with impaired development of mature OLs ($O4^+$) at later age[35]. Notably, previous studies show that the EoP model was not associated with myelin changes when injected in P6-P10 pups (compared to P1-P5)[180] – suggesting that OL development is too advanced at P6 to be affected by the more mild nature of neuroinflammation induced by systemic IL-1β injections.

Our research supports that oxytocin promotes an overall anti-inflammation-phenotypic shift in reactive microglia induced by TBI and IL-1β injury. Previous research demonstrated that a pro-($iNOS^+$) to anti-inflammatory($Arg\text{-}1^+$) shift enhances remyelination after injury – and blocking of the $Arg\text{-}1^+$ phenotype inhibits OL differentiation[186]. Moreover, the presence of specifically pro-inflammatory ($COX2^+$) microglia was required to induce MBP deficiencies in a model of EoP[63]. In addition to this general transcriptomic shift, oxytocin promoted expression of specific microglial genes involved in myelination

and axon development in pups subjected to TBI and EoP. Oxytocin upregulated Endothelin-1 expression in microglia from female IL-1β pups. This signaling molecule is associated with OL differentiation and myelin development, and stimulation of Endothelin-1 signaling promotes OL maturation in a mouse model of perinatal white matter injury[201]. Oxytocin also increased expression of microglial Matn2 in female Il-1β pups, which is involved in remyelination after brain injury[202]. In both males and females, oxytocin promoted gene expression of Semaphorin genes in microglia from IL-1β pups, which is a protein family that stimulates axon and OPC guidance via chemo-attraction and chemo-repulsion processes[203]. In IL-1β females, oxytocin increased expression of Sema3f, which is known to induce OPC migration after myelin injury[204]. In microglia from TBI pups, oxytocin promoted gene expression of Cdon. Cdon is associated with OL maturation and myelination, and overexpression of this cell-surface protein increases myelin protein expression by oligodendrocytes in vitro[205]. Oxytocin increased expression of Axl after TBI, a gene that is important for maintaining axonal integrity and remyelination after injury: depletion of this gene causes increased OL apoptosis, reduced myelination and enhanced axonal damage after white matter injury in juvenile mice[206,207]. Finally, oxytocin modulated Wnt signaling in microglia. Downregulation of the microglial canonical Wnt/β-catenin pathway has been previously identified as key contributor to hypomyelination in a mouse model of EoP[63]. Agonistic activation of Wnt signaling prevented the white matter damage induced by EoP. Our data shows that oxytocin increases Wnt signaling in P3 microglia subjected to IL-1β. Oxytocin increased expression of Wnt pathway members Wif1 in females, Wnt9a and Wnt4 in males, and Fzd6 in both sexes, which is a gene whose depletion was functionally linked to the effects of microgliosis on hypomyelination in previous research[63].

This transcriptomic shift in microglia caused by chemogenetic oxytocin modulation thus strongly indicates improved OL development after injury, an assumption that is supported by a previous study showing restored mature OL numbers (APC^+) after oxytocin agonist administration to neonatal rats exposed to a double-hit model of perinatal brain damage[172]. Moreover, preclinical studies using environmental enrichment (EE) therapy after hypoxia show similar results. Forbes and colleagues[208] subjected neonatal rats to EE therapy after chronic hypoxia between P3-P11. Compared to untreated hypoxic rats, EE increased oligodendrogenesis, OL maturation, and specifically proliferation, it improved the production of myelin proteins MAG and MBP, increased the proportion of myelinated axons, and increased myelin thickness. Interestingly, they performed RNA sequencing on sorted OPCs and OLs from the corpus callosum, which generated a transcriptomic profile of the effect of EE: EE restored expression of genes involved in axon-OPC synapse formation that were depleted by the hypoxia. These genes were enriched for functions involving synapse formation, membrane formation, process extension, cell movement and dendritic growth – crucial processes for OPC functioning[209]. The authors found that the effect of EE on OPCs was transient over time, affecting different maturation processes for the different timepoints after injury (OPCs rebound from hypoxia by increasing maturation programs that are not seen in control OPCs). Although oxytocin levels were not directly measured in the study by Forbes and colleagues, previous studies strongly support that EE increases oxytocin expression: EE elevates oxytocin plasma levels[210,211], increases the density of oxytocin immunoreactivity in the PVN and SON[212], and shows comparable promoting effects on wound healing as oxytocin administration[213]. Collectively, these data suggest that the effects of EE found on oligodendrocyte development could be strongly and causally associated with increased oxytocinergic signaling. This is further emphasized by preclinical reports where the EE-induced increase in neuronal plasticity (via BDNF expression in the medial prefrontal cortex), was obliterated by blockade of oxytocin receptor functioning[211].

In summary, the long-term improvements to white matter and myelin structure we found in TBI and EoP mice after oxytocin release, is plausibly associated with improved oligodendrocyte and axon development through altered microglia gene expression (**Figure 4**).

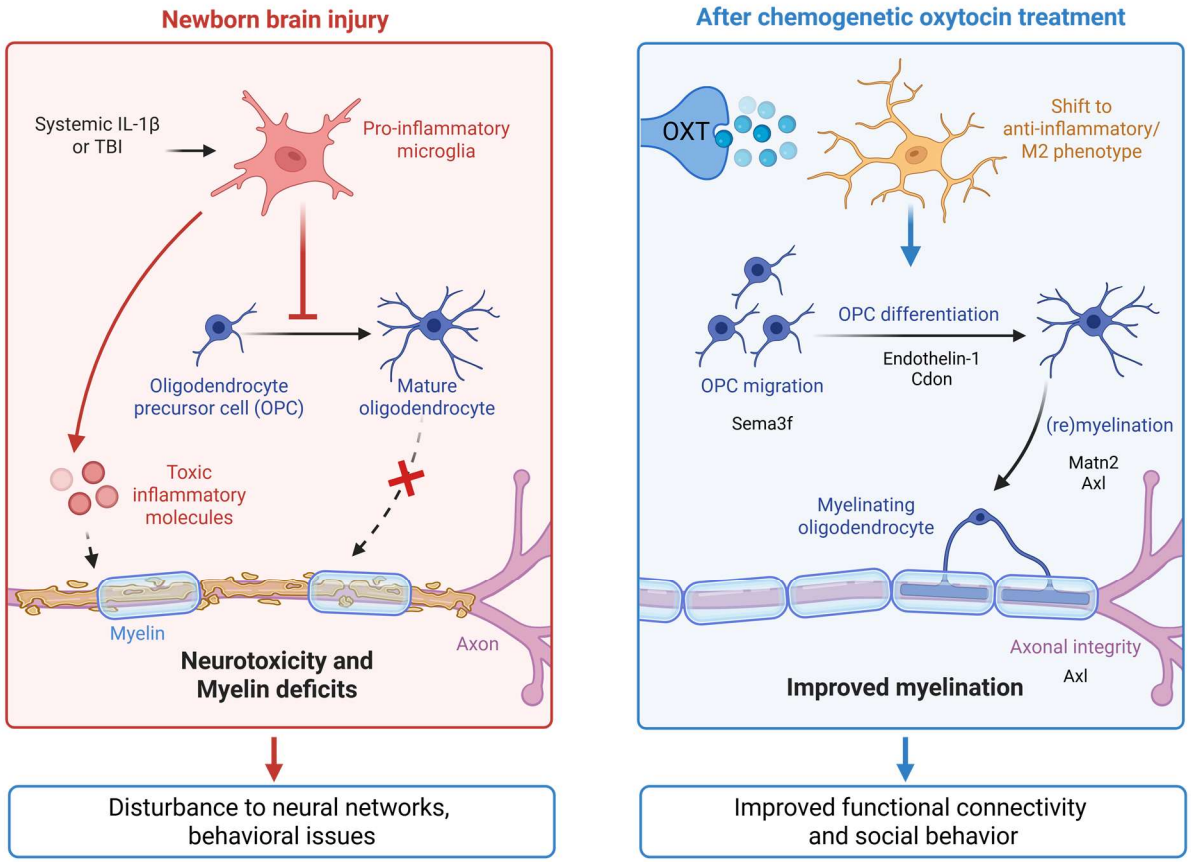

Figure 4: Transcriptomic effects of oxytocin on microglia that are associated with oligodendrocyte maturation. Left panel: in EoP (systemic IL-1β) and TBI, microglia become pro-inflammatory in response to injury and block the differentiation of OPCs into myelinating OLs. They also secrete damage-associated molecules that are toxic for neurons. Right panel: Summary of findings from our studies, showing the specific oligodendrocyte-associated genes in microglia that were upregulated after chemogenetic activation of oxytocinergic neurons, and their function in OL development. Created with Biorender.com

3. Intercellular signaling mechanism between oxytocin and microglia: implicating astrocytes?

An outstanding question is how oxytocin reaches microglia. Based on existing literature, there are several possible intercellular signaling pathways. To help answer this question, we wanted to assess if young mice demonstrate oxytocin receptor expression on microglia – something that was not shown yet consistently by previous RNA sequencing studies (reviewed in Knoop et al., 2022[112]). It is important to confirm oxytocin receptor expression in young mice because of the transient expression pattern throughout development[214–216]. Oxytocin receptor mapping is complicated by the lack of specific anti-OXTR antibodies[168], and the fact that RNA sequencing analyses are not sensitive to lowly expressed genes. Using RNA scope, an in-situ hybridization technique, we were able to consistently identify oxytocin receptor expression on microglia in the cortex and corpus callosum of brain slices from P5 mice. Thus, we found evidence – for the first time – that young mice express microglia oxytocin

receptors in vivo (in line with reports in vitro and in adult mice[155,158]), which suggests that oxytocin *can* influence microglia directly via receptor-ligand activation (**Figure 5**, pathway 1). We found a notably higher degree of oxytocin receptor mRNA expression in cortical microglia compared to white matter microglia, which could suggest that cortical microglia respond better to oxytocin treatment. This aligns with the more moderate long-term effects we found of oxytocin on subcortical white matter microstructure, compared to cortical myelination and functional connectivity. This difference is potentially associated with the unequal distribution of axonal projections of hypothalamic oxytocin neurons in the brain, showing higher innervation of gray matter rather than white matter regions[217]. Such a spatial heterogeneity in microglial oxytocin responsiveness will be important to explore in future studies.

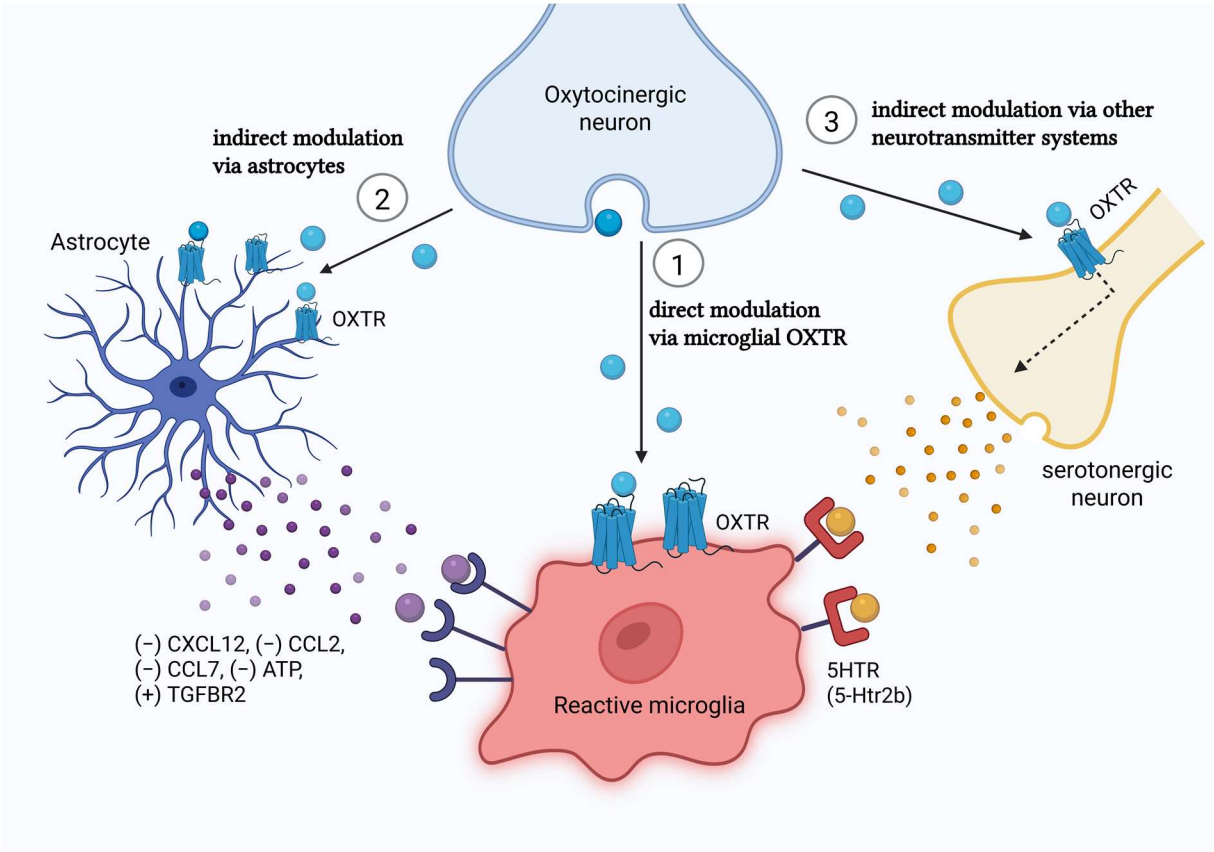

Figure 5: Possible intercellular signaling pathways between oxytocin and microglial cells in neuroinflammation. (1) Oxytocin can influence microglia directly through oxytocin receptor expression on microglia. (2) Oxytocin can influence microglia through astrocytes. It can bind to oxytocin receptors on astrocytes, and reduce the reactivity of microglial cells indirectly by decreasing ("–") secretion of chemokines such as CXCL12, CCL2, CCL7 and ATP from astrocytes, as well as increasing ("+") activation of microglial TGFB2 receptor. (3) A third possible pathway of effect involves additional neurotransmitter systems such as serotonin (5-HT). Oxytocin can induce serotonin release through activation of oxytocin receptors on serotonergic neurons. Serotonin can bind to microglia via microglial 5-HTR (5-Htr2b) expression and reduce pro-inflammatory cytokine expression. OXTR = oxytocin receptor. Adapted from Knoop et al., 2022.

Another possibility is that oxytocin alters microglia through astrocytes (**Figure 5**, pathway 2). We demonstrated oxytocin receptor mRNA expression on P5 astrocytes, which is in line with widely accepted concept that astrocytes can be influenced by oxytocin via oxytocin receptors in vitro and in

vivo. Oxytocin receptor expression on astrocytes is found in all major brain regions – hypothalamus, hippocampus, frontal cortex, ventral striatum and amygdala (reviewed in Baudon et al., 2022[218]). Moreover, oxytocinergic signaling in astrocytes has been functionally validated in vivo, for example in modulating anxiolytic effects in the amygdala[100,219].

There is strong microglia-astrocyte crosstalk in homeostasis and neuroinflammation, where astrocytes and microglia can bi-directionally enhance and reduce each other's inflammatory functioning[45,66]. For example, astrocytic IL-3 induces pro-inflammatory responses from microglia in the pathology of MS[220]. But astrocytes can also attenuate microglia reactivity: astrocytic production of Orm2 reduces microglia reactivity in response to LPS in vitro[221], and TGF-β produced by astrocytes decreases pro-inflammatory cytokine expression by microglia[45]. Moreover, astrocytes can reduce microglia reactivity through the Sema4B/Plexin-B2 pathway[222]. Although the body of work on oxytocin's effect on astrocytes is much smaller compared to microglia, studies do suggest that oxytocin administration promotes anti-inflammatory properties in astrocytes. In adult rats, oxytocin decreased GFAP immunoreactivity in the SON, suggesting anti-inflammatory effects on astrocyte activity[223]. This is in line with reports showing that oxytocin inhibits astrocytic NLRP3 inflammasome activation[224]. Additionally, oxytocin application in vitro makes astrocytes retract their processes from the synapse, which could link to reduced neurotoxic effects on neurons by reactive astrocytes in inflammatory settings[218]. The fact that oxytocin induces anti-inflammatory responses in astrocytes, combined with the fact that anti-inflammatory astrocytes induce anti-inflammatory effects in microglia through cross-talk, suggests that the effects we found of oxytocin on microglia *could* be mediated through astrocytes.

The intricate microglia-astrocyte crosstalk raises the question which glia type is more affected by oxytocin, and thus more responsible for the improvements to brain development we witnessed. We aimed to assess this in the TBI study, where we performed RNA sequencing on both microglia and astrocytes 24h post-TBI. In astrocytes, we found a notable reduction in pro-inflammatory gene expression 24h post-injury, which is shown to prevent neurotoxicity after injury in vitro[46]. In microglia, oxytocin did not change the pro-inflammatory profile as much after TBI, but rather induced a clear promotion of brain-development functions – in line with previous studies[225]. Both effects likely contribute to improved neuroprotection after oxytocin, but its effects on microglia gene expression show a more direct association with improved brain outcomes. It will be interesting to further explore the individual contribution of microglia versus astrocytes to oxytocin-induced changes in neuroinflammation. A trans-well cell culture setup would be ideal to separately pre-treat microglia and astrocytes with oxytocin in monoculture, before combining the two cell types in co-culture and subject them to inflammatory challenge such as IL-1β mixed with IFN-γ[172]. Similarly, their respective contributions to oxytocin-induced improved brain development could be assessed *in vivo* with selective knockout of astrocytes and microglia using Adeno-associated viral vectors with GFAP- and CX3CR1 promotors, respectively, during the oxytocin treatment window and compare the recovery of the brain injury.

Another factor that likely underlies the different effect of oxytocin on microglia and astrocytes that we found after TBI is timeline after injury. The number of differentially expressed genes induced by oxytocin in the acute post-TBI phase was 5 times higher in microglia compared to astrocytes. This suggests that oxytocin possibly had a larger effect on microglia compared to astrocytes 24h post-injury. As first responders, microglia generally react faster to newborn brain injury than astrocytes, who react later[226]. In line with the different temporal profiles of the two glia types after injury[35,227,228], it is plausible that oxytocin's effect on astrocytes and microglia could be different for more subacute phases after injury. For example, IL-1 receptor agonism in the acute phase after TBI reduced astrocyte proliferation

2 weeks later, but did not affect microglia at that subacute timepoint[229]. It will be interesting to assess with transcriptomic profiling oxytocin's effect on the two glia cell types at later post-injury stages.

A final option in the mechanism of effect between oxytocin and microglia implicates other neurotransmitter systems (**Figure 5**, pathway 3). In addition to the oxytocin receptor expression we found, microglia express a myriad of other neurotransmitter receptors, including glutamate, GABA, norepinephrine, cannabinoid, acetylcholine and serotonin[230]. These neurotransmitters are able to influence microglia functioning, including its phagocytic activity, and the expression of chemokines and cytokines (TNF-α and interleukins) and free radicals[230]. One notable possibility pertains the serotonin system. Microglia express 5-Hrt2b serotonin receptors, and knockout of these receptors increases the neuroinflammatory response to LPS[231]. Interestingly, oxytocin is known to interact with the serotonin system: serotonergic neurons express oxytocin receptors, and activation of these receptors by oxytocin strengthens serotonin axon length[232,233] and induces serotonin release (which caused anxiolytic effects in the raphe nuclei)[234]. This underlines that oxytocin can induce serotonin release, which could be a third pathway of effect between oxytocin and microglia. Future mechanistic assessments will reveal which pathway is most responsible for relaying oxytocin's therapeutic effects on microglia after newborn brain injury.

4. General positive effects of oxytocin on newborn brain development

The neural oxytocin system is vast and wide-spread. It has axonal projections to and receptor expression in virtually all major brain regions, including the limbic system, olfactory system, basal ganglia, cortical areas, and the hippocampus[100,235]. Stimulation of those connections is known to contribute to transient brain developmental processes[113,215,236]. It is therefore quite likely that the neuroprotective effects we found for chemogenetic activation of oxytocinergic neurons after injury are modulated by *overall* stimulating effects of oxytocin signaling for brain development. A specific example of this is the rescue of USV in the EoP study, as oxytocin receptors are widely expressed in regions that have been identified as key regulators for USV emission with whole-brain mapping of c-Fos expression (such as amygdala and hypothalamus)[237]. Neonatal oxytocin has many long-term effects on behavior, which is associated to structural and functional modifications to neural circuitry (reviewed in Miller & Caldwell, 2015[238]). Indeed, oxytocin contributes to neurite growth and formation of neural circuits[96], especially in experience-dependent cortical development[239]. Manipulating the oxytocin system in early development can influence the trajectory of the brain and change neural chemistry, circuitry and behavior[240]. It is therefore possible that the non-inflammation effects of oxytocin on brain development were different in the EoP and TBI models. In the EoP study, we increased oxytocinergic activity in the P1-P5 mouse brain. In the TBI study, oxytocin was increased between P7-P10. These ages in mice are characterized by different developmental milestones (**Table 3**) and different temporal windows of transient oxytocin receptor expression in developing brain regions (see Knoop et al., 2022 Figure 1). Moreover, P7 mice have more oxytocin cells in hypothalamic areas compared to P1 mice[241], suggesting a potentially increased oxytocin release induced by DREADD activation in mice of the TBI study compared to the EoP study. In summary, these differences could contribute to distinct effects of oxytocin on brain development, dependent on age of modulation.

Table 3: Key developmental milestones taking place in the respective oxytocin treatment windows of the EoP study (P1-P5) and the TBI study (P7-P10). Repeated chemogenetic activation of oxytocinergic neurons could have distinct general effects on brain development as a result of the different ages in mice of these models. Reproduced from Semple et al., 2017

Human	Rodent	Developmental milestones	References
23-32 wk gestation (preterm infant)	P1-P3	Oligodendrocyte maturation state changes – predominance of mitotically active pre-OLs	Craig et al. (2003), Lodygensky et al. (2010), Dean et al. (2011a,b)
		Immune system development	Holsapple et al. (2003)
		Establishment of the blood-brain barrier	Engelhardt (2003), Daneman et al. (2010)
36-40 wk gestation (term infant)	P7-P10	Peak brain growth spurt	Dobbing and Sands (1979), Bockhorst et al. (2008)
		Peak in gliogenesis	Catalani et al. (2002), Kriegstein and Alvarez-Buylla (2009)
		Increasing axonal and dendritic density	Cowan (1979), Bockhorst et al. (2008), Baloch et al. (2009)
		Oligodendrocyte maturation state changes – switch to a predominance of immature OLs	Craig et al. (2003), Dean et al. (2011a,b)
		Consolidation of the immune system	Holsapple et al. (2003)

We found that oxytocin specifically has general positive effect on brain development via microglia functioning. With RNA sequencing of P3 microglia from pups injected with DREADD-activating CNO *versus* controls, we found that oxytocin release has a general positive effect on brain development by increasing expression of gene pathways in microglia involved in many aspects of brain development (including axons, synapse, neurons, genesis, migration, differentiation). So even in a non-inflammatory milieu, microglia could be the connecting factor in the general improving effects of oxytocin on child development. This is in line with increasing reports that oxytocin is a notable positive modulator of the immune system. In homeostatic conditions, studies show that oxytocin controls bone marrow and thymus activity, and that it modulates activity of the hypothalamic-pituitary-immune axes and the autonomic nervous sustem[242]. This likely contributes to improved healing after brain injury. One notable observation was that oxytocin did not affect long-term (social) behavior in healthy mice in our control experiments, while it did improve behavior in IL-1β subjected mice. Forbes and colleagues report a similar observation, where neuroprotective effects of (oxytocin-associated) EE were not as evident in control mice compared to hypoxic mice. They argue that the injury selectively opens a window of developmental plasticity, where treatment such as EE enhances endogenous repair and restored behavioral function[208]. This is in line with reports from a separate EE study as well[243], and with a study that reports oxytocin-induced changes to stress-hormone levels of the HPA axis, but only in stressful situations, not in healthy situations[244]. A similar mechanism could be at play in the adult behavioral experiments of our studies.

5. Sexual dimorphism in the protective effects of oxytocin on perinatal brain injury

In the EoP study, we explored sex-specific effects of oxytocin and found that males and females had notably different therapeutic responses to increased oxytocinergic release: females showed more anti-inflammatory effects on P3 microgliosis, and more long-term improvements to social behavior than males. Sex differences in the early-life oxytocin system in mice potentially influenced these sex-specific effects. Females express Oxt mRNA earlier in development – at E16.5 versus P2 for males – and the amount of Oxt and Oxt receptor mRNA expressed just before birth and in the first postnatal days is higher in females than males[245]. Similar effects of sex were found for Oxt receptor density and Oxt receptor signaling in juvenile rats[246]. Given the widespread expression of oxytocin receptors throughout

the brain, sex-differences in the innate oxytocin system likely underlie additional, non-inflammation, effects of oxytocin on brain development. This is in line with a study of social and physical EE in healthy rats, that demonstrated increased benefits of the treatment in females[211]. Studies further show that neonatal manipulation of oxytocin levels can change rodent brain development. In mandarin voles, oxytocin administration at P0 changed partner preference in the adult age, which was accompanied by changes to oxytocin c-FOS activity in neural regions associated with social behavior[247]. Interestingly, this effect on mating was also sex-dependent: embryonic disruption of oxytocin receptor signaling affected adult social behavior in males but not females[240]. These reports emphasize the sex-differences in early-life oxytocin signaling, and in the consequences of neonatal manipulation. They are in line with our sex-specific findings, where females showed more long-term social improvements to the CNO-induced oxytocin treatment than males in EoP.

The observation that oxytocin mRNA is only found later in postnatal development specifically in *male* mice could also explain the different magnitude of oxytocin's neuroprotective effects that were observed in the TBI model versus the EoP model in males. In the TBI study, which included only males, chemogenetic activation of oxytocin neurons between P7 and P10 induced robust positive effects on microgliosis and brain outcome after P7 injury, effects that were far less prominent in EoP males treated with P1-P5 activation of oxytocinergic neurons. The report that male mice potentially do not express oxytocin mRNA until P2[245], and that the number of oxytocinergic neurons increases with development[233,248] could explain how oxytocin was more effective in males in the TBI study compared to the EoP study.

It will be important for future research to map the sex-specific, and age-specific, differences in oxytocin responsiveness, to enhance the mechanistic understanding of oxytocin's effect on brain injury, and to optimize individualized care based on inter-individual differences in oxytocin signaling (as is proving effective in clinical trials of ASD[249]).

6. Effects of repeated chemogenetic oxytocin stimulation on the endogenous oxytocin system

An outstanding question is whether CNO-induced activation of oxytocin neurons had a sustained effect on the activity of the oxytocin system after cessation of the treatment. This is important because it gives evidence on if acute modulation was sufficient for the long-term effects, or if oxytocin had sustained effects. Many studies agree that the immediate phase after injury is the most optimal window for treatment[16,208]. This supports that oxytocin upregulation *could* be strong enough to exert long-lasting positive effects on the brain, which was demonstrated in a model of ASD where early oxytocin treatment showed to re-shape long-term brain circuitry[250]. However, it is plausible that repeated activation of oxytocinergic neurons in the neonatal period affects the development of the oxytocin system, as early exposure to hormones is known to longitudinally alter the responsiveness of a hormone receptor (a concept known as *hormonal imprinting*[251,252]). Previous work shows that repeated intranasal oxytocin exposure in children with ASD induced elevated salivary oxytocin levels 24 hours later. Although these elevations returned to baseline 4 weeks later, reductions in oxytocin receptor DNA methylation were still observed, suggesting sustained epigenetic changes to the reception of oxytocin[253]. Preclinically, oxytocin treatment to Magel2-kock-out mouse pups (a genetic model of ASD and Prader-Wili syndrome) during the first week of life normalized the activity of the oxytocin system at adulthood[254]. Similarly, oxytocin administration to 1-day old female mice increased oxytocin immunoreactivity in the PVN 20 days later[248]. However, no changes were found after oxytocin administration to P1 males. Congruently, other studies report that the long-lasting effects of hormonal imprinting are subject to type of treatment, age, sex and species[238].

An important observation to make is that these studies all used exogenous oxytocin application. When scanning the preclinical DREADD landscape, very few studies report long-lasting effects of DREADD activation on endogenous neuronal activity. The electrophysiological response seems to peak 45-50 minutes after injection[255]. Yet some studies report that CNO enhances neuronal activity for many hours[256]. One thing to consider specifically with the use of DREADD to stimulate neurons is potential receptor desensitization and downregulation after prolonged activation. Multiple studies report desensitization-like effects after prolonged activation of DREADDs, yet these studies predominantly use inhibitory Gi DREADDs. The Hm3Dq *Gq* DREADD is less prone to desensitization compared to the inhibitory *Gi* DREADD, because of its high expression[256]. We confirmed this in our oxytocin-Hm3Dq mouse line, showing 80% DREADD expression on oxytocin neurons in the PVN. Some studies do report Hm3Dq DREADD receptor desensitization, and a reduction in endogenous neuronal activity, yet this was found after chronic activation for 11 days[257], and 16 days[258], respectively. The 4 and 5 days of chemogenetic oxytocin activation in our respective TBI and EoP treatment models, is likely less prone to this effect. It will be interesting for future studies to track the activity of oxytocin neurons after the CNO treatment window, to determine when and which developmental mechanisms it is influencing.

7. Strengths and limitations

This work has several strengths and limitations. The main strength concerns the translational value of study methodology. Translation of preclinical therapeutic success to the clinic is a known problem in biomedical research. This "valley of death" between bench and bedside is aided by suboptimal methodology where rodent disease models differ from mechanisms in humans, and treatment application methods can have different mechanisms of effect[88]. The methodology used in our studies could benefit from increased translational potential to the clinic. First, this concerns the injury models. The postnatal systemic IL-1β mouse model of EoP shows close resemblance to the clinical symptoms of EoP seen in preterm infants, including microgliosis, astrogliosis, white matter injury, dysmaturation of OLs, axonopathy and interneuronopathy, altered neural microstructure and behavioral impairments[63,180,192,259,260] (reviewed in Van Steenwinckel et al., 2024[34]). This model has been previously predominantly studied in OF1 mice. Here, we were able to replicate this EoP phenotype in mice with a C57BL/6 background. Similar to EoP, there are different models to study TBI (reviewed in Kochanek et al., 2017[261]). Most studies use penetrating controlled-cortical-impact (CCI) models to study pediatric TBI, because of their robust effects and optimal consistency between subjects. Although penetrating TBI occurs in adult clinical cases, the nature of TBI in newborns and children is predominantly non-penetrating physical impact[13,262]. This distinction is important because penetrating TBI and closed-head TBI do not cause the same injury mechanisms[263]. As such, the closed-head TBI model likely has preferred relevance to study the TBI mechanisms of newborns.

Secondly, our administration method of oxytocin likely benefits from enhanced clinical relevance. Exogenous application of chemicals – including oxytocin – can induce different mechanisms of effect than endogenous activity itself does[171]. As such, we stressed activation of body-own oxytocin release with use of the DREADD construct. CNO is the most widely used DREADD agonist, preferred for its rapid penetration to and distribution in the brain[264]. However, high doses of CNO may have side effects. CNO is a metabolite of atypical antipsychotic drug clozapine. It has been demonstrated in mice and rats that in high dosages, CNO back-transforms into clozapine and binds to non-DREADD receptors where it induces physiological and behavioral changes[265]. For that reason, chemogenetic research requires thorough control assessment of the CNO substance. We emphasized rigorous assessment of such potential side-effects in our studies. CNO administration to Oxt-Hm3Dq$^{-/-}$ mice (which have OXT-Cre but do not express the Hm3Dq-DREADD) did not affect microglia inflammatory cytokine expression,

nor did it affect behavior, in both injury models. This confirms that the neuroprotective effects demonstrated with our studies are indeed attributed to elevated oxytocin release itself and not induced or attenuated by CNO. Altogether, the pathological mechanisms studied in our preclinical models and the modulation method of oxytocin likely have close resemblance to processes in human infants.

An important limitation of our work concerns the lack of single cell-level assessment of microglia transcriptomics in our studies. As repeatedly evidenced (and elegantly summarized in Paolicelli et al., 2022[266]), microglia cells are too dynamic and heterogeneous to reduce to a mere M1 *versus* M2, or pro-inflammatory *versus* anti-inflammatory phenotype. Single cell sequencing studies consistently show the wide range of microglia sub-clusters in the mouse and human brain, especially in the developing brain[76,77,163,267]. Bulk RNA sequencing does not possess methodological precision to make such detailed distinctions[268], and so there are likely more detailed effects on microglia subtypes that we did not see. It will be of high interest to elucidate which microglia sub-clusters are most affected by oxytocin modulation.

Another limitation pertains unclarity regarding any peripheral effects of oxytocin, which could be especially relevant for the EoP study. Chemogenetic activation of oxytocinergic neurons evokes both central and peripheral oxytocin release[269]. Studies show that plasmic oxytocin possesses similar modulatory properties on peripheral immune cells including macrophages, monocytes and neurotrophils, where it can reduce pro-inflammatory cytokine expression and improve recovery of peripheral organs[270]. Importantly, peripheral immune cells can infiltrate the brain in response to injury, where they aggravate inflammatory processes[271]. Given that the IL-1β EoP model is a model of initial *systemic* inflammation that turns into *neuro*inflammation after peripheral inflammatory cytokines reach microglia in the brain (through various possible mechanisms, see Gressens, Volpe 2024[3]), anti-inflammatory effects on peripheral inflammatory processes via increased plasmic oxytocin concentrations likely contribute to faster alleviation of inflammatory symptoms in the brain. That said, the concentration of oxytocin in the brain is 100 to 1000-fold higher than in blood plasma[272], so the magnitude of any peripheral effects of oxytocin remains to be proven.

8. Implications of findings

In the neonatal intensive care unit (NICU), there is abundant evidence that skin-to-skin exposure, voice/music exposure and family-oriented care can improve a newborn's survival, reduce the risk of sepsis and severe infection, decrease hypothermia, increase a baby's growth, stimulate breastfeed and induce successful attachment[273]. Specifically for the brain, these non-pharmacological interventions can improve cortical connectivity[130], cognitive development[129], social and language skills[127], it can increase brain volumes, and improve white matter development[125]. Despite this growing evidence, oxytocin-associated interventions are not yet a prominent part of caregiving in the NICU or pediatric ICU (PICU). To accommodate often understaffed nursing teams, professional caregiving is focused on efficiency, with open bay units where babies lie in close proximity and are constantly exposed to alarms, noise and bright lights. The overlooking of oxytocin-associated clinical interventions as a real treatment option is aided by the lack of knowledge that explains the biological effects observed. Our studies provide biological support for a neuroprotective effect of oxytocin, that can be achieved by non-pharmacological, natural elevation. This supports the potential of developmental care practices that stimulate non-pharmacological oxytocin interventions. Developmental care, and personalized and family-centered care practices are interventions focused on minimizing aversive stimuli for the child (noise from alarms or crying from other infants, light and stress), while promoting interaction with intimate family, through skin-to-skin contact and voice/music exposure[82,129,274]. These interactions with

family members are important because they are natural protective mechanisms crucial for optimization of outcomes after injury that professional caregiving and technology cannot provide[275,276]. One concrete idea that contributes to developmental care are private room NICU's instead of open bay units, which limit the amount of stressors, enhance family bonding, and have shown positive outcomes to the child's development[277]. Interventions like these are costly, which likely explains the absence of wide application so far. However, given the annual costs of preterm birth (~26 billion USD[12]) and pediatric TBI (~13 billion USD[27]), it could even be financially beneficial to implement these practices.

Although the biological mechanism underlying the mechanism between oxytocin and improved brain outcomes needs to be further explored, the existing data supports oxytocin as a promising therapeutic target. Also, this therapy option benefits from the fact that it stimulates a mechanism that seems naturally occurring: studies show that the brain increases its natural responsiveness to the effects of oxytocin by upregulating expression of oxytocin receptors[278]. Secondly, these non-pharmacological interventions do not compete with traditional medicine. This suggests that helping the brain elevate its oxytocin levels is a safe therapeutic option for newborns. Moreover, the therapy could have a positive correlation between duration of treatment and outcomes: preclinical studies show substantially higher improvements to oligodendrocyte development after hypoxia when treated with oxytocin-associated EE for 30 days compared to just 10 days[208]. This could suggest that there is little risk of too much oxytocin elevation, which will of course have to be tailored to the developmental care program in the ICU. Finally, it is important that brain repair interventions can take place as soon as possible after injury. Preclinical research widely support a critical time-window for the most regenerative potential after newborn brain injury[16,208], the sooner intervention is started the better the outcome. Oxytocin-associated clinical interventions such a skin-to-skin care can be implemented immediately after birth, meaning that oxytocin can profit from this critical treatment window after injury. A remaining clinical question is whether we would be able to identify the social/clinical intervention associated with the most substantial oxytocin release and whether this effect may be subject to inter individual variability.

Modulation of post-injury neuroinflammation is a hot topic in translational research and we are not the first to explore therapeutic targets for the developing brain. Previous preclinical studies on additional inflammation-based therapies to newborn brain injury likewise report beneficial effects decreasing microgliosis and inflammation post-injury. However, they focus on short-term effects[229,279–282], or require many treatment sessions[283] (including pre-treatment[227,284]). In our studies, we demonstrate long-term neuroprotection after EoP and pediatric TBI that persist after oxytocin modulation is discontinued, with only a few treatment sessions required. As such, oxytocin could benefit from improved translational relevance for clinical use. Our data support increased implementation of non-pharmacological interventions associated with oxytocin in the standard care routine after brain injury to newborns, while in parallel more (preclinical) research is conducted to elaborate on the underlying biological mechanism and see how the treatment can be adjusted and optimized per brain injury mechanism and per individual.

9. Conclusions

Given the dominant role of neuroinflammation in the aggravation of brain injury in EoP and pediatric TBI, immune-modulatory interventions have a high potential to promote neuroprotection after injury. Clinical data point suggest that oxytocin-associated non-pharmacological intervention improves brain development in infants born preterm, yet how this happens largely remained a scientific black box. In this thesis, we studied this mechanism in preclinical models of newborn brain injury and found biological basis for the observed effect in the clinic (**Figure 6**). Our results suggest that oxytocin has a neuroprotective effect after brain development by modulating the glia response to injury, reducing the

astrocyte reactivity, altering the inflammatory profile of microglia and stimulating their support functions for brain development and oligodendrocyte development. We found that on the long term, oxytocin improves cerebrovascular recovery and correlation of functional brain connectivity, that it improves white matter microstructural properties, and that it restores the development of neurotypical social behavior. These data are in line with previous work of our group showing neuroprotective properties of oxytocin receptor agonist to a model of intra-uterine growth retardation. And, similar protective effects are found for chemogenetic oxytocinergic stimulation in a model of neonatal hypoxic-ischemic injury (Schirmbeck, Sanches, Knoop et al., *in prep*.). These data strongly support that oxytocin is a valid therapeutic target for newborn brain injury, with unprecedented non-invasive and easy-to-implement characteristics, and supports improved use of oxytocin-associated intervention in the clinic.

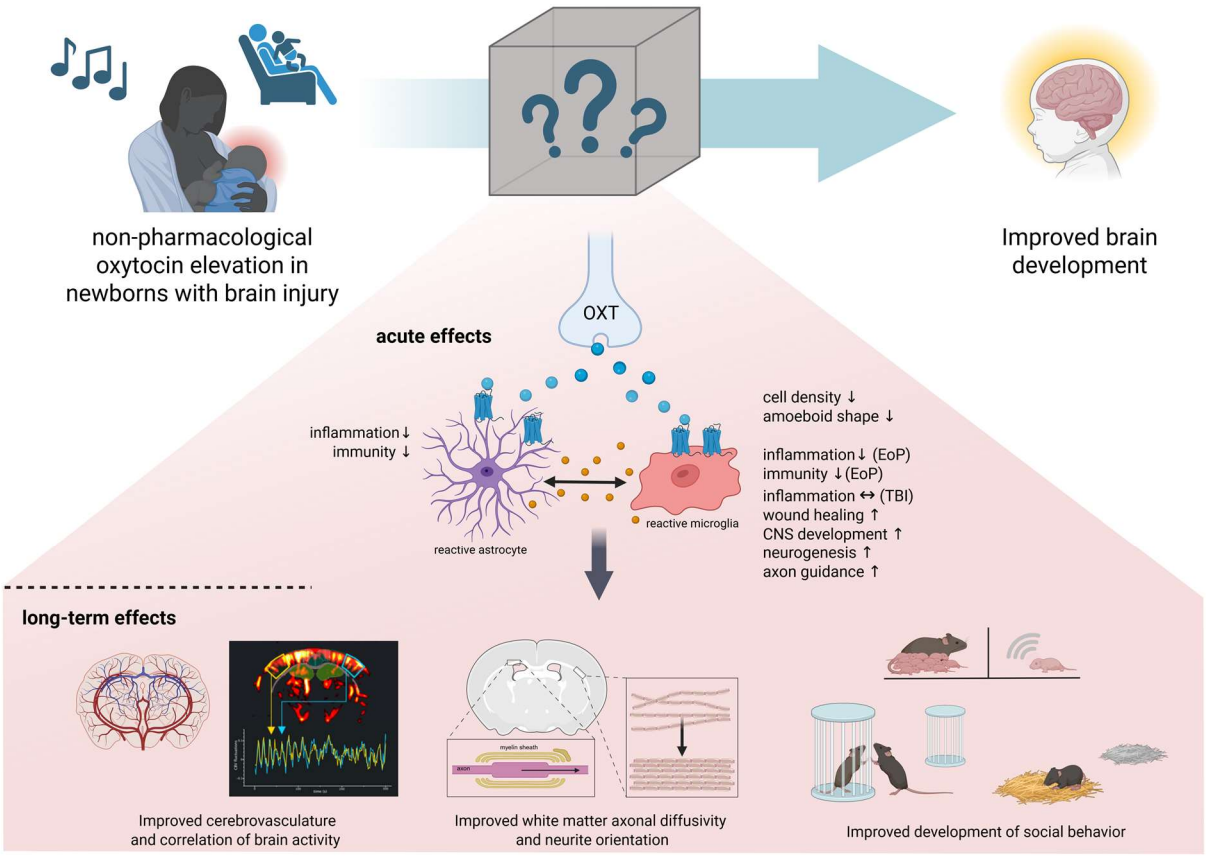

Figure 6: Summary of findings of this thesis. Our preclinical findings shed light on the black box between elevated oxytocin and improved brain development after injury that is observed in the clinic. In neuroinflammation-associated brain injury models of EoP and pediatric TBI, we show that oxytocin modulates acute gliosis after injury, and that this is associated with improved long-term development of brain vasculature, functional connectivity, white matter microstructure and social development. Created with Biorender.com

References

1. Gale, C. *et al.* Neonatal brain injuries in England: population-based incidence derived from routinely recorded clinical data held in the National Neonatal Research Database. *Arch Dis Child Fetal Neonatal Ed* **103**, F301–F306 (2018).
2. Volpe, J. J. Brain injury in premature infants: a complex amalgam of destructive and developmental disturbances. *Lancet Neurol* **8**, 110–124 (2009).
3. Gressens, P. Chapter 17 - Inflammation and the Newborn Brain. in *Volpe's Neurology of the Newborn (Seventh Edition)* (ed. Volpe, J. J.) 494-505.e4 (Elsevier, St. Louis (MO), 2025). doi:10.1016/B978-0-443-10513-5.00017-6.
4. ARAKI, T., YOKOTA, H. & MORITA, A. Pediatric Traumatic Brain Injury: Characteristic Features, Diagnosis, and Management. *Neurol Med Chir (Tokyo)* **57**, 82–93 (2017).
5. Fair, D. & Schlaggar, B. L. Brain Development. in *Encyclopedia of Infant and Early Childhood Development* (eds. Haith, M. M. & Benson, J. B.) 211–225 (Academic Press, San Diego, 2008). doi:10.1016/B978-012370877-9.00027-X.
6. Rashid, M. *et al.* The impact of pediatric traumatic brain injury (TBI) on family functioning: a systematic review. *J Pediatr Rehabil Med* **7**, 241–254 (2014).
7. Tonmukayakul, U. *et al.* Systematic review of the economic impact of cerebral palsy. *Res Dev Disabil* **80**, 93–101 (2018).
8. Bourke-Taylor, H., Cotter ,Claire & and Stephan, R. Complementary, Alternative, and Mainstream Service use Among Families with Young Children with Multiple Disabilities: Family Costs to Access Choices. *Physical & Occupational Therapy In Pediatrics* **35**, 311–325 (2015).
9. Van Steenwinckel, J. *et al.* Brain damage of the preterm infant: new insights into the role of inflammation. *Biochem Soc Trans* **42**, 557–563 (2014).
10. Vanes, L. D., Murray, R. M. & Nosarti, C. Adult outcome of preterm birth: Implications for neurodevelopmental theories of psychosis. *Schizophr Res* **247**, 41–54 (2022).
11. Phibbs, C. S. *et al.* Birth Hospitalization Costs and Days of Care for Mothers and Neonates in California, 2009-2011. *J Pediatr* **204**, 118-125.e14 (2019).

12. Behrman, R. E., Butler, A. S. & Outcomes, I. of M. (US) C. on U. P. B. and A. H. Societal Costs of Preterm Birth. in *Preterm Birth: Causes, Consequences, and Prevention* (National Academies Press (US), 2007).
13. Dewan, M. C., Mummareddy, N., Wellons, J. C. & Bonfield, C. M. Epidemiology of Global Pediatric Traumatic Brain Injury: Qualitative Review. *World Neurosurgery* **91**, 497-509.e1 (2016).
14. Lozano, D. *et al.* Neuroinflammatory responses to traumatic brain injury: etiology, clinical consequences, and therapeutic opportunities. *Neuropsychiatr Dis Treat* **11**, 97–106 (2015).
15. Adams, J. H., Graham, D. I. & Gennarelli, T. A. Head Injury in Man and Experimental Animals: Neuropathology. in *Trauma and Regeneration* (ed. Adams, J. H.) 15–30 (Springer, Vienna, 1983). doi:10.1007/978-3-7091-4147-2_2.
16. Jacquens, A. *et al.* Neuro-Inflammation Modulation and Post-Traumatic Brain Injury Lesions: From Bench to Bed-Side. *International Journal of Molecular Sciences* **23**, 11193 (2022).
17. Fraunberger, E. & Esser, M. Neuro-Inflammation in Pediatric Traumatic Brain Injury—from Mechanisms to Inflammatory Networks. *Brain Sciences* **9**, 319 (2019).
18. Kooper, C. C. *et al.* Long-Term Neurodevelopmental Outcome of Children With Mild Traumatic Brain Injury. *Pediatric Neurology* **160**, 18–25 (2024).
19. Kyösti, E. *et al.* Long-Term Quality of Life After Pediatric Traumatic Brain Injury Treated in the Intensive Care Unit. *Pediatric Neurology* **157**, 50–56 (2024).
20. Dennis, E. L. *et al.* White Matter Disruption in Pediatric Traumatic Brain Injury: Results From ENIGMA Pediatric Moderate to Severe Traumatic Brain Injury. *Neurology* **97**, e298–e309 (2021).
21. Botchway, E. *et al.* Resting-state network organisation in children with traumatic brain injury. *Cortex* **154**, 89–104 (2022).
22. van der Horn, H. J. *et al.* Dynamic Functional Connectivity in Pediatric Mild Traumatic Brain Injury. *NeuroImage* **285**, 120470 (2024).
23. GERRARD-MORRIS, A. *et al.* Cognitive development after traumatic brain injury in young children. *J Int Neuropsychol Soc* **16**, 157–168 (2010).

24. Bellesi, G., Barker, E. D., Brown, L. & Valmaggia, L. Pediatric traumatic brain injury and antisocial behavior: are they linked? A systematic review. *Brain Inj* **33**, 1272–1292 (2019).
25. Ashwal, S., Siebold, L., Krueger, A. C. & Wilson, C. G. Post-traumatic Neuroinflammation: Relevance to Pediatrics. *Pediatric Neurology* **122**, 50–58 (2021).
26. Taylor, C. A., Bell, J. M., Breiding, M. J. & Xu, L. Traumatic Brain Injury-Related Emergency Department Visits, Hospitalizations, and Deaths - United States, 2007 and 2013. *MMWR Surveill Summ* **66**, 1–16 (2017).
27. Miller, T. R. *et al.* Lifetime Cost of Abusive Head Trauma at Ages 0–4, USA. *Prev Sci* **19**, 695–704 (2018).
28. Arambula, S. E., Reinl, E. L., El Demerdash, N., McCarthy, M. M. & Robertson, C. L. Sex differences in pediatric traumatic brain injury. *Experimental Neurology* **317**, 168–179 (2019).
29. Kelly, L. A., Branagan, A., Semova, G. & Molloy, E. J. Sex differences in neonatal brain injury and inflammation. *Front. Immunol.* **14**, (2023).
30. Blencowe, H. *et al.* Born Too Soon: The global epidemiology of 15 million preterm births. *Reproductive Health* **10**, S2 (2013).
31. Coronado, V. G. *et al.* Surveillance for traumatic brain injury-related deaths--United States, 1997-2007. *MMWR Surveill Summ* **60**, 1–32 (2011).
32. McCarthy, M. M. Multifaceted origins of sex differences in the brain. *Philos Trans R Soc Lond B Biol Sci* **371**, 20150106 (2016).
33. Flanagan, K. L. Sexual dimorphism in biomedical research: a call to analyse by sex. *Transactions of The Royal Society of Tropical Medicine and Hygiene* **108**, 385–387 (2014).
34. Van Steenwinckel, J. *et al.* Key roles of glial cells in the encephalopathy of prematurity. *Glia* **72**, 475–503 (2024).
35. Jacquens, A. *et al.* Deleterious effect of sustained neuroinflammation in pediatric traumatic brain injury. *Brain, Behavior, and Immunity* **120**, 99–116 (2024).
36. Li, Q. & Barres, B. A. Microglia and macrophages in brain homeostasis and disease. *Nat Rev Immunol* **18**, 225–242 (2018).

37. Menassa, D. A. *et al.* The spatiotemporal dynamics of microglia across the human lifespan. *Developmental Cell* **57**, 2127-2139.e6 (2022).
38. Alliot, F., Godin, I. & Pessac, B. Microglia derive from progenitors, originating from the yolk sac, and which proliferate in the brain. *Brain Res Dev Brain Res* **117**, 145–152 (1999).
39. Thion, M. S. & Garel, S. On place and time: microglia in embryonic and perinatal brain development. *Current Opinion in Neurobiology* **47**, 121–130 (2017).
40. Lawrence, A. R. *et al.* Microglia maintain structural integrity during fetal brain morphogenesis. *Cell* **187**, 962-980.e19 (2024).
41. Réu, P. *et al.* The Lifespan and Turnover of Microglia in the Human Brain. *Cell Rep* **20**, 779–784 (2017).
42. von Bartheld, C. S., Bahney, J. & Herculano-Houzel, S. The Search for True Numbers of Neurons and Glial Cells in the Human Brain: A Review of 150 Years of Cell Counting. *J Comp Neurol* **524**, 3865–3895 (2016).
43. Hickman, S. E. *et al.* The microglial sensome revealed by direct RNA sequencing. *Nat Neurosci* **16**, 1896–1905 (2013).
44. Lively, S. & Schlichter, L. C. Microglia Responses to Pro-inflammatory Stimuli (LPS, IFNγ+TNFα) and Reprogramming by Resolving Cytokines (IL-4, IL-10). *Front Cell Neurosci* **12**, 215 (2018).
45. Matejuk, A. & Ransohoff, R. M. Crosstalk Between Astrocytes and Microglia: An Overview. *Frontiers in Immunology* **11**, (2020).
46. Liddelow, S. A. *et al.* Neurotoxic reactive astrocytes are induced by activated microglia. *Nature* **541**, 481–487 (2017).
47. Liu, W., Tang, Y. & Feng, J. Cross talk between activation of microglia and astrocytes in pathological conditions in the central nervous system. *Life Sci* **89**, 141–146 (2011).
48. Liu, L.-R., Liu, J.-C., Bao, J.-S., Bai, Q.-Q. & Wang, G.-Q. Interaction of Microglia and Astrocytes in the Neurovascular Unit. *Front Immunol* **11**, 1024 (2020).
49. Colonna, M. & Butovsky, O. Microglia Function in the Central Nervous System During Health and Neurodegeneration. *Annu Rev Immunol* **35**, 441–468 (2017).

50. Glass, C. K., Saijo, K., Winner, B., Marchetto, M. C. & Gage, F. H. Mechanisms underlying inflammation in neurodegeneration. *Cell* **140**, 918–934 (2010).
51. Basha, S., Surendran, N. & Pichichero, M. Immune Responses in Neonates. *Expert Rev Clin Immunol* **10**, 1171–1184 (2014).
52. Schimmel, S. J., Acosta, S. & Lozano, D. Neuroinflammation in traumatic brain injury: A chronic response to an acute injury. *Brain Circ* **3**, 135–142 (2017).
53. Simon, D. W. *et al.* The far-reaching scope of neuroinflammation after traumatic brain injury. *Nat Rev Neurol* **13**, 171–191 (2017).
54. Pang, Y. *et al.* Lipopolysaccharide-activated microglia induce death of oligodendrocyte progenitor cells and impede their development. *Neuroscience* **166**, 464–475 (2010).
55. Talbott, J. F. *et al.* CNTF promotes the survival and differentiation of adult spinal cord-derived oligodendrocyte precursor cells in vitro but fails to promote remyelination in vivo. *Exp Neurol* **204**, 485–489 (2007).
56. Bona, E. *et al.* Chemokine and Inflammatory Cell Response to Hypoxia-Ischemia in Immature Rats. *Pediatr Res* **45**, 500–509 (1999).
57. Vaes, J. E. G. *et al.* Intranasal mesenchymal stem cell therapy to boost myelination after encephalopathy of prematurity. *Glia* **69**, 655–680 (2021).
58. Benincasa, B. C., Rieck, L. G. B., Procianoy, R. S. & Silveira, R. C. Cytokine Levels in Neonates: Unveiling the Impact of Perinatal Inflammation on Prematurity. *Am J Perinatol* **41**, 1554–1559 (2024).
59. Verney, C. *et al.* Microglial Reaction in Axonal Crossroads Is a Hallmark of Noncystic Periventricular White Matter Injury in Very Preterm Infants. *Journal of Neuropathology & Experimental Neurology* **71**, 251–264 (2012).
60. Supramaniam, V. *et al.* Microglia activation in the extremely preterm human brain. *Pediatr Res* **73**, 301–309 (2013).
61. Loane, D. J. & Kumar, A. Microglia in the TBI Brain: The Good, The Bad, And The Dysregulated. *Exp Neurol* **275**, 316–327 (2016).

62. Kumar, A., Alvarez-Croda, D.-M., Stoica, B. A., Faden, A. I. & Loane, D. J. Microglial/Macrophage Polarization Dynamics following Traumatic Brain Injury. *Journal of Neurotrauma* **33**, 1732–1750 (2016).
63. Van Steenwinckel, J. *et al.* Decreased microglial Wnt/β-catenin signalling drives microglial pro-inflammatory activation in the developing brain. *Brain* **142**, 3806–3833 (2019).
64. Da Pozzo, E. *et al.* Microglial Pro-Inflammatory and Anti-Inflammatory Phenotypes Are Modulated by Translocator Protein Activation. *Int J Mol Sci* **20**, 4467 (2019).
65. Arroyo, D. S., Soria, J. A., Gaviglio, E. A., Rodriguez-Galan, M. C. & Iribarren, P. Toll-like receptors are key players in neurodegeneration. *Int Immunopharmacol* **11**, 1415–1421 (2011).
66. Jha, M. K., Jo, M., Kim, J.-H. & Suk, K. Microglia-Astrocyte Crosstalk: An Intimate Molecular Conversation. *Neuroscientist* **25**, 227–240 (2019).
67. Scott, M. C., Bedi, S. S., Olson, S. D., Sears, C. M. & Cox, C. S. MICROGLIA AS THERAPEUTIC TARGETS AFTER NEUROLOGICAL INJURY: Strategy for Cell Therapy. *Expert Opin Ther Targets* **25**, 365–380 (2021).
68. Piano, I. *et al.* Anti-inflammatory reprogramming of microglia cells by metabolic modulators to counteract neurodegeneration; a new role for Ranolazine. *Sci Rep* **13**, 20138 (2023).
69. Zhang, W. *et al.* Microglia-associated neuroinflammation is a potential therapeutic target for ischemic stroke. *Neural Regen Res* **16**, 6–11 (2020).
70. Kwon, M.-S. Advanced therapeutic strategies targeting microglia: beyond neuroinflammation. *Arch. Pharm. Res.* **45**, 618–630 (2022).
71. Safieh-Garabedian, B., Haddad, J. J. & Saadé, N. E. Cytokines in the central nervous system: targets for therapeutic intervention. *Curr Drug Targets CNS Neurol Disord* **3**, 271–280 (2004).
72. Figuera-Losada, M., Rojas, C. & Slusher, B. S. Inhibition of Microglia Activation as a Phenotypic Assay in Early Drug Discovery. *SLAS Discovery* **19**, 17–31 (2014).
73. Szalay, G. *et al.* Microglia protect against brain injury and their selective elimination dysregulates neuronal network activity after stroke. *Nat Commun* **7**, 11499 (2016).
74. Palsamy, K. *et al.* Microglial depletion after brain injury prolongs inflammation and impairs brain repair, adult neurogenesis and pro-regenerative signaling. *Glia* **71**, 2642–2663 (2023).

75. Harry, G. J. & Kraft, A. D. Microglia in the developing brain: a potential target with lifetime effects. *Neurotoxicology* **33**, 191–206 (2012).
76. Hammond, T. R. *et al.* Single-Cell RNA Sequencing of Microglia throughout the Mouse Lifespan and in the Injured Brain Reveals Complex Cell-State Changes. *Immunity* **50**, 253-271.e6 (2019).
77. Li, Q. *et al.* Developmental Heterogeneity of Microglia and Brain Myeloid Cells Revealed by Deep Single-Cell RNA Sequencing. *Neuron* **101**, 207-223.e10 (2019).
78. Kochanek, P. M. *et al.* Guidelines for the Management of Pediatric Severe Traumatic Brain Injury, Third Edition: Update of the Brain Trauma Foundation Guidelines. *Pediatr Crit Care Med* **20**, S1–S82 (2019).
79. Adelson, P. D. *et al.* Phase II Clinical Trial of Moderate Hypothermia after Severe Traumatic Brain Injury in Children. *Neurosurgery* **56**, 740 (2005).
80. Beca, J. *et al.* Hypothermia for Traumatic Brain Injury in Children—A Phase II Randomized Controlled Trial*. *Critical Care Medicine* **43**, 1458 (2015).
81. Ream, M. A. & Lehwald, L. Neurologic Consequences of Preterm Birth. *Curr Neurol Neurosci Rep* **18**, 48 (2018).
82. Molloy, E. J. *et al.* Neuroprotective therapies in the NICU in preterm infants: present and future (Neonatal Neurocritical Care Series). *Pediatr Res* **95**, 1224–1236 (2024).
83. Marlow, N., Wolke, D., Bracewell, M. A., Samara, M., & EPICure Study Group. Neurologic and developmental disability at six years of age after extremely preterm birth. *N Engl J Med* **352**, 9–19 (2005).
84. Marret, S. *et al.* Brain injury in very preterm children and neurosensory and cognitive disabilities during childhood: the EPIPAGE cohort study. *PLoS One* **8**, e62683 (2013).
85. Dubner, S. E., Rose, J., Bruckert, L., Feldman, H. M. & Travis, K. E. Neonatal white matter tract microstructure and 2-year language outcomes after preterm birth. *Neuroimage Clin* **28**, 102446 (2020).
86. Jacobs, S. E. *et al.* Cooling for newborns with hypoxic ischaemic encephalopathy. *Cochrane Database Syst Rev* **2013**, CD003311 (2013).

87. Chang, Y. S., Ahn, S. Y., Sung, S. & Park, W. S. Stem Cell Therapy for Neonatal Disorders: Prospects and Challenges. *Yonsei Med J* **58**, 266–271 (2017).
88. Seyhan, A. A. Lost in translation: the valley of death across preclinical and clinical divide – identification of problems and overcoming obstacles. *Translational Medicine Communications* **4**, 18 (2019).
89. Brummelte, S. *et al.* Procedural pain and brain development in premature newborns. *Ann Neurol* **71**, 385–396 (2012).
90. Matsunaga, W. *et al.* LPS-induced Fos expression in oxytocin and vasopressin neurons of the rat hypothalamus. *Brain Res* **858**, 9–18 (2000).
91. *Behavioral Pharmacology of Neuropeptides: Oxytocin*. (Springer International Publishing : Imprint: Springer, Cham, 2018). doi:10.1007/978-3-319-63739-6.
92. Ludwig, M. & Stern, J. Multiple signalling modalities mediated by dendritic exocytosis of oxytocin and vasopressin. *Philos Trans R Soc Lond B Biol Sci* **370**, 20140182 (2015).
93. Ludwig, M., Apps, D., Menzies, J., Patel, J. C. & Rice, M. E. Dendritic release of neurotransmitters. *Compr Physiol* **7**, 235–252 (2016).
94. Goaillard, J.-M., Moubarak, E., Tapia, M. & Tell, F. Diversity of Axonal and Dendritic Contributions to Neuronal Output. *Frontiers in Cellular Neuroscience* **13**, (2020).
95. Chini, B., Verhage, M. & Grinevich, V. The Action Radius of Oxytocin Release in the Mammalian CNS: From Single Vesicles to Behavior. *Trends Pharmacol Sci* **38**, 982–991 (2017).
96. Bakos, J., Srancikova, A., Havranek, T. & Bacova, Z. Molecular Mechanisms of Oxytocin Signaling at the Synaptic Connection. *Neural Plast* **2018**, 4864107 (2018).
97. Son, S. *et al.* Whole-Brain Wiring Diagram of Oxytocin System in Adult Mice. *J Neurosci* **42**, 5021–5033 (2022).
98. Jurek, B. & Neumann, I. D. The Oxytocin Receptor: From Intracellular Signaling to Behavior. *Physiological Reviews* **98**, 1805–1908 (2018).
99. Grinevich, V., Knobloch-Bollmann, H. S., Eliava, M., Busnelli, M. & Chini, B. Assembling the Puzzle: Pathways of Oxytocin Signaling in the Brain. *Biological Psychiatry* **79**, 155–164 (2016).

100. Knobloch, H. S. *et al.* Evoked axonal oxytocin release in the central amygdala attenuates fear response. *Neuron* **73**, 553–566 (2012).

101. Eliava, M. *et al.* A New Population of Parvocellular Oxytocin Neurons Controlling Magnocellular Neuron Activity and Inflammatory Pain Processing. *Neuron* **89**, 1291–1304 (2016).

102. Busnelli, M. *et al.* Functional selective oxytocin-derived agonists discriminate between individual G protein family subtypes. *J Biol Chem* **287**, 3617–3629 (2012).

103. Olff, M. *et al.* The role of oxytocin in social bonding, stress regulation and mental health: An update on the moderating effects of context and interindividual differences. *Psychoneuroendocrinology* **38**, 1883–1894 (2013).

104. Jones, C., Barrera, I., Brothers, S., Ring, R. & Wahlestedt, C. Oxytocin and social functioning. *Dialogues Clin Neurosci* **19**, 193–201 (2017).

105. Filippa, M. *et al.* Pain, Parental Involvement, and Oxytocin in the Neonatal Intensive Care Unit. *Front Psychol* **10**, 715 (2019).

106. Dubrovsky, B., Harris, J., Gijsbers, K. & Tatarinov, A. Oxytocin induces long-term depression on the rat dentate gyrus: Possible ATPase and ectoprotein kinase mediation. *Brain Research Bulletin* **58**, 141–147 (2002).

107. Tomizawa, K. *et al.* Oxytocin improves long-lasting spatial memory during motherhood through MAP kinase cascade. *Nat Neurosci* **6**, 384–390 (2003).

108. Lin, Y.-T., Chen, C.-C., Huang, C.-C., Nishimori, K. & Hsu, K.-S. Oxytocin stimulates hippocampal neurogenesis via oxytocin receptor expressed in CA3 pyramidal neurons. *Nat Commun* **8**, 537 (2017).

109. Rajamani, K. T., Wagner, S., Grinevich, V. & Harony-Nicolas, H. Oxytocin as a Modulator of Synaptic Plasticity: Implications for Neurodevelopmental Disorders. *Front. Synaptic Neurosci.* **10**, (2018).

110. Ben-Ari, Y. Oxytocin and Vasopressin, and the GABA Developmental Shift During Labor and Birth: Friends or Foes? *Front Cell Neurosci* **12**, 254 (2018).

111. Grinevich, V. & Ludwig, M. The multiple faces of the oxytocin and vasopressin systems in the brain. *Journal of Neuroendocrinology* **33**, e13004 (2021).

112. Knoop, M. *et al.* The Role of Oxytocin in Abnormal Brain Development: Effect on Glial Cells and Neuroinflammation. *Cells* **11**, 3899 (2022).

113. Cratty, B. J. Perceptual and Motor Development in Infants and Children. Second Edition. (1979).

114. Peters, S. & Crone, E. A. Increased striatal activity in adolescence benefits learning. *Nat Commun* **8**, 1983 (2017).

115. Hammock, E. A. D. & Levitt, P. Oxytocin receptor ligand binding in embryonic tissue and postnatal brain development of the C57BL/6J mouse. *Frontiers in Behavioral Neuroscience* 8 (2013).

116. Onaka, T. & Takayanagi, Y. The oxytocin system and early-life experience-dependent plastic changes. *J Neuroendocrinol* **33**, e13049 (2021).

117. Loewy, J., Stewart, K., Dassler, A.-M., Telsey, A. & Homel, P. The effects of music therapy on vital signs, feeding, and sleep in premature infants. *Pediatrics* **131**, 902–918 (2013).

118. Yue, W., Han, X., Luo, J., Zeng, Z. & Yang, M. Effect of music therapy on preterm infants in neonatal intensive care unit: Systematic review and meta-analysis of randomized controlled trials. *J Adv Nurs* **77**, 635–652 (2021).

119. Ormston, K., Howard, R., Gallagher, K., Mitra, S. & Jaschke, A. The Role of Music Therapy with Infants with Perinatal Brain Injury. *Brain Sci* **12**, 578 (2022).

120. Yakobson, D. *et al.* Effects of Live Music Therapy on Autonomic Stability in Preterm Infants: A Cluster-Randomized Controlled Trial. *Children (Basel)* **8**, 1077 (2021).

121. Wang, Y., Zhao, T., Zhang, Y., Li, S. & Cong, X. Positive Effects of Kangaroo Mother Care on Long-Term Breastfeeding Rates, Growth, and Neurodevelopment in Preterm Infants. *Breastfeed Med* **16**, 282–291 (2021).

122. Cristóbal Cañadas, D., Bonillo Perales, A., Galera Martínez, R., Casado-Belmonte, M. D. P. & Parrón Carreño, T. Effects of Kangaroo Mother Care in the NICU on the Physiological Stress Parameters of Premature Infants: A Meta-Analysis of RCTs. *Int J Environ Res Public Health* **19**, 583 (2022).

123. Cristóbal Cañadas, D., Parrón Carreño, T., Sánchez Borja, C. & Bonillo Perales, A. Benefits of Kangaroo Mother Care on the Physiological Stress Parameters of Preterm Infants and Mothers in Neonatal Intensive Care. *Int J Environ Res Public Health* **19**, 7183 (2022).

124. Zengin, H. *et al.* The effects of kangaroo mother care on physiological parameters of premature neonates in neonatal intensive care unit: A systematic review. *J Pediatr Nurs* **71**, e18–e27 (2023).

125. Charpak, N. *et al.* Kangaroo mother care had a protective effect on the volume of brain structures in young adults born preterm. *Acta Paediatr* **111**, 1004–1014 (2022).

126. Nimbalkar, S. M., Chaudhary, N. S., Gadhavi, K. V. & Phatak, A. Kangaroo Mother Care in reducing pain in preterm neonates on heel prick. *Indian J Pediatr* **80**, 6–10 (2013).

127. Lilliesköld, S. *et al.* Skin-to-Skin Contact at Birth for Very Preterm Infants and Mother-Infant Interaction Quality at 4 Months: A Secondary Analysis of the IPISTOSS Randomized Clinical Trial. *JAMA Netw Open* **6**, e2344469 (2023).

128. Linnér, A. *et al.* Immediate skin-to-skin contact may have beneficial effects on the cardiorespiratory stabilisation in very preterm infants. *Acta Paediatr* **111**, 1507–1514 (2022).

129. Welch, M. G. *et al.* Family Nurture Intervention in the Neonatal Intensive Care Unit improves social-relatedness, attention, and neurodevelopment of preterm infants at 18 months in a randomized controlled trial. *J Child Psychol Psychiatry* **56**, 1202–1211 (2015).

130. Yrjölä, P. *et al.* Facilitating early parent-infant emotional connection improves cortical networks in preterm infants. *Sci Transl Med* **14**, eabq4786 (2022).

131. Head, L. M. The Effect of Kangaroo Care on Neurodevelopmental Outcomes in Preterm Infants. *The Journal of Perinatal & Neonatal Nursing* **28**, 290 (2014).

132. Pavlyshyn, H., Sarapuk, I., Horishna, I., Slyva, V. & Skubenko, N. Skin-to-skin contact to support preterm infants and reduce NICU-related stress. *Int J Dev Neurosci* **82**, 639–645 (2022).

133. Bergman, N. J. New policies on skin-to-skin contact warrant an oxytocin-based perspective on perinatal health care. *Front. Psychol.* **15**, (2024).

134. Vittner, D. *et al.* Increase in Oxytocin From Skin-to-Skin Contact Enhances Development of Parent-Infant Relationship. *Biol Res Nurs* **20**, 54–62 (2018).

135. Moberg, K. U., Handlin, L. & Petersson, M. Neuroendocrine mechanisms involved in the physiological effects caused by skin-to-skin contact – With a particular focus on the oxytocinergic system. *Infant Behavior and Development* **61**, 101482 (2020).

136. Chanda, M. L. & Levitin, D. J. The neurochemistry of music. *Trends Cogn Sci* **17**, 179–193 (2013).

137. Wulff, V. *et al.* The effects of a music and singing intervention during pregnancy on maternal well-being and mother–infant bonding: a randomised, controlled study. *Arch Gynecol Obstet* **303**, 69–83 (2021).

138. Lammertink, F. *et al.* Early-life stress exposure and large-scale covariance brain networks in extremely preterm-born infants. *Transl Psychiatry* **12**, 1–9 (2022).

139. Urfer, A. *et al.* Consequences of Prematurity on Cortisol Regulation and Adjustment Difficulties: A 9-Year Longitudinal Study. *Children (Basel)* **9**, 9 (2021).

140. Pavlyshyn, H., Sarapuk, I. & Kozak, K. The relationship between neonatal stress in preterm infants and developmental outcomes at the corrected age of 24–30 months. *Front. Psychol.* **15**, (2024).

141. Uvnäs-Moberg, K., Gross, M. M., Calleja-Agius, J. & Turner, J. D. The Yin and Yang of the oxytocin and stress systems: opposites, yet interdependent and intertwined determinants of lifelong health trajectories. *Front. Endocrinol.* **15**, (2024).

142. Pavlyshyn, H. & Sarapuk, I. Skin-to-skin contact-An effective intervention on pain and stress reduction in preterm infants. *Front Pediatr* **11**, 1148946 (2023).

143. Arya, S. *et al.* Effect on neonatal sepsis following immediate kangaroo mother care in a newborn intensive care unit: a post-hoc analysis of a multicentre, open-label, randomised controlled trial. *EClinicalMedicine* **60**, 102006 (2023).

144. Seltzer, L. J., Ziegler, T. E. & Pollak, S. D. Social vocalizations can release oxytocin in humans. *Proc Biol Sci* **277**, 2661–2666 (2010).

145. Ooishi, Y., Mukai, H., Watanabe, K., Kawato, S. & Kashino, M. Increase in salivary oxytocin and decrease in salivary cortisol after listening to relaxing slow-tempo and exciting fast-tempo music. *PLoS One* **12**, e0189075 (2017).

146. Karelina, K. *et al.* Oxytocin mediates social neuroprotection after cerebral ischemia. *Stroke* **42**, 3606–3611 (2011).

147. Etehadi Moghadam, S. *et al.* Neuroprotective Effects of Oxytocin Hormone after an Experimental Stroke Model and the Possible Role of Calpain-1. *Journal of Stroke and Cerebrovascular Diseases* **27**, 724–732 (2018).

148. Selles, M. C. *et al.* Oxytocin attenuates microglial activation and restores social and non-social memory in APP/PS1 Alzheimer model mice. *iScience* **26**, 106545 (2023).

149. Takahashi, J. *et al.* Oxytocin reverses Aβ-induced impairment of hippocampal synaptic plasticity in mice. *Biochemical and biophysical research communications* **528**, 174–178 (2020).

150. Sünnetçi, E., Solmaz, V. & Erbaş, O. Chronic Oxytocin treatment has long lasting therapeutic potential in a rat model of neonatal hypercapnic-hypoxia injury, through enhanced GABAergic signaling and by reducing hippocampal gliosis with its anti-inflammatory feature. *Peptides* **135**, 170398 (2021).

151. Andari, E. *et al.* Promoting social behavior with oxytocin in high-functioning autism spectrum disorders. *Proc Natl Acad Sci U S A* **107**, 4389–4394 (2010).

152. Vargas, D. L., Nascimbene, C., Krishnan, C., Zimmerman, A. W. & Pardo, C. A. Neuroglial activation and neuroinflammation in the brain of patients with autism. *Ann Neurol* **57**, 67–81 (2005).

153. Koyama, R. & Ikegaya, Y. Microglia in the pathogenesis of autism spectrum disorders. *Neurosci Res* **100**, 1–5 (2015).

154. Inoue, T. *et al.* Oxytocin Suppresses Inflammatory Responses Induced by Lipopolysaccharide through Inhibition of the eIF-2α–ATF4 Pathway in Mouse Microglia. *Cells* **8**, 527 (2019).

155. Yuan, L. *et al.* Oxytocin inhibits lipopolysaccharide-induced inflammation in microglial cells and attenuates microglial activation in lipopolysaccharide-treated mice. *J Neuroinflammation* **13**, 77 (2016).

156. Bennett, M. L. *et al.* New tools for studying microglia in the mouse and human CNS. *Proc Natl Acad Sci U S A* **113**, E1738-1746 (2016).

157. Marsh, S. E. *et al.* Dissection of artifactual and confounding glial signatures by single-cell sequencing of mouse and human brain. *Nat Neurosci* **25**, 306–316 (2022).

158. Guttenplan, K. A. *et al.* Knockout of reactive astrocyte activating factors slows disease progression in an ALS mouse model. *Nat Commun* **11**, 3753 (2020).

159. Szeto, A. *et al.* Regulation of the macrophage oxytocin receptor in response to inflammation. *Am J Physiol Endocrinol Metab* **312**, E183–E189 (2017).

160. Momenabadi, S. *et al.* Oxytocin Reduces Brain Injury and Maintains Blood-Brain Barrier Integrity After Ischemic Stroke in Mice. *Neuromolecular Med* **22**, 557–571 (2020).

161. Chen, W., Man, X., Zhang, Y., Yao, G. & Chen, J. Medial prefrontal cortex oxytocin mitigates epilepsy and cognitive impairments induced by traumatic brain injury through reducing neuroinflammation in mice. *Sci Rep* **13**, 5214 (2023).

162. Wu, G. *et al.* Oxytocin attenuates hypothalamic injury-induced cognitive dysfunction by inhibiting hippocampal ERK signaling and Aβ deposition. *Transl Psychiatry* **14**, 208 (2024).

163. Yaqubi, M. *et al.* Analysis of the microglia transcriptome across the human lifespan using single cell RNA sequencing. *Journal of Neuroinflammation* **20**, 132 (2023).

164. Veening, J. G. & Olivier, B. Intranasal administration of oxytocin: behavioral and clinical effects, a review. *Neurosci Biobehav Rev* **37**, 1445–1465 (2013).

165. Kang, Y. S. & Park, J. H. Brain uptake and the analgesic effect of oxytocin--its usefulness as an analgesic agent. *Arch Pharm Res* **23**, 391–395 (2000).

166. Meidahl, A. C. *et al.* Intranasal Oxytocin Attenuates Reactive and Ongoing, Chronic Pain in a Model of Mild Traumatic Brain Injury. *Headache: The Journal of Head and Face Pain* **58**, 545–558 (2018).

167. Parker, K. J. *et al.* Intranasal oxytocin treatment for social deficits and biomarkers of response in children with autism. *Proc Natl Acad Sci U S A* **114**, 8119–8124 (2017).

168. Althammer, F., Muscatelli, F., Grinevich, V. & Schaaf, C. P. Oxytocin-based therapies for treatment of Prader-Willi and Schaaf-Yang syndromes: evidence, disappointments, and future research strategies. *Transl Psychiatry* **12**, 318 (2022).

169. Djupesland, P. G., Skretting, A., Winderen, M. & Holand, T. Breath actuated device improves delivery to target sites beyond the nasal valve. *Laryngoscope* **116**, 466–472 (2006).

170. Chung, S. *et al.* The nose has it: Opportunities and challenges for intranasal drug administration for neurologic conditions including seizure clusters. *Epilepsy Behav Rep* **21**, 100581 (2022).

171. Carter, C. S. *et al.* Is Oxytocin "Nature's Medicine"? *Pharmacological Reviews* **72**, 829–861 (2020).

172. Mairesse, J. *et al.* Oxytocin receptor agonist reduces perinatal brain damage by targeting microglia. *Glia* **67**, 345–359 (2019).

173. Johnson, M. C. *et al.* Effects of oxytocin receptor agonism on acquisition and expression of pair bonding in male prairie voles. *Transl Psychiatry* **14**, 286 (2024).

174. Franklin, R. J. M. & Simons, M. CNS remyelination and inflammation: From basic mechanisms to therapeutic opportunities. *Neuron* **110**, 3549–3565 (2022).

175. Medzhitov, R. The spectrum of inflammatory responses. *Science* **374**, 1070–1075 (2021).

176. Stary, C. M. *et al.* Nursing Markedly Protects Postpartum Mice From Stroke: Associated Central and Peripheral Neuroimmune Changes and a Role for Oxytocin. *Front. Neurosci.* **13**, (2019).

177. Yang, M. *et al.* Oxytocin Improves Intracerebral Hemorrhage Outcomes by Suppressing Neuronal Pyroptosis and Mitochondrial Fission. *Stroke* **54**, 1888–1900 (2023).

178. Devost, D., Wrzal, P. & Zingg, H. H. Oxytocin receptor signalling. in *Progress in Brain Research* (eds. Neumann, I. D. & Landgraf, R.) vol. 170 167–176 (Elsevier, 2008).

179. Ye, C. *et al.* Oxytocin Nanogels Inhibit Innate Inflammatory Response for Early Intervention in Alzheimer's Disease. *ACS Appl Mater Interfaces* **14**, 21822–21835 (2022).

180. Favrais, G. *et al.* Systemic inflammation disrupts the developmental program of white matter. *Ann Neurol* **70**, 550–565 (2011).

181. Klein, L. *et al.* A unique cerebellar pattern of microglia activation in a mouse model of encephalopathy of prematurity. *Glia* **70**, 1699–1719 (2022).

182. Semple, B. D., Blomgren, K., Gimlin, K., Ferriero, D. M. & Noble-Haeusslein, L. J. Brain development in rodents and humans: Identifying benchmarks of maturation and vulnerability to injury across species. *Prog Neurobiol* **0**, 1–16 (2013).

183. Obenaus, A. *et al.* A single mild juvenile TBI in male mice leads to regional brain tissue abnormalities at 12 months of age that correlate with cognitive impairment at the middle age. *Acta Neuropathol Commun* **11**, 32 (2023).

184. Kalafatakis, I. & Karagogeos, D. Oligodendrocytes and Microglia: Key Players in Myelin Development, Damage and Repair. *Biomolecules* **11**, 1058 (2021).

185. Yang, X. *et al.* Oxytocin Regulated Neuroinflammation through OTR/Mitochondria Mediated Pathway to Improve Hypoxia-Induced Brain Injury. *Mol Neurobiol* (2025) doi:10.1007/s12035-025-05061-7.

186. Miron, V. E. *et al.* M2 microglia and macrophages drive oligodendrocyte differentiation during CNS remyelination. *Nat Neurosci* **16**, 1211–1218 (2013).

187. Kumar, A. *et al.* NOX2 drives M1-like microglial/macrophage activation and neurodegeneration following experimental traumatic brain injury. *Brain Behav Immun* **58**, 291–309 (2016).

188. Zveik, O., Rechtman, A., Brill, L. & Vaknin-Dembinsky, A. Anti- and pro-inflammatory milieu differentially regulate differentiation and immune functions of oligodendrocyte progenitor cells. *Immunology* **171**, 618–633 (2024).

189. Forshammar, J. *et al.* Anti-inflammatory substances can influence some glial cell types but not others. *Brain Research* **1539**, 34–40 (2013).

190. Matcovitch-Natan, O. *et al.* Microglia development follows a stepwise program to regulate brain homeostasis. *Science* **353**, aad8670 (2016).

191. Meyer, U. *et al.* The time of prenatal immune challenge determines the specificity of inflammation-mediated brain and behavioral pathology. *J Neurosci* **26**, 4752–4762 (2006).

192. Dufour, A. *et al.* Neonatal inflammation impairs developmentally-associated microglia and promotes a highly reactive microglial subset. *Brain Behav Immun* **123**, 466–482 (2025).

193. Nemes-Baran, A. D., White, D. R. & DeSilva, T. M. Fractalkine-Dependent Microglial Pruning of Viable Oligodendrocyte Progenitor Cells Regulates Myelination. *Cell Reports* **32**, 108047 (2020).

194. Lawrence, K. E. *et al.* White matter microstructure shows sex differences in late childhood: Evidence from 6797 children. *Human Brain Mapping* **44**, 535–548 (2023).

195. Bartnik-Olson, B. *et al.* Evolving White Matter Injury following Pediatric Traumatic Brain Injury. *J Neurotrauma* **38**, 111–121 (2021).

196. Irzan, H. *et al.* White matter analysis of the extremely preterm born adult brain. *Neuroimage* **237**, 118112 (2021).

197. Ment, L. R., Hirtz, D. & Hüppi, P. S. Imaging biomarkers of outcome in the developing preterm brain. *Lancet Neurol* **8**, 1042–1055 (2009).

198. Nishiyama, A., Shimizu, T., Sherafat, A. & Richardson, W. D. Life-long oligodendrocyte development and plasticity. *Semin Cell Dev Biol* **116**, 25–37 (2021).

199. van Tilborg, E. *et al.* Combined fetal inflammation and postnatal hypoxia causes myelin deficits and autism-like behavior in a rat model of diffuse white matter injury. *Glia* **66**, 78–93 (2018).

200. Billiards, S. S. *et al.* RESEARCH ARTICLE: Myelin Abnormalities without Oligodendrocyte Loss in Periventricular Leukomalacia. *Brain Pathology* **18**, 153–163 (2008).

201. Du, M. *et al.* Endothelin-1–Endothelin receptor B complex contributes to oligodendrocyte differentiation and myelin deficits during preterm white matter injury. *Front Cell Dev Biol* **11**, 1163400 (2023).

202. Lloyd, A. F. *et al.* Central nervous system regeneration is driven by microglia necroptosis and repopulation. *Nat Neurosci* **22**, 1046–1052 (2019).

203. Garcia-Areas, R., Libreros, S. & Iragavarapu-Charyulu, V. Semaphorin7A: branching beyond axonal guidance and into immunity. *Immunol Res* **57**, 81–85 (2013).

204. Williams, A. *et al.* Semaphorin 3A and 3F: key players in myelin repair in multiple sclerosis? *Brain* **130**, 2554–2565 (2007).

205. Wang, L.-C. & Almazan, G. Cdon, a cell surface protein, mediates oligodendrocyte differentiation and myelination. *Glia* **64**, 1021–1033 (2016).

206. Hoehn, H. J. *et al.* Axl−/− mice have delayed recovery and prolonged axonal damage following cuprizone toxicity. *Brain Research* **1240**, 1–11 (2008).

207. Ray, A. K. *et al.* Loss of Gas6 and Axl signaling results in extensive axonal damage, motor deficits, prolonged neuroinflammation, and less remyelination following cuprizone exposure. *Glia* **65**, 2051–2069 (2017).

208. Forbes, T. A. *et al.* Environmental enrichment ameliorates perinatal brain injury and promotes functional white matter recovery. *Nat Commun* **11**, 964 (2020).

209. Bergles, D. E. & Richardson, W. D. Oligodendrocyte Development and Plasticity. *Cold Spring Harb Perspect Biol* **8**, a020453 (2016).

210. Faraji, J. *et al.* Oxytocin-mediated social enrichment promotes longer telomeres and novelty seeking. *Elife* **7**, e40262 (2018).

211. Faraji, J. *et al.* Regional Differences in BDNF Expression and Behavior as a Function of Sex and Enrichment Type: Oxytocin Matters. *Cereb Cortex* **32**, 2985–2999 (2022).

212. Neal, S., Kent, M., Bardi, M. & Lambert, K. G. Enriched Environment Exposure Enhances Social Interactions and Oxytocin Responsiveness in Male Long-Evans Rats. *Front Behav Neurosci* **12**, 198 (2018).

213. Vitalo, A. *et al.* Nest Making and Oxytocin Comparably Promote Wound Healing in Isolation Reared Rats. *PLOS ONE* **4**, e5523 (2009).

214. Grinevich, V., Desarménien, M. G., Chini, B., Tauber, M. & Muscatelli, F. Ontogenesis of oxytocin pathways in the mammalian brain: late maturation and psychosocial disorders. *Front Neuroanat* **8**, 164 (2015).

215. Newmaster, K. T. *et al.* Quantitative cellular-resolution map of the oxytocin receptor in postnatally developing mouse brains. *Nat Commun* **11**, 1885 (2020).

216. Yoshimura, R., Kimura, T., Watanabe, D. & Kiyama, H. Differential expression of oxytocin receptor mRNA in the developing rat brain. *Neuroscience Research* **24**, 291–304 (1996).

217. Liao, P.-Y., Chiu, Y.-M., Yu, J.-H. & Chen, S.-K. Mapping Central Projection of Oxytocin Neurons in Unmated Mice Using Cre and Alkaline Phosphatase Reporter. *Front Neuroanat* **14**, 559402 (2020).

218. Baudon, A., Clauss Creusot, E., Althammer, F., Schaaf, C. P. & Charlet, A. Emerging role of astrocytes in oxytocin-mediated control of neural circuits and brain functions. *Progress in Neurobiology* **217**, 102328 (2022).

219. Wahis, J. *et al.* Astrocytes mediate the effect of oxytocin in the central amygdala on neuronal activity and affective states in rodents. *Nat Neurosci* **24**, 529–541 (2021).

220. Kiss, M. G. *et al.* Interleukin-3 coordinates glial-peripheral immune crosstalk to incite multiple sclerosis. *Immunity* **56**, 1502-1514.e8 (2023).

221. Jo, M. *et al.* Astrocytic Orosomucoid-2 Modulates Microglial Activation and Neuroinflammation. *J Neurosci* **37**, 2878–2894 (2017).

222. Casden, N., Belzer, V., El Khayari, A., El Fatimy, R. & Behar, O. Astrocyte-to-microglia communication via Sema4B-Plexin-B2 modulates injury-induced reactivity of microglia. *Proceedings of the National Academy of Sciences* **121**, e2400648121 (2024).

223. Wang, P., Qin, D. & Wang, Y.-F. Oxytocin Rapidly Changes Astrocytic GFAP Plasticity by Differentially Modulating the Expressions of pERK 1/2 and Protein Kinase A. *Frontiers in Molecular Neuroscience* **10**, (2017).

224. Zhu, J. & Tang, J. LncRNA Gm14205 induces astrocytic NLRP3 inflammasome activation via inhibiting oxytocin receptor in postpartum depression. *Bioscience Reports* **40**, BSR20200672 (2020).

225. Basrai, H. S., Christie, K. J., Turbic, A., Bye, N. & Turnley, A. M. Suppressor of Cytokine Signaling-2 (SOCS2) Regulates the Microglial Response and Improves Functional Outcome after Traumatic Brain Injury in Mice. *PLoS One* **11**, e0153418 (2016).

226. Karve, I. P., Taylor, J. M. & Crack, P. J. The contribution of astrocytes and microglia to traumatic brain injury. *Br J Pharmacol* **173**, 692–702 (2016).

227. Witcher, K. G. *et al.* Traumatic brain injury-induced neuronal damage in the somatosensory cortex causes formation of rod-shaped microglia that promote astrogliosis and persistent neuroinflammation. *Glia* **66**, 2719–2736 (2018).

228. Todd, B. P. *et al.* Traumatic brain injury results in unique microglial and astrocyte transcriptomes enriched for type I interferon response. *Journal of Neuroinflammation* **18**, 151 (2021).

229. Semple, B. D. *et al.* Interleukin-1 Receptor in Seizure Susceptibility after Traumatic Injury to the Pediatric Brain. *J Neurosci* **37**, 7864–7877 (2017).

230. Liu, H., Leak, R. K. & Hu, X. Neurotransmitter receptors on microglia. *Stroke Vasc Neurol* **1**, 52–58 (2016).

231. Béchade, C. *et al.* The serotonin 2B receptor is required in neonatal microglia to limit neuroinflammation and sickness behavior in adulthood. *Glia* **69**, 638–654 (2021).

232. Eaton, J. L. *et al.* Organizational effects of oxytocin on serotonin innervation. *Developmental Psychobiology* **54**, 92–97 (2012).

233. Muscatelli, F., Desarménien, M. G., Matarazzo, V. & Grinevich, V. Oxytocin Signaling in the Early Life of Mammals: Link to Neurodevelopmental Disorders Associated with ASD. *Curr Top Behav Neurosci* **35**, 239–268 (2018).

234. Yoshida, M. *et al.* Evidence That Oxytocin Exerts Anxiolytic Effects via Oxytocin Receptor Expressed in Serotonergic Neurons in Mice. *Journal of Neuroscience* **29**, 2259–2271 (2009).

235. Raam, T., McAvoy, K. M., Besnard, A., Veenema, A. H. & Sahay, A. Hippocampal oxytocin receptors are necessary for discrimination of social stimuli. *Nat Commun* **8**, 2001 (2017).

236. Rokicki, J. *et al.* Oxytocin receptor expression patterns in the human brain across development. Preprint at https://doi.org/10.31219/osf.io/j3b5d (2021).

237. Mai, L., Inada, H. & Osumi, N. Whole-brain mapping of neuronal activity evoked by maternal separation in neonatal mice: An association with ultrasound vocalization. *Neuropsychopharmacology Reports* **43**, 239–248 (2023).

238. Miller, T. V. & Caldwell, H. K. Oxytocin during Development: Possible Organizational Effects on Behavior. *Front Endocrinol (Lausanne)* **6**, 76 (2015).

239. Zheng, J.-J. *et al.* Oxytocin mediates early experience–dependent cross-modal plasticity in the sensory cortices. *Nat Neurosci* **17**, 391–399 (2014).

240. Aulino, E. A. & Caldwell, H. K. Pharmacological manipulation of oxytocin receptor signaling during mouse embryonic development results in sex-specific behavioral effects in adulthood. *Hormones and Behavior* **135**, 105026 (2021).

241. Madrigal, M. P. & Jurado, S. Specification of oxytocinergic and vasopressinergic circuits in the developing mouse brain. *Commun Biol* **4**, 1–16 (2021).

242. Li, T., Wang, P., Wang, S. C. & Wang, Y.-F. Approaches Mediating Oxytocin Regulation of the Immune System. *Front. Immunol.* **7**, (2017).

243. Makinodan, M., Rosen, K. M., Ito, S. & Corfas, G. A critical period for social experience-dependent oligodendrocyte maturation and myelination. *Science* **337**, 1357–1360 (2012).

244. Nishimura, H. *et al.* Endogenous oxytocin exerts anti-nociceptive and anti-inflammatory effects in rats. *Commun Biol* **5**, 907 (2022).

245. Tamborski, S., Mintz, E. M. & Caldwell, H. K. Sex Differences in the Embryonic Development of the Central Oxytocin System in Mice. *Journal of Neuroendocrinology* **28**, (2016).

246. Sabihi, S., Durosko, N. E., Dong, S. M. & Leuner, B. Oxytocin in the prelimbic medial prefrontal cortex reduces anxiety-like behavior in female and male rats. *Psychoneuroendocrinology* **45**, 31–42 (2014).

247. Jia, R., Tai, F., An, S., Broders, H. & Sun, R. Neonatal manipulation of oxytocin influences the partner preference in mandarin voles (Microtus mandarinus). *Neuropeptides* **42**, 525–533 (2008).

248. Yamamoto, Y. *et al.* Neonatal manipulations of oxytocin alter expression of oxytocin and vasopressin immunoreactive cells in the paraventricular nucleus of the hypothalamus in a gender-specific manner. *Neuroscience* **125**, 947–955 (2004).

249. Watanabe, T. *et al.* Oxytocin receptor gene variations predict neural and behavioral response to oxytocin in autism. *Social Cognitive and Affective Neuroscience* **12**, 496–506 (2017).

250. Bertoni, A. *et al.* Oxytocin administration in neonates shapes hippocampal circuitry and restores social behavior in a mouse model of autism. *Mol Psychiatry* **26**, 7582–7595 (2021).

251. Csaba, G. Hormonal imprinting: its role during the evolution and development of hormones and receptors. *Cell Biology International* **24**, 407–414 (2000).

252. Csaba, G. The biological basis and clinical significance of hormonal imprinting, an epigenetic process. *Clin Epigenetics* **2**, 187–196 (2011).

253. Moerkerke, M. *et al.* Chronic oxytocin administration stimulates the oxytocinergic system in children with autism. *Nat Commun* **15**, 58 (2024).

254. Meziane, H. *et al.* An Early Postnatal Oxytocin Treatment Prevents Social and Learning Deficits in Adult Mice Deficient for Magel2, a Gene Involved in Prader-Willi Syndrome and Autism. *Biol Psychiatry* **78**, 85–94 (2015).

255. Alexander, G. M. *et al.* Remote Control of Neuronal Activity in Transgenic Mice Expressing Evolved G Protein-Coupled Receptors. *Neuron* **63**, 27–39 (2009).

256. Roth, B. L. DREADDs for Neuroscientists. *Neuron* **89**, 683–694 (2016).

257. Libbrecht, S. *et al.* Chronic chemogenetic stimulation of the anterior olfactory nucleus reduces newborn neuron survival in the adult mouse olfactory bulb. *Journal of Neurochemistry* **158**, 1186–1198 (2021).

258. Chohan, M. O., Fein, H., Mirro, S., O'Reilly, K. C. & Veenstra-VanderWeele, J. Repeated chemogenetic activation of dopaminergic neurons induces reversible changes in baseline and amphetamine-induced behaviors. *Psychopharmacology (Berl)* **240**, 2545–2560 (2023).

259. Krishnan, M. L. *et al.* Integrative genomics of microglia implicates DLG4 (PSD95) in the white matter development of preterm infants. *Nat Commun* **8**, 428 (2017).

260. Schang, A.-L. *et al.* Epigenetic priming of immune/inflammatory pathways activation and abnormal activity of cell cycle pathway in a perinatal model of white matter injury. *Cell Death Dis* **13**, 1038 (2022).

261. Kochanek, P. M., Wallisch, J. S., Bayır, H. & Clark, R. S. B. Pre-clinical models in pediatric traumatic brain injury-challenges and lessons learned. *Childs Nerv Syst* **33**, 1693–1701 (2017).

262. Pinto, P. S., Poretti, A., Meoded, A., Tekes, A. & Huisman, T. A. G. M. The unique features of traumatic brain injury in children. Review of the characteristics of the pediatric skull and brain, mechanisms of trauma, patterns of injury, complications and their imaging findings--part 1. *J Neuroimaging* **22**, e1–e17 (2012).

263. Rostami, E. *et al.* The Terminal Pathway of the Complement System Is Activated in Focal Penetrating But Not in Mild Diffuse Traumatic Brain Injury. *Journal of Neurotrauma* **30**, 1954–1965 (2013).

264. Bender, D., Holschbach, M. & Stöcklin, G. Synthesis of n.c.a. carbon-11 labelled clozapine and its major metabolite clozapine-N-oxide and comparison of their biodistribution in mice. *Nucl Med Biol* **21**, 921–925 (1994).

265. Manvich, D. F. *et al.* The DREADD agonist clozapine N-oxide (CNO) is reverse-metabolized to clozapine and produces clozapine-like interoceptive stimulus effects in rats and mice. *Sci Rep* **8**, 3840 (2018).

266. Paolicelli, R. C. *et al.* Microglia states and nomenclature: A field at its crossroads. *Neuron* **110**, 3458–3483 (2022).

267. Eze, U. C., Bhaduri, A., Haeussler, M., Nowakowski, T. J. & Kriegstein, A. R. Single-cell atlas of early human brain development highlights heterogeneity of human neuroepithelial cells and early radial glia. *Nat Neurosci* **24**, 584–594 (2021).

268. Gerrits, E., Heng, Y., Boddeke, E. W. G. M. & Eggen, B. J. L. Transcriptional profiling of microglia; current state of the art and future perspectives. *Glia* **68**, 740–755 (2020).

269. Grund, T. *et al.* Chemogenetic activation of oxytocin neurons: Temporal dynamics, hormonal release, and behavioral consequences. *Psychoneuroendocrinology* **106**, 77–84 (2019).

270. An, X. *et al.* Protective effect of oxytocin on LPS-induced acute lung injury in mice. *Sci Rep* **9**, 2836 (2019).

271. Greenhalgh, A. D., David, S. & Bennett, F. C. Immune cell regulation of glia during CNS injury and disease. *Nat Rev Neurosci* **21**, 139–152 (2020).

272. Landgraf, R. & Neumann, I. D. Vasopressin and oxytocin release within the brain: a dynamic concept of multiple and variable modes of neuropeptide communication. *Frontiers in Neuroendocrinology* **25**, 150–176 (2004).

273. Browne, J. V., Jaeger, C. B., Kenner, C., & Gravens Consensus Committee on Infant and Family Centered Developmental Care. Executive summary: standards, competencies, and recommended best practices for infant- and family-centered developmental care in the intensive care unit. *J Perinatol* **40**, 5–10 (2020).

274. Macho, P. Individualized Developmental Care in the NICU: A Concept Analysis. *Adv Neonatal Care* **17**, 162–174 (2017).

275. Hodgson, C. R., Mehra, R. & Franck, L. S. Infant and Family Outcomes and Experiences Related to Family-Centered Care Interventions in the NICU: A Systematic Review. *Children* **12**, 290 (2025).

276. Duke, T. New WHO standards for improving the quality of healthcare for children and adolescents. *Arch Dis Child* **103**, 625–627 (2018).

277. Lyngstad, L. T. *et al.* Ten Years of Neonatal Intensive Care Adaption to the Infants' Needs: Implementation of a Family-Centered Care Model with Single-Family Rooms in Norway. *Int J Environ Res Public Health* **19**, 5917 (2022).

278. McKay, E. C. *et al.* Peri-Infarct Upregulation of the Oxytocin Receptor in Vascular Dementia. *J Neuropathol Exp Neurol* **78**, 436–452 (2019).

279. Gu, X. *et al.* Pharmacologically Induced Hypothermia Attenuates Traumatic Brain Injury in Neonatal Rats. *Exp Neurol* **267**, 135–142 (2015).

280. Chhor, V. *et al.* Role of microglia in a mouse model of paediatric traumatic brain injury. *Brain Behav Immun* **63**, 197–209 (2017).

281. Hanlon, L. A., Huh, J. W. & Raghupathi, R. Minocycline Transiently Reduces Microglia/Macrophage Activation but Exacerbates Cognitive Deficits Following Repetitive Traumatic Brain Injury in the Neonatal Rat. *J Neuropathol Exp Neurol* **75**, 214–226 (2016).

282. Hamood, Y. *et al.* Sex specific effects of buprenorphine on behavior, astrocytic opioid receptor expression and neuroinflammation after pediatric traumatic brain injury in mice. *Brain Behav Immun Health* **22**, 100469 (2022).

283. Fletcher, J. L. *et al.* Acute treatment with TrkB agonist LM22A-4 confers neuroprotection and preserves myelin integrity in a mouse model of pediatric traumatic brain injury. *Exp Neurol* **339**, 113652 (2021).

284. Webster, K. M. *et al.* Targeting high-mobility group box protein 1 (HMGB1) in pediatric traumatic brain injury: Chronic neuroinflammatory, behavioral, and epileptogenic consequences. *Experimental Neurology* **320**, 112979 (2019).

Acknowledgements

There are many people to thank for the creation of this thesis. They helped in multiple stages of the last 4 and a half years, and from multiple countries. They have been invaluable in guiding me through this PhD journey. Although my gratitude cannot be expressed in words, I will give it a try.

Olivier. The first big thanks of course goes out to you. We made it! I still remember the first time we met, in the lobby of the HUG in November 2020. With big plans and dreams, and here we are now. I feel lucky to have done this adventure with you as a boss. You have been so very empathetic, understanding, warm and kind. I very much appreciate that you saw me as a person beyond the PhD student, and I felt very supported in the whole journey. I am proud of the work we achieved together, and I will keep the things you taught me with me for the rest of my career.

Stéphane. The second big thank you goes out to my co-supervisor. Thank you for spontaneously accepting me as you PhD-student this last year. We did not have that many interactions but your calming presence was a welcome influence in the last months. And! You introduced me to my new love: Indian food.

Eduardo. The undisputed barbecue master. I cannot express how thankful I am for you. You grew from just a funny colleague in the beginning into a real mentor, confidant and friend in the end. Crazy Dutch and Zwarte Piet. You and your office fridge of beers have been the cheapest and most welcome therapy session these last 2 years ("come have a beer, girl"). Your work ethic has been a true inspiration. Every time I had to work late nights, you were also there. Every time I had to come in on the weekend, you were also there. I think I would have gone crazy without you, so thank you for keeping my sanity. Together with Gabriel, you two Brazilian-boys have led me to the finish line, and I so enjoyed the many *many* beers, Inglewood Gorgodzilla nights, PhD memes and chicken-heart skewers it took in the process. Once, with a glass of free wine in hand looking out over the vinyards of Lavaux you spoke the now-famous words "You know, I don't deserve anything less in life". Thank you for making me believe that I don't, either.

Gabriel. The other part of the Brazilian-boys, and third member of the Zwarte Pieten lab. O how you were an angel sent by a higher power. I don't want to say that you saved my PhD, but I don't see I could have gotten so much done without your help in the last year of experiments. Your knowledge, expertise, can-do attitude and creativity are unmatched and I am *very* thankful that Schmidheiny brought you into my life. It has been a joy sharing my office with you, talking about your time in Groningen, ranting about the Annemasse train, and coming up with ways to make a stable income in Paris (selling Eiffel towers seems lucrative).

I would also like to thank past members of the Baud lab: **Jerome**, for taking me under your wing and showing me around the lab those first months. **Marie-Laure**, for introducing me to (social) life in Switzerland, for teaching me the importance of a nice, French, lunch ("sad lunch" no more), and for being my first friend in Geneva. **Alice**, for your calmness in the lab and your guidance in life. And, maybe more importantly, for introducing me to my great love: Sézane. Also many thanks to **Yohan**, **Noemi**, **Chloe**, **Roxanna**, **Dini** and **Laura**, for a very joyful 4 years in our joint Sizonenko-Baud lab.

To my students: **Ines**, **Giorgia**, **Nico**, and **Gabrielle**, I have very much enjoyed guiding you and seeing you develop as a scientist and a person. You were all different and I like to think we helped each other grow. I hope you are doing well wherever you are!

There is one student I want to thank especially: **Ece**. My prodigy. My confidant. My friend. In the 2 years that we worked intensely together, you became my right hand, left hand, and both my feet. Not only in the lab, but we also grew very close over lunch and coffee sessions. The outings we had together with Gabriel and Eduardo are some of my favorite moments from the past 4 years. Not only are you a great human-being, a great friend, but also a fantastic scientist. I am proud to see you thrive in another lab, and I look forward to the next trip to Paris you will take so I can stalk you again with all my tips.

Not only the direct colleagues were important in the creation of this thesis, but also the work environment in general. So I would like to thank all the people from the 3rd floor of La Tulipe: **Philippe**, **Ben**, **Stergios**, **Pia**, **Kelly**, **Laurène**, and **Aurélien** from the Millet lab. Thank you for your insights into my research, but also just for the fun times, the culinary lessons you taught me ("Gouda is not cheese"), helping me translate French, or even being my personal assistants handling my administration *bordels*. I know it must not have been easy in an all-French environment having this one girl speak English, but we made it work (and we became *très* good at speaking Frenglish, *non*?). I want to thank in particular **Quentin**. You were the first PhD friend I had. I have learned so much from you and it was an inspiration seeing your thrive and make it to the finish line! You have become a confidant, a car vendor (!), and my personal guide through the intricate thesis submission shenanigans. I know that I have a friend for life in you, **Nathalie** and **Sofia**. Then, from Menicon (R.I.P.), thanks to **Melody**, **Verena**, **Maryam** and **Paul**. I sort of sneakily invaded your company's lunch sessions, which you kindly turned into an open invitation. It was always fun to chat, vent, and be inspired. I wish you all the best in your new ventures.

Paolo. The guardian of the most important room of La Tulipe: the animal facility. Thank you so much for taking such good care of my mice, it must have not been easy with my never-ending breeding schedule and constant checking of births. I truly enjoyed our intense collaboration, which was heavily complicated by our language barrier – but we made it work. And I apologize again for scaring you with a blue mouse that one time.

Jean-Luc. Weren't you just a little gift out of nowhere. I already very much enjoyed our (shockingly efficient!) professional collaboration, but once we found out that we both play basketball, *c'etait partiiiiii*. You stepped above and beyond your job description to advise me on my project, with the climax that you even went back in the lab after 10 years to perform an experiment for me (that ended up being the most beautiful immuno of the whole thesis – you f*cker). Thank you so much for the many joy-filled coffee chats and lunch sessions – except for that one time when you proudly showed me photos of your ~~ugly~~ car. I am still recovering from that. *À la prochaine*!

And then the people in Geneva who were as important to the last four years, not necessarily for the scientific content of this book, but for the existence of this book in general, as they are the people who took me in and created my home away from home.

First of all, my girl-boss partners-in-crime, my fellow-PhD troopers **Martina** and **Abigail**. Walking into that first class of the MRI course in fall of 2022 I never thought I was going to meet friends for life. I thought I was doing fine without many social contacts at Unige, but your friendship turned out to be the gift I didn't know I needed. Although our research areas are so very different – it always gave me great pleasure wowing you with stories and footage of new mouse experiments – we go through the same things and you were always there to hear out my rants, to give me advice and even to provide a shoulder

to cry on. And how fun has it been to exchange stories of how things are done in America, Italy and the Netherlands, and trying to pronounce vowels in ways that our cultural heritage just doesn't allow (Ma*rrrrrr*tina - impossible). Your constant support and perpetual believe in me is truly invaluable and our sisterhood has been a magical thing to experience. Brunch sessions, sushi dates, (very bad) Indian food, concerts, walks in the sun, running in the rain, ice-cream and wine nights, beach-time, and auntie cuddle sessions with future girl-boss babygirl **Ayris**; You girls are my light and my joy, and I cannot wait to see all the places we go.

Esther. My dear Esther. Sometimes you have an immediate connection with someone and that is how I felt with you, that first practice at International basketball club summer of 2021. We immediately bonded over our exchange experiences in Toronto and our shared humor (remember your old-school basketball shorts?!). So when I quit the team later that summer, I was very sad to not see you again and so I "asked you out" for a drink. A strange experience but I am very happy I did because you have become a lifelong friend ever since. From battling on the court for three seasons of rivalry basketball matchups (more fun for me in the beginning, before you started beating us ;p), to us making all kinds of plans and then just always ending up in the bar. Let the record show that we did hike that 1 time (and watched a documentary about hiking). You and **Manu** are always there for me and your calming presence and "*t'inquiète,* it will be fine" attitude has been so valuable for keeping my sanity.

My **St Jean basketball team**. In all the foreign countries I have lived, basketball has been a way to find a basis, a home. And such was the case in Geneva as well, when I joined St Jean Basket in September 2021. It was a new experience to get used to basketball terms in French (you would think "screen" is still "screen", but no) and I so enjoyed learning about culture from the wide range of personalities and job types that our team was made up from. **Prisca, Pierrine, Bomba, Georges, Nono, Nora, Christine, Jackie, Randy, Anna**, thank you all for the fun times, and the 3 trophies we collected over the years! Some people I want to mention in particular. **Ghju** and **Alex**. You took care of me and were there for me literally 24/7. And how many times did you drive me home after a game or a practice?! I really felt taken care of in a foreign place and that was because of you. Thank you. **Ced**. Coach Ced. My man. O what big dreams we had. I remember the first time I saw you and I nearly beat you in a game of horse. Mind you, I shot 90%, but it still wasn't enough to beat you. We instantly bonded over our love of American (college) basketball and I so very enjoyed that season you were our coach. Your believe in me on the court was so empowering, and I learned so much from your guidance and your stories. And then of course **Candela**. Mamacita Candelita. How many times did you have me running in circles trying to chase you on the basketball court?! Speedy Gonzales. Your warmth and joy and love are unmatched and I am so happy we developed a profound friendship. The sound of your laughter ("kast!") has been the best medicine in difficult times. You are among the kindest, warmest people I know, and I cannot express how grateful I am to all that you and your family have done for me this last year. Mi corazón canta cuando está contigo. Thank you for your friendship.

I say Geneva has been my home away from home, and there are so many people in my *home* home that have supported me in the past 4 years, and in particular the final 6 months. So now I switch to Dutch, to thank my family and my friends back home, in Utrecht, me stadsie.

Jim. De Paul van mijn Simone. Ik ben heel dankbaar voor onze band, die sinds 4 VWO alleen maar sterker is geworden. Je bent als een broer voor me. En **Margreet** en **Piet** voelen ook als familie. Jij en je piano staan altijd klaar voor me (danwel vergezeld door een fles Limoncello om moed in te drinken) en dat brengt m'n hart zo'n plezier. Jij kent me als geen ander, bij jou hoef ik niks uit te leggen. Je bent

een inspiratie, in het leven, en zeker tijdens het afronden van de PhD. *"Wat moet ik nou, zo zonder jou?"* Gelukkig hoef ik me daar geen zorgen om te maken.

Rennie. Lieve Ren. Van samen noedelsoep koken en NPO documentaires kijken op onze kleine studentenkamers op de Braamstraat in 2015, naar het delen van de meest diepgaande en moeilijke gedachtes over een glas limonade (zonder vodka shot) op SOIA 10 jaar later. Mijn ziel voelt zich verbonden met de jouwe en ik kan bij jou met alles terecht. Bedankt voor de vele jaren onszelf zijn. Op tien duizend luchtballonnen en nog vele K3 dansjes!

Jordy. Bedankt voor al je steun en het geloven in mij en mijn dromen.

Mijn basketbalfamilie. Weetje, het is echt moeilijk geweest om aan mensen in Geneve uit te leggen hoe diep onze band is, frankly omdat ze zich dat gewoon niet voor kunnen stellen. Ik dacht ook dat het vrij normaal was, hoe hecht het team is, maar hoe meer verschilende plekken ik woon, hoe meer ik reminded wordt van onze speciale band als teammates and friends. Bedankt aan alle meiden en coaches van **Bulls dames 1**, voor het omarmen van me in het team en de heerlijke feestjes die we samen bouwen (Shots! Shots! Shots, shots, shots, shots!). Ook veel dank aan **Oud Maar Goud**. Hoewel we al lang niet meer allemaal in hetzelfde team zitten ben ik blij en trots hoe we nog verbonden zijn. Ik heb me de afgelopen 4 jaar steeds zo welkom en betrokken gevoeld door jullie, op afstand, en natuurlijk toen jullie me allemaal kwamen opzoeken en we ons moesten beschermen tegen Pierre de koe (maar gelukkig was Jacques er om ons te beschermen). Jullie zijn denk ik wel mijn meest invloedrijke vrienden van de afgelopen 10 jaar, en dat neem ik niet voor lief.

En dan in het bijzonder nog even Tammie en Shanta. **Tammie**, jouw PhD journey is zo inspirerend geweest voor me. De herinnering van hoe jij aan het shinen was op je verdediging heeft me meerdere malen op de been gehouden tijdens m'n eigen afrondingsproces. Het is zo fijn geweest mijn frustraties met je te delen – die je altijd moeiteloos begreep – en ik heb zo geteerd op jouw lieve aanmoediging en steun in de rug. Dat kun je je niet voorstellen. En natuurlijk de laatste maanden, toen je letterlijk je huis aan me hebt opengesteld en deed alsof dat de gewoonste zaak van de wereld was. En dan **Shanta**, de mayonaise van mijn patat, de scorer van mijn assist. Tien jaar geleden maakte ik oogcontact met jouw resting bitch face en mijn leven is nooit meer hetzelfde geweest. In sickness en in health, voor de meest onnozele dingen, en de meest moeilijke dingen. Je bent er altijd voor me. Bedankt voor je onvoorwaardelijke vriendschap.

De **Knoopjes**. Lieve **Tom**, **Renske**, **Niek**, **Nella**, **Maike** en **Martin**. Little baby Marit is all grown up! Heel veel dank aan mijn lieve grote (schoon) broers en zussen die me hebben laten opgroeien, me hebben uitgedaagd en me hebben gemaakt tot de persoon die ik ben. Bedankt voor de support over de jaren, allemaal op jullie eigen manier. Ik prijs me heel gelukkig met onze familie, die alleen maar mooier is geworden door de leuke nichtjes en het leuke neefje die jullie me hebben gegeven: **Max**, **Ymke**, **Noa** en **Anne**. Enneh, ik verwacht vanaf nu dat elke verjaardagskaart geaddresseerd wordt aan Dr. Marit :P

Mama en **papa**. Mijn OG chearleaders. Ik heb door jullie altijd gevoeld dat ik alles kan wat ik wil. Geen lat ligt te hoog, geen plan is te mal. Bedankt voor jullie onvoorwaardelijke steun en vertrouwen in mij en mijn dromen. Jullie staan 24/7 voor me klaar en nemen altijd de telefoon op, ook al is het midden in de nacht, en van duizenden kilometers ver weg (en moet je ineens om 2 uur 's nachts instructies geven hoe een Franse waterpomp te ontlasten). Dat gevoel is heel bijzonder. Ik hoop dat ik jullie trots heb gemaakt met het behalen van dit graad, maar tegelijkertijd wil ik jullie ook bedanken voor het gevoel dat dit graad helemaal niet uitmaakt voor jullie. Jullie zijn altijd trots. En ik op jullie, ik hou van jullie.

I would like to finish my acknowledgements with some **final words**. Doing a PhD in translational neuroscience is something I have dreamed of since the first year of my Bachelor studies. It has long been the main goal of my life, the compass guiding my decisions. Having completed it now feels like the greatest achievement of my life. Do not get me wrong – I hugely underestimated it and there were many lows along the way. But it taught me so much. About science, about life, about different cultures, and about myself. I am so proud of what I achieved, and that has been because of all of you. This thesis was written in Pâquis, Eaux-Vives, Champel, Nyon, Zuilen, Kattenbroek, Kanaleneiland and Oog-in-al, in the homes of dear friends who opened their doors for me in times of need. I have felt so loved, and so supported. I am proud of this work, but I am even prouder of the wonderful people I have gathered around me over the years. That has been the real accomplishment. Thank you.

Publications and awards

List of published articles associated with this thesis

1. **Knoop, M.**, Possovre, ML., Trak, E., Van de Looij, Y., Sanches, E., Tsartsalis, S., Pansiot, J., Schirmbeck, G. & Baud, O. (*submitted to Nature Comms*). Neonatal oxytocin release mitigates neuroinflammation and rescues neural correlates of encephalopathy of prematurity

2. **Knoop, M.**, Trak, E., Possovre, ML., Van de Looij, Y., Schirmbeck, G., Ceyzériat, K., Pitetti, JL., Sanches, E., Musardo, S., Millet, P., Tsartsalis, S., Tournier, BB., Bellone, C., Sizonenko, S., Jacquens, A., & Baud, O. (2025). Oxytocin release modulates acute neuroinflammation and improves brain development after pediatric traumatic brain injury. bioRxiv 2025.06.02.652172; doi: https://doi.org/10.1101/2025.06.02.652172

3. Baud, O., & **Knoop, M.** (2024). Oxytocine et neuroprotection en période néonatale : évidences conceptuelles et précliniques [Oxytocin as a neuroprotective strategy in neonates: concept and preclinical evidence]. Gynecologie, obstetrique, fertilite & senologie, 52(6), 418–424. https://doi.org/10.1016/j.gofs.2023.12.005

4. Baud, O., **Knoop, M.**, Jacquens, A., & Possovre, M. L. (2022). Ocytocine : une nouvelle cible de neuroprotection ? [Oxytocin: a new target for neuroprotection?]. Biologie aujourd'hui, 216(3-4), 145–153. https://doi.org/10.1051/jbio/2022012

5. **Knoop, M.**, Possovre, M. L., Jacquens, A., Charlet, A., Baud, O., & Darbon, P. (2022). The Role of Oxytocin in Abnormal Brain Development: Effect on Glial Cells and Neuroinflammation. Cells, 11(23), 3899. https://doi.org/10.3390/cells11233899

6. Musardo, S., Contestabile, A., **Knoop, M.**, Baud, O., & Bellone, C. (2022). Oxytocin neurons mediate the effect of social isolation via the VTA circuits. eLife, 11, e73421. https://doi.org/10.7554/eLife.73421

7. Zinni, M., Pansiot, J., Colella, M., Faivre, V., Delahaye-Duriez, A., Guillonneau, F., Bruce, J., Salnot, V., Mairesse, J., **Knoop, M.**, Possovre, M. L., Vaiman, D., & Baud, O. (2021). Impact of Fetal Growth Restriction on the Neonatal Microglial Proteome in the Rat. Nutrients, 13(11), 3719. https://doi.org/10.3390/nu13113719

List of international congresses where work of this thesis was presented

1. *2024 SFAR congress, Paris*: Oxytocin as a novel therapeutic target to reduce neuroinflammation and protect neural development following pediatric traumatic brain injury in mice. **M. Knoop**, E. Trak, ML. Possovre, K. Ceyzeriat, A. Jacquens, O. Baud

2. *2024 FENS Forum, Vienna*: Oxytocin as a novel therapeutic target to reduce neuroinflammation and protect brain development following pediatric traumatic brain injury. **Marit Knoop**, Ece Trak, Marie-Laure Possovre, Kelly Ceyzeriat, Yohan Van de Looij, Alice Jacquens, & Olivier Baud

3. *2023 Glia meeting, Berlin*: Increased oxytocin activity via chemogenetic modulation positively affects microglial reactivity and brain development in a mouse model of neonatal inflammation. **Marit Knoop**, Marie-Laure Possovre, Yohan Van de Looij, Nicolas Marti Mencias, Ece Trak, Gabrielle Michon, Jerôme Mairesse, Alice Jacquens, Kelly Ceyzeriat & Olivier Baud

4. *2023 DNF Symposium, Lausanne*: Increased oxytocin activity via chemogenetic modulation alleviates microglial reactivity and restores normal brain development in a new mouse model of neonatal inflammation. **Marit Knoop**, Marie-Laure Possovre, Ece Trak, Kelly Ceyzeriat, Alice Jacquens, Yohan Van de Looij & Olivier Baud

5. *2022 FENS-Hertie winter school, Obergurgl*: The effect of oxytocin on reactive microglia in a mouse model of neonatal neuroinflammation. **Marit Knoop**, Marie-Laure Possovre, Alice Jacquens, Stefano Musardo, Yohan Van de looij, Camilla Bellone, Olivier Baud,

Awards and stipends won for the work associated with this thesis

1. 2024: Winner of the Jean Falk-Vairant award for best clinical neuroscience PhD presentation in the Annual Meeting of the NeuroLeman Network and Doctoral Schools

2. 2022: Laureate of the fonds Jean Falk-Vairant travel grant for the FENS-Hertie Winter school "Neuroimmune interactions in health and disease" in Obergurgl, Austria

Curriculum Vitae

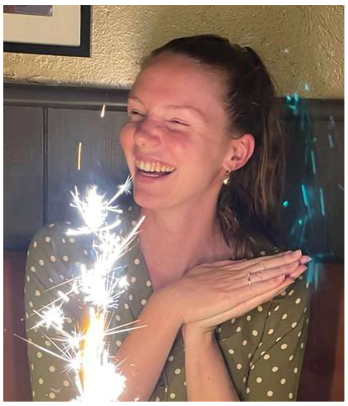

Marit Susan Knoop was born on the 13th of July in Amersfoort, the Netherlands, as the youngest of four children. She started her studies in 2014, with Biological Psychology at Utrecht University. She was accepted into the Honors Program, joined the faculty as a teaching-assistant and spent an exchange semester at the University of Toronto studying molecular neuroscience. In Toronto, she received the Outstanding Community Member award for her contributions to the campus residence community. She obtained her Bachelor's degree in 2018, with cum-laude distinctions. Marit continued her studies with the Master's program Neuroscience & Cognition at Utrecht University. After extensive research internships at the VU university medical center, Utrecht university medical center and Wilhelmina Children's Hospital, Marit graduated from her Master's program in 2020 with a degree in Translational Neuroscience. In Spring of 2021, she moved to Geneva, Switzerland, to start her PhD research on oxytocin as a neuroprotectant for newborn brain injury in the laboratory of Prof. Dr. Olivier Baud. The findings of said research are presented in the current thesis. During her PhD, Marit supervised 4 master thesis students and 1 bachelor thesis student, published papers in peer-reviewed journals and presented her findings at international conferences. In 2024, she received the Jean Falk-Vairant prize for best clinical neuroscience PhD presentation in the Lake Geneva region, for her work on oxytocin as a neuroprotectant in pediatric traumatic brain injury. After obtaining her doctorate, Marit plans to go on a nice vacation, and then find a job where she can continue her translational research on finding therapeutic targets for the injured brain.

Appendices

Appendix A: The role of oxytocin in abnormal brain development: effect on glial cells and neuroinflammation. (2022). *Cells*

Appendix B: Oxytocin release modulates acute neuroinflammation and improves brain development after pediatric traumatic brain injury *(submitted to Annals of Neurology)*

Appendix C: Neonatal oxytocin release mitigates neuroinflammation and rescues neural correlates of encephalopathy of prematurity *(submitted to Nature Communications)*

Appendix D: Immunohistochemistry of CD68+ phagocytic activity 24h after TBI

Appendix A

The role of oxytocin in abnormal brain development: effect on glial cells and neuroinflammation

Knoop M, Possovre ML, Jacquens A, Charlet A, Baud O, and Darbon P. *Cells*. **2022**, *11*, 3899. doi: 10.3390/cells11233899. PMID: 36497156.

Appendix B

Oxytocin release modulates acute neuroinflammation and improves brain development after pediatric traumatic brain injury

Knoop M, Trak E, Possovre ML, Van de Looij Y, Schirmbeck G, Ceyzériat K, Pitetti JL, Sanches E, Musardo S, Millet P, Tsartsalis S, Tournier BB, Bellone C, Sizonenko S, Jacquens A, and Baud O. bioRxiv 2025.06.02.652172; doi: https://doi.org/10.1101/2025.06.02.652172

Oxytocin release modulates acute neuroinflammation and improves brain development after pediatric traumatic brain injury

(1) Authors:

Marit Knoop, MSc,[1] Ece Trak, MSc,[1] Marie-Laure Possovre, PhD,[1] Yohan van de Looij, PhD,[1,2] Gabriel Schirmbeck, PhD,[1] Kelly Ceyzériat, PhD,[3] Jean-Luc Pitetti, PhD,[4] Eduardo Sanches, PhD,[1] Stefano Musardo, PhD,[5] Philippe Millet, MD, PhD,[6] Stergios Tsartsalis, MD, PhD,[6] Benjamin B. Tournier, PhD,[6] Camilla Bellone, PhD,[5] Stéphane V. Sizonenko, MD, PhD,[1] Alice Jacquens, MD, PhD[7,8#] & Olivier Baud, MD, PhD[1,7,9,10#,*]

(2) Affiliations:

[1] Department of Child Growth and Development, Faculty of Medicine, University of Geneva, 1205 Geneva, Switzerland

[2] Center for Biomedical Imaging (CIBM), Animal Imaging Technology Section, Ecole Polytechnique Fédérale de Lausanne (EPFL), Lausanne, Switzerland: Yohan van de Looij

[3] Center for Biomedical Imaging (CIBM), University of Geneva, 1205 Geneva, Switzerland

[4] Laboratory animal facility, University of Geneva, 1205 Geneva, Switzerland

[5] Department of Basic Neuroscience, Faculty of Medicine, University of Geneva, 1205 Geneva, Switzerland

[6] Department of Psychiatry, University Hospital of Geneva and University of Geneva, 1205 Geneva, Switzerland

[7] Faculty of Medicine, Université Paris Cité, Inserm, NeuroDiderot, 75019 Paris, France

[8] Sorbonne University, GRC 29, AP-HP, DMU DREAM, Department of Anaesthesiology and Critical Care Medicine, Pitié-Salpêtrière Hospital, 75013 Paris, France

[9] Obstetric, Perinatal, Paediatric and Life Course Epidemiology Team (OPPaLE), Center for Research in Epidemiology and StatisticS (CRESS), Alimentation Et L'Environnement (INRAe), Institut National Pour La Santé Et La Recherche Médicale (INSERM, French Institute for Health and Medical ResearchInstitut National de Recherche Pour L'Agriculture, Paris Cité University, Paris, France

[10] Department of Neonatal Medicine, FHU Prem'Impact, Cochin-Port Royal Hospital, Assistance Publique-Hôpitaux de, Paris Cité University , 75014, Paris, France

[#] These authors contributed equally

*Corresponding author

(3) Corresponding author's contact information:

Pr Olivier Baud, MD-PhD

tel: +33158412423 fax: +3358413641 email:olivier.baud@aphp.fr

(4) number of characters in the title: 107 (spaces excluded)

(5) Number of words:

Abstract: 246

Introduction: 309

Discussion: 1128

Body of manuscript (Introduction, Methods, Results and Discussion combined): 4499

(6) Number of figures (color): 8

Number of supplementary tables: 2

Number of supplementary figures (color): 7

Abstract

Objective: Pediatric traumatic brain injury (TBI) is a leading cause of death and disability in infants, whose neurodevelopmental consequences currently lack effective treatment. Since TBI is associated with neuroinflammation, modulation of the post-injury neuroinflammatory response is a promising strategy. Oxytocin is suggested to possess anti-inflammatory properties, and seems to play a role in clinical interventions that improve brain development in neonates. However, the underlying mechanisms remain unclear, as does its applicability to acute brain injury.

Methods: Here, we assess the effects of chemogenetic activation of oxytocinergic neurons on acute neuroinflammation and on long-term brain development after TBI in postnatal day 7 (P7) male mice. Immunohistochemistry, RNA sequencing, *ex-vivo* MRI-diffusion tensor imaging, *in-vivo* functional ultrasound imaging and behavioral assays are used for assessment. Oxytocinergic neurons were activated daily between P7 and P10.

Results: We show that oxytocin release mitigates the acute neuroinflammatory response to TBI 24h post-injury, where it reduces the expression of immune and inflammation-related genes in astrocytes and promotes brain repair and development gene pathways in microglia. In the long-term, early-life oxytocin exposure improves subcortical and cortical white matter damage after TBI, prevents hyperactivity and loss of social behavior, and restores TBI-induced alterations in resting-state functional connectivity of the isocortex. These therapeutic effects were found 35 days after the last oxytocin activation session.

Conclusion: These findings enhance our understanding of neuroinflammation modulation by oxytocin and its long-term effects, and further support intervention associated with endogenous oxytocin release as a promising neuroprotective strategy in pediatric TBI.

Introduction

Pediatric traumatic brain injury (TBI) is a leading cause of death and disability in children aged 0 to 4 years caused by falls, motor vehicle injuries or physical abuse.[1,2] The developing brain is particularly vulnerable to physical trauma due to an underdeveloped immune system where early-life microglia are more implicated in functions related to brain development rather than immune processes.[3] Simultaneously, TBI can interrupt key maturational processes leading to long-lasting impact on a child's functioning in all facets of life.[4,5]

Current treatments for pediatric TBI are invasive, minimally effective, and not tailored to the pediatric population.[6] A novel promising approach to tackle TBI-induced neuroinflammatory is the modulation of microglia and astrocytes activation and phenotypes to positively brain injury outcomes.[7]

One treatment option with strong clinical potential is oxytocin, a nonapeptide secreted by hypothalamic neurons, that project to all major regions of the brain – including the limbic and cortical areas.[8] Historically known for its social properties, oxytocin is gaining interest for its importance in the postnatal period and its association to brain development.[9] Clinical interventions that indirectly increase oxytocin levels in the newborn – such as skin-to-skin exposure or music therapy – were associated with improved neurodevelopment of the child.[10,11] Some preclinical studies also suggest a link between oxytocin agonists exposure and modulation of microglial cells reactivity in brain injury models different from TBI.[12–14] However, whether endogenous oxytocin release could affect inflammation in the developing brain and specifically in pediatric TBI remains to be explored.

In this study, we assessed endogenous oxytocin release as a treatment for pediatric TBI in newborn male mice, using a clinically-relevant model of pediatric TBI and a chemogenetic tool to manipulate oxytocinergic neuron activity. We found that only a few sessions of oxytocinergic neurons burst firing within the 4 days following TBI are sufficient to mitigate acute-phase neuroinflammation and to exert long-term positive effects on brain development.

Methods

An extended version of the methods is available as Supplementary materials.

Animal models

This study was approved by Ethical Committee for Animal Experiments of the University of Geneva and the Veterinary Office of Geneva (cantonal no. GE155A; national no. 34289).

Cre-dependent Hm3Dq-DREADD (Designer Receptors Exclusively Activated by Designer Drugs) mice (B6N;129-Tg(CAG-CHRM3*,-mCitrine)1Ute/J, Jackson stock #026220) were crossed with Oxytocin-Ires-Cre mice (B6;129S-Oxttm1.1(cre)Dolsn/J, Jackson stock #024234) to create Oxt-Hm3Dq mice (B6;129S-Oxt-Cre;R26-LSL-hM3Dq-DREADD), which express the excitatory DREADD under the oxytocin promotor gene.

A model of closed-head weight-drop impact acceleration injury to male P7 mice was used, adapted from Jacquens et al., 2024.[15] Only male mice were used in this study, due to the increased occurrence and susceptibility of pediatric TBI seen in male infants.[16]

Mice of the TBI-oxytocin treatment group received daily CNO injections (10mg/kg, Enzo Life, BML-NS-105-0025) starting at P7, 4h post-TBI, and subsequently every morning at P8, P9 and P10 to activate the excitatory DREADDs, which causes a temporary increase in neuronal oxytocin firing. Non-treated mice received NaCl injections at the same time points.

Evans Blue assay of cerebrovascular rupture

P7 mice were i.p. injected with 50 µl of 1% Evans Blue (Sigma-Aldrich E2129) 4h before TBI or Sham-operation. Mice were sacrificed 4h post-surgery, brains fixed and imaged using iBright FL1500 Imaging System (ThermoFisher) at AlexaFluor 633 wavelength.

Immunohistochemistry

Brains were collected at P8 (24h post-TBI) and P45 (38 days post-TBI). Coronal free-floating frozen sections corresponding to slide 70 to 75 of Allen brain atlas (atlas.brain-map.org) were selected for immunofluorescent assays, corresponding to the Bregma level of TBI impact. They were labelled using rabbit anti-cleaved-caspase 3 (1:200; Cell Signaling D175), goat anti-Iba1 (1:500; Abcam ab5076), rabbit anti-Iba1 (1:1000; Fujifilm Wako 019-19741) and rat anti-CD68 (1:1000, Bio-rad FA-11), and mouse anti-MBP (1:500, Sigma-Aldrich MAB382).

Image acquisition and analysis

For measuring the degree of apoptotic cell death and microglia response at P8, brain sections were imaged with a ZEISS Axioscan.Z1 (Zeiss, Oberkochen, Germany) at 10x. Other immunohistochemistry assays were imaged using a ZEISS LSM 800 Airyscan confocal microscope (Zeiss, Oberkochen, Germany), at different magnitudes. Images were analyzed using FIJI/ImageJ[17].Quantifications were performed by researchers blinded to experimental conditions.

Morphological analysis of single microglia

To assess the morphological characteristics of microglia on a single-cell level, individual microglia were isolated and reconstructed from the 40x z-stack micrographs, and analyzed using the Shape Filter plugin[18] and Sholl plugin[19] of ImageJ.

WM microstructure

Analysis of WM (WM) microstructure at P45 was performed in ImageJ as previously reported.[15,20] Subcortical WM microstructure and the integrity of myelinated axons in the cortex were based on myelin base protein (MBP) immunoreactivity.

RT-qPCR and transcriptomic profiling of glia

Microglia (anti-mouse CD11b microbeads (Miltenyi Biotech)) and astrocytes (anti-mouse ACSA-2 microbeads) were sorted from P8 mice using magnetic cell sorting technology as previously described.[21]

Gene expression of a selection of pro-inflammatory cytokines was assessed, based on previous findings.[15] Primers were designed with Primer-BLAST and primer sequences are listed in Supplementary Table S2.

The microglial and astrocytic RNAs were sequenced in bulk with Illumina NovaSeq 6000 next-generation sequencer. Quality control was performed with FastQC (v.0.1.1.9), and the reads were mapped to the reference mouse genome (Ensemble / GRCm39) using STAR aligner (v.2.7.10b).

Differential gene expression (DEG) analysis was performed with edgeR (v.3.42.4). Differentially expressed genes were estimated using a quasi-likelihood (QL) F-test with rigorous type I error rate control. Corrections for multiple testing were performed with False Discovery Rate (FDR) and the Benjamini & Hochberg correction (BH). Significant genes were filtered on cut-off values of ≥ 1.5 fold-change and $p < .05$. DEG analysis was performed for the comparisons TBI versus Sham, and TBI+OXT versus TBI.

Gene set enrichment analysis on differentially expressed genes was performed using DAVID Functional Annotation Tool (DAVID Knowledgebase v2024q1, National Institutes of Health). Databases of biological processes and KEGG pathways were investigated.

The RNA Seq experiments were performed at the iGE3 Genomics Platform of the University of Geneva (https://ige3.genomics.unige.ch).

Ex-vivo brain structure assessment using MRI-diffusion tensor imaging

Ex-vivo MRI experiments were performed with a 2.5 cm diameter birdcage coil, on an 9.4T/31cm actively shielded horizontal-bore magnet (Magnex Scientific, Yarnton, UK). Several brain regions were assessed in the ipsilateral hemisphere, ROIs were delineated on the fractional anisotropy maps. We calculated DTI derived parameters, neurite orientation dispersion, and density imaging (NODDI) metrics. These parameters were calculated for 5 Ipsilateral ROIs for each animal: corpus callosum (CC), cingulum (Cg), external capsule (EC), primary motor cortex (M1Cx) and primary somatosensory cortex (S1Cx).

In-vivo brain connectivity imaging with functional ultrasound (fUS)

We performed *in-vivo* resting-state functional ultrasound (fUS) imaging of the brain at P45, using the previously reported methodology.[12,15,22]

Individual CBV patterns were transformed into connectivity correlation matrices between a selection of 10 ROIs of the atlas, based on previous findings.[15] We analyzed connectivity between these regions, and within ipsilateral and contralateral hemispheres.

To perform a holistic network analysis of brain connectivity, we measured CBV variations in 212 ROIs across 3 coronal planes (Bregma -1, -1.5, -2). This large connectivity matrix was loaded into Gephi[23] and transformed into a 3D neural network of nodes (ROIs) and edges (connections between ROIs). We categorized the 212 ROIs into cerebral structures (e.g., “sensorimotor cortex”) and transcending structural “hubs” (e.g., “isocortex”), to enable assessment of larger collections of structures in the network. See full list of ROIs and their categorization in Supplementary Table S1.

Behavior

Mouse behavior was tracked and analyzed using Ethovision (Noldus, Wageningen, the Netherlands). Mice performed the P14 homing test, representing early-life sociability, P45 open field test, to analyze general motor activity and anxiety, and P45 three-chamber test, as an adult measure of sociability.

Statistical analyses

Statistical analysis was performed with Graphpad/Prism version 10.4.0 for Windows (GraphPad Software, Boston, Massachusetts USA, www.graphpad.com). Comparisons between experimental groups were performed with Student's t-test, Mann-Whitney U test, paired t-test, One-way ANOVA or two-way ANOVA, as appropriate. The alpha was set at 0.05, and tested two-tailed. Unless specified otherwise, graphs show Mean + SEM values.

Results

Traumatic brain injury causes acute neural damage and neuroinflammation in P7 male mice

TBI in P7 male OXT-Hm3Dq DREADD mice with a C57BL/6N background created cerebrovascular tissue rupture around the cortical impact site as soon as 4h post-injury lasting >3 days (Fig 1a,b,c). It was associated with blood accumulation in the ipsilateral subcortical WM (Fig 1d), and increased apoptotic cell death in both the ipsilateral subcortical WM and the ipsilateral cortex at 24h post-injury (Fig 1e-g). TBI mice showed increased CD68 phagocytic activity in the primary somatosensory cortex (Fig 1h,i) and subcortical WM (Fig 1j,k). The increase in CD68 signal 24h after TBI was higher in the ipsilateral cortex compared to WM (Fig 1l), consistent with a significant upregulation of microglia genes encoding for inflammatory cytokines was observed in the ipsilateral hemisphere (Fig 1m-q).

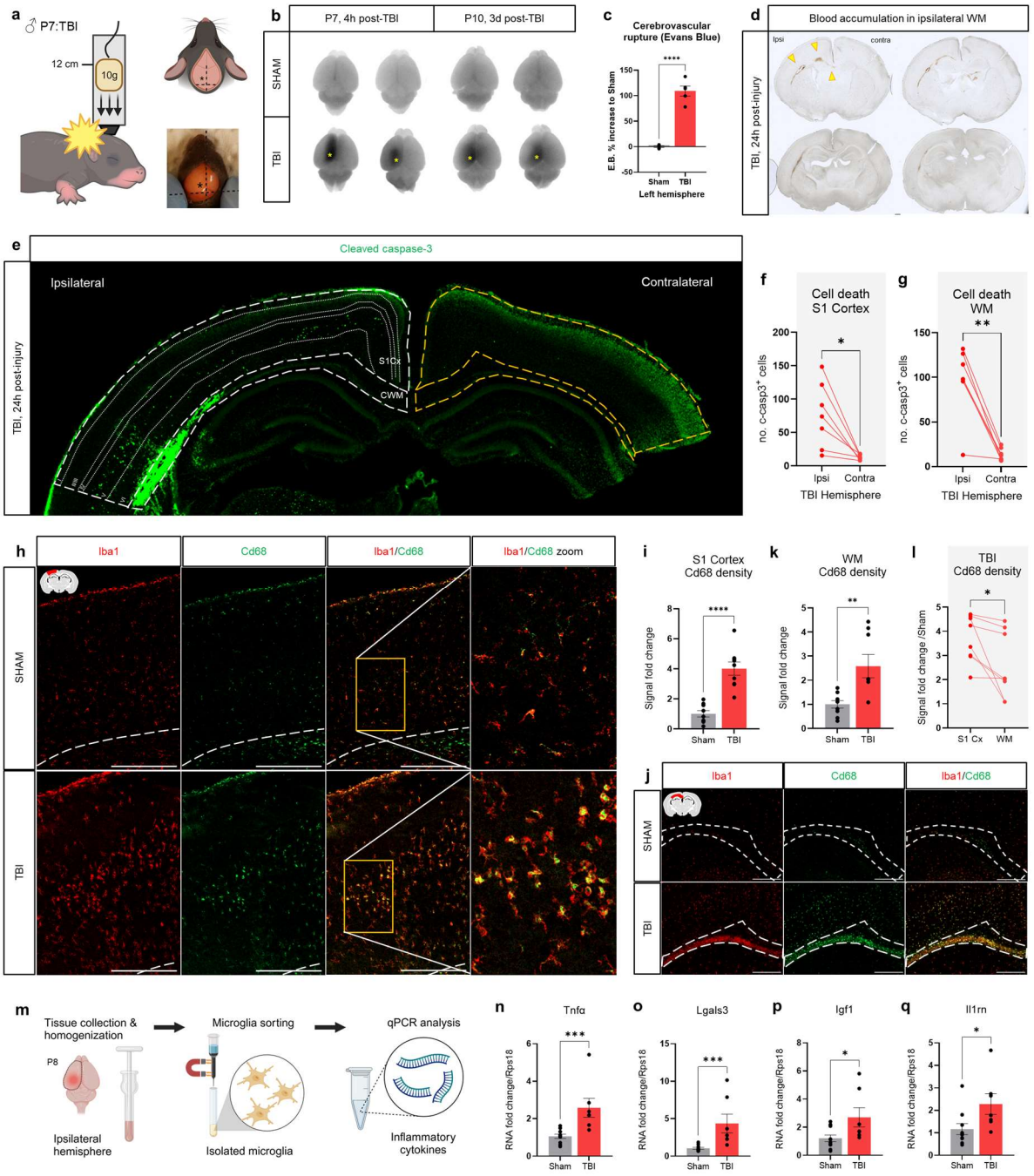

Fig. 1: Closed-head weight drop model of pediatric TBI causes acute neural damage and neuroinflammation in P7 male mice. a) Graphical representation of the closed-head accelerated weight-drop model of TBI in P7 male mice, where a 10g weight is dropped from 12 cm distance to create mechanical impact directly on the exposed skull. Asterisk represents placement of impact with the dropping weight. **b)** Representative images of Evans Blue assay showing cerebrovascular rupture in the ipsilateral cortex 4 hours and 3 days after TBI injury. Yellow asterisks indicate aimed placement of the TBI dropping weight. **c)** Quantification of Evans Blue signal showing a substantial increase in cerebrovascular damage in TBI mice compared to sham. **d)** Representative images of cerebrovascular

spillage into the brain 24h post-TBI. Blood accumulation is found around the ipsilateral subcortical white matter (arrows) at multiple bregma levels. **e)** Representative micrograph of cleaved-caspase 3 (green) immunohistochemistry of apoptotic cell death in the ipsilateral cortex and white matter 24 hours post-TBI. Cortical cell death was found mostly in cell layers V and VI. **f, g)** Quantification of cleaved-caspase 3 signal in ipsilateral versus contralateral hemisphere in TBI animals for S1 cortex **(f)** and cingulate white matter **(g)**, showing a unilateral injury effect of TBI for the ipsilateral hemisphere. **h,j)** Representative micrographs of Iba1 (red) and CD68 (green) signal in Sham and TBI groups 24h post-injury, as a representation of microglia/macrophage phagocytic activity in the ipsilateral cortex **(h)** and white matter **(j)**. Scale bar = 200 μm. **i,k)** Quantification of CD68 signal fold change showed that TBI increased phagocytic activity compared to sham, in both the ipsilateral cortex **(i)** and white matter **(k)**. **l)** The increase in CD68 phagocytosis in TBI mice was higher in the cortex than in the white matter. **m)** Graphical representation of qPCR assessment of microglia magnetically sorted from the ipsilateral hemisphere 24h post-TBI. **n-q)** Quantification of gene expression revealed an upregulation of neuroinflammation cytokine expression in microglia from TBI mice compared to sham mice, including Tnfα **(n)**, Lgals3 **(o)**, Igf1 **(p)**, and Il1rn **(q)**. In **(i)** Unpaired t-test ($t(16) = 6.20$, ****$p < .0001$, Sham: $n = 9$, TBI: $n = 9$). In **(k)** Unpaired t-test ($t(15) = 3.28$, **$p = .005$, Sham: $n = 9$, TBI: $n = 8$). In **(l)** Paired t-test ($t(7) = 2.66$, *$p = .032$, $n = 8$). In **(n)** Mann-Whitney U test ($U = 2$, ***$p = .0004$, Sham: $n = 10$, TBI: $n = 7$). In **(o)** Mann-Whitney U test ($U = 2$, ***$p = .0004$, Sham: $n = 10$, TBI: $n = 7$). In **(p)** Mann-Whitney U test ($U = 13$, *$p = .033$, Sham: $n = 10$, TBI: $n = 7$). In **(q)** Mann-Whitney U test ($U = 11$, *$p = .019$, Sham: $n = 10$, TBI: $n = 7$). Bar and line graphs represent Mean ± SEM. Each circle represents an individual sample.

Oxytocin reduces microglia reactivity in the acute post-TBI phase

Oxytocin release was achieved by injecting CNO which selectively activates the Hm3Dq receptors and increases firing of oxytocin neurons (Supplementary Fig S1). Importantly, the CNO substance itself – in absence of functional DREADD expression – did not cause significant changes in readouts of this study (Supplementary Fig S2).

We assessed the effect of oxytocin on acute-phase inflammation post-TBI (Fig 2a). At 24h post-injury, pediatric TBI mice showed an increase in cleaved caspase-3 (c-casp3) apoptotic cell death in the ipsilateral cortex, the location of the direct mechanical impact (Fig 2b,c).

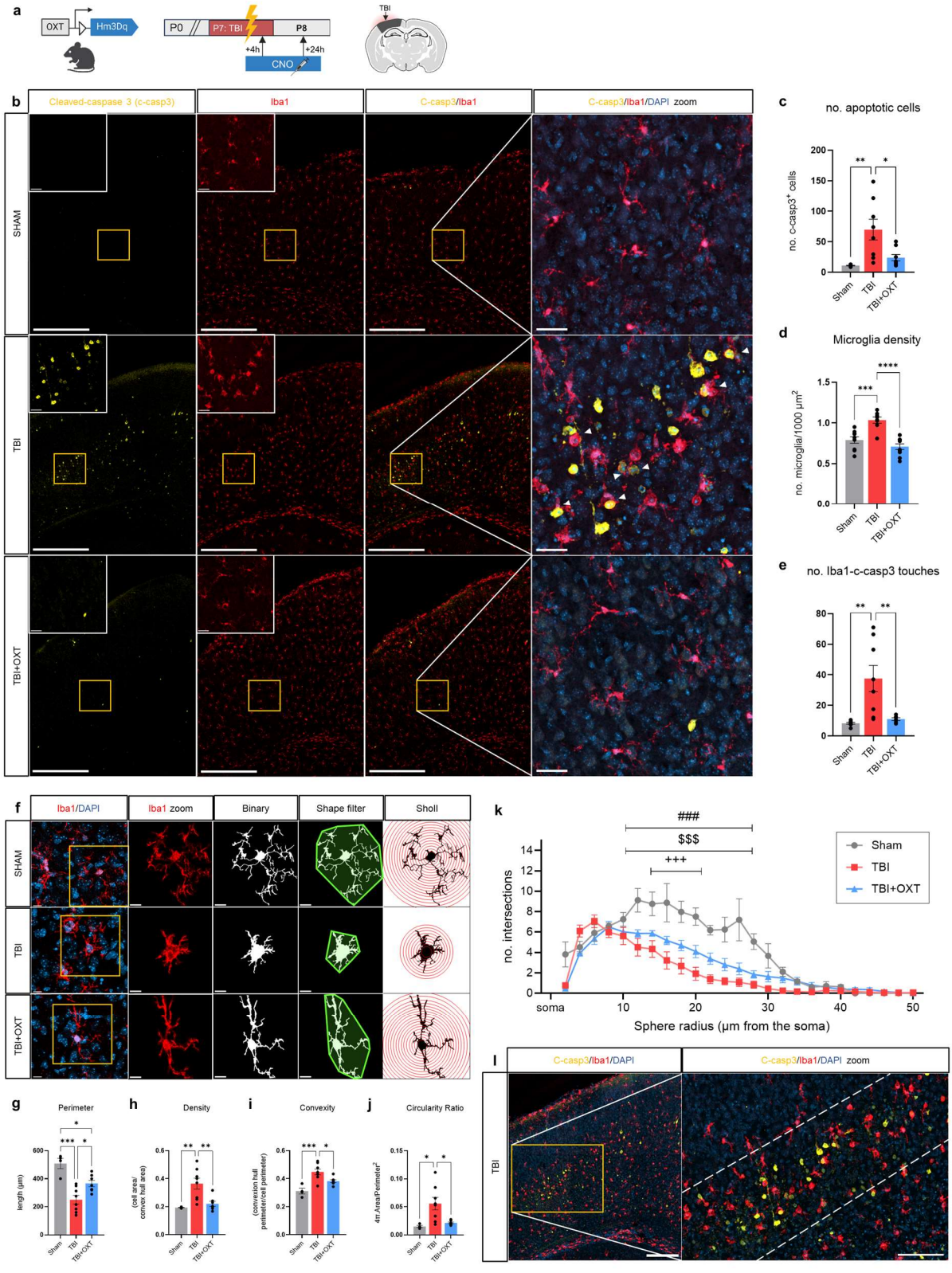

Fig. 2: Oxytocin decreases cortical microglial reactivity 24h post-TBI. a) Graphical timeline of P8 immunohistochemistry experiment after P7 TBI and 2 sessions of oxytocin treatment via CNO injections, and indication of the ipsilateral somatosensory cortex ROI. **b)** Representative micrographs of apoptotic cell death (cleaved caspase-3; yellow), and microglia (Iba1; red) in the ipsilateral

somatosensory cortex in Sham, TBI and TBI+OXT treatment groups. Scale bar = 200 µm (inserts: scale bar = 30 µm). Cleaved caspase-3/Iba1 co-labeling indicating apoptotic cells that are touched by a microglial cell with white arrows **(b, right column)**. **c)** Quantification of number of apoptotic cells showed an increase in TBI compared to sham, and a reverse in TBI+OXT groups. **d)** Microglia density was increased in TBI compared to sham, as was the number of Iba1-cleaved caspase-3 touches **(e)**. Both measures were reduced in the TBI+OXT group, compared to TBI **(d,e)**. **f)** Representative micrographs of individual cortical microglia in Sham, TBI and TBI+OXT groups, visualizing the processing steps for Shape filter and Sholl analysis. Scale bar = 10 µm. **g-j)** Parameters of microglia shape filter analysis revealed a more amoeboid-phenotype in TBI vs. Sham mice: decreased cell perimeter **(g)**, increased cell density **(h)**, increased cell convexity **(i)** and increased cell circularity ratio **(j)**. All shape filter parameters of cortical microglia were reversed in the TBI+OXT group compared to TBI **(g-j)**, reflecting a ramified microglia morphology similar to Sham mice. **k)** Quantification of microglia Sholl analysis showing the number of process intersections per sphere radius from the soma. ### Significant difference TBI *vs* Sham, $$$ significant difference TBI+OXT *vs* Sham, +++ significant difference TBI+OXT *vs* TBI. Sholl analysis showed that TBI microglia are less ramified than sham, and that oxytocin treatment increases the ramification degree partially. **l)** Representative micrograph of TBI mice showing an accumulation of amoeboid-shaped microglia around the cleaved caspase-3^+ apoptotic cells in the cortex. This "amoeboid microglial line" is indicated by dashed lines. Scale bar = 100 µm (insert: scale bar = 50 µm). TBI = traumatic brain injury. CNO = clozapine n-oxide, ROI = region of interest, OXT = oxytocin. In **(c)** ANOVA ($F(2,21) = 11.60$, $^{**}p = .0015$, Sham: $n = 8$, TBI: $n = 8$, TBI+OXT: $n = 8$). Tukey's (Sham vs. TBI: $^{**}p = .0016$, Sham vs. TBI+OXT: $p = .65$, TBI vs. TBI+OXT: $^{*}p = .013$). In **(d)** ANOVA ($F(2,24) = 19.51$, $^{****}p < .0001$, Sham: $n = 9$, TBI: $n = 9$, TBI+OXT: $n = 10$). Tukey's (Sham vs. TBI: $^{***}p = .0005$, Sham vs. TBI+OXT: $p = .27$, TBI vs. TBI+OXT: $^{****}p < .0001$). In **(e)** ANOVA ($F(2,19) = 9.16$, $^{**}p = .0016$, Sham: $n = 8$, TBI: $n = 8$, TBI+OXT: $n = 6$). Tukey's (Sham vs. TBI: $^{**}p = .0024$, Sham vs. TBI+OXT: $p = .94$, TBI vs. TBI+OXT: $^{**}p = .0098$). In **(g)** ANOVA ($F(2,16) = 15.97$, $^{***}p = .0002$, Sham: $n = 4$, TBI: $n = 8$, TBI+OXT: $n = 7$). Tukey's (Sham vs. TBI: $^{***}p = .0001$, Sham vs. TBI+OXT: $^{*}p = .021$, TBI vs. TBI+OXT: $^{*}p = .023$). In **(h)** ANOVA ($F(2,16) = 8.93$, $^{***}p = .0002$, Sham: $n = 4$, TBI: $n = 8$, TBI+OXT: $n = 7$). Tukey's (Sham vs. TBI: $^{**}p = .0074$, Sham vs. TBI+OXT: $p = .85$, TBI vs. TBI+OXT: $^{**}p = .0075$). In **(i)** ANOVA ($F(2,16) = 12.59$, $^{***}p = .0005$, Sham: $n = 4$, TBI: $n = 8$, TBI+OXT: $n = 7$). Tukey's (Sham vs. TBI: $^{***}p = .0004$, Sham vs. TBI+OXT: $p = .059$, TBI vs. TBI+OXT: $^{*}p = .032$). In **(j)** ANOVA ($F(2,16) = 7.17$, $^{**}p = .0060$, Sham: $n = 4$, TBI: $n = 8$, TBI+OXT: $n = 7$). Tukey's (Sham vs. TBI: $^{*}p = .016$, Sham vs. TBI+OXT: $p = .88$, TBI vs. TBI+OXT: $^{*}p = .016$). In **(k)** Two-way ANOVA ($F(48,400) = 5.00$, $^{****}p < .0001$. Sham: $n = 4$, TBI: $n = 8$, TBI+OXT: $n = 7$). See Supplementary Data S1 for Tukey's post-hoc statistical details. Bar graphs represent Mean ± SEM. Each circle represents an individual sample.

Co-labeling with NeuN showed that the majority of the c-casp3$^+$ cells were neurons (60-80%; Supplementary Fig S3). TBI mice had a higher Iba1$^+$ microglial cell density in the ipsilateral cortex compared to sham (Fig 2b,d). Single-cell analysis of microglia shape revealed a significant increase in amoeboid morphology parameters in TBI mice, including a more circular shape, higher cell density and lower number of cell ramifications (Fig 2f-k). We found an accumulation of amoeboid-shaped microglia around the c-casp3$^+$ cells in TBI mice, forming an "amoeboid microglial line" around the dying cells in the ipsilateral cortex (Fig 2l). The number of Iba1$^+$ / c-casp3$^+$ touching cells was increased in TBI compared to sham (Fig 2e), with 57% of c-casp3$^+$cells being touched by Iba1$^+$ cells in TBI mice. We also found an increase in CD68 phagocytosis immunoreactivity in TBI compared to sham (Fig 1h,i). Compared to untreated TBI animals, exposure to oxytocin release after TBI was associated with a reduction in microglia density in the ipsilateral cortex, a reversal of amoeboid morphology 24h post-injury, (Fig 2b,d,f-k), and a reduction in apoptotic cell death (Fig 2b,c). While the proportion of apoptotic neurons was unaffected by endogenous oxytocin release (Supplementary Fig S3), it reduced the degree of contact between microglia and c-casp3$^+$ apoptotic cells in the cortex, compared to untreated TBI (Fig 2b,e). Similar effects were found in the ipsilateral white matter (Fig 3), with the exception that apoptotic signal and number of Iba1$^+$/c-casp3$^+$ contacts were unaltered by oxytocin release 24h post-injury (Fig 3b,c,e). Altogether, these data strongly suggest that oxytocin release has a significant effect on the morphologic and functional aspects of cortical microglia subjected to TBI.

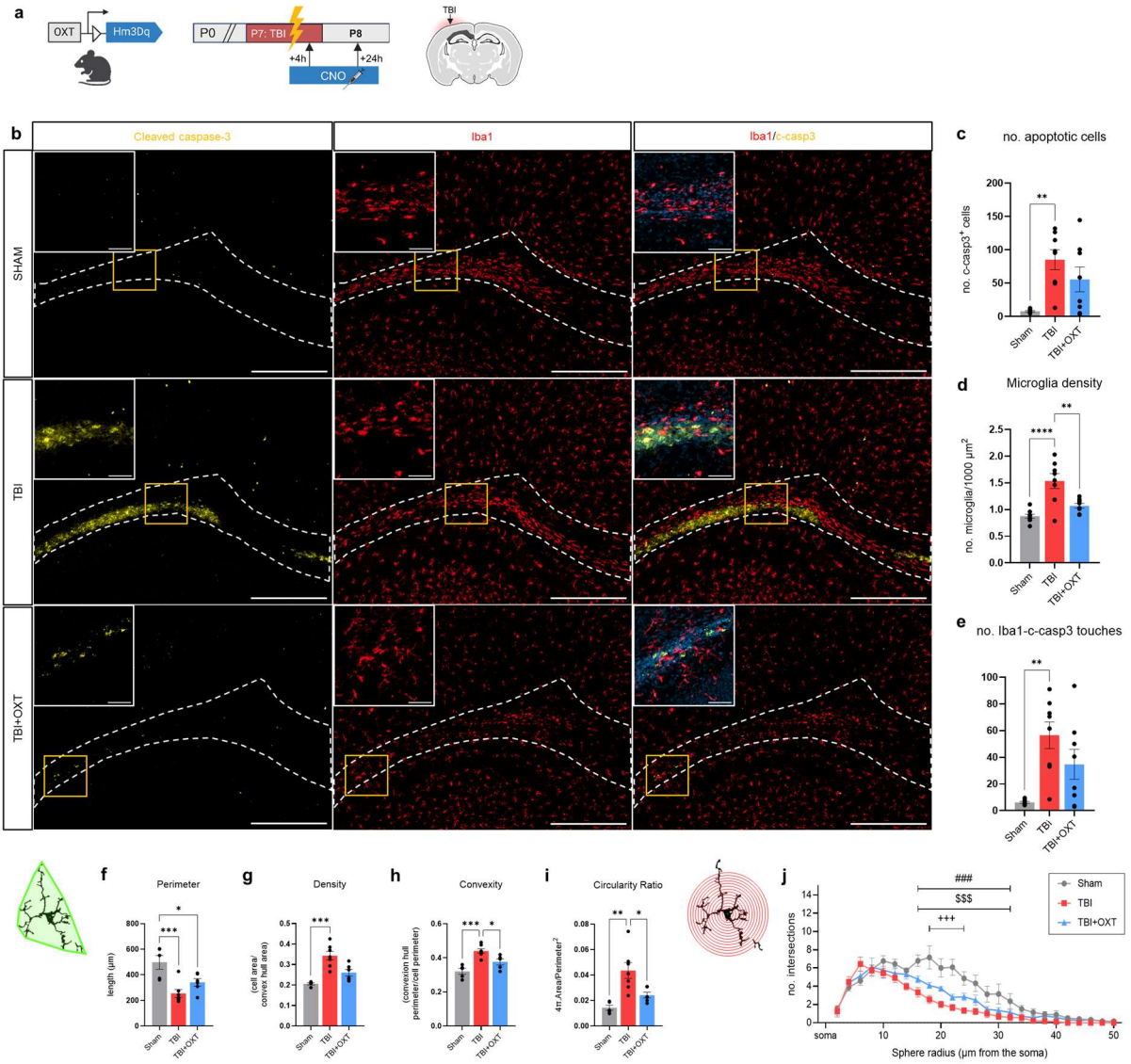

Fig. 3: Oxytocin partially reduces white matter microglial reactivity 24h post-TBI. a) Graphical timeline of P8 immunohistochemistry experiment after P7 TBI and 2 sessions of oxytocin treatment via CNO injections, and graphical indication of ROI in the ipsilateral WM. **b)** Representative micrographs of apoptotic cell death (cleaved caspase-3; yellow) and microglia (Iba1; red) in the ipsilateral white matter in Sham, TBI and TBI+OXT treatment groups. Scale bar = 200 µm (inserts: 30 µm). **c)** Quantification of number of apoptotic cells showed an increase in TBI vs Sham mice, that was unaffected by the oxytocin treatment. **d)** TBI mice showed an increase in WM microglia density compared to sham. This was reduced in the TBI+OXT group compared to TBI. **e)** The number of touches between apoptotic cells and microglia was increased in TBI vs Sham, and remained high in the TBI+OXT group. **f-i)** Shape filter analysis of single microglia in the WM revealed an increase in amoeboid-morphological parameters in TBI vs Sham, including reduced cell perimeter **(f)**, increased cell density **(g)**, increased cell convexity **(h)** and increased cell circularity ratio **(i)**. TBI+OXT mice showed a partial

reverse of amoeboid parameters, including a reduction in cell convexity **(h)** and cell circularity ratio **(i)**. **j)** Quantification of Sholl analysis of single microglia showed a decrease in number of intersections per sphere radius between TBI and sham groups, which was partially increased in the TBI+OXT group. ### Significant difference TBI *vs* Sham, $$$ significant difference TBI+OXT *vs* Sham, +++ significant difference TBI+OXT *vs* TBI. TBI = traumatic brain injury. CNO = clozapine n-oxide, ROI = region of interest, OXT = oxytocin. In **(c)** ANOVA ($F(2,21) = 7.93$, $^{**}p = .0027$, Sham: $n = 8$, TBI: $n = 8$, TBI+OXT: $n = 8$). Tukey's (Sham vs. TBI: $^{**}p = .0002$, Sham vs. TBI+OXT: $p = .06$, TBI vs. TBI+OXT: $p = .31$). In **(d)** ANOVA ($F(2,22) = 15.94$, $^{****}p < .0001$, Sham: $n = 9$, TBI: $n = 8$, TBI+OXT: $n = 8$). Tukey's (Sham vs. TBI: $^{****}p < .0001$, Sham vs. TBI+OXT: $p = .25$, TBI vs. TBI+OXT: $^{**}p = .0028$). In **(e)** ANOVA ($F(2,21) = 8.41$, $^{**}p = .0021$, Sham: $n = 8$, TBI: $n = 8$, TBI+OXT: $n = 8$). Tukey's (Sham vs. TBI: $^{**}p = .0015$, Sham vs. TBI+OXT: $p = .076$, TBI vs. TBI+OXT: $p = .20$). In **(f)** ANOVA ($F(2,15) = 10.60$, $^{**}p = .0014$, Sham: $n = 5$, TBI: $n = 7$, TBI+OXT: $n = 6$). Tukey's (Sham vs. TBI: $^{***}p = .0010$, Sham vs. TBI+OXT: $^{*}p = .030$, TBI vs. TBI+OXT: $p = .23$). In **(g)** Kruskal-Wallis test ($F(3) = 13.40$, $^{****}p < .0001$, Sham: $n = 5$, TBI: $n = 7$, TBI+OXT: $n = 6$). Dunn's (Sham vs. TBI: $^{***}p = .0008$, Sham vs. TBI+OXT: $p = .17$, TBI vs. TBI+OXT: $p = .23$). In **(h)** ANOVA ($F(2,14) = 15.17$, $^{***}p = .0003$, Sham: $n = 5$, TBI: $n = 7$, TBI+OXT: $n = 5$). Tukey's (Sham vs. TBI: $^{***}p = .0002$, Sham vs. TBI+OXT: $p = .0582$, TBI vs. TBI+OXT: $^{*}p = .028$). In **(i)** ANOVA ($F(2,16) = 10.71$, $^{**}p = .0013$, Sham: $n = 5$, TBI: $n = 7$, TBI+OXT: $n = 6$). Tukey's (Sham vs. TBI: $^{**}p = .0013$, Sham vs. TBI+OXT: $p = .34$, TBI vs. TBI+OXT: $^{*}p = .019$). In **(j)** Two-way ANOVA ($F(48,375) = 3.10$, $^{****}p < .0001$. Sham: $n = 5$, TBI: $n = 7$, TBI+OXT: $n = 6$). See Supplementary Data S2 for Tukey's post-hoc statistical details. Bar graphs represent Mean ± SEM. Each circle represents an individual sample.

<u>Oxytocin promotes gene expression of brain repair functions in microglia 24h post-TBI</u>

We investigated the microglia transcriptome with RNA sequencing of sorted microglia from brains collected 24h post-injury at P8 (Fig 4a, Supplementary Fig S4). Unsupervised PCA analysis revealed a separation of microglia transcriptome between the 3 experimental groups (Fig 4b). From the 15'933 genes sequenced, 908 genes were differentially expressed between TBI and sham microglia, of which 513 upregulated and 395 downregulated (Fig 4c,d). Gene set enrichment analysis revealed a strong upregulation of glycolytic metabolic pathways and associated pathways gluconeogenesis, response to hypoxia and HIF-1 signaling in TBI *vs* sham microglia (Fig 4e). These data suggest a transcriptomic shift from homeostatic oxidative phosphorylation towards pro-inflammatory glycolysis in TBI. Conversely,

TBI microglia showed a downregulation of genes involved in angiogenesis, axon guidance and regulation of cell migration and differentiation, compared to sham (Fig 4e). Many signaling pathways linked to pro-inflammatory microglia function and hypo-myelination in the developing mouse brain[24] were downregulated in TBI *vs* sham microglia (Fig 4e). Oxytocin signaling was also downregulated in TBI *vs* sham microglia (Fig 4e).

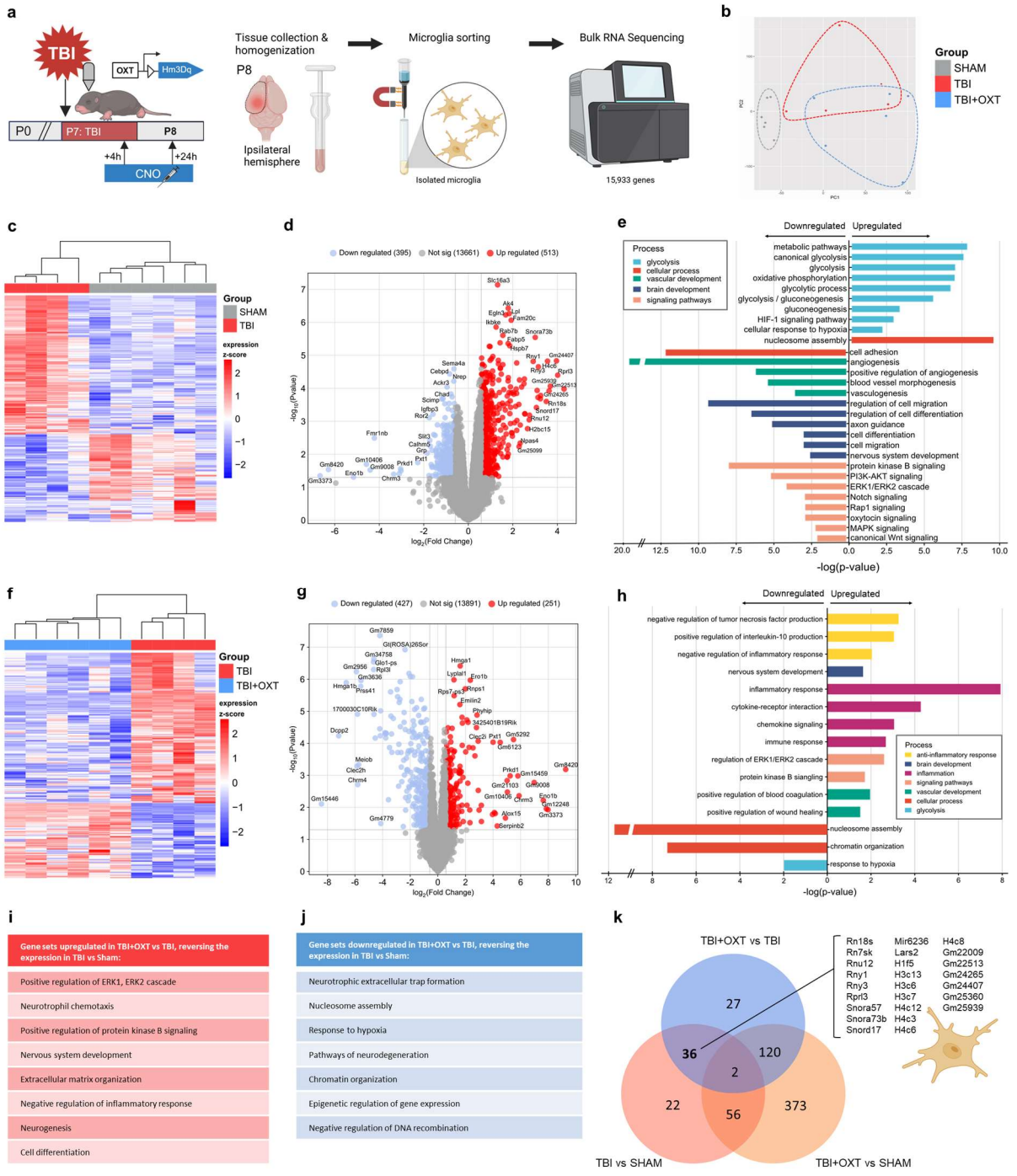

Fig. 4: Oxytocin promotes brain repair gene pathways in microglia transcriptome 24h post-TBI. a) Graphical timeline of P8 microglia RNA sequencing experiment after P7 TBI and 2 sessions of oxytocin treatment via CNO injections. Microglia were magnetically sorted from ipsilateral hemispheres of P8 mice and sequenced in bulk (15'933 genes). **b)** PCA plot showing segregation of the 3 experimental groups, based on microglia transcriptomic profile. **c)** Unsupervised heatmap analysis of top deregulated genes shows separation of TBI and Sham samples into their respective treatment groups. **d)** Volcano plot showing 908 differentially expressed genes between TBI and sham microglia, including 395 downregulated (blue) and 513 upregulated (red) genes. **e)** Bar graph showing enriched gene pathways between TBI and sham microglia, assessed with gene set enrichment analysis of biological processes and KEGG repositories. TBI microglia showed an upregulation of glycolysis pathways, and a downregulation of pathways involved in vascular development, brain development and cell signaling. **f)** Unsupervised heatmap analysis of top deregulated genes between TBI+OXT and TBI microglia shows separation of TBI+OXT and TBI samples into their respective treatment groups. **g)** Volcano plot showing 678 differentially expressed genes in TBI+OXT microglia compared to TBI microglia, of which 427 downregulated (blue) and 251 upregulated (red). **h)** Bar graph of significantly enriched gene pathways in TBI+OXT microglia vs. TBI shows an upregulation of (anti-) inflammatory pathways, a rescue of vascular development and brain development pathways, and a downregulation of glycolysis and cellular processes. **i,j)** Tables highlighting gene sets upregulated **(i)** and downregulated **(j)** in TBI+OXT vs TBI, reversing the transcriptomic effect of TBI vs Sham in sorted microglia. **k)** Venn diagram of differentially expressed genes between treatment groups revealed 36 genes common genes between TBI vs. Sham and TBI+OXT vs. TBI comparisons. These genes were associated with histone and chromatin compartments. These data suggest that oxytocin treatment promotes anti-inflammatory gene expression in microglia 24h post-TBI, as well as improved expression of brain and cerebrovascular development gene pathways. TBI = traumatic brain injury. CNO = clozapine n-oxide, OXT = oxytocin. DEG = differentially expressed gene, GSEA = gene set enrichment analysis. RNA Seq analysis was performed with > 1.5 thresholds for fold change, and with FDR-corrected p-value < .05 for the DEG analysis and $p < .05$ for the GSEA analysis. In **(e,h)** enrichment is represented as the negative log of the p value. Upregulated pathways are positioned on the right side of the y-axis, and downregulated pathways on the left.

Oxytocin treatment affected expression of 678 microglial genes compared to untreated TBI microglia, of which 251 upregulated and 427 downregulated (Fig 4f,g). The upregulated genes in TBI+OXT microglia were enriched for pathways associated with anti-inflammatory functions and repair (Fig 4h).

Neurodegeneration was one of the pathways that was downregulated in TBI+OXT microglia, as were general cellular processes such as nucleosome assembly and chromatin organization (Fig 4h).

We identified several pathways whose differential upregulation in TBI *vs* sham microglia was directly reversed by endogenous oxytocin release (Fig 4i,j), including neurogenesis, cell differentiation, nervous system development, tissue repair, ERK1/ERK2 and protein kinase B (Fig 4i). Likewise, oxytocin reversed the upregulation of pathways involved in neurodegeneration and hypoxia found in TBI, as well as epigenetic pathways such as chromatin organization (Fig 4j). Notably, the epigenetic effects were the most significant of all the transcriptomic pathways that were affected by oxytocin. Moreover, the 36 overlapping genes that were differentially expressed by TBI (*vs* sham) and also by TBI+OXT (*vs* TBI) showed an enrichment for histone (cluster 3 and 4) and chromatin compartments (Fig 4k).

Oxytocin differently affects the astrocyte transcriptome from microglia 24h post-TBI

Using RNA scope *in situ* hybridization on P5 brain sections, we found support that both microglia and astrocytes express oxytocin receptor mRNA *in-vivo*, in both cortical and WM regions (Supplementary Fig S5), as previously reported.[13,25] We then performed RNA seq on highly-enriched sorted astrocytes samples to understand transcriptomic changes caused by TBI and oxytocin exposure, to complement the microglia results (Fig 5a,b, Supplementary Fig S4b).

We sequenced 17’460 genes and found 357 genes expressed differentially between TBI *vs* sham astrocytes, of which 269 upregulated and 88 downregulated (Fig 5c,d). Gene set enrichment analysis revealed a significant upregulation of pathways involved in the immune, pro-inflammatory response in TBI astrocytes compared to sham. Downregulated gene pathways in TBI astrocytes involved synaptic functioning (Fig 5e).

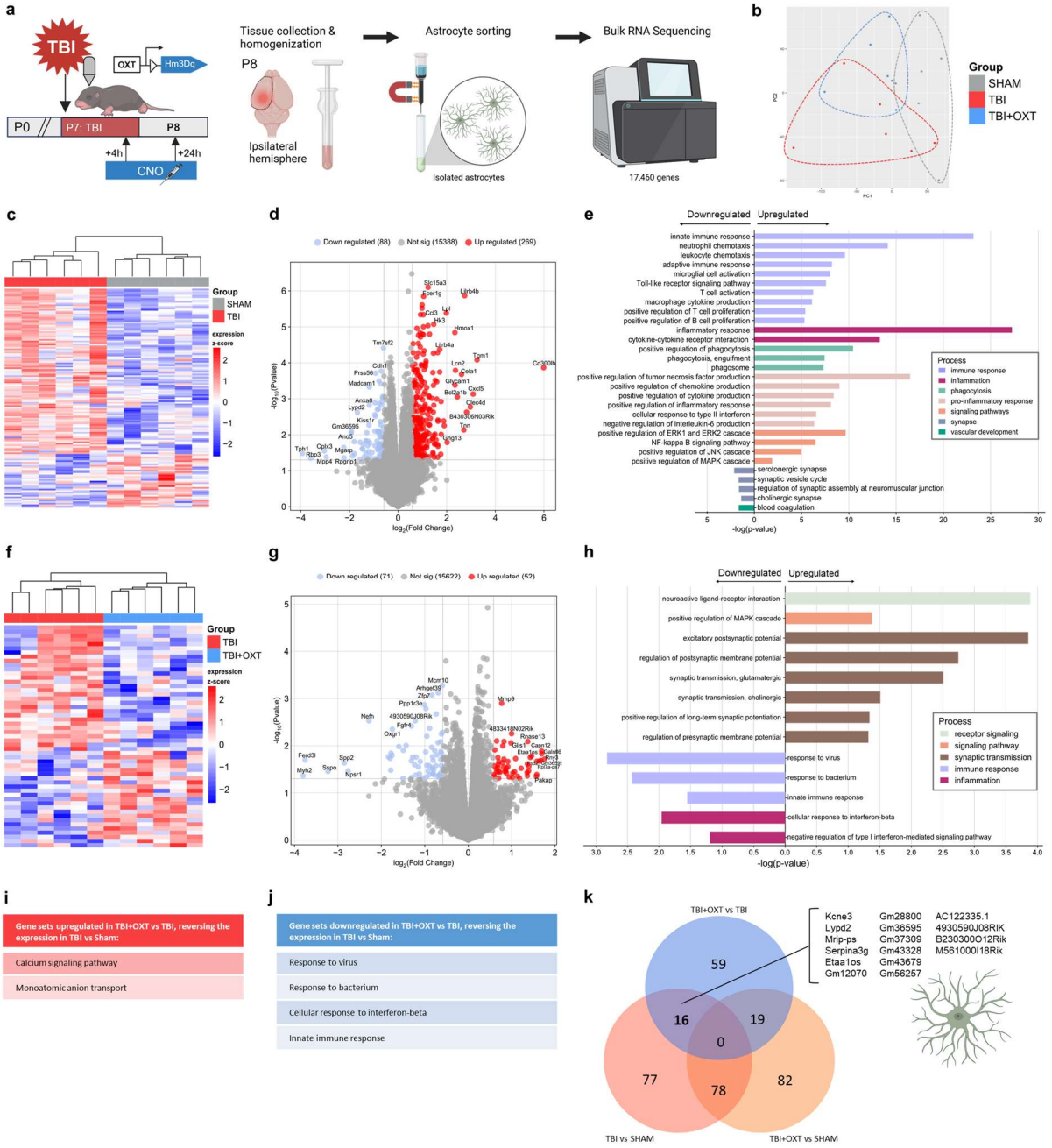

Fig. 5: Oxytocin dampens immune and inflammation gene pathways in astrocyte transcriptome 24h post-TBI. a) Graphical timeline of P8 astrocyte RNA sequencing experiment after P7 TBI and 2 sessions of oxytocin treatment via CNO injections. Astrocytes were magnetically sorted from ipsilateral hemispheres of P8 mice and sequenced in bulk (17'460 genes). **b)** PCA plot showing segregation of the 3 treatment groups, based astrocyte transcriptomic profile. **c)** Unsupervised heatmap analysis of top deregulated genes shows separation of TBI and Sham samples into their respective treatment groups. **d)** Volcano plot showing 357 differentially expressed genes between TBI and sham astrocytes, including 88 downregulated (blue) and 269 upregulated (red) genes. **e)** Bar graph showing significantly enriched gene pathways between TBI and sham astrocytes, assessed with gene set enrichment analysis

of Biological processes and KEGG repositories. TBI astrocytes showed a strong upregulation of immune and inflammation gene pathways, and a downregulation of synaptic pathways. **f)** Unsupervised heatmap analysis of top deregulated genes between TBI+OXT and TBI astrocytes shows separation of TBI+OXT and TBI samples into their respective treatment groups. **g)** Volcano plot showing 123 differentially expressed genes in TBI+OXT astrocytes compared to TBI astrocytes, of which 71 downregulated (blue) and 52 upregulated (red). **h)** Bar graph of significantly enriched gene pathways in TBI+OXT astrocytes vs. TBI shows an upregulation of synaptic processes and a downregulation of immune and inflammation pathways. **i,j)** Tables highlighting gene sets upregulated **(i)** and downregulated **(j)** in TBI+OXT vs TBI, reversing the transcriptomic effect of TBI vs Sham in sorted astrocytes **k)** Venn diagram of differentially expressed genes between treatment groups revealed 16 genes commonly shared between TBI vs. Sham and TBI+OXT vs. TBI comparisons. These genes were not associated with any particular processes or cellular compartments. The data suggest that oxytocin treatment reduces the pro-inflammatory and immune response in astrocytes 24h post-TBI. No effects on brain development pathways were found for astrocytes. TBI = traumatic brain injury. CNO = clozapine n-oxide, OXT = oxytocin. DEG = differentially expressed gene, GSEA = gene set enrichment analysis. RNA Seq analysis was performed with > 1.5 thresholds for fold change, and with FDR-corrected p-value < .05 for the DEG analysis and p < .05 for the GSEA analysis. In **(e,h)** enrichment is represented as the negative log of the p value. Upregulated pathways are positioned on the right side of the y-axis, and downregulated pathways on the left.

Astrocytes sorted from TBI+OXT pups had 123 genes differentially expressed compared to astrocytes from untreated TBI pups, of which 52 upregulated and 71 downregulated (Fig 5f,g). Oxytocin was found to reverse upregulated pathways involved in inflammation and the immune response observed in TBI *vs* sham, including response to type 1 interferon (Fig 5h). Pathways associated with regulation of the MAPK cascade and synaptic transmission, including presynaptic and postsynaptic processes, were found to be upregulated by oxytocin (Fig 5h). Unlike its effect on microglia, oxytocin did not regulate genes involved in vascular tissue recovery or brain development in TBI astrocytes.

Immune response and response to virus pathways, increased in TBI *vs* sham, were downregulated by oxytocin release (Fig 5j). The 16 overlapping genes between TBI+OXT (*vs* TBI) and TBI (*vs* sham) microglia were not enriched for any specific functions or cellular compartments (Fig 5k). These data

suggest that oxytocin induces a reduction of immune-associated pro-inflammatory gene pathways upregulated by TBI in astrocytes.

Long-term WM microstructural deficiencies following TBI are prevented by oxytocin release

TBI mice had smaller corpus callosum thickness at P45, which was reversed in the TBI+OXT group (Fig 6a-c), but ipsilateral external capsule was unaffected (Fig 6d,e). TBI mice showed lower MBP density and reduced myelin coverage of axons compared to sham mice in the ipsilateral S1 cortex (the "TBI impact site") (Fig 6f-h), and oxytocin fully reversed these deficits. Finally, coherency of cortical myelin – an inverted measure of fiber integrity[21] – was not different between groups (Fig 6i).

To further explore WM integrity, we performed P45 *ex-vivo* magnetic resonance diffusion tensor imaging (Fig 6j-m). Compared to sham, TBI mice showed reductions in fractional anisotropy in the EC, cingulum and a trend for the CC (Fig 6n). TBI mice had significantly lower axial diffusivity in the EC, reflecting axonal damage (Fig 6o). Increased radial diffusivity was found in the CC in TBI mice, indicating damage to the myelin sheaths (Fig 6p). NODDI analysis of neurite microstructure further revealed increased orientation dispersion in the EC and cingulum in TBI mice compared to sham, which reflects a loss of coherence in axon orientation (Fig 6q). TBI+OXT mice showed, in the EC, a significant rescue of axial diffusivity and a trend for fractional anisotropy damage compared to TBI mice (Fig 6o,n).

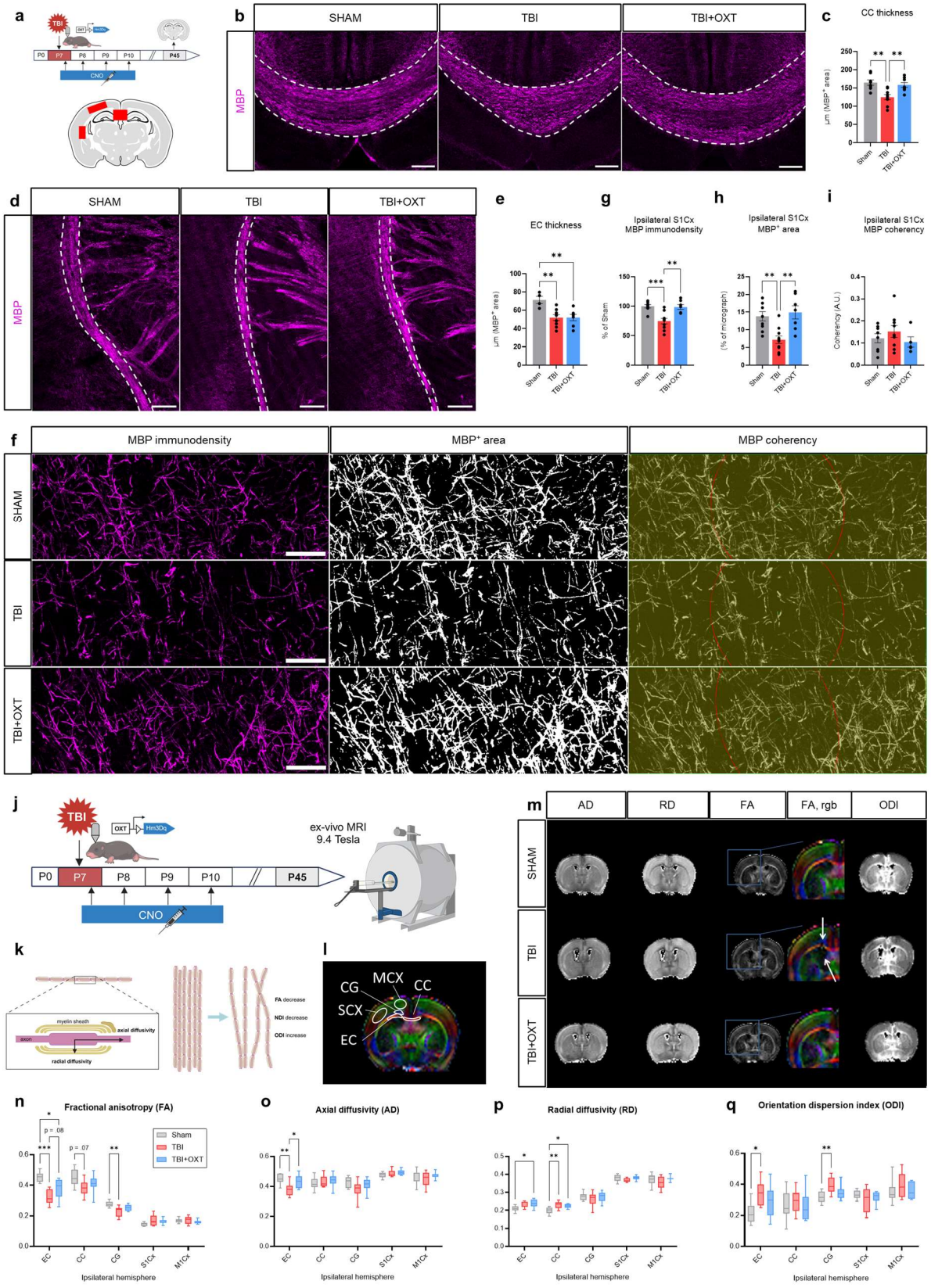

Fig. 6: Long-term white matter microstructural deficiencies following TBI are affected by oxytocin treatment. a) Graphical timeline of the P45 myelin base protein (MBP) immunohistochemistry

experiment, with the 3 ROIs in red. **b,d**) Representative micrographs of MBP signal (magenta) in the CC **(b)** and EC **(d)** for Sham, TBI and TBI+OXT groups. Scale bar = 100 µm. **c)** Quantification of CC thickness shows a reduction in TBI and a rescue in the TBI+OXT group. **e)** Quantification of EC thickness shows a reduction in TBI vs. Sham mice, and no effect of the oxytocin treatment. **f)** Representative micrographs of MBP immunodensity (left), MBP^+ area (middle) and MBP coherency (right) of ipsilateral cortical white matter for Sham, TBI and TBI+OXT groups. Scale bar = 20 µm. **g-i)** Quantification of cortical WM measures shows a decrease in MBP immunodensity **(g)** and MBP^+ area **(h)** in TBI, which were both rescued in TBI+OXT mice. MBP coherency was not affected by treatment group **(i)**. **j)** Graphical timeline of the P45 *ex-vivo* DTI-MRI experiment after P7 TBI and P7-P10 oxytocin treatment via CNO injections. **k)** Graphical representation of the DTI and NODDI parameters, illustrating the different aspects of white matter microstructure they reflect. **l)** Atlas of ipsilateral ROIs that were quantified from MRI scans: 3 WM ROIs (CC, EC, CG) and 2 gray matter ROIs (MCX and SCX). **m)** Representative MRI sections of Sham, TBI and TBI+OXT mice showing the AD, RD, FA, ODI and NDI signals in the ROIs. Arrows emphasize FA damage in WM regions of TBI mice. **n-r)** Quantification of DTI **(n-p)** and NODDI **(q)** parameters between Sham (gray), TBI (red) and TBI+OXT (blue) groups. AD **(o)** and RD **(p)** are expressed in $x10^{-2}$ $mm^2.s^{-1}$. Compared to sham mice, TBI mice showed a reduction in FA **(n)** for all WM ROIs, reduced AD **(o)** in the EC, increased RD **(p)** in the EC and CC, and increased ODI **(q)** in the EC and CG. Compared to TBI mice, TBI+OXT mice showed an increased FA **(n)** in the EC, and an increased AD **(o)** in the EC. TBI = traumatic brain injury, CNO = clozapine n-oxide, CC = corpus callosum, EC = external capsule, CG = cingulum, MCX = primary motor cortex, SCX = primary somatosensory cortex, AD = axonal diffusion, RD = radial diffusivity, FA = fractional anisotropy, ODI = orientation dispersion index, NDI = neurite density index. DTI = diffusion tensor imaging, NODDI = neurite orientation dispersion and density imaging, WM = white matter, MBP = myelin base protein. In **(c)** ANOVA ($F(2,22) = 9.71$, $***p = .0009$, Sham: $n = 8$, TBI: $n = 9$, TBI+OXT: $n = 8$). Tukey's (Sham vs. TBI: $**p = .0014$; Sham vs. TBI+OXT: $p = .80$; TBI vs. TBI+OXT: $**p = .0067$). In **(e)** ANOVA ($F(2,17) = 7.21$, $**p = .0052$, Sham: $n = 4$, TBI: $n = 9$, TBI+OXT: $n = 7$). Tukey's (Sham vs. TBI: $**p = .0065$; Sham vs. TBI+OXT: $**p = .0092$; TBI vs. TBI+OXT: $p = 1$). In **(g)** ANOVA ($F(2,22) = 12.96$, $***p = .0002$, Sham: $n = 8$, TBI: $n = 10$, TBI+OXT: $n = 8$). Tukey's (Sham vs. TBI: $***p = .0005$; Sham vs. TBI+OXT: $p = .97$; TBI vs. TBI+OXT: $**p = .0013$). In **(h)** ANOVA ($F(2,23) = 9.86$, $***p = .0008$, Sham: $n = 9$, TBI: $n = 10$, TBI+OXT: $n = 7$). Tukey's (Sham vs. TBI: $**p = .0041$; Sham vs. TBI+OXT: $p = .85$; TBI vs. TBI+OXT: $**p = .0019$). In **(i)** ANOVA ($F(2,19) = 0.91$, $p = .42$, Sham: $n = 8$, TBI: $n = 9$, TBI+OXT: $n = 5$). In **(n-q)** See Supplementary Data S3 for statistical details. Bar graphs and box plots represent Mean ± SEM. Each circle represents an individual sample.

Oxytocin improves loss of long-term functional brain connectivity after TBI

We assessed the long-term neural correlates of pediatric TBI and oxytocin exposure using functional ultrasound (fUS), an innovative *in-vivo* imaging technique based on cerebral blood volume (CBV) analysis (Fig 7a-c).[22] fUS revealed a loss of CBV in the ipsilateral hemisphere in P45 TBI mice injured at P7, compared to sham (Fig 7d,e). TBI+OXT mice showed increased, sham-equivalent CBV in the ipsilateral hemisphere compared to untreated TBI (Fig 7d,e), suggesting improved long-term cerebrovascular integrity after early-life oxytocin release.

Functional connectivity analysis of a selection of ROIs[15] (Fig 7b,f) revealed that TBI reduces resting-state functional brain connectivity at P45 (Fig 7g,h). Intra-hemispheric connectivity of the primary somatosensory (S1) cortex regions was reduced in TBI animals in the ipsilateral, but not the contralateral hemisphere (Fig 7j,k). Inter-hemispheric cortical connectivity was similarly reduced in TBI versus sham mice (Fig 7l,m). Early-life oxytocin exposure after TBI was able to restore functional connectivity within the ipsilateral cortical regions (Fig 7j), and between hemispheric cortical regions (Fig 7l,m), compared to untreated TBI animals. Similar effects of TBI and oxytocin were found on connectivity in corpus callosum regions (Supplementary Fig S6).

Next, we performed network analysis and visualization using Gephi[23] on fUS connectivity between 212 ROIs across 3 coronal planes, to explore neural connectivity in more depth (see methods). Fig 7n shows the average isocortex neural networks for Sham, TBI and TBI+OXT groups, divided into strong and weak connections, and color-coded for the 5 substructures.

Network analysis revealed that TBI mice had significantly fewer strong connections in the isocortex compared to sham, showing a reduction in both weighted degree of connections (Fig 7o), and eigenvector centrality measures of nodes (Fig 7p). Oxytocin treatment reversed the weighted degree of strong connections in the perirhinal cortex, but not in other substructures (Fig 7s). TBI+OXT mice showed a rescue of centrality in the isocortex as a whole (Fig 7p), as well as for the sensorimotor and retrosplenial substructures (Fig 7t).

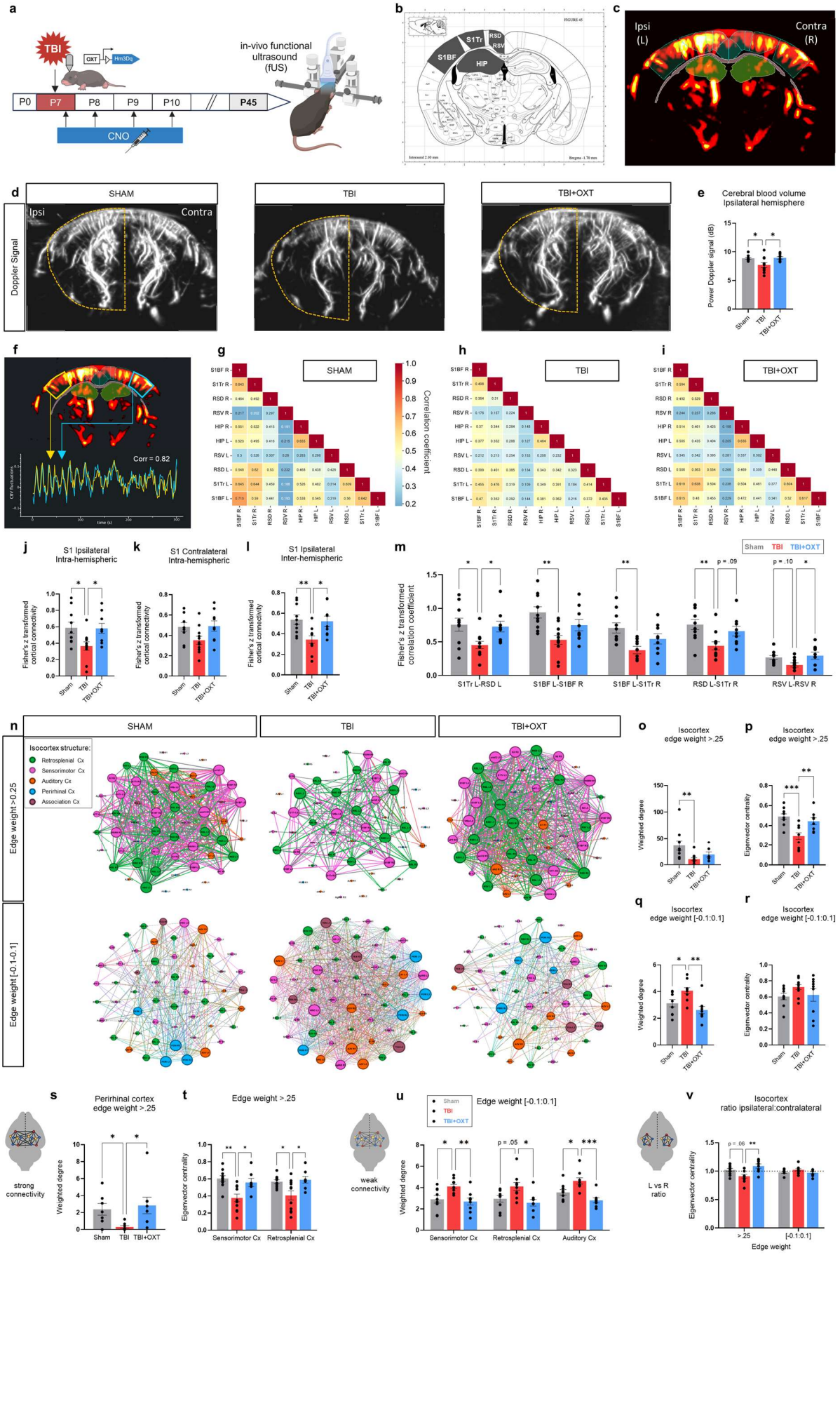
a
TBI
OXT
Hm3Dq
P0
P7
P8
P9
P10
P45
CNO
in-vivo functional ultrasound (fUS)
b
S1Tr
RSD
RSV
S1BF
HIP
c
Ipsi (L)
Contra (R)
d
SHAM
TBI
TBI+OXT
Doppler Signal
Ipsi
Contra
e
Cerebral blood volume Ipsilateral hemisphere
Power Doppler signal (dB)
Sham
TBI
TBI+OXT
f
Corr = 0.82
time (s)
g
SHAM
Correlation coefficient
h
TBI
i
TBI+OXT
j
S1 Ipsilateral Intra-hemispheric
k
S1 Contralateral Intra-hemispheric
l
S1 Ipsilateral Inter-hemispheric
Fisher's z transformed cortical connectivity
m
Sham
TBI
TBI+OXT
Fisher's z transformed correlation coefficient
p = .09
p = .10
S1Tr L-RSD L
S1BF L-S1BF R
S1BF L-S1Tr R
RSD L-S1Tr R
RSV L-RSV R
n
SHAM
TBI
TBI+OXT
Edge weight >0.25
Edge weight [-0.1:0.1]
Isocortex structure:
Retrosplenial Cx
Sensorimotor Cx
Auditory Cx
Perirhinal Cx
Association Cx
o
Isocortex edge weight >.25
Weighted degree
p
Isocortex edge weight >.25
Eigenvector centrality
q
Isocortex edge weight [-0.1:0.1]
Weighted degree
r
Isocortex edge weight [-0.1:0.1]
Eigenvector centrality
s
strong connectivity
Perirhinal cortex edge weight >.25
Weighted degree
t
Edge weight >.25
Eigenvector centrality
Sensorimotor Cx
Retrosplenial Cx
u
weak connectivity
Edge weight [-0.1:0.1]
Weighted degree
Auditory Cx
v
L vs R ratio
Isocortex ratio ipsilateral:contralateral
Eigenvector centrality
p = .06
>.25
[-0.1:0.1]
Edge weight

Fig. 7: Oxytocin improves long-term functional brain connectivity after TBI. **a)** Graphical timeline of the P45 *in-vivo* resting-state fUS experiment after P7 TBI and P7-P10 oxytocin treatment via CNO injections. **b)** Visualization of the bregma plane and the 10 ROIs that were selected for correlation connectivity analysis: S1Bf, S1Tr, RSV, RSD, HIP, in the ipsilateral and contralateral hemisphere. **c)** Example of the cerebral blood volume signal of a mouse with the ROIs superimposed. Lighter colors represent higher CBV, red colors represent lower CBV volumes. **d)** Representative images of the CBV as a measure of cerebrovascular integrity in the Sham (left), TBI (middle) and TBI+OXT (right) groups, with ipsilateral hemisphere delineated with dotted line. **e)** Quantification of CBV in the ipsilateral hemisphere shows a reduction in TBI mice versus Sham, and a rescue in the TBI+OXT group. **f)** Visualization of how the functional connectivity was calculated: as a correlation coefficient between the CBV variations between 2 ROIs. This example shows high correlation (r = .82). **(g-i)** Average correlation coefficient matrices of functional connectivity between the 10 ROIs for Sham **(g)**, TBI **(h)** and TBI+OXT **(i)** groups. **j-l)** Quantification of cortical functional connectivity in the S1 regions, divided into intra-hemispheric ipsilateral **(j)**, intra-hemispheric contralateral **(k)** and inter-hemispheric **(l)** connectivity. TBI mice showed a reduction, and TBI+OXT mice a rescue, for ipsilateral intra-hemispheric connectivity **(j)**, inter-hemispheric connectivity **(l)**, but no effect was found on contralateral intra-hemispheric connectivity **(k)**. **m)** Quantification of functional connectivity between a selection of ROI-pairs for Sham (gray), TBI (red) and TBI+OXT (blue) groups. **n-w)** Network analysis of functional connectivity on fUS registrations from 212 ROIs across 3 bregma planes. **n)** Average isocortex networks of the Sham (left), TBI (middle) and TBI+OXT (right) groups, separated into strong connections (edge weight >.25; top) and weak connections (edge weight between -0.1 and 0.1; bottom). Visualized with the Fruchterman-Reingold force-directed layout algorithm[26]. Node size represents eigenvector centrality (EC), and edge size represents weighted degree (= strength; WD). Colors represent the 5 isocortex substructures: retrosplenial cortex (green), sensorimotor cortex (magenta), auditory cortex (orange), perirhinal cortex (blue) and association cortex (mauve). **o,p)** Quantification of WD **(o)** and EC **(p)** measures for strong connections of the isocortex shows a decrease in both WD **(o)** and EC **(p)** in the TBI group versus sham, and a rescue of EC **(p)** in the TBI+OXT group. **q,r)** Quantification of WD **(q)** and EC **(r)** for weak connections of the isocortex showed an increase in TBI and a reverse in TBI+OXT for WD **(q)**. No effect on EC was found for weak isocortex connections **(r)**. **s)** Quantification of strong connectivity WD revealed a decrease in TBI and increase in TBI+OXT mice for the perirhinal cortex. **t)** Quantification of strong connectivity EC showed a decrease in TBI (red) and reversal in TBI+OXT (blue) for the sensorimotor and retrosplenial cortices. **u)** Quantification of weak connectivity WD for a selection of isocortex substructures for Sham (gray), TBI (red) and TBI+OXT (blue) groups, showed an increase in TBI and rescue in TBI+OXT for the sensorimotor, retrosplenial and auditory cortices. **v)** Quantification of the ratio of EC between ipsilateral/left and contralateral/right isocortex regions as a

representation of hemispheric balance revealed a preference for the contralateral regions in TBI (red) and a restoration of equal balance in the TBI+OXT (blue) mice for strong connectivity. No effect on weak connectivity EC ratio was found. Dotted line represents no preference (ratio = 1). TBI = traumatic brain injury; CNO = clozapine n-oxide; fUS = functional ultrasound; ROI = region of interest; CBV = cerebral blood volume; S1Bf = primary somatosensory cortex, barrel field; S1Tr = primary somatosensory cortex, trunk region; RSV = ventral retrosplenial cortex; RSD = dorsal retrosplenial cortex; HIP = hippocampus; WD = weighted degree; EC = eigenvector centrality. See Supplementary Data S4 for statistical details. In **(b)** Atlas source: Paxinos & Franklin, 2007[27]. Bar graphs represent Mean ± SEM. Each circle represents an individual sample.

The weighted degree of weak connections of the isocortex was increased in TBI versus sham, and rescued by OXT (Fig 7q,u) in the retrosplenial, somatosensory and auditory networks. Treatment group did not affect centrality of weak isocortex connections for the whole network (Fig 7r). These data suggest that TBI mice increase their weak connections of the isocortex, at the cost of strong connections, and that this pattern is reversed by early-life oxytocin treatment.

Finally, centrality between the ipsilateral and contralateral cortex for the 3 experimental groups were investigated by assessing ratio of ipsilateral versus contralateral eigenvector centrality for isocortex strong connectivity. TBI mice showed a reduction of this ratio, favoring the contralateral hemisphere in network centrality (Fig 7v). TBI+OXT mice had a fully restored equal balance in centrality between ipsilateral and contralateral isocortex regions, similar to sham mice (Fig 7v).

Oxytocin release rescues long-term behavioral deficits induced by TBI

Mice from the 3 experimental groups had comparable body growth, and were subjected to a behavioral test battery at the juvenile (P14) and adult age (P45) (Fig 8a,b). Using the homing test (Fig 8c), an early-life indicator of sociability and attachment[28], TBI mice lost preference for the home-cage nest bedding compared to bedding from an unfamiliar nest at P14 (Fig 8d). This impaired early social behavior persisted in the adult age, as shown using 3-chamber test at P45(Fig 8d,h,i). TBI mice further

demonstrated hyperactive behavior during the open field test at P45, showing increased average velocity and total distance traveled compared to sham (Fig 8e-g).

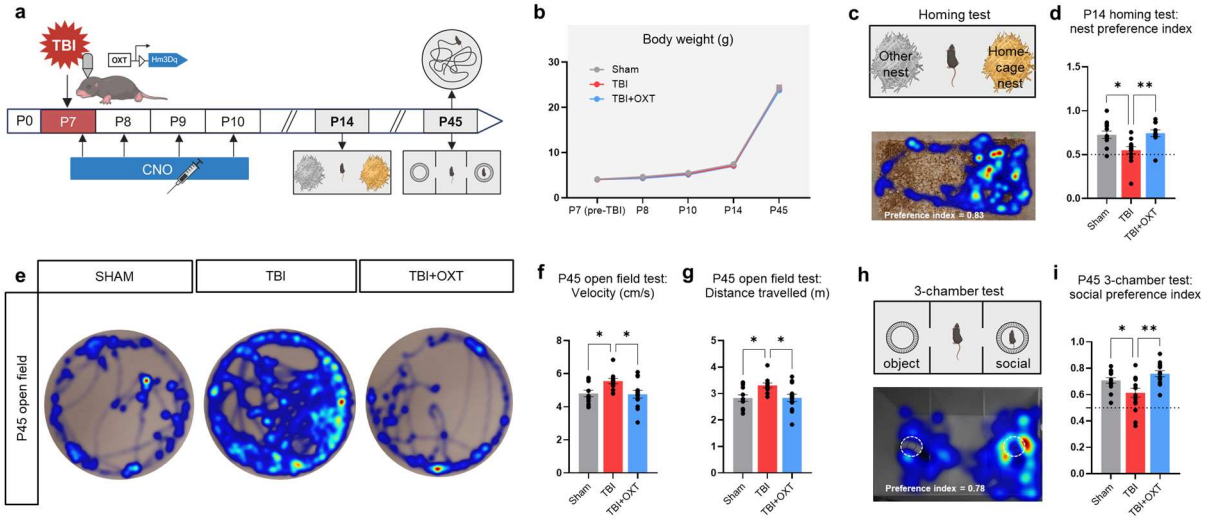

Fig. 8: Long-term behavioral deficits of TBI are rescued by oxytocin treatment. a) Graphical timeline of behavioral experiments after P7 TBI and P7-P10 oxytocin treatment via CNO injections. **b)** Body weight was not affected by TBI or oxytocin treatment. **c)** Graphical representation and representative sham-level performance of the P14 homing test. **d)** Quantification of the P14 homing test nest preference index (PI) showed a decreased nest preference in TBI mice and a rescue in TBI+OXT mice. Dotted line represents no nest preference (PI = 0.5). **e)** Representative behavior of sham (left), TBI (middle) and TBI+OXT (right) mice during the P45 open field test. **f,g)** Quantification of the P45 open field test revealed an increase in velocity **(f)** and distance traveled **(g)** in the TBI mice, and a rescue of both behaviors in the TBI+OXT treatment group. **h)** Graphical representation and representative sham-level performance of the 3-chamber test at P45. **i)** Quantification of the P45 3-chamber test showed a decrease in social preference in the TBI mice and a rescue in the TBI+OXT mice. Dotted line represents no social preference (PI = 0.5). In **(b)** Mixed-effects analysis ($F(8,161) = 0.34$, $p = .95$, Sham: $n = 15$, TBI: $n = 16$, TBI+OXT: $n = 14$). In **(d)** ANOVA ($F(2,34) = 6.91$, $^{**}p = .003$, Sham: $n = 13$, TBI: $n = 13$, TBI+OXT: $n = 11$). Tukey's (Sham vs. TBI: $^{*}p = .01$; Sham vs. TBI+OXT: $p = .95$; TBI vs. TBI+OXT: $^{**}p = .0067$). In **(n)** ANOVA ($F(2,38) = 0.34$, $p = .71$, Sham: $n = 13$, TBI: $n = 15$, TBI+OXT: $n = 13$). In **(f)** ANOVA ($F(2,33) = 4.54$, $^{*}p = .0181$, Sham: $n = 12$, TBI: $n = 11$, TBI+OXT: $n = 13$). Tukey's (Sham vs. TBI: $^{*}p = .043$; Sham vs. TBI+OXT: $p = .98$; TBI vs. TBI+OXT: $^{*}p = .026$). In **(g)** ANOVA ($F(2,33) = 4.73$, $^{*}p = .016$, Sham: $n = 12$, TBI: $n = 11$, TBI+OXT: $n = 13$). Tukey's (Sham vs. TBI: $^{*}p = .029$; Sham vs. TBI+OXT: $p = .99$; TBI vs. TBI+OXT: $^{*}p = .029$). In **(i)** ANOVA ($F(2,39) = 7.21$, $^{**}p = .0022$, Sham: $n = 14$, TBI: $n = 15$, TBI+OXT: $n = 13$). Tukey's (Sham vs. TBI: $^{*}p = .049$; Sham vs. TBI+OXT: $p = .405$; TBI vs. TBI+OXT: $^{**}p = .0018$). Bar and line graphs represent Mean ± SEM. Each circle represents an individual sample.

Early-life oxytocin release prevented the long-term impairments in social behavior induced by TBI. TBI+OXT mice showed a fully restored preference for their home-cage nest bedding at P14 (Fig 8d) and for the social stimulus at P45 (Fig 8i), and prevented the hyperactivity observed at P45 (Fig 8f,g).

Following the long-term effects of pediatric TBI on P45 brain functioning, we investigated the neuroinflammatory profile at P45. TBI mice showed no increase in cortical and WM microglia density (Fig S7c,d), astrocyte signal density (Fig S7e,f), or cortical TSPO expression (Fig S7g-h) at P45 compared to sham, nor did oxytocin treatment have an effect. This suggests that the TBI-induced deficits found at P45 may be considered as long-term consequences of TBI-induced acute neuroinflammation.

Discussion

This study shows that early-life chemogenetic activation of oxytocinergic neurons dampens the neuroinflammatory response 24h post-injury in a model of pediatric TBI, mitigating immune and pro-inflammatory gene pathways in astrocytes, and improving cerebrovascular repair and brain development mechanisms in microglial cells. The modulation of acute phase neuroinflammation prevented long-term damage to subcortical and cortical WM tracts, to resting-state functional connectivity loss in the isocortex, and ultimately to social behavior and hyperactivity disorders induced by TBI.

Consistent with previous studies,[29,30] we report widespread TBI-induced WM injury, with reduced long-term axonal integrity, myelin integrity and fiber tract thickness. Release of endogenous oxytocin spared corpus callosum thickness and axonal integrity in the external capsule. It also improved myelination in the cortical TBI impact region. In agreement, clinical studies demonstrate improved fractional anisotropy in the whole brain and specifically in the external capsule in preterm infants exposed to music therapy[11] – known to elevate oxytocin release.[31]

Second, we found alterations in the resting-state functional brain connectivity after pediatric TBI as also reported in clinical and preclinical studies.[15,32,33] fUS imaging showed improved long-term functional connectivity in the TBI isocortex 35 days after oxytocin release. The isocortex – specifically its prefrontal modules – contains the neural correlates underlying social behavior in mice,[34] and has positive correlations with pro-social effects of oxytocin.[35] With network analysis, we further revealed that oxytocin can shift the centrality of cortical hubs within brain networks after TBI, an important balance for executive functioning and information processing,[36] which can be distorted in children with TBI.[32] Moreover, fUS imaging revealed restored long-term cerebral blood flow in oxytocin-treated TBI mice. Vascular growth improves recovery of brain function and is a known therapeutic target following TBI.[37]

Third, we found that early-life endogenous oxytocin release was associated with restoration of typical social behavior in TBI-injured animals. A previous study performing TBI in P11 rats similarly observed a rescue of adolescent sociability after intranasal oxytocin administration 1h before testing,[35] and another study showed that improved social behavior after TBI treatment in rats associates with increased levels of oxytocin and oxytocin receptor expression.[38] Finally, pediatric TBI causes hyperactive disorders at adulthood[30]. This was prevented by oxytocin release

We found that long-term positive effects of oxytocin release just after TBI related to specific effects on neuroinflammation during the acute post-injury phase - a major contributor to disease progression, not only in TBI but after any insult to the developing brain.[7,39] Such anti-inflammatory effects, known to improve disease progression after brain insult, were previously suggested using a oxytocinergic analog,[12] and the current study further confirm these effects induced by endogenous oxytocin in the developing brain.

Microgliosis in developing WM can impair oligodendrocyte viability and development, which causes long-term myelination deficits.[40] Impaired oligodendrocyte development induced by the acute local microgliosis could explain the long-term integrity loss found in WM of TBI mice, a notion supported by

decreased Wnt signaling we found in TBI microglia, which causes hypomyelination.[24] Previous studies report a rescue of oligodendrocyte maturation following oxytocin receptor agonist exposure in a perinatal brain injury model in rats.[12]

Transcriptomic profiling of microglia and astrocytes after TBI provided insights into the ongoing inflammatory processes. On a transcriptomic level, oxytocin positively regulated genes encoding for tissue repair and brain development processes in TBI microglia. It increased the expression of genes related to vascular recovery, which likely contributes to the long-term vascular improvements we found at P45. Moreover, oxytocin reversed the transcriptomic increase of epigenetic processes in TBI microglia. Following an inflammatory insult as associated with TBI, microglia can undergo epigenetic reprogramming that heightens their response to secondary stressors.[41] In humans, such a two-hit model of inflammation and stress can lead to increased anxiety-like and depressive behaviors in adulthood.[42] Our findings suggest that oxytocin potentially reduces this pre-conditioning, which could protect the brain against future secondary insults. In astrocytes, oxytocin exposure increased expression of synaptic pathways, which are involved in the development of neural connectivity.[43] More notable was oxytocin's reduction of the inflammation and immune pathways upregulated after TBI. This was linked to type 1 interferon signaling, a pathway whose downregulation is a known neuroprotective following TBI.[44]

The transcriptomic signatures suggest a differential effect of oxytocin release on astrocytes and microglia in the acute phase after injury. First, the number of affected genes was 5 times higher in microglia than in astrocytes. Second, the transcriptomic changes induced by oxytocin showed a different profile in astrocytes and microglia. During neuroinflammation, astrocytes and microglia shift between pro- and anti-inflammatory activity, where anti-inflammatory functions are traditionally associated with tissue-repair and take over later in the post-injury timeline.[45] We found that oxytocin mostly reduced pro-inflammatory processes in astrocytes, and mostly increased anti-inflammatory processes in microglia. This double-edged and cell-specific effect suggests that oxytocin accelerates

the microglial shift towards a neuroprotective phenotype. Glial crosstalk during neuroinflammation is a known complex mechanism,[46] further complicated by the fact that the dynamic post-TBI transcriptomic profiles of microglia and astrocytes are highly susceptible to injury severity,[44] and timeline.[47] A practical distinction in neuroinflammation therapy research is whether to decrease toxic pro-inflammatory activity or increase protective anti-inflammatory activity[48,49], a dual mechanism potentially targeted by oxytocin, depending on glia type.

This study demonstrates that early life endogenous oxytocin release has acute anti-inflammatory effects after trauma in the developing brain with long-term benefits that persist long after oxytocin modulation is discontinued. As neuroinflammation is a key symptom of most types of perinatal brain injury,[39] the current study may act as a proof-of-concept for other brain injuries observed in young children. Translation of preclinical treatments is a general challenge for the pediatric population, but methodology of the current study may contribute to improve the translational potential of the therapeutic findings. Indeed, chemogenetic manipulation of endogenous oxytocin via the DREADD construct – rather than exogenous oxytocin administration – mimics the naturally elevated oxytocin levels observed in clinical studies of music therapy, skin-to-skin contact, and environmental enrichment in infants.[10,31] Clinical intervention associated with oxytocin release is non-invasive and does not compete with traditional medication. It should be noted that this study only included male mice – due to the increased occurrence and susceptibility of pediatric TBI seen in boys.[16] Given the increasing evidence for sexual dimorphism in early-life microglia,[50] in the inflammatory response to and outcomes of TBI,[51] consideration of findings from this study should be limited to males and invite future assessment in females.

Conclusions

In summary, this preclinical study describes a biological foundation for a protective effect of endogenous oxytocin activity on brain development following experimental pediatric TBI. We show a

multi-faceted improvement on brain functioning that persisted long after the treatment period, linked to changes to the microglial and astrocytic profile in the acute phase after injury. This identifies oxytocin as a novel, easy-to-implement treatment option for pediatric TBI in the clinical practice, which invites further exploration into its use.

Acknowledgements

This study was funded by the Swiss National Science Foundation (grant number 197462), and supported by La Fondation des Gueules Cassées and La Société Française d'Anesthésie et de Réanimation. Author ST was supported by the Swiss National Science Foundation (grant number 223414). We thank the CIBM Center for Biomedical Imaging for providing expertise and resources for the PET experiment. Figures were made with BioRender (https://www.biorender.com/), and SRplot[52].

Author Contributions

OB and MK contributed to conception and design of the study; MK developed experimental methods, performed data collection and analysis, and wrote the manuscript; ET performed data collection and analysis. YL performed and analyzed fUS and MRI imaging experiments; JLP performed the c-casp3/Iba1/NeuN immunohistochemistry experiment; KC and PM analyzed the TSPO experiment. BBT and PM provided materials for the TSPO experiment; SM performed and analyzed the electrophysiology experiment; ST contributed to data analysis of RNA Seq experiments; GS and ES contributed to development of experimental methods and to data collection; MLP and AJ contributed to development of experimental methods and to supplementary data collection and analysis; All authors edited the manuscript; AJ and OB acquired funding and supervised the project.

Potential conflicts of interest

Nothing to report

Data availability

All data necessary to evaluate the conclusions in this paper are included within the main text and Supplementary Materials. Source data are provided upon reasonable request.

References

1. Dewan, M. C., Mummareddy, N., Wellons, J. C. & Bonfield, C. M. Epidemiology of Global Pediatric Traumatic Brain Injury: Qualitative Review. *World Neurosurgery* **91**, 497-509.e1 (2016).
2. ARAKI, T., YOKOTA, H. & MORITA, A. Pediatric Traumatic Brain Injury: Characteristic Features, Diagnosis, and Management. *Neurol Med Chir (Tokyo)* **57**, 82–93 (2017).
3. Matcovitch-Natan, O. *et al.* Microglia development follows a stepwise program to regulate brain homeostasis. *Science* **353**, aad8670 (2016).
4. Kooper, C. C. *et al.* Long-Term Neurodevelopmental Outcome of Children With Mild Traumatic Brain Injury. *Pediatric Neurology* **160**, 18–25 (2024).
5. Kyösti, E. *et al.* Long-Term Quality of Life After Pediatric Traumatic Brain Injury Treated in the Intensive Care Unit. *Pediatric Neurology* **157**, 50–56 (2024).
6. Figaji, A. An update on pediatric traumatic brain injury. *Childs Nerv Syst* **39**, 3071–3081 (2023).
7. Jacquens, A. *et al.* Neuro-Inflammation Modulation and Post-Traumatic Brain Injury Lesions: From Bench to Bed-Side. *International Journal of Molecular Sciences* **23**, 11193 (2022).
8. Rokicki, J. *et al.* Oxytocin receptor expression patterns in the human brain across development. Preprint at https://doi.org/10.31219/osf.io/j3b5d (2021).
9. Knoop, M. *et al.* The Role of Oxytocin in Abnormal Brain Development: Effect on Glial Cells and Neuroinflammation. *Cells* **11**, 3899 (2022).
10. Moberg, K. U., Handlin, L. & Petersson, M. Neuroendocrine mechanisms involved in the physiological effects caused by skin-to-skin contact – With a particular focus on the oxytocinergic system. *Infant Behavior and Development* **61**, 101482 (2020).

11. Sa de Almeida, J. *et al.* Music enhances structural maturation of emotional processing neural pathways in very preterm infants. *NeuroImage* **207**, 116391 (2020).

12. Mairesse, J. *et al.* Oxytocin receptor agonist reduces perinatal brain damage by targeting microglia. *Glia* **67**, 345–359 (2019).

13. Yuan, L. *et al.* Oxytocin inhibits lipopolysaccharide-induced inflammation in microglial cells and attenuates microglial activation in lipopolysaccharide-treated mice. *J Neuroinflammation* **13**, 77 (2016).

14. Sünnetçi, E., Solmaz, V. & Erbaş, O. Chronic Oxytocin treatment has long lasting therapeutic potential in a rat model of neonatal hypercapnic-hypoxia injury, through enhanced GABAergic signaling and by reducing hippocampal gliosis with its anti-inflammatory feature. *Peptides* **135**, 170398 (2021).

15. Jacquens, A. *et al.* Deleterious effect of sustained neuroinflammation in pediatric traumatic brain injury. *Brain, Behavior, and Immunity* **120**, 99–116 (2024).

16. Arambula, S. E., Reinl, E. L., El Demerdash, N., McCarthy, M. M. & Robertson, C. L. Sex differences in pediatric traumatic brain injury. *Experimental Neurology* **317**, 168–179 (2019).

17. Schindelin, J. *et al.* Fiji: an open-source platform for biological-image analysis. *Nat Methods* **9**, 676–682 (2012).

18. IJBlob: An ImageJ Library for Connected Component Analysis and Shape Analysis. *Journal of Open Research Software* **1**, e6 (2013).

19. Ferreira, T. A. *et al.* Neuronal morphometry directly from bitmap images. *Nat Methods* **11**, 982–984 (2014).

20. van Tilborg, E. *et al.* A quantitative method for microstructural analysis of myelinated axons in the injured rodent brain. *Sci Rep* **7**, 16492 (2017).

21. Bokobza, C. *et al.* Magnetic Isolation of Microglial Cells from Neonate Mouse for Primary Cell Cultures. *JoVE* 62964 (2022) doi:10.3791/62964.

22. Macé, E. *et al.* Functional ultrasound imaging of the brain. *Nat Methods* **8**, 662–664 (2011).

23. Bastian, M., Heymann, S. & Jacomy, M. Gephi: An Open Source Software for Exploring and Manipulating Networks. *ICWSM* **3**, 361–362 (2009).

24. Van Steenwinckel, J. *et al.* Decreased microglial Wnt/β-catenin signalling drives microglial pro-inflammatory activation in the developing brain. *Brain* **142**, 3806–3833 (2019).

25. Guttenplan, K. A. *et al.* Knockout of reactive astrocyte activating factors slows disease progression in an ALS mouse model. *Nat Commun* **11**, 3753 (2020).

26. Fruchterman, T. M. J. & Reingold, E. M. Graph drawing by force-directed placement. *Software: Practice and Experience* **21**, 1129–1164 (1991).

27. Paxinos, G. & PhD, K. B. J. F., MA. *The Mouse Brain in Stereotaxic Coordinates*. (Elsevier Science, 2007).

28. Scattoni, M. L., Puopolo, M., Calamandrei, G. & Ricceri, L. Basal forebrain cholinergic lesions in 7-day-old rats alter ultrasound vocalisations and homing behaviour. *Behavioural Brain Research* **161**, 169–172 (2005).

29. Dikranian, K. *et al.* Mild traumatic brain injury to the infant mouse causes robust white matter axonal degeneration which precedes apoptotic death of cortical and thalamic neurons. *Experimental Neurology* **211**, 551–560 (2008).

30. Obenaus, A. *et al.* A single mild juvenile TBI in male mice leads to regional brain tissue abnormalities at 12 months of age that correlate with cognitive impairment at the middle age. *Acta Neuropathol Commun* **11**, 32 (2023).

31. Chanda, M. L. & Levitin, D. J. The neurochemistry of music. *Trends Cogn Sci* **17**, 179–193 (2013).

32. Botchway, E. *et al.* Resting-state network organisation in children with traumatic brain injury. *Cortex* **154**, 89–104 (2022).

33. van der Horn, H. J. *et al.* Dynamic Functional Connectivity in Pediatric Mild Traumatic Brain Injury. *NeuroImage* **285**, 120470 (2024).

34. Harris, J. A. *et al.* Hierarchical organization of cortical and thalamic connectivity. *Nature* **575**, 195–202 (2019).

35. Runyan, A., Lengel, D., Huh, J. W., Barson, J. R. & Raghupathi, R. Intranasal Administration of Oxytocin Attenuates Social Recognition Deficits and Increases Prefrontal Cortex Inhibitory Postsynaptic Currents following Traumatic Brain Injury. *eNeuro* **8**, ENEURO.0061-21.2021 (2021).

36. Fagerholm, E. D., Hellyer, P. J., Scott, G., Leech, R. & Sharp, D. J. Disconnection of network hubs and cognitive impairment after traumatic brain injury. *Brain* **138**, 1696–1709 (2015).

37. Ma, X. *et al.* Angiogenic peptide hydrogels for treatment of traumatic brain injury. *Bioact Mater* **5**, 124–132 (2020).

38. Wei, Z. Z. *et al.* Intracranial Transplantation of Hypoxia-Preconditioned iPSC-Derived Neural Progenitor Cells Alleviates Neuropsychiatric Defects after Traumatic Brain Injury in Juvenile Rats. *Cell Transplant* **25**, 797–809 (2016).

39. Hagberg, H. *et al.* The role of inflammation in perinatal brain injury. *Nat Rev Neurol* **11**, 192–208 (2015).

40. Favrais, G. *et al.* Systemic inflammation disrupts the developmental program of white matter. *Ann Neurol* **70**, 550–565 (2011).

41. Huang, M. *et al.* Microglial immune regulation by epigenetic reprogramming through histone H3K27 acetylation in neuroinflammation. *Front. Immunol.* **14**, (2023).

42. Quagliato, L. A., de Matos, U. & Nardi, A. E. Maternal immune activation generates anxiety in offspring: A translational meta-analysis. *Transl Psychiatry* **11**, 1–6 (2021).

43. Budak, M. & Zochowski, M. Synaptic Failure Differentially Affects Pattern Formation in Heterogenous Networks. *Front. Neural Circuits* **13**, (2019).

44. Todd, B. P. *et al.* Traumatic brain injury results in unique microglial and astrocyte transcriptomes enriched for type I interferon response. *Journal of Neuroinflammation* **18**, 151 (2021).

45. Andrew, P. M. *et al.* Shifts in the spatiotemporal profile of inflammatory phenotypes of innate immune cells in the rat brain following acute intoxication with the organophosphate diisopropylfluorophosphate. *J Neuroinflammation* **21**, 285 (2024).

46. Matejuk, A. & Ransohoff, R. M. Crosstalk Between Astrocytes and Microglia: An Overview. *Frontiers in Immunology* **11**, (2020).

47. Witcher, K. G. *et al.* Traumatic Brain Injury Causes Chronic Cortical Inflammation and Neuronal Dysfunction Mediated by Microglia. *J. Neurosci.* **41**, 1597–1616 (2021).

48. Michelucci, A., Heurtaux, T., Grandbarbe, L., Morga, E. & Heuschling, P. Characterization of the microglial phenotype under specific pro-inflammatory and anti-inflammatory conditions: Effects of oligomeric and fibrillar amyloid-beta. *J Neuroimmunol* **210**, 3–12 (2009).

49. Szpakowski, P., Ksiazek-Winiarek, D., Turniak-Kusy, M., Pacan, I. & Glabinski, A. Human Primary Astrocytes Differently Respond to Pro- and Anti-Inflammatory Stimuli. *Biomedicines* **10**, 1769 (2022).

50. Schwarz, J. M., Sholar, P. W. & Bilbo, S. D. Sex differences in microglial colonization of the developing rat brain. *Journal of Neurochemistry* **120**, 948–963 (2012).

51. Villapol, S., Loane, D. J. & Burns, M. P. Sexual dimorphism in the inflammatory response to traumatic brain injury. *Glia* **65**, 1423–1438 (2017).

52. Tang, D. *et al.* SRplot: A free online platform for data visualization and graphing. *PLoS One* **18**, e0294236 (2023).

Oxytocin release modulates acute neuroinflammation and improves brain development after pediatric traumatic brain injury

Marit Knoop, Ece Trak, Marie-Laure Possovre, Yohan van de Looij, Gabriel Schirmbeck, Kelly Ceyzériat, Jean-Luc Pitetti, Eduardo Sanches, Stefano Musardo, Philippe Millet, Stergios Tsartsalis, Benjamin B. Tournier, Camilla Bellone, Stéphane V. Sizonenko, Alice Jacquens & Olivier Baud

Supplementary materials

Extended methods:

Animals

Cre-dependent Hm3Dq-DREADD (Designer Receptors Exclusively Activated by Designer Drugs)[1] mice (B6N;129-Tg(CAG-CHRM3*,-mCitrine)1Ute/J, Jackson stock #026220) were crossed with Oxytocin-Ires-Cre mice (B6;129S-Oxttm1.1(cre)Dolsn/J, Jackson stock #024234) to create Oxt-Hm3Dq mice (B6;129S-Oxt-Cre;R26-LSL-hM3Dq-DREADD), which express the excitatory DREADD under the oxytocin promotor gene. This genetic profile allowed temporally increased neuronal firing of endogenous oxytocin neurons following injections of clozapine-N oxide solution (Enzo Life, BML-NS-105-0025).

Mice were housed in the SPF area in IVC-filtered top cages, under a light-dark cycle of 12 hours, with water and food access *ad libitum*. Room temperature and hygrometry were between 20-24°C and between 30% and 70%, respectively. Experimental cages included 2 dams with pups, and pups were randomly assigned to experimental groups. To prevent litter effects, each litter was divided into at least 2 experimental groups and every experiment consisted of at least 3 litters of animals. All surgeries and experiments were performed at the same hour across different litters. Only male mice were used in this study, due to the increased occurrence and susceptibility of pediatric TBI seen in male infants in the clinic.[2]

This study was approved by Ethical Committee for Animal Experiments of the University of Geneva and the Veterinary Office of Geneva (cantonal no. GE155A; national no. 34289). The animal facility of the UNIGE Faculty of Medicine is approved by the General Direction on Health of Geneva and meets all the requirements defined by Swiss regulations and laws.

Pediatric traumatic brain injury model

A model of closed-head weight-drop impact acceleration injury to male P7 mice was used, adapted from Jacquens et al., 2024.[3] In brief, P7 mice were anesthetized with 4% isoflurane, confirmed by the loss of the toe-pinch reflex. An incision was made to the scalp to expose the skull, and the head was placed under a trauma contusion device consisting of a stainless-steel cylinder, which guides a 10 g weight falling onto a foot plate (2 mm diameter; RWD Stereotaxic Model 68093). The foot plate was positioned above the TBI location on the brain: on the left parietal bone, 1mm lateral and 2 mm anterior to lambda. The footplate was lowered until it contacted the skull, and then it was further depressed by 0.5 cm. Once fixated, the 10 g weight was dropped from a 12 cm distance onto the foot plate to induce the weight-drop impact acceleration injury to the skull. After the procedure, the scalp was closed with surgical glue (3M Vetbond 1469SB). Pups were kept under an infrared lamp until they woke up, after which they were put back in their home-cage. Before reintroduction in the home-cage, pups were gently rubbed with home-cage bedding to ensure successful re-acceptance by the dam. Sham-operated mice were anesthetized, their skull surface was exposed and then their skin was closed with surgical glue. The TBI injury was administered by the same experimenter to assure consistency across samples.

Pharmacological increase of endogenous oxytocin

Mice of the TBI-oxytocin treatment group received Clozapine-N oxide (CNO) injections to activate the excitatory DREADDs on oxytocin neurons, which causes a temporary increase in endogenous neuronal oxytocin firing.[4] CNO was dissolved in NaCl at a concentration of 10mg/kg and injected intraperitoneally (i.p.) at a volume of 10 µl. Mice from the oxytocin treatment group received daily CNO injections starting at P7, 4 hours post-TBI (when major inflammatory cytokines are peaking)[5], and subsequently every morning at P8, P9 and P10. Non-treated mice received NaCl injections at the same time points. CNO solutions were prepared fresh daily.

This study had 3 experimental groups: Sham-operated mice, receiving NaCl injections (“Sham mice”), TBI-operated mice, receiving NaCl injections (“TBI mice”), and TBI-operated mice, receiving oxytocin-increasing CNO injections (“TBI+OXT mice”).

Evans Blue assay of cerebrovascular rupture

To assess blood-brain-barrier integrity loss in the TBI model, and to quantify rupture of cortical vasculature in response to the TBI procedure, we performed an Evans Blue assay at P7. Mice were i.p. injected with 50 µl of 1% Evans Blue (Sigma-Aldrich E2129) and put back in the home-cage to let the solution circulate and reach the brain vasculature. 4 hours post-injection, mice were subjected to TBI or Sham-operation. Mice were sacrificed 4 hours post-surgery with decapitation after pentobarbital anesthesia (150 mg/kg). Brains were immersed in 4% PFA for 48 hours, washed with PBS1x and imaged using iBright FL1500 Imaging System (ThermoFisher) at AlexaFluor 633 wavelength. Cerebrovascular rupture was assessed with ImageJ as an invert measure of ipsilateral hemisphere Evans Blue immunodensity fold change for TBI mice versus Sham littermate controls.

Immunohistology

Immunohistology was performed at P8 (24h post-TBI) and P45 (38 days post-TBI). Animals were anesthetized with i.p. injections of pentobarbital (150 mg/kg), confirmed by the loss of the toe-pinch reflex, and transcardially perfused with PBS and 4% paraformaldehyde (PFA) in PBS1x. Brains were post-fixated overnight in 4% PFA, and embedded in 15% sucrose (morning) and 30% sucrose (afternoon) solution the following day. Brains were snap-frozen in isopentane at -45°C and stored at -20°C until cutting. Brains were cut with a cryostat into free-floating coronal sections of 50 µm and stored in PBS+0.3%Azide solution. Coronal sections corresponding to slide 70 to 75 of Allen brain atlas (atlas.brain-map.org) were selected for immunofluorescent assays, corresponding to the Bregma level of TBI impact.

Immunofluorescence

Free-floating brain sections were blocked with 0.2% Triton+10% BSA in PBS1x for 1 hour. Following a 5 min wash in PBS, sections were incubated overnight at 4°C with primary antibodies in a solution of 0.2%Triton+3% BSA in PBS1x. Primary antibodies included rabbit anti-cleaved-caspase 3 (1:200; Cell Signaling D175), goat anti-Iba1 (1:500; Abcam ab5076), rabbit anti-Iba1 (1:1000; Fujifilm Wako 019-19741) and rat anti-CD68 (1:1000, Bio-rad FA-11), to assess (neuronal) cell death, microglia reactivity and their phagocytic activity at P8, and mouse anti-MBP (1:500, Sigma-Aldrich MAB382) was used to investigate myelination at P45. Following 3x 10 min washes in PBS1x, sections were incubated with secondary antibodies in a solution of 0.2%Triton+10% BSA in PBS1x for 1 hour and 30 minutes. Secondary antibodies were goat anti rabbit 594 (1:500, Abcam ab150080), goat anti rat 488 (1:500, Abcam ab150165), goat anti mouse 647 (1:500, Abcam ab150115), donkey anti rabbit 488 (1:500; Abcam ab150061), chicken anti goat 647 (1:500, Invitrogen A21469). After a final wash in PBS1x,

sections were mounted and coverslipped on microscopy slides (ThermoFisher) with flouromount medium that includes DAPI (Abcam ab104139). Slides were stored at 4°C.

Image acquisition

For measuring the degree of apoptotic cell death and microglia response at P8, brain sections were imaged with a ZEISS Axioscan.Z1 (Zeiss, Oberkochen, Germany) at 10x. Other immunohistochemistry assays were imaged using a ZEISS LSM 800 Airyscan confocal microscope (Zeiss, Oberkochen, Germany), at different magnitudes. All images were taken in the hemisphere ipsilateral to the brain injury. Micrographs were acquired by researchers blinded to experimental conditions.

For measuring the number of microglia and CD68 signal immunodensity, 3x4 tiles of 10x magnification were taken in two ROIs: the medial somatosensory cortex (layers I-VI), and the medial corpus callosum including the cingulate bundle. Both ROIs were taken at a horizontal localization superimposing the hippocampal CA1 region.

For single-cell microglia morphological analysis, 4 40X z-stack images (0.23 µm step size) were taken per animal, in 2 ROIs: in the medial somatosensory cortex layers IV/V, and at the medial corpus callosum including the cingulate bundle (superimposing the hippocampal CA1 region).

For analysis of corpus callosum thickness, 3x3 10x tiles were taken in the center of the structure, at the hemispheric division. For analysis of the external capsule, 3x4 10x tiles were taken. For analysis of cortical myelination, 3 40x z-stack images (0.23 µm step size) were taken per animal, in adjacent regions of cortical layers IV/V superimposing the hippocampal CA1 and CA2 regions.

Image analysis

Images were analyzed using FIJI/ImageJ[6] and QuPath[7]. Quantifications were performed by researchers blinded to experimental conditions.

- Apoptotic cell death and microglial proliferation

To quantify the degree of apoptotic cell death in the S1 cortex and white matter (WM), we counted the number of cleaved caspase-3$^+$ (c-casp3) cells, and the proportion of NeuN$^+$/c-casp3$^+$ cells. We also counted the number of microglia that were touching or engulfing c-casp3$^+$ cells. Microglia density in the S1 and WM was quantified as the number of Iba1$^+$ cells in the ROIs. Data from 3 micrographs per animal were averaged.

- Morphological analysis of single microglia

To assess the morphological characteristics of microglia on a single-cell level, individual microglia were isolated and reconstructed from the 40x z-stack micrographs, and saved as binary images for further analysis with the Shape Filter plugin[8] and Sholl plugin[9] of ImageJ.

Shape filter analysis[8] was performed on individual microglia to extract detailed parameters of overall cell morphology: Cell perimeter (CP) in µm, Cell density (CD), which is the ratio between cell area and cell perimeter, Cell convexity, which is the perimeter of the convex hull divided by the perimeter of the cell. Finally, a "Cell Circularity" measure was calculated with the following formula: circularity = 4π x CA / CP^2. Measures from 4-5 microglia were averaged per ROI per animal.

To measure the ramification of microglial cells, Sholl analysis[9] was performed on individual microglia. Sholl analysis was performed with a 2 µm radius step size, to generate a readout of number of intersections per radius step. 4-5 microglia were averaged per ROI per animal.

- Microglia phagocytic compartment

Phagocytic engulfment of dead or dying cells by microglia was assessed as the number of c-casp3$^+$-Iba1$^+$ touching cells, determined by manual counting. To further assess the phagocytic activity, the CD68$^+$ microglial compartment was measured as fluorescence density from a 3x4 10x tile micrograph. For each animal, an integrated CD68 density measure was calculated from a selected ROI. Fluorescence of 3 separate background readings per ROI was averaged and subtracted from the CD68 integrated density while controlling for ROI size using the formula: Corrected CD68 fluorescence = Integrated Density – (Area size of selected region x Mean fluorescence of background readings). Corrected CD68$^+$ fluorescence was normalized on the Sham group and reported as a fold change.

- White matter microstructure

Analysis of white matter microstructure at P45 was performed in ImageJ and based on the methods reported previously.[10] Subcortical white matter and the integrity of myelinated axons in the cortex were based on myelin base protein (MBP) immunoreactivity.

Subcortical white matter microstructure was assessed as the size (µm) of the medial corpus callosum and the external capsule based on 10x micrographs.

The MBP immunodensity and MBP$^+$ area measures were based on 40x z-stack micrographs taken as 3 adjacent regions in the somatosensory cortex (cortical layers IV/V). MBP immunodensity was measured as the mean signal intensity measure of the whole micrograph, subtracted by the background signal intensity. The MBP immunodensity was normalized on Sham group values, which were set on 100%. For each animal, measures from the 3 micrographs were averaged.

For the MBP^+ area analysis, a threshold for the MBP signal was applied to the whole micrographs, creating a binary image of all MBP^+ tissue and removing the background. The area proportion of MBP^+ signal was then calculated. Measures from 3 micrographs were averaged per animal.

MBP fiber coherency is an inverted measure of fiber complexity.[10] This was assessed in 3 adjacent 40x z-stack micrographs of the ipsilateral cortex, with the 'OrientationJ measure' function of the ImageJ plugin OrientationJ, as described previously.[10,11] Data from 3 micrographs were averaged per animal.

Transcriptomic profiling of glia

Magnetic isolation of microglia and astrocytes

To enable *in-vivo* assessment of the acute microglia and astrocyte transcriptome following TBI and the oxytocin treatment, microglia and astrocytes were sorted from P8 mice using magnetic cell sorting technology as described previously.[12] Briefly, P8 pups were anesthetized with pentobarbital i.p. injection (150 mg/kg) and transcardially perfused with PBS to remove macrophages. Brains were dissected, olfactory bulb and cerebellum removed, and the hemisphere ipsilateral to the injury was selected for further processing. Brain tissue was dissociated using the MACS® neural dissociation kit (Miltenyi Biotech). Microglia cells were isolated from brain homogenates via incubation with magnetic anti-mouse CD11b microbeads (Miltenyi Biotech) and collected using the MultiMACS® cell separator apparatus (Miltenyi Biotech). A separate sorting experiment was executed to collect astrocytes (using anti-mouse ACSA-2 microbeads). Sorted microglia and astrocytes were stored at -80°C.

Microglia real-time qPCR

For validation of the TBI model, RNA was extracted from P8 MACS-sorted microglia using the Nucleospin RNA Plus XS extraction kit (Macherey-Nagel). RNA quantity was measured with Nanodrop 2000 and was normalized across samples. RNA was subjected to reverse transcriptase using the MLV-RT kit (Promega; M1701). Real-time quantitative transcription polymerase chain reaction (RT-qPCR) was performed in duplicates with PowerUp™ SYBR™ Green Master Mix (ThermoFischer) for 40 cycles with a 2-step program (15 sec of denaturation at 95°C and 1 min of annealing/extension at 60°C). mRNA amplification values were normalized on Rps18 housekeeping gene and calculated as mRNA fold change measures normalized on the Sham group following the ΔΔCt analysis method. Gene expression of a selection of pro-inflammatory cytokines was assessed, based on previous findings[42]. Primers were designed with Primer-BLAST.[13] Primer sequences are provided in supplementary Table S2.

Microglia and astrocyte RNA sequencing

RNA was extracted from P8 sorted microglia using the Nucleospin RNA Plus XS extraction kit (Macherey-Nagel). RNA quantification was performed with a Qubit fluorometer (ThermoFisher Scientific) and RNA integrity assessed with a Bioanalyzer (Agilent Technologies). The microglial RNA was sequenced in bulk with Illumina NovaSeq 6000 next-generation sequencer. Quality control was performed with FastQC (v.0.1.1.9), and the reads were mapped to the reference mouse genome (Ensembl / GRCm39) using STAR aligner (v.2.7.10b).

MACS cell sorting purity was assessed with Expression Weighted Cell-type Enrichment analysis[14] of the top 250 expressed genes in the Sham group, based on normalized gene expression. The analysis was run with default parameters, with the number of repetitions for bootstrap enrichment set to 10.000. Enrichment significance was set at $p < .05$.

Differential gene expression (DEG) analysis was performed with edgeR (v.3.42.4). Lowly expressed genes (< 10 raw counts) were filtered out, and gene expression was normalized according to the library size and RNA composition. Differentially expressed genes were estimated using a quasi-likelihood (QL) F-test with rigorous type I error rate control. Corrections for multiple testing were performed with False Discovery Rate (FDR) and the Benjamini & Hochberg correction (BH). Significant genes were filtered on cut-off values of ≥ 1.5 fold-change and $p < .05$. DEG analysis was performed for the comparisons TBI versus Sham, and TBI+OXT versus TBI. Unidentified DEGs were excluded from the results.

Gene set enrichment analysis on differentially expressed genes was performed using DAVID Functional Annotation Tool (DAVID Knowledgebase v2024q1, National Institutes of Health). The upregulated DEGs were analyzed separately from the downregulated DEGs. Databases of biological processes and KEGG pathways were investigated. Pathways with a p value of < .05 were considered.

The same methodology was applied to astrocyte RNA sequencing, with the exception that a batch effect was discovered for astrocyte samples with PCA analysis, which was corrected for in downstream RNA Seq analyses.

The RNA Seq experiments were performed at the iGE3 Genomics Platform of the University of Geneva (https://ige3.genomics.unige.ch).

Ex-vivo brain structure assessment with MRI-diffusion tensor imaging

We performed microscopic diffusion analysis of white and grey matter in the ipsilateral hemisphere with *ex-vivo* MRI imaging to assess long-term microstructural brain development. At P45, animals were anesthetized with i.p. injections of pentobarbital (150 mg/kg), confirmed by the loss of the toe-pinch reflex, and transcardially perfused with PBS and 4% paraformaldehyde (PFA) in PBS1x. Brains were kept in PFA overnight, then changed and kept in PBS1x for 6 weeks until scanning.

Image acquisition

Ex-vivo MRI experiments were performed with a 2.5 cm diameter birdcage coil, on an 9.4T/31cm actively shielded horizontal-bore magnet (Magnex Scientific, Yarnton, UK), B-GA12S HP shielded gradient set (114mm ID, 660 mT/m peak strength and 4570 T/m/s slew rate, Bruker BioSpin, Ettlingen, Germany) interfaced to a Bruker BioSpec console with AVANCE NEO electronics running ParaVision 360 v3.5. A multi-b-value shell protocol was acquired using a spin-echo sequence (FOV = 21 × 16 mm^2, matrix size = 120 × 80, 20 slices of 0.6 mm, 4 averages with TE/TR = 22/2000ms). 82 DWI were acquired, 6 b0 images and 76 separated in 3 shells (noncollinear and uniformly distributed in each shell with δ/Δ = 4.5/12 ms) with number of directions/b-value in s/mm^2: 16/1500, 30/3000 and 30/5000.

Microscopic diffusion analysis with DTI and NODDI techniques

Diffusion data processing started by MP-PCA denoising[15] then the diffusion tensor was estimated using a weighted linear least squares algorithm.[16] Diffusion weighted data were fitted using the AMICO model.[17] Several brain regions were assessed in the ipsilateral hemisphere, ROIs were delineated on the fractional anisotropy maps. We calculated DTI derived parameters, including Axial diffusivity (AD), representing axonal integrity, Radial diffusivity (RD), representing myelin sheath integrity, and Fractional anisotropy (FA), reflecting axonal diameter, fiber density and myelination. We also calculated neurite orientation dispersion and density imaging (NODDI) metrics, including Neurite density index (NDI), relating to the packing density of axons or dendrites, Orientation dispersion index (ODI), an inverse measure of fiber alignment, and Free water fraction (FWF), which reflects contamination of the CSF. These parameters were calculated for 5 Ipsilateral ROIs for each animal: corpus callosum (CC), cingulum (Cg), external capsule (EC), primary motor cortex (M1Cx) and primary somatosensory cortex (S1Cx). Data were averaged for the coronal planes and statistically tested between groups using one-way ANOVA tests with Tukey's post-hoc.

In-vivo brain connectivity imaging with functional ultrasound (fUS)

We performed *in-vivo* resting-state functional ultrasound (fUS) imaging of the brain at P45 as a readout of long-term functional brain connectivity. This method uses cerebrovascular blood volume (CBV)

variations to analyze the correlation of resting-state neuronal activity, between ROIs in the same (intra-hemispheric connectivity) and opposite hemispheres (inter-hemispheric connectivity).[18] The mouse P56 coronal brain atlas from Allen Institute (atlas.brain-map.org) was used as ROI map.

fUS data acquisition

The experiment was performed as previously described.[3,19] Briefly, P45 animals were anesthetized with 1:10 Ketamine mixed with 1:20 Domitor in NaCl, injected i.p. at a concentration of 100 ul/kg body weight. After ensuring anesthesia by the loss of the toe-pinch reflex, the scalp was cut to expose the skull. The animal was placed in a stereotaxic frame, on top of a heating pad kept at 37°C. Ultrasound coupling gel was applied to the skull and the ultrasonic probe (Vermon, Tours, France) was positioned directly above the parietal bone.

An initial 3D anatomic scan was performed for every mouse to function as a reference atlas to align the ROI map to. The probe was vertically positioned directly above Bregma level -1. From this position, a 10-minute ultrasonic acquisition scan was conducted at a frame-rate of 500 Hz, with tilted plane waves oriented at 5 different angles to allow optimal detection of blood volume variation.

fUS data analysis

Connectivity correlation analysis

For each animal, CBV patterns were transformed into connectivity correlation matrices between a selection of 10 ROIs of the atlas, based on previous findings[3]: barrel field of the somatosensory cortex (S1BF), trunk region of the somatosensory cortex (S1Tr), ventral retrosplenial cortex (RSV), dorsal retrosplenial cortex (RSD) and CA1 region of the hippocampus (HIP), in both hemispheres. We analyzed connectivity between these regions, and for connectivity in the cortex (averaging the S1Tr, S1BF, RSV, and RSD regions) in the ipsilateral and contralateral hemispheres. For statistical testing between groups, the Pearson correlation coefficients were transformed using a Fisher z transformation, and tested with One-way ANOVAs.

Neural network analysis

To perform a holistic network analysis of brain connectivity, we measured CBV variations in 212 ROIs across 3 coronal planes (Bregma -1, -1.5, -2). This created a large connectivity matrix that was loaded into Gephi[43] where it was transformed into a 3D neural network of nodes (ROIs) and edges (connections between ROIs). We categorized the 212 ROIs into cerebral structures (e.g., “sensorimotor cortex”) and transcending structural “hubs” (e.g., “isocortex”), to enable assessment of larger

collections of structures in the network. See full list of ROIs and their categorization in Supplementary Table S1.

Neural networks were filtered on structural hub, edge weight (strong *vs* weak connections), underlying structure and hemisphere. We analyzed for every structural hub and for a selection of underlying structures the total connectivity (as average weighted degree and average eigenvector centrality) and the ratio between ipsilateral and contralateral hemispheres for the eigenvector centrality measures. Weighted degree reflects the average strength of connections of the network, and eigenvector centrality also includes the strength of connecting nodes[20] – meaning that it is a measure of how central the node is in the entire network. Statistical comparison between treatment groups was performed with One-way ANOVA with Tukey's post-hoc assessment.

Behavior

Mouse behavior was tracked and analyzed using Ethovision.[21] Behavioral experiments were performed by the same researcher to ensure a consistent testing environment.

Body growth

Body growth was measured at P7 (before TBI procedure), P8, P10, P14 and P45 to assess effects of the TBI and the oxytocin treatment on general well-being of the mouse.

Homing test

At P14, the homing test was performed to analyze early-life sociability: a pup was placed in a 32x16x18 cm (lxwxh) cage with bedding and was allowed free exploration during 3 minutes. The cage was divided in length into 2 outer zones of 12 cm. The middle zone (8 cm) had fresh bedding, one zone on the far side had bedding from the pup's home-cage nest, and the other far-side zone had bedding from an unfamiliar nest with pups. Time spent in each zone was calculated and converted to a preference index for the home-cage zone versus the unfamiliar nest zone. The cage orientation was alternated between trials and fresh bedding from the 2 nests was added between every trial to equalize odor strength between trials.

Open field test

The open field test was performed at P45 to analyze general motor activity and anxiety. Animals were placed in a circular arena (35 cm diameter, 22 cm tall) and were allowed free exploration during 10 minutes. Readouts were velocity (m/s), total distance travelled (m), and time spent in the center zone (s) as an indirect measure of anxiety.

Three chamber test

The three-chamber test was performed at P45 as an adult measure of sociability. In an arena divided in 3 connected chambers of 20x40x25 cm (lxwxh), the two outer chambers include either an empty mesh-bar enclosure (9 cm diameter, 17 cm tall) or an enclosure containing an unfamiliar mouse (one week younger than the experimental mouse). After a 10 min habituation phase, the 2 enclosures were placed and the animal was allowed free exploration during 5 minutes. Data was analyzed as time spent interacting with both enclosures (object versus social), by tracking the total time the animal's nose was within 2 cm proximity from the enclosure. We analyzed the social preference score by calculating the time spent interacting with the social enclosure divided by the total time interacting with the social + empty enclosure.

Statistical analysis

Statistical analysis was performed with Graphpad/Prism version 10.4.0 for Windows (GraphPad Software, Boston, Massachusetts USA, www.graphpad.com). All data was checked for outliers with the ROUT method (Q = 0.1%), and tested for normality using Kolmogorov-Smirnov test (α = .05) and QQ plot inspection. The *n* indicated in each figure legend represents sample size after outlier removal. Comparisons between 2 treatment groups were performed with Student's t-test for normally distributed data and a Mann-Whitney U test for non-normally distributed data. Analyses of phagocytosis between cortex and white matter in the TBI group was performed with paired t-test. Analyses between all 3 treatment groups was performed with a One-way ANOVA with Tukey's post-hoc for normal distributed data, or Kruskal-Wallis test with Dunn's post-hoc for non-normally distributed data. Sholl analysis of microglia ramification was performed with a two-way ANOVA of treatment x sholl radius. Behavioral assays of repetitive assessments (e.g., body growth) were analyzed with a two-way ANOVA of treatment x postnatal age. The alpha was set at 0.05, and tested two-tailed. Unless specified otherwise, graphs show Mean + SEM values. Non-significant post-hoc comparisons are not shown in the graphs.

References

1. Zhu, H. *et al.* Cre dependent DREADD (Designer Receptors Exclusively Activated by Designer Drugs) mice. *Genesis (New York, N.Y. : 2000)* **54**, 439 (2016).
2. Arambula, S. E., Reinl, E. L., El Demerdash, N., McCarthy, M. M. & Robertson, C. L. Sex differences in pediatric traumatic brain injury. *Experimental Neurology* **317**, 168–179 (2019).

3. Jacquens, A. *et al.* Deleterious effect of sustained neuroinflammation in pediatric traumatic brain injury. *Brain, Behavior, and Immunity* **120**, 99–116 (2024).
4. Grund, T. *et al.* Chemogenetic activation of oxytocin neurons: Temporal dynamics, hormonal release, and behavioral consequences. *Psychoneuroendocrinology* **106**, 77–84 (2019).
5. Delage, C., Taib, T., Mamma, C., Lerouet, D. & Besson, V. C. Traumatic Brain Injury: An Age-Dependent View of Post-Traumatic Neuroinflammation and Its Treatment. *Pharmaceutics* **13**, 1624 (2021).
6. Schindelin, J. *et al.* Fiji: an open-source platform for biological-image analysis. *Nat Methods* **9**, 676–682 (2012).
7. Bankhead, P. *et al.* QuPath: Open source software for digital pathology image analysis. *Sci Rep* **7**, 16878 (2017).
8. IJBlob: An ImageJ Library for Connected Component Analysis and Shape Analysis. *Journal of Open Research Software* **1**, e6 (2013).
9. Ferreira, T. A. *et al.* Neuronal morphometry directly from bitmap images. *Nat Methods* **11**, 982–984 (2014).
10. van Tilborg, E. *et al.* A quantitative method for microstructural analysis of myelinated axons in the injured rodent brain. *Sci Rep* **7**, 16492 (2017).
11. Effect of Aging on Elastin Functionality in Human Cerebral Arteries | Stroke. https://www.ahajournals.org/doi/10.1161/STROKEAHA.108.528091?url_ver=Z39.88-2003&rfr_id=ori:rid:crossref.org&rfr_dat=cr_pub%20%200pubmed.
12. Bokobza, C. *et al.* Magnetic Isolation of Microglial Cells from Neonate Mouse for Primary Cell Cultures. *JoVE* 62964 (2022) doi:10.3791/62964.
13. Ye, J. *et al.* Primer-BLAST: A tool to design target-specific primers for polymerase chain reaction. *BMC Bioinformatics* **13**, 134 (2012).
14. Skene, N. G. & Grant, S. G. N. Identification of Vulnerable Cell Types in Major Brain Disorders Using Single Cell Transcriptomes and Expression Weighted Cell Type Enrichment. *Front. Neurosci.* **10**, (2016).
15. Veraart, J., Fieremans, E. & Novikov, D. S. Diffusion MRI noise mapping using random matrix theory. *Magn Reson Med* **76**, 1582–1593 (2016).
16. Veraart, J., Sijbers, J., Sunaert, S., Leemans, A. & Jeurissen, B. Weighted linear least squares estimation of diffusion MRI parameters: Strengths, limitations, and pitfalls. *NeuroImage* **81**, 335–346 (2013).
17. Daducci, A. *et al.* Accelerated Microstructure Imaging via Convex Optimization (AMICO) from diffusion MRI data. *NeuroImage* **105**, 32–44 (2015).
18. Macé, E. *et al.* Functional ultrasound imaging of the brain. *Nat Methods* **8**, 662–664 (2011).

19. Mairesse, J. *et al.* Oxytocin receptor agonist reduces perinatal brain damage by targeting microglia. *Glia* **67**, 345–359 (2019).
20. Bonacich, P. Factoring and weighting approaches to status scores and clique identification. *Journal of Mathematical Sociology* (1972).
21. Noldus, L. P. J. J., Spink, A. J. & Tegelenbosch, R. A. J. EthoVision: A versatile tracking system for automation of behavioral experiments. *Behavior Research Methods, Instruments & Computers* **33**, 398–414 (2001).

Methods of supplementary figures:

A Supplementary experiments to validate the OXT-Hm3Dq DREADD construct

A.1 Immunohistochemistry

A.1.1 Hm3Dq DREADD expression on oxytocin neurons

Validation immunohistochemistry of the OXT-Hm3Dq mouse line was performed to assess the degree of DREADD expression on oxytocin cells in the periventricular nucleus (PVN) – the principal production region of oxytocin[1]. Untreated OXT-Hm3Dq mice were anesthetized and sacrificed as described in the main methods. 50 µm free-floating coronal sections were cut with a vibratome. The immunohistochemistry was a 5-day experiment. Day 1: Sections were incubated for 1h in blocking solution (10%BSA + 3% NGS in PBS1x), and incubated at 4°C for 48h with mouse anti-HA-Tag (cell signaling 2367; 1:200) in incubation solution (3%BSA + 1%NGS+0.2%TritonX in PBS1x). Day 3: Sections were washed in 0.2%TritonX+PBS1x and incubated at RT for 2h with goat anti-mouse Alexa 594 (Abcam ab150116; 1:500). Sections were washed in 0.1%TritonX in PBS1x, blocked for 45 min in blocking solution and subsequently incubated at 4°C for 48h with rabbit anti oxytocin (Millipore Ab911; 1:500) in incubation solution. Day 5: Sections were washed in 0.2%TritonX+PBS1x and incubated at RT for 2h with goat anti rabbit Alexa 488 (Abcam ab150077; 1:500). Slides were washed, mounted and coverslipped with Fluoromount (Abcam ab104139).

A.1.2 c-FOS activation upon CNO injection

We validated the increase in PVN cell firing after CNO injection with immunohistochemistry of immediate-early-gene c-FOS[2]. OXT-Hm3Dq mice were injected with saline or CNO solution, and sacrificed under anesthesia 1h post-injection. Brains were collected and cut into 50 µm floating sections with a vibratome. Sections were blocked for 1h in 10% BSA + 3%NGS + 0.2% TritonX in PBS 1x, and incubated at 4°C for 24h with guinea pig anti-c-Fos (synaptic systems 226 308; 1:5000) in 3% BSA + 1%NGS + 0.2% TritonX in PBS1x. Sections were washed in PBS1x and incubated with sheep anti guinea pig FITC (Abcam ab136790; 1:500) in PBS1x + 0.1% TritonX for 2h at RT. Sections were washed, mounted and coverslipped with Fluoromount (Abcam ab104139).

A.1.3 Image acquisition

Brain sections were imaged with a ZEISS LSM 800 Airyscan confocal microscope (Zeiss, Oberkochen, Germany). Images of the PVN were acquired as 3x4 tiles of 20x z-stack images with 0.49 µm step size.

A.1.4 Image analysis

Image analysis was performed with FIJI/ImageJ[3] via manual counting by researchers blinded to experimental conditions. The degree of HA-Tag coverage of OXT cells in the PVN was determined as the number of $HATag^{+}/OXT^{+}$ cells divided by the total number of OXT^{+} cells. For the cFOS quantification, $cFOS^{+}$ cells were counted and transformed as a percentage relative to the average cFOS signal of the saline injected group ("% of baseline").

A.2 Electrophysiology

Coronal sections of the midbrain, 250 µm thick and including the PVN, were obtained from mice of the OXT-Hm3Dq DREADD line. Brain slicing was performed using a cutting solution composed of 90.89 mM choline chloride, 24.98 mM glucose, 25 mM NaHCO3, 6.98 mM MgCl2, 11.85 mM ascorbic acid, 3.09 mM sodium pyruvate, 2.49 mM KCl, 1.25 mM NaH2PO4, and 0.50 mM CaCl2. The sections were maintained in the same solution for 20–30 minutes at 35°C. Subsequently, the slices were transferred to artificial cerebrospinal fluid (aCSF) composed of 119 mM NaCl, 2.5 mM KCl, 1.3 mM MgCl2, 2.5 mM CaCl2, 1.0 mM NaH2PO4, 26.2 mM NaHCO3, and 11 mM glucose, continuously bubbled with a gas mixture of 95% O2 and 5% CO2 at room temperature. Electrophysiological recordings, in either whole-cell voltage-clamp or current-clamp mode, were performed at 35–37°C with slices submerged in aCSF perfused at 2–3 ml/min. The internal solution for recording pipettes consisted of 140 mM K-Gluconate, 2 mM MgCl2, 5 mM KCl, 0.2 mM EGTA, 10 mM HEPES, 4 mM Na2ATP, 0.3 mM Na3GTP, and 10 mM creatine-phosphate. Oxytocinergic neurons were identified by stimulating the tissue with a 594 nm LED to detect mCitrine fluorescence. The resting membrane potential (measured in mV) was recorded using a Multiclamp 700B Commander (Molecular Devices) under zero current injection conditions (I=0) immediately after establishing whole-cell configuration. Action potentials were induced in current-clamp mode by applying depolarizing current steps of 100 pA lasting 500 ms. Following baseline acquisition, CNO (20 µM, Enzo Life Sciences, BML-NS-105-0025) was administered to the bath solution and subsequently washed out. Throughout the experiment, the number of action potentials and resting membrane potential values were systematically monitored.

<u>B Supplementary experiments to assess side-effects of the CNO substance</u>

B.1 Animals

Cre-dependent Hm3Dq-DREADD (Designer Receptors Exclusively Activated by Designer Drugs) mice (B6N;129-Tg(CAG-CHRM3*,-mCitrine)1Ute/J[4], Jackson stock #026220) were crossed with Oxytocin-Ires-Cre mice (B6;129S-Oxttm1.1(cre)Dolsn/J, Jackson stock #024234) to create $OXT^{+/-}$-$Hm3Dq^{-/-}$ mice. We used these mice to test side-effects of the CNO substance because they come from the same breeding colony and they share the exact same genetic background as the OXT-Hm3Dq experimental

mice, but without DREADD expression. As such, the CNO substance could be tested isolated from its functional effects on the Gq designer receptors.

TBI injury and CNO treatment were administered to the $OXT^{+/-}$-$Hm3Dq^{-/-}$ animals as described in the main methods.

B.2 real-time qPCR

RNA was extracted from P8 ipsilateral neural tissue using the Nucleospin RNA XS extraction kit (Macherey-Nagel). RNA quantity was measured with Nanodrop 2000 and was normalized across samples. RNA was subjected to reverse transcriptase using the MLV-RT kit (Promega; M1701). Real-time quantitative transcription polymerase chain reaction (RT-qPCR) was performed in duplicates with PowerUp™ SYBR™ Green Master Mix (ThermoFischer) for 40 cycles with a 2-step program (15 sec of denaturation at 95°C and 1 min of annealing/extension at 60°C). mRNA amplification values were normalized on Rps18 housekeeping gene and calculated as mRNA fold change measures normalized on the TBI+saline group following the ΔΔCt analysis method. We tested a selection of microglia-related inflammation genes, based on previous findings[5]: Nos2, Ptgs2, Tnf-α, Lgals3, Igf1, and IL1rn. Primers were designed with Primer-BLAST [6]. Primer sequences are provided in Table S2.

B.3 Behavior

To assess long-term side-effects of CNO on behavior, we subjected the CNO-treated and saline-treated $OXT^{+/-}$-$Hm3Dq^{-/-}$ TBI mice to P45 3-chamber test and P45 open field test. Data acquisition and analysis was performed as described in the main methods.

C Supplementary experiment on *in-vivo* oxytocin receptor mRNA expression

To assess oxytocin receptor (OXTR) expression on microglia and astrocytes *in-vivo* in young mice (P5), we performed RNA Scope in situ hybridization of Oxtr mRNA expression.

C.1 Fluorescent RNAscope in situ hybridization

RNA in situ hybridization was performed using RNAScope® Multiplex Fluorescent V2 Assay with the ACD HybEZ™ II Hybridization System (Advanced Cell Diagnostics, Hayward, California, USA), according to the manufacturer's protocol. Mouse-specific probes for oxytocin receptor (RNAscope® Probe #412171), Cd11b (RNAscope® Probe #311491-C2) and Gfap (RNAscope® Probe #313211-C3) mRNA were used to identify OXTR expression on microglia and astrocytes, respectively. Probes were amplified and fluorescently labeled using TSA Vivid Fluorofore kits 520 (#7523), 570 (#7526) and 650 (#7527). Slides were coverslipped with DAPI-immersed mounting medium to visualize cell nuclei.

C.2 Image acquisition

Fluorescent brain sections were imaged with a ZEISS LSM 800 Airyscan confocal microscope (Zeiss, Oberkochen, Germany) at 20x magnitude. 5 separate images were taken in the cortex and white matter, for each animal.

C.3 Image analysis

Images analysis was performed with FIJI/ImageJ[3]. Astrocytes and microglia cells were counted based on co-labeling of DAPI cell nuclei with Gfap and Cd11b mRNA, respectively. The degree of $OXTR^+$ astrocytes/microglia was calculated as the number of $OXTR^+$ astrocytes/microglia divided by the total number of astrocyte/microglia cells. Data from 5 images was averaged for each sample. Quantification was performed separately for the cortex and white matter.

D Supplementary experiment on acute neuronal cell death

To assess the proportion neuronal cell death after TBI and oxytocin exposure, we performed immunohistochemistry on P8 mouse brains from TBI and TBI+OXT groups.

D.1 Immunohistochemistry

Immunohistochemistry was performed on P8 brain sections as described in the main methods. Primary antibodies used were mouse anti-NeuN (Sigma-Aldrich MAB377; 1:200) and rabbit anti-cleaved-caspase 3 (Cell Signaling D175; 1:200). Secondary antibodies used were donkey anti mouse 555 (Abcam ab150106; 1:500) and donkey anti rabbit 488 (Abcam ab150061; 1:500).

D.2 Image acquisition

Brain sections were imaged with a ZEISS Axioscan.Z1 (Zeiss, Oberkochen, Germany) at 10x.

D.3 Image analysis

Image analysis was performed by researchers blinded to experimental conditions. NeuN and cleaved-caspase 3 signals were quantified in the cortex ipsilateral to the brain injury, by manual counting. The degree of neuronal apoptotic cell death was quantified per animal as the number of $NeuN^+$/cleaved-caspase-3^+ cells divided by the total number of cleaved-caspase 3^+ cells.

E Supplementary experiments on long-term neuroinflammation after TBI

To assess the long-term neuroinflammatory profile of our TBI model, we performed P45 experiments of microglia and astrocyte reactivity in sham, TBI and TBI+OXT groups.

E.1 P45 Immunohistochemistry

Immunohistochemistry of Iba1^{+} (microglia) and Gfap^{+} (astrocyte) reactivity was performed on free-floating sections from P45 brains as described in the main methods. Microglia and astrocyte density were analyzed in the ipsilateral somatosensory cortex and white matter as described in the main methods. Analysis was performed by a researcher blinded to experimental conditions. Microglia were manually counted, and astrocyte density was analyzed per sample as mean signal intensity measures corrected for background signal.

E.2 P45 TSPO quantification

To complement the microgliosis assay, we set out to measure the presence of 18 kDa Translocator Proteins (TSPO) at P45, which are proteins expressed by glia, that can act as a biomarker of neuroinflammation (reviewed in Cumbers et al., 2024[7]).

E.2.1 [^{18}F]PBR111 PET imaging and processing

P45 animals were anaesthetised with isoflurane (4% induction, maintained at 2%) and injected with [^{18}F]PBR111 in the tail vein immediately prior to imaging – [^{18}F]PBR111 is a second-generation PET ligand that specifically binds the TSPO. To maintain the same specific activity between animals at the time of injection, all syringes were prepared at the same time, the injected dose consequently varied from 33.54 MBq to 5.76 MBq. A CT image was acquired, followed by a dynamic PET acquisition of 50 minutes per animal (5x10 min), during which body temperature was maintained using a heated bed. Images were acquired on a FLEX TriumphTM preclinical PET-CT scanner (Gamma Medica-Ideas, Nortridge, CA).

[^{18}F]PBR111 dynamic images were co-registered to a T2-weighted MRI atlas using PMOD (v4.401, PMOD Technologies LLC). A factorial analysis was applied to extract the signal component attributed to defluorination-related accumulation in the skull, using PET data processed with Pixies (Apteryx), as previously described[8]. Static images were then created for the last 15 min of scan. Standard uptake values (SUV) corrected for injected dose and weight were then generated using Statistical Parametric Mapping (SPM12) with the Small Animal Molecular Imaging Toolbox (SAMIT; v3.0). A volume of interest (VOI) was then manually created in the TBI-targeted area and analysed in both hemispheres using PMOD.

E.2.2 *Ex-vivo* radioactivity counting

Radioactive concentrations in targeted TBI area and the contralateral area were measured on an automatic γ counting system (Wizard 3”, PerkinElmer). Data are expressed in percentage of the injected dose (% ID)/g of tissue for each animal.

References

1. Matsunaga, W. *et al.* LPS-induced Fos expression in oxytocin and vasopressin neurons of the rat hypothalamus. *Brain Res* **858**, 9–18 (2000).
2. Hoffman, G. E., Smith, M. S. & Verbalis, J. G. c-Fos and related immediate early gene products as markers of activity in neuroendocrine systems. *Front Neuroendocrinol* **14**, 173–213 (1993).
3. Schindelin, J. *et al.* Fiji: an open-source platform for biological-image analysis. *Nat Methods* **9**, 676–682 (2012).
4. Zhu, H. *et al.* Cre dependent DREADD (Designer Receptors Exclusively Activated by Designer Drugs) mice. *Genesis (New York, N.Y. : 2000)* **54**, 439 (2016).
5. Jacquens, A. *et al.* Deleterious effect of sustained neuroinflammation in pediatric traumatic brain injury. *Brain, Behavior, and Immunity* **120**, 99–116 (2024).
6. Ye, J. *et al.* Primer-BLAST: A tool to design target-specific primers for polymerase chain reaction. *BMC Bioinformatics* **13**, 134 (2012).
7. Cumbers, G. A., Harvey-Latham, E. D., Kassiou, M., Werry, E. L. & Danon, J. J. Emerging TSPO-PET Radiotracers for Imaging Neuroinflammation: A Critical Analysis. *Seminars in Nuclear Medicine* **54**, 856–874 (2024).
8. Millet, P. *et al.* Quantification of dopamine D2/3 receptors in rat brain using factor analysis corrected [18F]Fallypride images. *NeuroImage* **62**, 1455–1468 (2012).

Supplementary Figures:

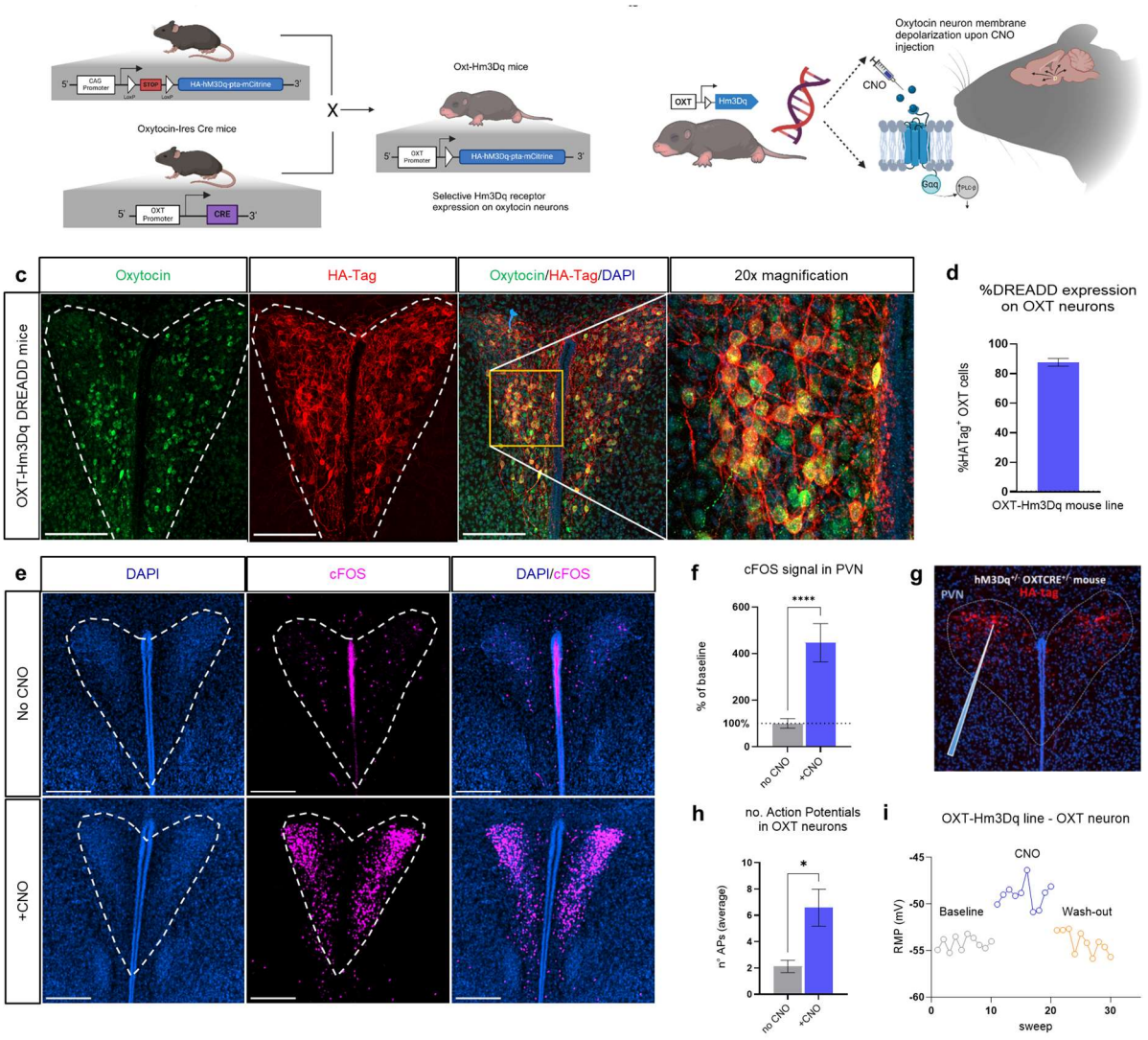

Fig. S1: Validation of the OXT-Hm3Dq DREADD construct. a) Graphical representation of the creation of the OXT-Hm3Dq DREADD mouse line. **b)** Graphic representing the theoretical concept of the OXT-Hm3Dq DREADD construct: Upon activation by the selective CNO ligand, designer Hm3Dq (Gq) receptors on oxytocin neurons cause membrane depolarization which creates firing of the neuron. **c)** Representative micrograph of immunohistochemistry of oxytocin (green) and HA-Tag (red) labeling, showing high coverage of Hm3Dq-DREADD receptors on oxytocin neurons (mean = 88%) in the PVN of the hypothalamus **(d).** Scale bar = 100 µm. **e)** Representative micrographs of immediate-early-gene cFOS (magenta) immunohistochemistry in the PVN in mice 1h after saline (top panel) or CNO injection (bottom panel). Scale bar = 200 µm. **f)** Signal quantification revealed a 300% increase in PVN cFOS activity in CNO-injected mice compared to the saline group. **g-i)** Electrophysiological recordings were performed on oxytocinergic neurons, identified by mCitrine fluorescence in reaction to stimulation

with a 594 nm LED. Oxytocinergic neurons showed an increase in action potentials **(h)** and resting membrane potential **(i)** upon CNO administration. Based on these validation experiments, we concluded that CNO successfully causes endogenous increases in oxytocin firing, and thus formed a valid tool to execute oxytocin treatment in this study. OXT = oxytocin; DREADD = designer receptors exclusively activated by designer drugs; CNO = clozapine-n-oxide; PVN = periventricular nucleus; TBI = traumatic brain injury. In **(f)** Mann-Whitney U test (U = 0, ****$p < .0001$, no CNO: $n = 8$, +CNO: $n = 9$). In **(h)** Paired t-test ($t(4) = 2.83$, *$p = .048$, $n = 5$). Bar graphs represent Mean ± SEM.

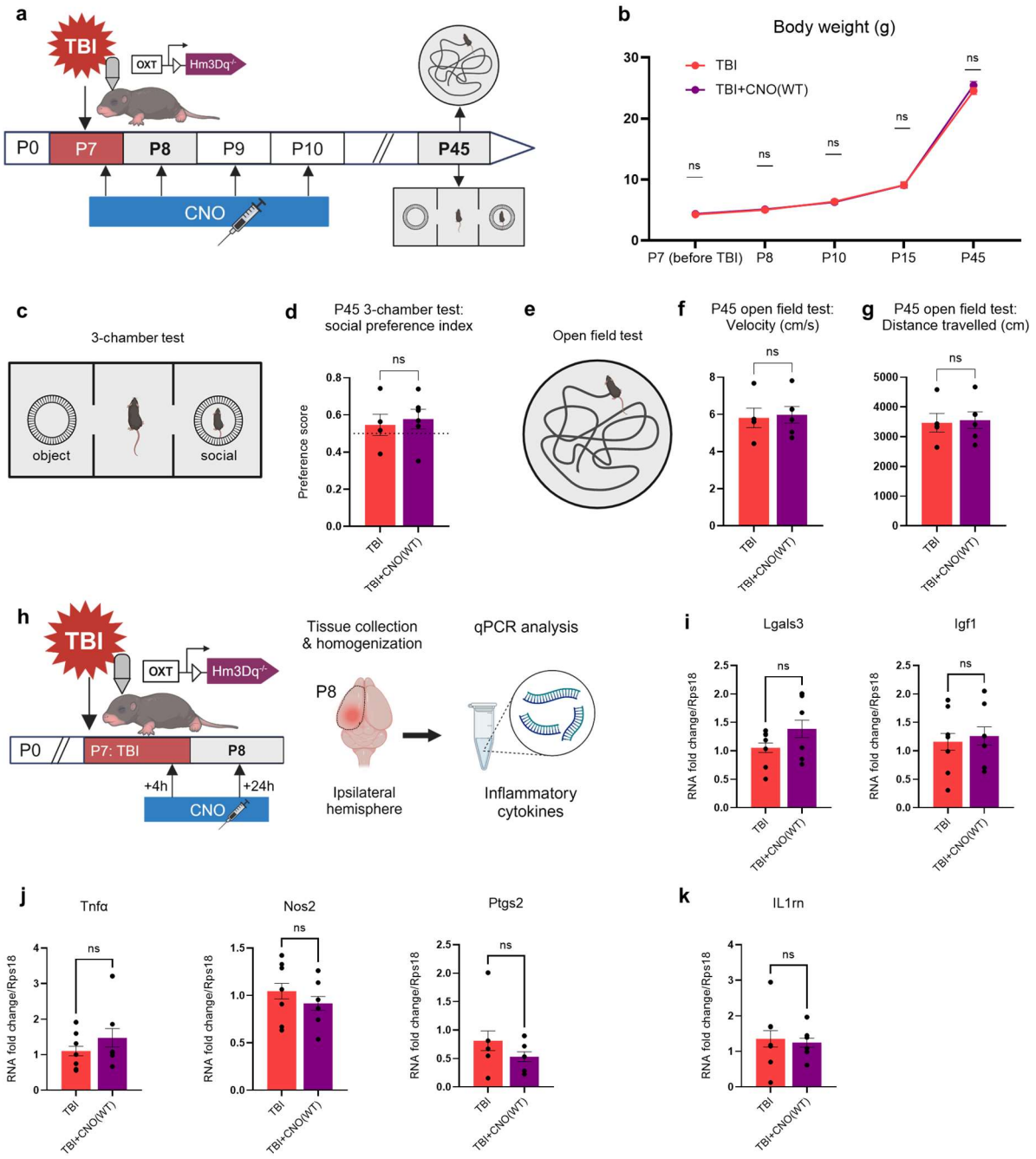

Fig. S2: The CNO treatment paradigm of this study did not have side-effects on long-term behavior or acute neuroinflammation following TBI. CNO in high dosages can bind to non-DREADD receptors and it can metabolize into clozapine, which is an atypical antipsychotic that can create physiological and behavioral effects in mice[1]. To assess if CNO had side-effects on readouts of our TBI model, we performed experiments on OXT-Hm3Dq$^{-/-}$ mice (which have OXT-Cre but are WT for the Hm3Dq-DREADD) subjected to TBI and treated with saline ("TBI"; red) or CNO ("TBI+CNO(WT)"; violet). **a)** Graphical timeline of behavioral experiments following P7 TBI and P7-P10 CNO treatment in WT mice. No effects of CNO were found on body weight and growth **(b)**, on social behavior during P45 3-chamber

test **(c,d)**, and on activity levels during the P45 open field **(e-g)**. We performed qPCR of P8 ipsilateral neural tissue to assess the effect of CNO on neuroinflammation 24 post-injury in OXT-Hm3Dq$^{-/-}$ mice **(h)**. We did not observe a difference between TBI mice and TBI+CNO(WT) mice in anti-inflammatory **(i)**, pro-inflammatory **(j)**, and immune-regulatory **(k)** cytokine expression. These data show that the CNO treatment used in this study did not have side-effects on the acute neuroinflammatory response following TBI, nor on long-term behavior. Any therapeutic effects found by the CNO treatment in our study can thus be attributed to increased oxytocin activity, and not CNO itself. TBI = traumatic brain injury, CNO = clozapine n-oxide, WT = wild type. In **(b)** Two-way ANOVA ($F(4,36) = 1.77$, $p = 0.16$. TBI: $n = 5$, TBI+CNO(WT): $n = 6$). In **(i)** Lgals3: Mann-Whitney U test ($U = 56$, $p = 0.17$, TBI: $n = 14$, TBI+CNO(WT): $n = 12$). Igf1: Unpaired t test ($t(24) = 0.47$, $p = 0.64$, TBI: $n = 14$, TBI+CNO(WT): $n = 12$). In **(j)** Tnfα: Mann-Whitney U test ($U = 64$, $p = 0.33$, TBI: $n = 14$, TBI+CNO(WT): $n = 12$). Nos2: Unpaired t test ($t(24) = 1.16$, $p = 0.26$, TBI: $n = 14$, TBI+CNO(WT): $n = 12$). Ptgs2 : Mann-Whitney U test ($U = 48$, $p = 0.47$, TBI: $n = 12$, TBI+CNO(WT): $n = 10$). In **(k)** Unpaired t test ($t(24) = 0.39$, $p = .70$, TBI: $n = 14$, TBI+CNO(WT): $n = 12$). Bar graphs represent Mean ± SEM. Each circle corresponds to one animal.

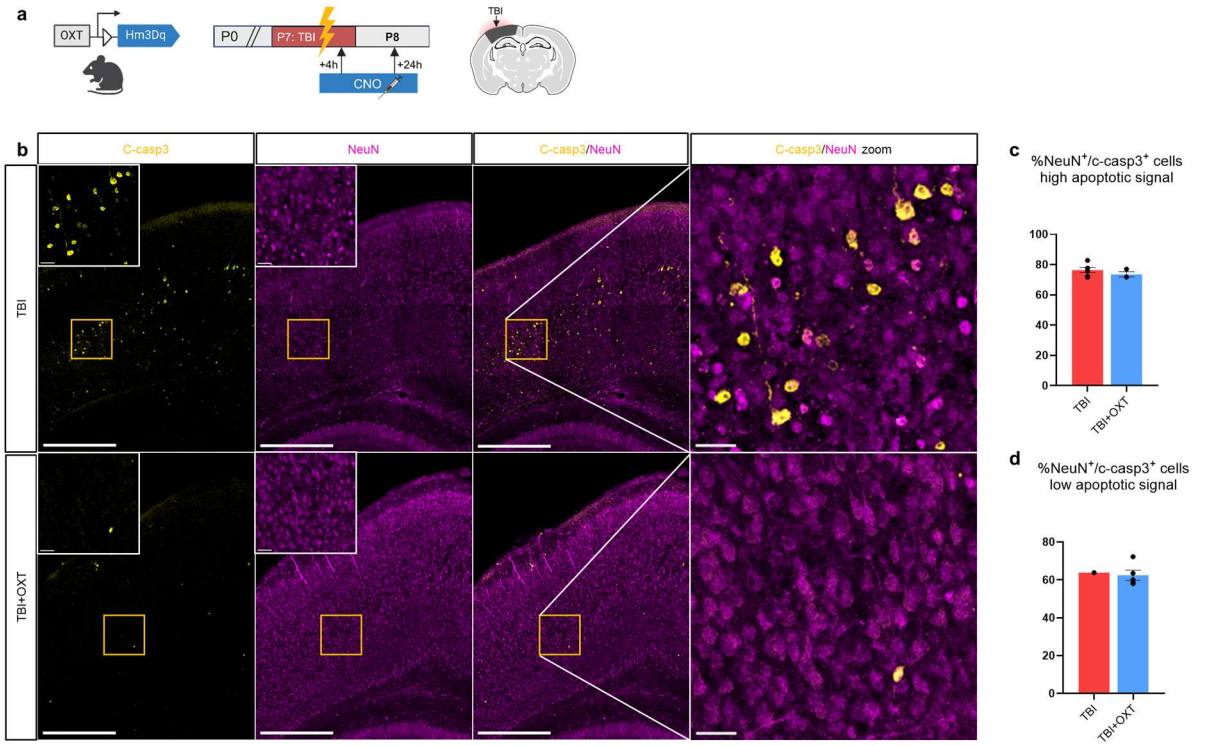

Fig. S3: Oxytocin does not affect the proportion neuronal apoptotic death following TBI. a) Graphical timeline of P8 immunohistochemistry experiment after P7 TBI and 2 sessions of CNO treatment, and graphical indication of the ipsilateral somatosensory cortex ROI. **b)** Representative micrographs of apoptotic cell death (cleaved-caspase 3; yellow) and neuron (NeuN; magenta) immunoreactivity in TBI (top row) and TBI+OXT (bottom row) mice. Scale bar = 200 µm (inserts: scale bar = 30 µm). To eliminate confounding effects of apoptotic signal degree on the proportion neuronal cell death, quantification was divided into high apoptotic and low apoptotic signal. **c,d)** Quantification of the proportion of neuronal cell death in samples with **(c)** high apoptotic and **(d)** low apoptotic reactivity showed no difference between TBI and TBI+OXT mice. TBI = traumatic brain injury. CNO = clozapine n-oxide, ROI = region of interest, c-casp3 = cleaved-caspase 3, OXT = oxytocin. In **(c)** Unpaired t-test ($t(7) = 1.04$, $p = .33$, TBI: $n = 6$, TBI+OXT: $n = 3$). In **(d)** sample size too small to perform statistical testing (TBI: $n = 1$, TBI+OXT: $n = 5$). Bar graphs represent Mean ± SEM. Each circle represents an individual sample.

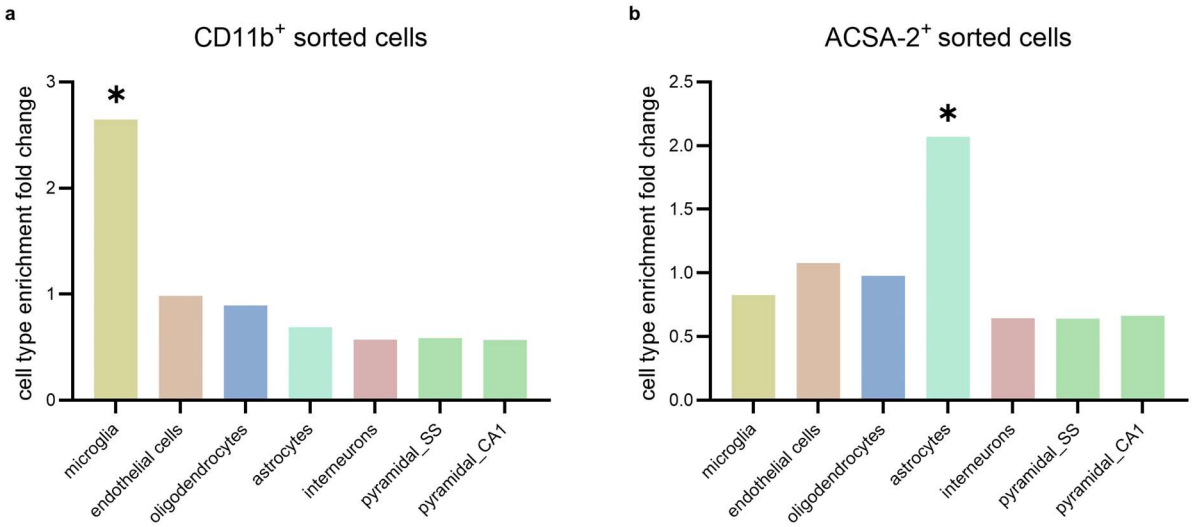

Fig S4: Cell type enrichment analysis confirms purity of magnetically sorted microglia and astrocytes. MACS® (Miltenyi Biotech) magnetic sorting purity of CD11b$^+$ and ACSA-2$^+$ cells was assessed with Expression Weighted Cell-type Enrichment (EWCE) analysis[2] based on top 250 expressed genes in the respective RNA Seq datasets. **a,b)** Bar graphs showing enrichment fold change of neural cell type marker gene expression in our transcriptomic datasets, including microglia, endothelial cells, oligodendrocytes, astrocytes, interneurons and pyramidal cells. Asterisks represent cell type enrichment with $p < .05$. **a)** EWCE analysis revealed a significant enrichment of only microglia cells in the CD11b$^+$ transcriptomic dataset. **b)** EWCE analysis revealed a significant enrichment of only astrocytes in the ACSA-2$^+$ transcriptomic dataset. This analysis confirms that the CD11b$^+$ and ACSA-2$^+$ sorted cells were indeed microglia and astrocytes, respectively.

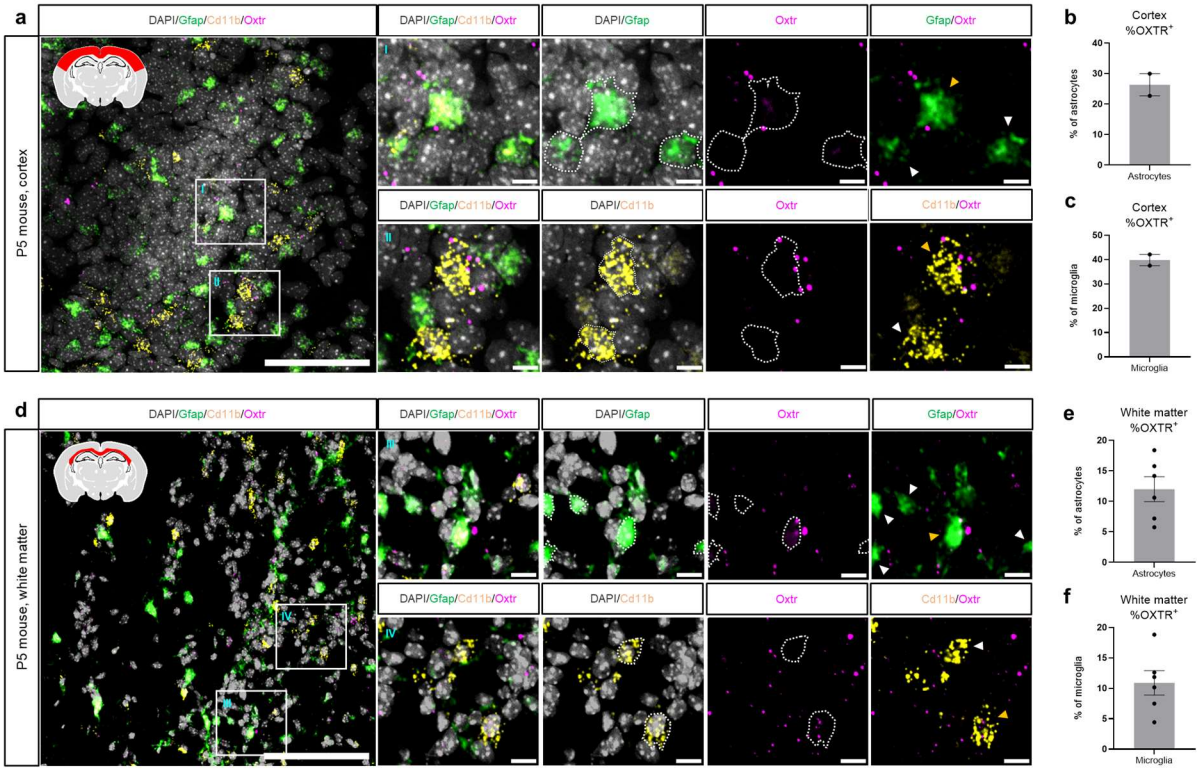

Fig. S5: RNA Scope in situ hybridization reveals OXT receptor expression on microglia and astrocytes in P5 mice. To assess if microglia and astrocytes express oxytocin receptors (OXTR) *in-vivo* in mouse pups, we performed RNA Scope in situ hybridization on brain sections from untreated P5 OXT-Hm3Dq mice. **a)** ROI indication (red) and representative micrograph from cortex showing reactivity of oxytocin receptor (*Oxtr*; magenta), microglia (*CD11b*; yellow), and astrocyte (*Gfap*; green) mRNA. Scale bar = 100 µm. Inserts highlight cortical astrocytes (top row) and microglia (bottom row) with (yellow arrow) and without (white arrow) expression of *Oxtr* mRNA. Scale bar = 10 µm. **b,c)** Quantification of micrographs revealed that 26% of cortical astrocytes **(b)** and 39% of cortical microglia express OXTR **(c)**. **d)** ROI indication (red) and representative micrograph from white matter showing *Oxtr*, *Gfap* and *CD11b* mRNA reactivity in the white matter. Scale bar = 100 µm. Inserts highlight white matter astrocytes (top row) and microglia (bottom row) with (yellow arrow) and without (white arrow) expression of OXTR mRNA. Scale bar = 10 µm. **e,f)** Quantification of micrographs revealed that 12% of white matter astrocytes **(e)** and 11% of white matter microglia express OXTR **(f)**. These data confirm oxytocin receptor expression on microglia and astrocytes, suggesting both cell types can be directly influenced by neuronal oxytocin. Bar graphs represent Mean ± SEM. Each circle represents an individual sample.

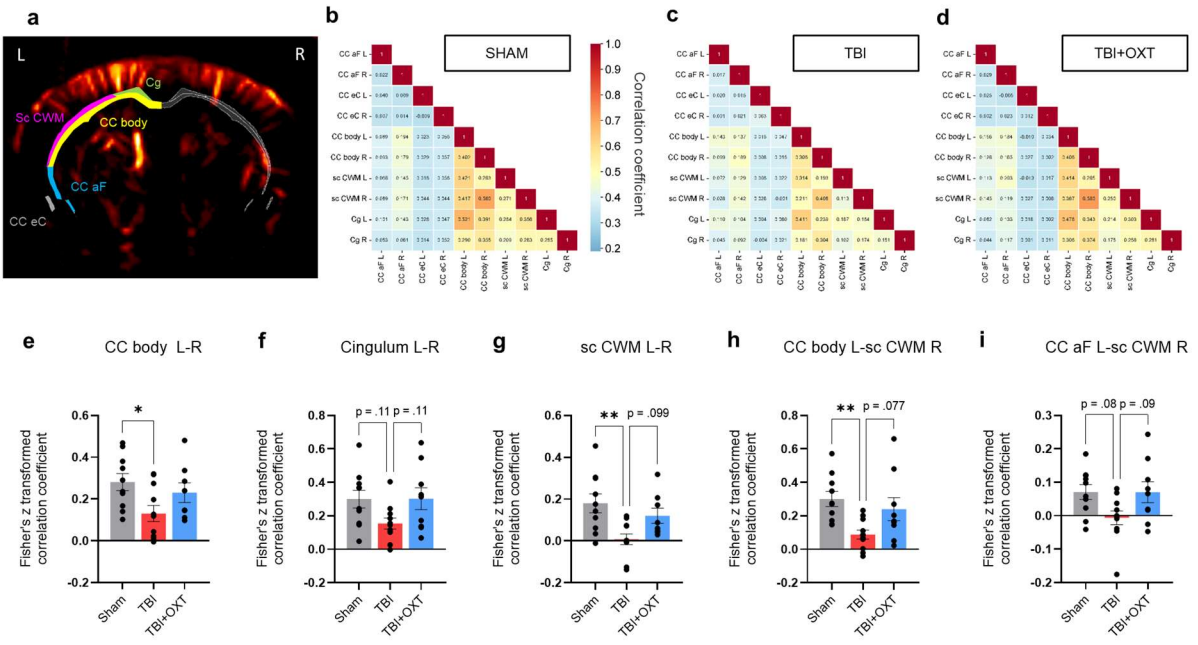

Fig. S6: Oxytocin affects long-term functional connectivity of white matter regions following TBI. a) Representative image of functional ultrasound (fUS) signal and the white matter ROIs in P45 mice: Cg (green), CC body (yellow), sc CWM (magenta), CC aF (blue), CC eC (gray). **b-d)** Average correlation coefficient matrices of functional connectivity between the white matter ROIs in the Sham **(b)**, TBI **(c)** and TBI+OXT **(d)** groups. **e-i)** Quantification of correlation coefficients between a selection of white matter ROI pairs, showing reduced functional connectivity in TBI, and reversed functional connectivity after oxytocin treatment. TBI = traumatic brain injury; CNO = clozapine n-oxide; fUS = functional ultrasound; ROI = region of interest; Cg = cingulum, CC body = corpus callosum body, sc CWM = supra-callosal cerebral white matter, CC aF = corpus callosum anterior forceps, CC eC = corpus callosum external capsule. In **(e)** ANOVA ($F(2,26) = 3.69$, $^*p = .039$, Sham: $n = 10$, TBI: $n = 11$, TBI+CNO: $n = 8$). Tukey's (Sham vs. TBI: $^*p = .034$; Sham vs. TBI+OXT: $p = .69$; TBI vs. TBI+OXT: $p = .24$). In **(f)** ANOVA ($F(2,27) = 2.98$, $p = .068$, Sham: $n = 10$, TBI: $n = 11$, TBI+CNO: $n = 9$). Tukey's (Sham vs. TBI: $p = .11$; Sham vs. TBI+OXT: $p = 1$; TBI vs. TBI+OXT: $p = .11$). In **(g)** ANOVA ($F(2,26) = 6.32$, $^{**}p = .006$, Sham: $n = 10$, TBI: $n = 11$, TBI+CNO: $n = 8$). Tukey's (Sham vs. TBI: $^{**}p = .005$; Sham vs. TBI+OXT: $p = .52$; TBI vs. TBI+OXT: $p = .099$). In **(h)** ANOVA ($F(2,27) = 5.69$, $^{**}p = .009$, Sham: $n = 10$, TBI: $n = 11$, TBI+CNO: $n = 9$). Tukey's (Sham vs. TBI: $^{**}p = .008$; Sham vs. TBI+OXT: $p = .66$; TBI vs. TBI+OXT: $p = .077$). In **(i)** ANOVA ($F(2,27) = 3.44$, $^*p = .047$, Sham: $n = 10$, TBI: $n = 11$, TBI+CNO: $n = 9$). Tukey's (Sham vs. TBI: $p = .077$; Sham vs. TBI+OXT: $p = 1$; TBI vs. TBI+OXT: $p = .089$). Bar graphs represent Mean ± SEM. Each circle represents an individual sample.

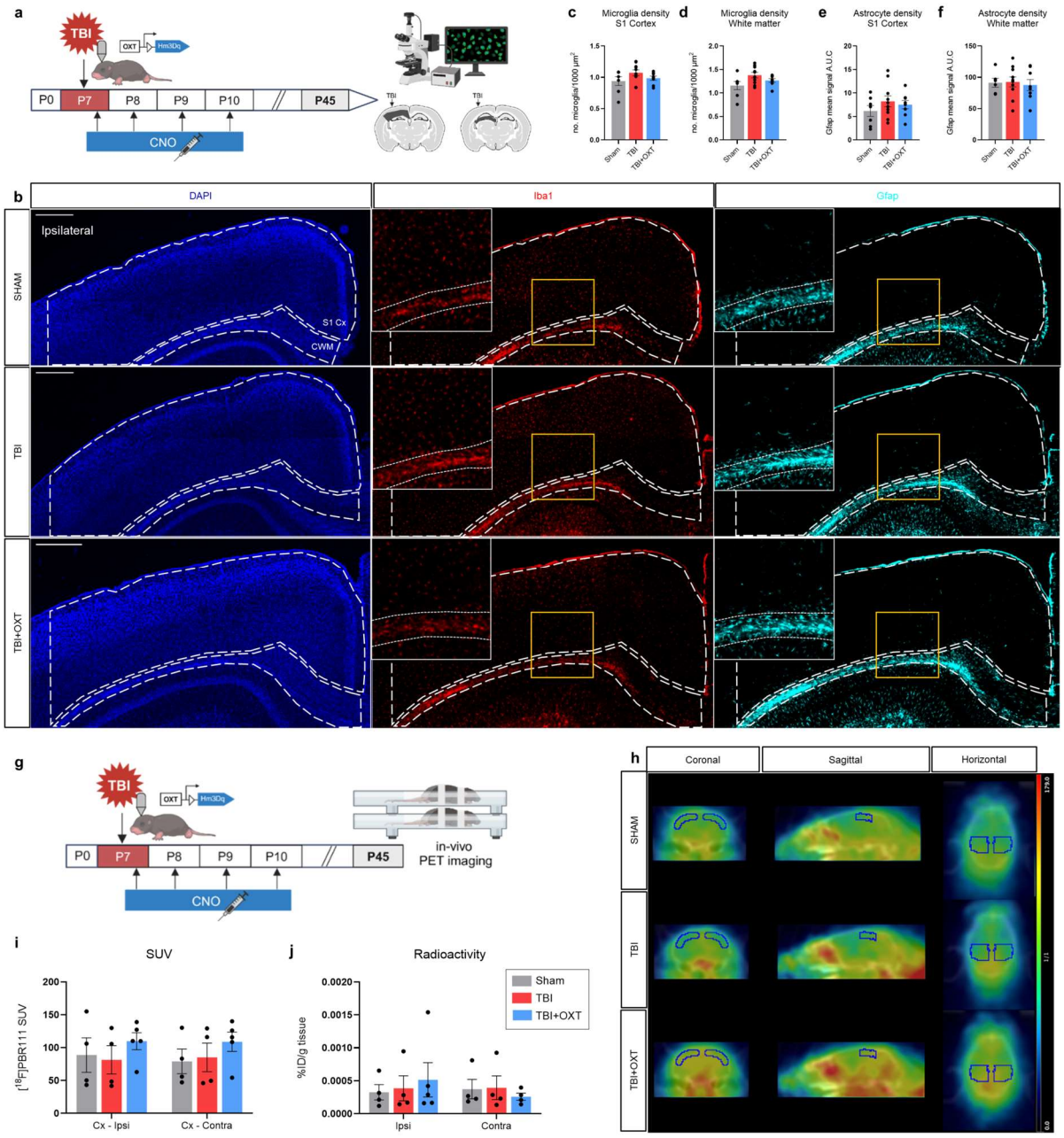

Fig. S7: Early-life TBI is not associated with long-term neuroinflammation. a) Graphical timeline of the P45 immunohistochemistry experiment with cortical and WM ROI (black) indication. **b)** Representative micrograph of Iba1$^+$ microglia (red) and GFAP$^+$ astrocytes (cyan) in ipsilateral S1 (dotted lines, top) and ipsilateral WM (dotted lines, bottom) for Sham, TBI and TBI+OXT groups. Scale bar = 400 µm. **c,d)** Quantification of number of microglia cells per 100 µm^2 in ipsilateral S1 **(c)**, and ipsilateral WM **(d)**, revealed no significant difference in microglia density between experimental groups at P45. **e,f)** Quantification of GFAP signal density in ipsilateral S1 **(e)**, and ipsilateral WM **(f)**, revealed no difference in astrocyte density between experimental groups at P45. **g)** Graphical timeline of P45 TSPO assessment using *in-vivo* positron emission tomography (PET) imaging and *ex-vivo* gamma counting. **h)** Average SUV images of [^{18}F]PBR111 acquired by PET imaging in sham, TBI and TBI+OXT animals, co-

registered to the CT in the coronal (left), sagittal (center) and horizontal (right) planes. Blue areas correspond to volumes of interest (VOIs). **i)** Quantification of [^{18}F]PBR111 SUV in ipsilateral and contralateral VOI in the three experimental groups. TSPO expression is not modulated by TBI or OXT treatment. **j)** Quantification of radioactivity (% injected dose (ID)/g of tissue) in the ipsilateral and contralateral VOI. Results confirm the absence of TSPO overexpression after TBI at long term. ROI = region of interest; S1 = primary somatosensory cortex; CWM = cingulate white matter; TBI = traumatic brain injury; OXT = oxytocin; TSPO = 18 kDa translocator protein; SUV = standard uptake value; VOI = volume of interest. In **(c)** ANOVA ($F(2,22) = 1.80$, $p = .19$, Sham: $n = 7$, TBI: $n = 10$, TBI+CNO: $n = 8$). In **(d)** ANOVA ($F(2,22) = 3.16$, $p = .06$, Sham: $n = 7$, TBI: $n = 10$, TBI+CNO: $n = 8$). In **(e)** ANOVA ($F(2,22) = 0.87$, $p = .43$, Sham: $n = 7$, TBI: $n = 10$, TBI+CNO: $n = 8$). In **(f)** ANOVA ($F(2,21) = 0.11$, $p = .90$, Sham: $n = 6$, TBI: $n = 10$, TBI+CNO: $n = 8$). In **(i)** Two-way ANOVA ($F(2,20) = 0.06$, $p = .94$, Sham: $n = 4$, TBI: $n = 5$, TBI+OXT: $n = 5$). In **(j)** Two-way ANOVA ($F(2,19) = 0.42$, $p = 0.66$. Sham: $n = 4$, TBI: $n = 5$, TBI+CNO: $n = 5$). Bar graphs represent Mean ± SEM. Each circle corresponds to one animal.

References

1. Manvich, D. F. *et al.* The DREADD agonist clozapine N-oxide (CNO) is reverse-metabolized to clozapine and produces clozapine-like interoceptive stimulus effects in rats and mice. *Sci Rep* **8**, 3840 (2018).
2. Skene, N. G. & Grant, S. G. N. Identification of Vulnerable Cell Types in Major Brain Disorders Using Single Cell Transcriptomes and Expression Weighted Cell Type Enrichment. *Front. Neurosci.* **10**, (2016).

Supplementary data files:

Table S1: fUS network analysis node list, used for Figure 7

Id	Region name	Structure	hemisphere	bregma slice	Structural hub
AgINS L3	(L) Agranular insular area slice 3	Sensorimotor	Left	3	Isocortex
VISa L2	(L) Anterior area slice 2	Sensorimotor	Left	2	Isocortex
adThal L3	(L) Anterior group of the dorsal thalamus slice 3	Thalamus	Left	3	Thalamus
aPT L1	(L) Anterior pretectal nucleus slice 1	Sensorimotor	Left	1	Isocortex
amV2 L1	(L) Anteromedial visual area slice 1	Sensorimotor	Left	1	Isocortex
ablAmyg L2	(L) Basolateral amygdalar nucleus, anterior part slice 2	Amygdala	Left	2	Striatum
ablAmyg L3	(L) Basolateral amygdalar nucleus, anterior part slice 3	Amygdala	Left	3	Striatum
pblAmyg L1	(L) Basolateral amygdalar nucleus, posterior part slice 1	Amygdala	Left	1	Striatum
pblAmyg L2	(L) Basolateral amygdalar nucleus, posterior part slice 2	Amygdala	Left	2	Striatum
pbmAmyg L2	(L) Basomedial amygdalar nucleus, posterior part slice 2	Amygdala	Left	2	Striatum
CP L2	(L) Caudoputamen slice 2	Basal ganglia	Left	2	Striatum
CP L3	(L) Caudoputamen slice 3	Basal ganglia	Left	3	Striatum
cAmyg L3	(L) Central amygdalar nucleus slice 3	Amygdala	Left	3	Striatum
cxAmyg L1	(L) Cortical amygdalar area slice 1	Amygdala	Left	1	Striatum
cxAmyg L2	(L) Cortical amygdalar area slice 2	Amygdala	Left	2	Striatum
cxAmyg L3	(L) Cortical amygdalar area slice 3	Amygdala	Left	3	Striatum
DG L1	(L) Dentate gyrus slice 1	Hippocampal formation	Left	1	Hippocampal formation
DG L2	(L) Dentate gyrus slice 2	Hippocampal formation	Left	2	Hippocampal formation
DG L3	(L) Dentate gyrus slice 3	Hippocampal formation	Left	3	Hippocampal formation
dA2 L1	(L) Dorsal auditory area slice 1	Auditory area	Left	1	Isocortex
dA2 L2	(L) Dorsal auditory area slice 2	Auditory area	Left	2	Isocortex
ECT L1	(L) Ectorhinal area slice 1	Hippocampal formation	Left	1	Hippocampal formation
ECT L2	(L) Ectorhinal area slice 2	Hippocampal formation	Left	2	Hippocampal formation
dEP L1	(L) Endopiriform nucleus, dorsal part slice 1	Olfactory area	Left	1	Piriform area
dEP L2	(L) Endopiriform nucleus, dorsal part slice 2	Olfactory area	Left	2	Piriform area
dEP L3	(L) Endopiriform nucleus, dorsal part slice 3	Olfactory area	Left	3	Piriform area
vEP L1	(L) Endopiriform nucleus, ventral part slice 1	Olfactory area	Left	1	Piriform area
vEP L2	(L) Endopiriform nucleus, ventral part slice 2	Olfactory area	Left	2	Piriform area
vEP L3	(L) Endopiriform nucleus, ventral part slice 3	Olfactory area	Left	3	Piriform area
ENT L1	(L) Entorhinal area, lateral part slice 1	Hippocampal formation	Left	1	Hippocampal formation
ENT L2	(L) Entorhinal area, lateral part slice 2	Hippocampal formation	Left	2	Hippocampal formation
epiThal L2	(L) Epithalamus slice 2	Thalamus	Left	2	Thalamus
epiThal L3	(L) Epithalamus slice 3	Thalamus	Left	3	Thalamus
FC L2	(L) Fasciola cinerea slice 2	Hippocampal formation	Left	2	Hippocampal formation
CA1 L1	(L) Field CA1 slice 1	Hippocampal formation	Left	1	Hippocampal formation
CA1 L2	(L) Field CA1 slice 2	Hippocampal formation	Left	2	Hippocampal formation
CA1 L3	(L) Field CA1 slice 3	Hippocampal formation	Left	3	Hippocampal formation
CA2 L1	(L) Field CA2 slice 1	Hippocampal formation	Left	1	Hippocampal formation
CA2 L2	(L) Field CA2 slice 2	Hippocampal formation	Left	2	Hippocampal formation

CA2 L3	(L) Field CA2 slice 3	Hippocampal formation	Left	3	Hippocampal formation
CA3 L1	(L) Field CA3 slice 1	Hippocampal formation	Left	1	Hippocampal formation
CA3 L2	(L) Field CA3 slice 2	Hippocampal formation	Left	2	Hippocampal formation
CA3 L3	(L) Field CA3 slice 3	Hippocampal formation	Left	3	Hippocampal formation
dThalGeni L1	(L) Geniculate group, dorsal thalamus slice 1	Thalamus	Left	1	Thalamus
dThalGeni L2	(L) Geniculate group, dorsal thalamus slice 2	Thalamus	Left	2	Thalamus
vThalGeni L1	(L) Geniculate group, ventral thalamus slice 1	Thalamus	Left	1	Thalamus
vThalGeni L2	(L) Geniculate group, ventral thalamus slice 2	Thalamus	Left	2	Thalamus
exGP L3	(L) Globus pallidus, external segment slice 3	Basal ganglia	Left	3	Striatum
lHyp L1	(L) Hypothalamic lateral zone slice 1	Hypothalamus	Left	1	Hypothalamus
lHyp L2	(L) Hypothalamic lateral zone slice 2	Hypothalamus	Left	2	Hypothalamus
lHyp L3	(L) Hypothalamic lateral zone slice 3	Hypothalamus	Left	3	Hypothalamus
mHyp L1	(L) Hypothalamic medial zone slice 1	Hypothalamus	Left	1	Hypothalamus
mHyp L2	(L) Hypothalamic medial zone slice 2	Hypothalamus	Left	2	Hypothalamus
mHyp L3	(L) Hypothalamic medial zone slice 3	Hypothalamus	Left	3	Hypothalamus
ildThal L2	(L) Intralaminar nuclei of the dorsal thalamus slice 2	Thalamus	Left	2	Thalamus
ildThal L3	(L) Intralaminar nuclei of the dorsal thalamus slice 3	Thalamus	Left	3	Thalamus
lAmyg L2	(L) Lateral amygdalar nucleus slice 2	Amygdala	Left	2	Striatum
lAmyg L3	(L) Lateral amygdalar nucleus slice 3	Amygdala	Left	3	Striatum
dlThal L1	(L) Lateral group of the dorsal thalamus slice 1	Thalamus	Left	1	Thalamus
dlThal L2	(L) Lateral group of the dorsal thalamus slice 2	Thalamus	Left	2	Thalamus
dlThal L3	(L) Lateral group of the dorsal thalamus slice 3	Thalamus	Left	3	Thalamus
mAmyg L3	(L) Medial amygdalar nucleus slice 3	Amygdala	Left	3	Striatum
mdThal L3	(L) Medial group of the dorsal thalamus slice 3	Thalamus	Left	3	Thalamus
MRN L1	(L) Midbrain reticular nucleus slice 1	Motor	Left	1	midbrain
MTN L3	(L) Midline group of the dorsal thalamus slice 3	Thalamus	Left	3	Thalamus
PAG L1	(L) Periaqueductal gray slice 1	Motor	Left	1	midbrain
PERI L1	(L) Perirhinal area slice 1	Perirhinal cortex	Left	1	Isocortex
PERI L2	(L) Perirhinal area slice 2	Perirhinal cortex	Left	2	Isocortex
PVN L2	(L) Periventricular region slice 2	Hypothalamus	Left	2	Hypothalamus
PVN L3	(L) Periventricular zone slice 3	Hypothalamus	Left	3	Hypothalamus
PIR L1	(L) Piriform area slice 1	Olfactory area	Left	1	Piriform area
PIR L2	(L) Piriform area slice 2	Olfactory area	Left	2	Piriform area
PIR L3	(L) Piriform area slice 3	Olfactory area	Left	3	Piriform area
Pir-Amyg L2	(L) Piriform-amygdalar area slice 2	Amygdala	Left	2	Striatum
Pir-Amyg L3	(L) Piriform-amygdalar area slice 3	Amygdala	Left	3	Striatum
pAmyg L1	(L) Posterior amygdalar nucleus slice 1	Amygdala	Left	1	Striatum
PoT L1	(L) Posterior triangular thalamic nucleus slice 1	Thalamus	Left	1	Thalamus
A1 L1	(L) Primary auditory area slice 1	Auditory area	Left	1	Isocortex
S1BF L2	(L) Primary somatosensory area, barrel field slice 2	Sensorimotor	Left	2	Isocortex
S1BF L3	(L) Primary somatosensory area, barrel field slice 3	Sensorimotor	Left	3	Isocortex
S1Tr L3	(L) Primary somatosensory area, trunk slice 3	Sensorimotor	Left	3	Isocortex
RT L3	(L) Reticular nucleus of the thalamus slice 3	Thalamus	Left	3	Thalamus
RSD L1	(L) Retrosplenial area, dorsal part slice 1	Retrosplenial cortex	Left	1	Isocortex
RSD L2	(L) Retrosplenial area, dorsal part slice 2	Retrosplenial cortex	Left	2	Isocortex

RSD L3	(L) Retrosplenial area, dorsal part slice 3	Retrosplenial cortex	Left	3	Isocortex
RSL L1	(L) Retrosplenial area, lateral agranular part slice 1	Retrosplenial cortex	Left	1	Isocortex
RSL L2	(L) Retrosplenial area, lateral agranular part slice 2	Retrosplenial cortex	Left	2	Isocortex
RSL L3	(L) Retrosplenial area, lateral agranular part slice 3	Retrosplenial cortex	Left	3	Isocortex
RSV L1	(L) Retrosplenial area, ventral part slice 1	Retrosplenial cortex	Left	1	Isocortex
RSV L2	(L) Retrosplenial area, ventral part slice 2	Retrosplenial cortex	Left	2	Isocortex
RSV L3	(L) Retrosplenial area, ventral part slice 3	Retrosplenial cortex	Left	3	Isocortex
VISRll L1	(L) Rostrolateral visual area slice 1	Sensorimotor	Left	1	Isocortex
SPF L1	(L) Subparafascicular nucleus slice 1	Thalamus	Left	1	Thalamus
S2 L2	(L) Supplemental somatosensory area slice 2	Sensorimotor	Left	2	Isocortex
S2 L3	(L) Supplemental somatosensory area slice 3	Sensorimotor	Left	3	Isocortex
TEA L1	(L) Temporal association areas slice 1	Association cortex	Left	1	Isocortex
TEA L2	(L) Temporal association areas slice 2	Association cortex	Left	2	Isocortex
valThal L3	(L) Ventral anterior-lateral complex of the thalamus slice 3	Thalamus	Left	3	Thalamus
A2V L1	(L) Ventral auditory area slice 1	Auditory area	Left	1	Isocortex
A2V L2	(L) Ventral auditory area slice 2	Auditory area	Left	2	Isocortex
VmThal L3	(L) Ventral medial nucleus of the thalamus slice 3	Thalamus	Left	3	Thalamus
VplThal L2	(L) Ventral posterolateral nucleus of the thalamus slice 2	Thalamus	Left	2	Thalamus
VplThal L3	(L) Ventral posterolateral nucleus of the thalamus slice 3	Thalamus	Left	3	Thalamus
VpplThal L2	(L) Ventral posterolateral nucleus of the thalamus, parvicellular part slice 2	Thalamus	Left	2	Thalamus
VpmThal L2	(L) Ventral posteromedial nucleus of the thalamus slice 2	Thalamus	Left	2	Thalamus
VpmThal L3	(L) Ventral posteromedial nucleus of the thalamus slice 3	Thalamus	Left	3	Thalamus
VppmThal L2	(L) Ventral posteromedial nucleus of the thalamus, parvicellular part slice 2	Thalamus	Left	2	Thalamus
VISC L3	(L) Visceral area slice 3	Sensorimotor	Left	3	Isocortex
AgINS R3	(R) Agranular insular area slice 3	Sensorimotor	Right	3	Isocortex
adThal R3	(R) Anterior group of the dorsal thalamus slice 3	Thalamus	Right	3	Thalamus
aPT R1	(R) Anterior pretectal nucleus slice 1	Sensorimotor	Right	1	Isocortex
amV2 R1	(R) Anteromedial visual area slice 1	Sensorimotor	Right	1	Isocortex
ablAmyg R2	(R) Basolateral amygdalar nucleus, anterior part slice 2	Amygdala	Right	2	Striatum
ablAmyg R3	(R) Basolateral amygdalar nucleus, anterior part slice 3	Amygdala	Right	3	Striatum
pblAmyg R1	(R) Basolateral amygdalar nucleus, posterior part slice 1	Amygdala	Right	1	Striatum
pblAmyg R2	(R) Basolateral amygdalar nucleus, posterior part slice 2	Amygdala	Right	2	Striatum
pbmAmyg R2	(R) Basomedial amygdalar nucleus, posterior part slice 2	Amygdala	Right	2	Striatum
CP R2	(R) Caudoputamen slice 2	Basal ganglia	Right	2	Striatum
CP R3	(R) Caudoputamen slice 3	Basal ganglia	Right	3	Striatum
cAmyg R3	(R) Central amygdalar nucleus slice 3	Amygdala	Right	3	Striatum
cxAmyg R1	(R) Cortical amygdalar area slice 1	Amygdala	Right	1	Striatum
cxAmyg R2	(R) Cortical amygdalar area slice 2	Amygdala	Right	2	Striatum
cxAmyg R3	(R) Cortical amygdalar area slice 3	Amygdala	Right	3	Striatum
DG R1	(R) Dentate gyrus slice 1	Hippocampal formation	Right	1	Hippocampal formation
DG R2	(R) Dentate gyrus slice 2	Hippocampal formation	Right	2	Hippocampal formation
DG R3	(R) Dentate gyrus slice 3	Hippocampal formation	Right	3	Hippocampal formation
dA2 R1	(R) Dorsal auditory area slice 1	Auditory area	Right	1	Isocortex
ECT R1	(R) Ectorhinal area slice 1	Hippocampal formation	Right	1	Hippocampal formation

ECT R2	(R) Ectorhinal area slice 2	Hippocampal formation	Right	2	Hippocampal formation
dEP R1	(R) Endopiriform nucleus, dorsal part slice 1	Olfactory area	Right	1	Piriform area
dEP R2	(R) Endopiriform nucleus, dorsal part slice 2	Olfactory area	Right	2	Piriform area
dEP R3	(R) Endopiriform nucleus, dorsal part slice 3	Olfactory area	Right	3	Piriform area
vEP R1	(R) Endopiriform nucleus, ventral part slice 1	Olfactory area	Right	1	Piriform area
vEP R2	(R) Endopiriform nucleus, ventral part slice 2	Olfactory area	Right	2	Piriform area
vEP R3	(R) Endopiriform nucleus, ventral part slice 3	Olfactory area	Right	3	Piriform area
ENT R1	(R) Entorhinal area, lateral part slice 1	Hippocampal formation	Right	1	Hippocampal formation
ENT R2	(R) Entorhinal area, lateral part slice 2	Hippocampal formation	Right	2	Hippocampal formation
epiThal R2	(R) Epithalamus slice 2	Thalamus	Right	2	Thalamus
epiThal R3	(R) Epithalamus slice 3	Thalamus	Right	3	Thalamus
FC R2	(R) Fasciola cinerea slice 2	Hippocampal formation	Right	2	Hippocampal formation
CA1 R1	(R) Field CA1 slice 1	Hippocampal formation	Right	1	Hippocampal formation
CA1 R2	(R) Field CA1 slice 2	Hippocampal formation	Right	2	Hippocampal formation
CA1 R3	(R) Field CA2 slice 1	Hippocampal formation	Right	1	Hippocampal formation
CA2 R2	(R) Field CA2 slice 2	Hippocampal formation	Right	2	Hippocampal formation
CA2 R3	(R) Field CA2 slice 3	Hippocampal formation	Right	3	Hippocampal formation
CA3 R1	(R) Field CA3 slice 1	Hippocampal formation	Right	1	Hippocampal formation
CA3 R2	(R) Field CA3 slice 2	Hippocampal formation	Right	2	Hippocampal formation
CA3 R3	(R) Field CA3 slice 3	Hippocampal formation	Right	3	Hippocampal formation
dThalGeni R1	(R) Geniculate group, dorsal thalamus slice 1	Thalamus	Right	1	Thalamus
dThalGeni R2	(R) Geniculate group, dorsal thalamus slice 2	Thalamus	Right	2	Thalamus
vThalGeni R1	(R) Geniculate group, ventral thalamus slice 1	Thalamus	Right	1	Thalamus
vThalGeni R2	(R) Geniculate group, ventral thalamus slice 2	Thalamus	Right	2	Thalamus
exGP R3	(R) Globus pallidus, external segment slice 3	Basal ganglia	Right	3	Pallidum
lHyp R1	(R) Hypothalamic lateral zone slice 1	Hypothalamus	Right	1	Hypothalamus
lHyp R2	(R) Hypothalamic lateral zone slice 2	Hypothalamus	Right	2	Hypothalamus
lHyp R3	(R) Hypothalamic lateral zone slice 3	Hypothalamus	Right	3	Hypothalamus
mHyp R1	(R) Hypothalamic medial zone slice 1	Hypothalamus	Right	1	Hypothalamus
mHyp R2	(R) Hypothalamic medial zone slice 2	Hypothalamus	Right	2	Hypothalamus
mHyp R3	(R) Hypothalamic medial zone slice 3	Hypothalamus	Right	3	Hypothalamus
ildThal R2	(R) Intralaminar nuclei of the dorsal thalamus slice 2	Thalamus	Right	2	Thalamus
ildThal R3	(R) Intralaminar nuclei of the dorsal thalamus slice 3	Thalamus	Right	3	Thalamus
lAmyg R2	(R) Lateral amygdalar nucleus slice 2	Amygdala	Right	2	Striatum
lAmyg R3	(R) Lateral amygdalar nucleus slice 3	Amygdala	Right	3	Striatum
ldThal R1	(R) Lateral group of the dorsal thalamus slice 1	Thalamus	Right	1	Thalamus
ldThal R2	(R) Lateral group of the dorsal thalamus slice 2	Thalamus	Right	2	Thalamus
ldThal R3	(R) Lateral group of the dorsal thalamus slice 3	Thalamus	Right	3	Thalamus
mAmyg R3	(R) Medial amygdalar nucleus slice 3	Amygdala	Right	3	Striatum
mdThal R3	(R) Medial group of the dorsal thalamus slice 3	Thalamus	Right	3	Thalamus
MiddThal R3	(R) Midline group of the dorsal thalamus slice 3	Thalamus	Right	3	Thalamus
PAG R1	(R) Periaqueductal gray slice 1	Motor	Right	1	midbrain
PERI R1	(R) Perirhinal area slice 1	Perirhinal cortex	Right	1	Isocortex
PERI R2	(R) Perirhinal area slice 2	Perirhinal cortex	Right	2	Isocortex

PVN R2	(R) Periventricular region slice 2	Hypothalamus	Right	2	Hypothalamus
PVN R3	(R) Periventricular zone slice 3	Hypothalamus	Right	3	Hypothalamus
PIR R1	(R) Piriform area slice 1	Olfactory area	Right	1	Piriform area
PIR R2	(R) Piriform area slice 2	Olfactory area	Right	2	Piriform area
PIR R3	(R) Piriform area slice 3	Olfactory area	Right	3	Piriform area
Pir-Amyg R2	(R) Piriform-amygdalar area slice 2	Amygdala	Right	2	Striatum
Pir-Amyg R3	(R) Piriform-amygdalar area slice 3	Amygdala	Right	3	Striatum
pAmyg R1	(R) Posterior amygdalar nucleus slice 1	Amygdala	Right	1	Striatum
ptThal R1	(R) Posterior triangular thalamic nucleus slice 1	Thalamus	Right	1	Thalamus
A1 R1	(R) Primary auditory area slice 1	Auditory area	Right	1	Isocortex
S1BF R2	(R) Primary somatosensory area, barrel field slice 2	Sensorimotor	Right	2	Isocortex
S1BF R3	(R) Primary somatosensory area, barrel field slice 3	Sensorimotor	Right	3	Isocortex
S1Tr R3	(R) Primary somatosensory area, trunk slice 3	Sensorimotor	Right	3	Isocortex
RThal R3	(R) Reticular nucleus of the thalamus slice 3	Thalamus	Right	3	Thalamus
RSD R1	(R) Retrosplenial area, dorsal part slice 1	Retrosplenial cortex	Right	1	Isocortex
RSD R2	(R) Retrosplenial area, dorsal part slice 2	Retrosplenial cortex	Right	2	Isocortex
RSD R3	(R) Retrosplenial area, dorsal part slice 3	Retrosplenial cortex	Right	3	Isocortex
RSL R1	(R) Retrosplenial area, lateral agranular part slice 1	Retrosplenial cortex	Right	1	Isocortex
RSL R2	(R) Retrosplenial area, lateral agranular part slice 2	Retrosplenial cortex	Right	2	Isocortex
RSL R3	(R) Retrosplenial area, lateral agranular part slice 3	Retrosplenial cortex	Right	3	Isocortex
RSV R1	(R) Retrosplenial area, ventral part slice 1	Retrosplenial cortex	Right	1	Isocortex
RSV R2	(R) Retrosplenial area, ventral part slice 2	Retrosplenial cortex	Right	2	Isocortex
RSV R3	(R) Retrosplenial area, ventral part slice 3	Retrosplenial cortex	Right	3	Isocortex
VISRll R1	(R) Rostrolateral visual area slice 1	Sensorimotor	Right	1	Isocortex
SPF R1	(R) Subparafascicular nucleus slice 1	Thalamus	Right	1	Thalamus
S2 R2	(R) Supplemental somatosensory area slice 2	Sensorimotor	Right	2	Isocortex
S2 R3	(R) Supplemental somatosensory area slice 3	Sensorimotor	Right	3	Isocortex
TEA R1	(R) Temporal association areas slice 1	Association cortex	Right	1	Isocortex
TEA R2	(R) Temporal association areas slice 2	Association cortex	Right	2	Isocortex
valThal R3	(R) Ventral anterior-lateral complex of the thalamus slice 3	Thalamus	Right	3	Thalamus
A2V R1	(R) Ventral auditory area slice 1	Auditory area	Right	1	Isocortex
A2V R2	(R) Ventral auditory area slice 2	Auditory area	Right	2	Isocortex
VMThal R3	(R) Ventral medial nucleus of the thalamus slice 3	Thalamus	Right	3	Thalamus
VplThal R2	(R) Ventral posterolateral nucleus of the thalamus slice 2	Thalamus	Right	2	Thalamus
VplThal R3	(R) Ventral posterolateral nucleus of the thalamus slice 3	Thalamus	Right	3	Thalamus
VpmThal R2	(R) Ventral posteromedial nucleus of the thalamus slice 2	Thalamus	Right	2	Thalamus
VpmThal R3	(R) Ventral posteromedial nucleus of the thalamus slice 3	Thalamus	Right	3	Thalamus
VppmThal R2	(R) Ventral posteromedial nucleus of the thalamus, parvicellular part slice 2	Thalamus	Right	2	Thalamus
VISC R3	(R) Visceral area slice 3	Sensorimotor	Right	3	Isocortex

Table S2: inflammatory cytokine qPCR primer sequences used for Figure 1 and S2

Gene	target protein	Forward	Reverse
Tnfa	Tumer necrosis factor alpha	GCC TC T T CT CAT TC C T GC TT	AGG GT C T GG GCC AT A G AA CT
Nos2	Nitric oxide synthase 2	CCC TT C A AT GGT TG G T AC ATG G	ACA TT G A TC TCC GT G A CA GCC
Ptgs2	Prostaglandin-Endoperoxide Synthase 2 (=Cox2)	TCA TT C A CC AGA CA G A TT GCT	AAG CG T T TG CGG TA C T CA TT
Lgals3	Lectin galactoside-binding soluble 3	GAT CA C A AT CAT GG G C AC AG	ATT GA A G CG GGG GT T A AA GT
Igf1	Insulin like growth factor 1	TGG ATG CTC TTC AGT TCG TG	GCA ACA CTC ATC CAC AAT GC
IL1rn	Interleukin 1 receptor antagonist	TTG TGC CAA GTC TGG AGA	TTC TCA GAG CGG ATG

Supplementary data:

Supplementary Data S1: 2-way ANOVA Tukey's post-hoc of panel Fig. 2k

Number of families	25
Number of comparisons per family	3
Alpha	0.05

Tukey's multiple comparisons test	Predicted (LS) mean diff.	95.00% CI of diff.	Below threshold?	Summary	Adjusted P Value
2					
Sham vs. TBI	3.043	1.121 to 4.965	Yes	***	0.0007
Sham vs. TBI+OXT	3.332	1.364 to 5.299	Yes	***	0.0002
TBI vs. TBI+OXT	0.2884	-1.336 to 1.913	No	ns	0.9084
4					
Sham vs. TBI	-1.586	-3.508 to 0.3362	No	ns	0.1286
Sham vs. TBI+OXT	0.5851	-1.382 to 2.552	No	ns	0.7638
TBI vs. TBI+OXT	2.171	0.5465 to 3.795	Yes	**	0.0051
6					
Sham vs. TBI	-1.146	-3.068 to 0.7755	No	ns	0.3402
Sham vs. TBI+OXT	0.5512	-1.416 to 2.518	No	ns	0.7873
TBI vs. TBI+OXT	1.698	0.07327 to 3.322	Yes	*	0.0381
8					
Sham vs. TBI	0.6045	-1.317 to 2.526	No	ns	0.7399
Sham vs. TBI+OXT	0.08215	-1.885 to 2.049	No	ns	0.9947
TBI vs. TBI+OXT	-0.5223	-2.147 to 1.102	No	ns	0.7299
10					
Sham vs. TBI	1.629	-0.2934 to 3.551	No	ns	0.1151
Sham vs. TBI+OXT	1.224	-0.7434 to 3.191	No	ns	0.3097
TBI vs. TBI+OXT	-0.4048	-2.029 to 1.220	No	ns	0.8276
12					
Sham vs. TBI	4.604	2.683 to 6.526	Yes	****	<0.0001
Sham vs. TBI+OXT	3.26	1.292 to 5.227	Yes	***	0.0003
TBI vs. TBI+OXT	-1.345	-2.969 to 0.2794	No	ns	0.1268
14					
Sham vs. TBI	4.431	2.509 to 6.353	Yes	****	<0.0001
Sham vs. TBI+OXT	2.885	0.9179 to 4.852	Yes	**	0.0018
TBI vs. TBI+OXT	-1.546	-3.170 to 0.07852	No	ns	0.066
16					
Sham vs. TBI	5.649	3.727 to 7.570	Yes	****	<0.0001
Sham vs. TBI+OXT	3.694	1.727 to 5.661	Yes	****	<0.0001

TBI vs. TBI+OXT	-1.954	-3.579 to -0.3301	Yes	*	0.0135
18					
Sham vs. TBI	5.314	3.392 to 7.236	Yes	****	<0.0001
Sham vs. TBI+OXT	3.29	1.323 to 5.257	Yes	***	0.0003
TBI vs. TBI+OXT	-2.024	-3.649 to -0.4001	Yes	**	0.0099
20					
Sham vs. TBI	5.599	3.677 to 7.521	Yes	****	<0.0001
Sham vs. TBI+OXT	3.423	1.456 to 5.390	Yes	***	0.0002
TBI vs. TBI+OXT	-2.176	-3.800 to -0.5515	Yes	**	0.005
22					
Sham vs. TBI	4.807	2.885 to 6.729	Yes	****	<0.0001
Sham vs. TBI+OXT	2.793	0.8263 to 4.761	Yes	**	0.0026
TBI vs. TBI+OXT	-2.013	-3.637 to -0.3887	Yes	*	0.0105
24					
Sham vs. TBI	5.071	3.149 to 6.993	Yes	****	<0.0001
Sham vs. TBI+OXT	3.442	1.474 to 5.409	Yes	***	0.0001
TBI vs. TBI+OXT	-1.63	-3.254 to -0.005401	Yes	*	0.049
26					
Sham vs. TBI	6.13	4.208 to 8.052	Yes	****	<0.0001
Sham vs. TBI+OXT	4.812	2.845 to 6.779	Yes	****	<0.0001
TBI vs. TBI+OXT	-1.318	-2.943 to 0.3062	No	ns	0.1374
28					
Sham vs. TBI	4.222	2.300 to 6.144	Yes	****	<0.0001
Sham vs. TBI+OXT	3.215	1.248 to 5.182	Yes	***	0.0004
TBI vs. TBI+OXT	-1.007	-2.631 to 0.6175	No	ns	0.3123
30					
Sham vs. TBI	3.215	1.293 to 5.137	Yes	***	0.0003
Sham vs. TBI+OXT	2.035	0.06734 to 4.002	Yes	*	0.0407
TBI vs. TBI+OXT	-1.18	-2.804 to 0.4443	No	ns	0.203
32					
Sham vs. TBI	1.852	-0.06988 to 3.774	No	ns	0.0617
Sham vs. TBI+OXT	0.6089	-1.358 to 2.576	No	ns	0.7469
TBI vs. TBI+OXT	-1.243	-2.868 to 0.3812	No	ns	0.1707
34					
Sham vs. TBI	1.002	-0.9199 to 2.924	No	ns	0.4382
Sham vs. TBI+OXT	-0.005948	-1.973 to 1.961	No	ns	>0.9999
TBI vs. TBI+OXT	-1.008	-2.632 to 0.6163	No	ns	0.3115
36					

Sham vs. TBI	0.4708	-1.451 to 2.393	No	ns	0.8329
Sham vs. TBI+OXT	-0.1994	-2.167 to 1.768	No	ns	0.9691
TBI vs. TBI+OXT	-0.6702	-2.295 to 0.9541	No	ns	0.5958
38					
Sham vs. TBI	0.425	-1.497 to 2.347	No	ns	0.8615
Sham vs. TBI+OXT	0.1131	-1.854 to 2.080	No	ns	0.99
TBI vs. TBI+OXT	-0.3119	-1.936 to 1.312	No	ns	0.8937
40					
Sham vs. TBI	0.3938	-1.528 to 2.316	No	ns	0.8799
Sham vs. TBI+OXT	0.244	-1.723 to 2.211	No	ns	0.9541
TBI vs. TBI+OXT	-0.1497	-1.774 to 1.475	No	ns	0.9744
42					
Sham vs. TBI	-0.1688	-2.091 to 1.753	No	ns	0.9768
Sham vs. TBI+OXT	-0.3988	-2.366 to 1.568	No	ns	0.8822
TBI vs. TBI+OXT	-0.2301	-1.854 to 1.394	No	ns	0.9407
44					
Sham vs. TBI	-0.1063	-2.028 to 1.816	No	ns	0.9907
Sham vs. TBI+OXT	-0.3512	-2.318 to 1.616	No	ns	0.9074
TBI vs. TBI+OXT	-0.2449	-1.869 to 1.379	No	ns	0.933
46					
Sham vs. TBI	-0.075	-1.997 to 1.847	No	ns	0.9954
Sham vs. TBI+OXT	-0.1786	-2.146 to 1.789	No	ns	0.9752
TBI vs. TBI+OXT	-0.1036	-1.728 to 1.521	No	ns	0.9877
48					
Sham vs. TBI	-0.05	-1.972 to 1.872	No	ns	0.9979
Sham vs. TBI+OXT	-0.07143	-2.039 to 1.896	No	ns	0.996
TBI vs. TBI+OXT	-0.02143	-1.646 to 1.603	No	ns	0.9995
50					
Sham vs. TBI	-0.0625	-1.984 to 1.859	No	ns	0.9968
Sham vs. TBI+OXT	-0.03571	-2.003 to 1.931	No	ns	0.999
TBI vs. TBI+OXT	0.02679	-1.598 to 1.651	No	ns	0.9992

Supplementary Data S2: 2-way ANOVA Tukey's post-hoc of panel Fig. 3j

Number of families	25
Number of comparisons per family	3
Alpha	0.05

Tukey's multiple comparisons test	Predicted (LS) mean diff.	95.00% CI of diff.	Below threshold?	Summary	Adjusted P Value
2					
Sham vs. TBI	0.3145	-1.264 to 1.893	No	ns	0.8859
Sham vs. TBI+OXT	0.2841	-1.348 to 1.916	No	ns	0.9117
TBI vs. TBI+OXT	-0.03037	-1.530 to 1.469	No	ns	0.9987
4					
Sham vs. TBI	-0.611	-2.189 to 0.9673	No	ns	0.6337
Sham vs. TBI+OXT	-0.5407	-2.173 to 1.091	No	ns	0.7159
TBI vs. TBI+OXT	0.07032	-1.429 to 1.570	No	ns	0.9933
6					
Sham vs. TBI	-1.853	-3.431 to -0.2749	Yes	*	0.0165
Sham vs. TBI+OXT	-0.5321	-2.164 to 1.100	No	ns	0.7234
TBI vs. TBI+OXT	1.321	-0.1785 to 2.821	No	ns	0.0969
8					
Sham vs. TBI	0.1112	-1.467 to 1.689	No	ns	0.985
Sham vs. TBI+OXT	-0.226	-1.858 to 1.406	No	ns	0.9432
TBI vs. TBI+OXT	-0.3372	-1.837 to 1.162	No	ns	0.8571
10					
Sham vs. TBI	1.328	-0.2502 to 2.906	No	ns	0.1186
Sham vs. TBI+OXT	0.9913	-0.6408 to 2.623	No	ns	0.3269
TBI vs. TBI+OXT	-0.3367	-1.836 to 1.163	No	ns	0.8575
12					
Sham vs. TBI	1.516	-0.06272 to 3.094	No	ns	0.0629
Sham vs. TBI+OXT	1.031	-0.6014 to 2.663	No	ns	0.2988
TBI vs. TBI+OXT	-0.4848	-1.984 to 1.015	No	ns	0.7273
14					
Sham vs. TBI	1.757	0.1791 to 3.336	Yes	*	0.0248
Sham vs. TBI+OXT	0.4278	-1.204 to 2.060	No	ns	0.8111
TBI vs. TBI+OXT	-1.33	-2.829 to 0.1700	No	ns	0.094
16					
Sham vs. TBI	3.459	1.880 to 5.037	Yes	****	<0.0001
Sham vs. TBI+OXT	2.031	0.3992 to 3.663	Yes	*	0.0101
TBI vs. TBI+OXT	-1.427	-2.927 to 0.07241	No	ns	0.066

18					
Sham vs. TBI	4.606	3.027 to 6.184	Yes	****	<0.0001
Sham vs. TBI+OXT	3.065	1.433 to 4.697	Yes	****	<0.0001
TBI vs. TBI+OXT	-1.541	-3.041 to -0.04142	Yes	*	0.0424
20					
Sham vs. TBI	3.999	2.421 to 5.577	Yes	****	<0.0001
Sham vs. TBI+OXT	2.257	0.6250 to 3.889	Yes	**	0.0035
TBI vs. TBI+OXT	-1.742	-3.242 to -0.2425	Yes	*	0.018
22					
Sham vs. TBI	4.396	2.818 to 5.974	Yes	****	<0.0001
Sham vs. TBI+OXT	3.291	1.659 to 4.924	Yes	****	<0.0001
TBI vs. TBI+OXT	-1.105	-2.604 to 0.3949	No	ns	0.1941
24					
Sham vs. TBI	3.526	1.948 to 5.104	Yes	****	<0.0001
Sham vs. TBI+OXT	2.012	0.3802 to 3.644	Yes	*	0.011
TBI vs. TBI+OXT	-1.514	-3.013 to -0.01411	Yes	*	0.0473
26					
Sham vs. TBI	3.094	1.515 to 4.672	Yes	****	<0.0001
Sham vs. TBI+OXT	1.838	0.2056 to 3.470	Yes	*	0.0228
TBI vs. TBI+OXT	-1.256	-2.756 to 0.2436	No	ns	0.1209
28					
Sham vs. TBI	2.142	0.5634 to 3.720	Yes	**	0.0043
Sham vs. TBI+OXT	1.65	0.01748 to 3.282	Yes	*	0.0469
TBI vs. TBI+OXT	-0.492	-1.992 to 1.008	No	ns	0.7204
30					
Sham vs. TBI	2.472	0.8939 to 4.050	Yes	***	0.0008
Sham vs. TBI+OXT	1.81	0.1778 to 3.442	Yes	*	0.0255
TBI vs. TBI+OXT	-0.6622	-2.162 to 0.8374	No	ns	0.5527
32					
Sham vs. TBI	1.753	0.1752 to 3.332	Yes	*	0.0252
Sham vs. TBI+OXT	1.218	-0.4141 to 2.850	No	ns	0.186
TBI vs. TBI+OXT	-0.5353	-2.035 to 0.9642	No	ns	0.6784
34					
Sham vs. TBI	0.9695	-0.6087 to 2.548	No	ns	0.3187
Sham vs. TBI+OXT	0.7966	-0.8355 to 2.429	No	ns	0.4849
TBI vs. TBI+OXT	-0.1729	-1.672 to 1.327	No	ns	0.9603
36					
Sham vs. TBI	0.9362	-0.6421 to 2.514	No	ns	0.3441
Sham vs. TBI+OXT	0.6014	-1.031 to 2.234	No	ns	0.6614

TBI vs. TBI+OXT	-0.3348	-1.834 to 1.165	No	ns	0.859
38					
Sham vs. TBI	0.7377	-0.8405 to 2.316	No	ns	0.5147
Sham vs. TBI+OXT	0.1645	-1.468 to 1.797	No	ns	0.9695
TBI vs. TBI+OXT	-0.5733	-2.073 to 0.9263	No	ns	0.6409
40					
Sham vs. TBI	0.7735	-0.8048 to 2.352	No	ns	0.482
Sham vs. TBI+OXT	0.2954	-1.337 to 1.928	No	ns	0.9049
TBI vs. TBI+OXT	-0.478	-1.978 to 1.022	No	ns	0.7337
42					
Sham vs. TBI	0.5	-1.078 to 2.078	No	ns	0.7366
Sham vs. TBI+OXT	0.1806	-1.452 to 1.813	No	ns	0.9633
TBI vs. TBI+OXT	-0.3194	-1.819 to 1.180	No	ns	0.8707
44					
Sham vs. TBI	0.4	-1.178 to 1.978	No	ns	0.8221
Sham vs. TBI+OXT	0.1639	-1.468 to 1.796	No	ns	0.9697
TBI vs. TBI+OXT	-0.2361	-1.736 to 1.263	No	ns	0.9271
46					
Sham vs. TBI	0.3333	-1.245 to 1.912	No	ns	0.8728
Sham vs. TBI+OXT	6.667E-08	-1.632 to 1.632	No	ns	>0.9999
TBI vs. TBI+OXT	-0.3333	-1.833 to 1.166	No	ns	0.8601
48					
Sham vs. TBI	0.1667	-1.412 to 1.745	No	ns	0.9665
Sham vs. TBI+OXT	-0.01389	-1.646 to 1.618	No	ns	0.9998
TBI vs. TBI+OXT	-0.1806	-1.680 to 1.319	No	ns	0.9567
50					
Sham vs. TBI	0.1667	-1.412 to 1.745	No	ns	0.9665
Sham vs. TBI+OXT	0.06944	-1.563 to 1.702	No	ns	0.9945
TBI vs. TBI+OXT	-0.09722	-1.597 to 1.402	No	ns	0.9873

Supplementary Data S3: One-way ANOVAs of panels Fig. 6n-q

Fig 6n:

EC: ANOVA ($F(2,21) = 13.07$, $^{***}p = .0002$, Sham: $n = 8$, TBI: $n = 8$, TBI+OXT: $n = 8$). Tukey's (Sham vs. TBI: $^{***}p = .0001$, Sham vs. TBI+OXT: $^{*}p = .027$, TBI vs. TBI+OXT: $p = .08$)

CC: ANOVA ($F(2,21) = 2.80$, $p = .08$, Sham: $n = 8$, TBI: $n = 8$, TBI+OXT: $n = 8$). Tukey's (Sham vs. TBI: $p = .07$, Sham vs. TBI+OXT: $p = .37$, TBI vs. TBI+OXT: $p = .60$)

CG: ANOVA ($F(2,21) = 6.76$, $^{**}p = .0054$, Sham: $n = 8$, TBI: $n = 8$, TBI+OXT: $n = 8$). Tukey's (Sham vs. TBI: $^{**}p = .0039$, Sham vs. TBI+OXT: $p = .16$, TBI vs. TBI+OXT: $p = .21$)

S1Cx: ANOVA ($F(2,21) = 2.07$, $p = .16$, Sham: $n = 8$, TBI: $n = 8$, TBI+OXT: $n = 8$).

M1Cx: ANOVA ($F(2,21) = 0.66$, $p = .53$, Sham: $n = 8$, TBI: $n = 8$, TBI+OXT: $n = 8$).

Fig 6o:

EC: ANOVA ($F(2,21) = 6.49$, $^{**}p = .0064$, Sham: $n = 8$, TBI: $n = 8$, TBI+OXT: $n = 8$). Tukey's (Sham vs. TBI: $^{**}p = .0067$, Sham vs. TBI+OXT: $p = .72$, TBI vs. TBI+OXT: $^{*}p = .038$)

CC: ANOVA ($F(2,21) = 0.40$, $p = .67$, Sham: $n = 8$, TBI: $n = 8$, TBI+OXT: $n = 8$).

CG: ANOVA ($F(2,21) = 2.19$, $p = .14$, Sham: $n = 8$, TBI: $n = 8$, TBI+OXT: $n = 8$).

S1Cx: ANOVA ($F(2,19) = 3.61$, $^{*}p = .047$, Sham: $n = 8$, TBI: $n = 6$, TBI+OXT: $n = 8$). Tukey's (Sham vs. TBI: $p = .81$, Sham vs. TBI+OXT: $p = .13$, TBI vs. TBI+OXT: $p = .055$)

M1Cx: ANOVA ($F(2,21) = 0.71$, $p = .50$, Sham: $n = 8$, TBI: $n = 8$, TBI+OXT: $n = 8$).

Fig 6p:

EC: ANOVA ($F(2,21) = 4.71$, $^{*}p = .02$, Sham: $n = 8$, TBI: $n = 8$, TBI+OXT: $n = 8$). Tukey's (Sham vs. TBI: $p = .14$, Sham vs. TBI+OXT: $^{*}p = .017$, TBI vs. TBI+OXT: $p = .56$)

CC: ANOVA ($F(2,21) = 7.44$, $^{**}p = .0036$, Sham: $n = 8$, TBI: $n = 8$, TBI+OXT: $n = 8$). Tukey's (Sham vs. TBI: $^{**}p = .0041$, Sham vs. TBI+OXT: $^{*}p = .022$, TBI vs. TBI+OXT: $p = .75$)

CG: ANOVA ($F(2,21) = 0.61$, $p = .55$, Sham: $n = 8$, TBI: $n = 8$, TBI+OXT: $n = 8$).

S1Cx: ANOVA ($F(2,21) = 1.95$, $p = .17$, Sham: $n = 8$, TBI: $n = 8$, TBI+OXT: $n = 8$).

M1Cx: ANOVA ($F(2,21) = 1.50$, $p = .25$, Sham: $n = 8$, TBI: $n = 8$, TBI+OXT: $n = 8$).

Fig 6q:

EC: ANOVA ($F(2,21) = 4.32$, $^{*}p = .027$, Sham: $n = 8$, TBI: $n = 8$, TBI+OXT: $n = 8$). Tukey's (Sham vs. TBI: $^{*}p = .02$, Sham vs. TBI+OXT: $p = .22$, TBI vs. TBI+OXT: $p = .47$)

CC: ANOVA ($F(2,21) = 0.35$, $p = .71$, Sham: $n = 8$, TBI: $n = 8$, TBI+OXT: $n = 8$).

CG: ANOVA ($F(2,21) = 5.52$, $^{*}p = .012$, Sham: $n = 8$, TBI: $n = 8$, TBI+OXT: $n = 8$). Tukey's (Sham vs. TBI: $^{**}p = .0094$, Sham vs. TBI+OXT: $p = .44$, TBI vs. TBI+OXT: $p = .13$)

S1Cx: ANOVA ($F(2,21) = 0.56$, $p = .58$, Sham: $n = 8$, TBI: $n = 8$, TBI+OXT: $n = 8$).

M1Cx: ANOVA ($F(2,21) = 0.80$, $p = .46$, Sham: $n = 8$, TBI: $n = 8$, TBI+OXT: $n = 8$).

Supplementary Data S4: Statistical tests of Fig. 7

In **(e)** ANOVA (F(2,25) = 5.39, **p* = .011. Sham: *n* = 10, TBI: *n* = 10, TBI+OXT: *n* = 8). Tukey's (Sham vs. TBI: **p* = .025; Sham vs. TBI+OXT: *p* = .98; TBI vs. TBI+OXT: **p* = .024).

In **(j)** ANOVA (F(2,27) = 4.77, **p* = .017. Sham: *n* = 10, TBI: *n* = 11, TBI+OXT: *n* = 9). Tukey's (Sham vs. TBI: **p* = .029; Sham vs. TBI+OXT: *p* = 1; TBI vs. TBI+OXT: **p* = .043).

In **(k)** ANOVA (F(2,27) = 3.33, *p* = .05. Sham: *n* = 10, TBI: *n* = 11, TBI+OXT: *n* = 9).

In **(l)** ANOVA (F(2,27) = 6.40, ***p* = .0053. Sham: *n* = 10, TBI: *n* = 11, TBI+OXT: *n* = 9). Tukey's (Sham vs. TBI: ***p* = .009; Sham vs. TBI+OXT: *p* = .97; TBI vs. TBI+OXT: **p* = .021).

In **(m)**

S1TrL-RSDL:	ANOVA (F(2,27) = 4.88, **p* = .016. Sham: *n* = 10, TBI: *n* = 11, TBI+OXT: *n* = 9). Tukey's (Sham vs. TBI: **p* = .023; Sham vs. TBI+OXT: *p* = .97; TBI vs. TBI+OXT: *p* = .049).
S1BFL-S1BFR:	ANOVA (F(2,27) = 7.25, ***p* = .0030. Sham: *n* = 10, TBI: *n* = 11, TBI+OXT: *n* = 9). Tukey's (Sham vs. TBI: ***p* = .002; Sham vs. TBI+OXT: *p* = .23; TBI vs. TBI+OXT: *p* = .14).
S1BFL-S1TrR:	ANOVA (F(2,27) = 6.05, ***p* = .0068. Sham: *n* = 10, TBI: *n* = 11, TBI+OXT: *n* = 9). Tukey's (Sham vs. TBI: ***p* = .0048; Sham vs. TBI+OXT: *p* = .25; TBI vs. TBI+OXT: *p* = .22).
RSDL-S1TrR:	ANOVA (F(2,27) = 5.66, ***p* = .0089. Sham: *n* = 10, TBI: *n* = 11, TBI+OXT: *n* = 9). Tukey's (Sham vs. TBI: ***p* = .008; Sham vs. TBI+OXT: *p* = .61; TBI vs. TBI+OXT: *p* = .09).
RSVL-RSVR:	ANOVA (F(2,27) = 3.95, **p* = .031. Sham: *n* = 10, TBI: *n* = 11, TBI+OXT: *n* = 9). Tukey's (Sham vs. TBI: *p* = .10; Sham vs. TBI+OXT: *p* = .88; TBI vs. TBI+OXT: **p* = .039).

In **(o)** Kruskall-Wallis test (F(3) = 10.38, ***p* = .0056. Sham: *n* = 10, TBI: *n* = 11, TBI+OXT: *n* = 7). Dunn's (Sham vs. TBI: ***p* = .004; Sham vs. TBI+OXT: *p* = .68; TBI vs. TBI+OXT: *p* = .29).

In **(p)** ANOVA (F(2,26) = 11.16, ****p* = .0003. Sham: *n* = 10, TBI: *n* = 11, TBI+OXT: *n* = 8). Tukey's (Sham vs. TBI: ****p* = .0003; Sham vs. TBI+OXT: *p* = .58; TBI vs. TBI+OXT: ***p* = .009).

In **(q)** ANOVA (F(2,25) = 8.39, ***p* = .0016. Sham: *n* = 9, TBI: *n* = 10, TBI+OXT: *n* = 9). Tukey's (Sham vs. TBI: **p* = .039; Sham vs. TBI+OXT: *p* = .37; TBI vs. TBI+OXT: ***p* = .001).

In **(r)** Kruskall-Wallis test (F(3) = 4.14, *p* = .13. Sham: *n* = 9, TBI: *n* = 11, TBI+OXT: *n* = 9).

In **(s)** Kruskall-Wallis test (F(3) = 9.71, ***p* = .0078. Sham: *n* = 7, TBI: *n* = 8, TBI+OXT: *n* = 8). Dunn's (Sham vs. TBI: **p* = .030; Sham vs. TBI+OXT: *p* = 1; TBI vs. TBI+OXT: *p* = .016).

In **(t)**

Sensorimotor Cx:	ANOVA (F(2,26) = 8.77, ***p* = .0012. Sham: *n* = 10, TBI: *n* = 11, TBI+OXT: *n* = 8). Tukey's (Sham vs. TBI: ***p* = .0014; Sham vs. TBI+OXT: *p* = .73; TBI vs. TBI+OXT: **p* = .017).
Retrosplenial Cx:	ANOVA (F(2,26) = 5.79, ***p* = .0083. Sham: *n* = 10, TBI: *n* = 11, TBI+OXT: *n* = 8). Tukey's (Sham vs. TBI: **p* = .026; Sham vs. TBI+OXT: *p* = .93; TBI vs. TBI+OXT: **p* = .016).

In **(u)**

Sensorimotor Cx:	ANOVA (F(2,23) = 6.83, ***p* = .0043. Sham: *n* = 9, TBI: *n* = 8, TBI+OXT: *n* = 9). Tukey's (Sham vs. TBI: **p* = .021; Sham vs. TBI+OXT: *p* = .87; TBI vs. TBI+OXT: ***p* = .0062).
Retrosplenial Cx:	ANOVA (F(2,25) = 5.98, ***p* = .0076. Sham: *n* = 9, TBI: *n* = 10, TBI+OXT: *n* = 9). Tukey's (Sham vs. TBI: *p* = .051; Sham vs. TBI+OXT: *p* = .71; TBI vs. TBI+OXT: ***p* = .0079).
Auditory Cx:	ANOVA (F(2,23) = 11.55, ****p* = .0003. Sham: *n* = 9, TBI: *n* = 9, TBI+OXT: *n* = 8). Tukey's (Sham vs. TBI: **p* = .022; Sham vs. TBI+OXT: *p* = .15; TBI vs. TBI+OXT: ****p* = .0002).

In **(v)**

Edge weight >.25:	ANOVA (F(2,25) = 7.28, ***p* = .0032. Sham: *n* = 10, TBI: *n* = 10, TBI+OXT: *n* = 8). Tukey's (Sham vs. TBI: *p* = .057; Sham vs. TBI+OXT: *p* = .33; TBI vs. TBI+OXT: ***p* = .0027).
Edge weight [-0.1:0.1]:	ANOVA (F(2,27) = 2.58, *p* = .09. Sham: *n* = 10, TBI: *n* = 11, TBI+OXT: *n* = 9).

Appendix C

Neonatal oxytocin release mitigates neuroinflammation and rescues neural correlates of encephalopathy of prematurity

Knoop M, Possovre ML, Trak E, Van de Looij Y, Sanches E, Tsartsalis S, Pansiot J, Schirmbeck G and Baud O. *under review (Nature Communications)*

Neonatal oxytocin release mitigates neuroinflammation and rescues neural correlates of encephalopathy of prematurity

Marit Knoop, Marie-Laure Possovre, Ece Trak, Yohan van de Looij, Eduardo Sanches, Stergios Tsartsalis, Julien Pansiot, Gabriel Schirmbeck and Olivier Baud.

Abstract

Every year, 15 million babies are born preterm (< 37 weeks of gestation) which puts them at increased risk for encephalopathy of prematurity (EoP). EoP is characterized by neuroinflammation and microglial reactivity that can aggravate injury mechanisms. Effective therapies against inflammation in the preterm brain remain elusive. However, therapies such as Kangaroo care and music therapy have a positive impact in newborn brain development – yet the underlying mechanism is largely unknown. Here, we assess the neuroprotective effects of endogenous oxytocin modulation on the neural correlates of EoP. Using a well-established mouse model of systemic interleukin-1β to induce EoP, we show that neonatal chemogenetic activation of oxytocinergic neurons has anti-inflammatory effects on microglial gene expression, restoring brain development functions including axonal integrity and oligodendrocyte maturation. In the long-term, oxytocin release improved microstructural development of the corpus callosum and motor cortex, and rescued typical social behavior including ultrasound vocalization profiles. The neuroprotective effects of oxytocin were more prominent in females, showing enhanced reduction of microgliosis and improved rescue of social behavior compared to males. This study supports early clinical interventions and further explains how developmental care, that stimulate endogenous oxytocin release, can induce neuroprotective effect against brain injury associated with prematurity.

1. Introduction

Preterm birth affects around 1 in every 10 live births worldwide[1] and is a leading risk factor for brain injury during neurodevelopment. The collection of neural and neurocognitive impairments that are associated with preterm birth are bundled in the clinical term *Encephalopathy of Prematurity* (EoP), which is characterized by cystic and non-cystic diffuse injury to developing white matter. Such lesions account for most cognitive, behavioral, attentional and social deficits occurring in more than 50% of children born preterm.[2]

The major causes of EoP are perinatal events creating an inflammatory environment in the developing brain, ie. amniotic infection, hypoxia-ischemia, neonatal sepsis, mechanical ventilation, and necrotizing enterocolitis[3]. The neuroinflammatory response then acts as a second insult with sufficient influence to further aggravate brain damage and impair neural development. Neuroinflammation in EoP is attributable to microglial cells[4]. Notably, major causal roles have been identified for microglia in white matter injury, a key feature of EoP: Microglia switch from a homeostatic phenotype that supports brain development, to a pro-inflammatory ("reactive") phenotype characterized by increased proliferation, amoeboid morphology and pro-inflammatory cytokine expression. Reactive microglia induce a maturational arrest in developing oligodendrocytes, leading to hypomyelation[5–7].

Modulation of microglia and the inflammatory response to injury seems a promising target for therapy in EoP. It has proven to reduce damage and improve outcomes in brain disease models associated with neuroinflammation, such as ischemic stroke[8], hypoxia-ischemia[9], and traumatic brain injury[10]. However, the magnitude of its neuroprotective effects is variable and inconsistent between different models and candidate molecules[11]. Moreover, the success of anti-inflammatory therapies for treating young infants has been, to date, mostly experimental, with no successful clinical translation. The need for a therapy that is safe, efficient and translational to the neonatal intensive care unit is therefore pressing.

A novel strategy with high translational potential for treating perinatal injuries involves the neuropeptide oxytocin, endogenously produced by the hypothalamus. Oxytocinergic system has projections throughout the brain, in particular in the white matter. Neural expression patterns of oxytocin receptor show fluctuations that correlate with the timeline of development of brain regions[12], suggesting that oxytocin is not only involved in sociability and bonding, but could be important during brain development and maturation. Clinical studies support this idea by showing positive associations between interventions such as music therapy, environmental enrichment, personalized care, maternal speech, and skin-to-skin contact and neurocognitive improvement in infants born preterm[13–15]. Some of these therapies were found to be associated with elevated oxytocin levels. Data from our group support the link between oxytocin and neuroprotection, by demonstrating improved brain development in a rat model of intra-uterine growth restriction after treatment with an exogenous oxytocin receptor agonist[7]. However, underlying mechanisms remain largely unclear and the neuroprotective effect of endogenous oxytocin remains to be demonstrated. Interestingly, sex-differences in innate oxytocin signaling make wonder how successful the therapy is in males and females[16], which is in line with the importance of sexual dimorphism in the mechanisms of neonatal EoP[17].

In this study, we assessed neonatal oxytocin release as a neuroprotectant for treating EoP using a mouse model of EoP induced by the systemic administration of pro-inflammatory cytokine interleukin-1β. We used chemogenetic DREADD technology to stimulate endogenous neuronal oxytocin activity and assessed its therapeutic effects on acute microglial inflammation and neuro-behavioral development in males and females. We found that oxytocin has anti-inflammatory effects on microgliosis, inducing transcriptomic changes that reduce toxic glial functions and promote brain developmental processes. On a systemic level, oxytocin exposure rescued deficits in white matter integrity and early-life social behavior in IL-1β exposed pups. The protective effects of oxytocin were more prominent in females than in males.

2. Results

2.1 EoP model induces microglial activation and long-term behavioral deficits in C57BL/6 mice

As a first experiment, we examined the cellular and neural correlates of the EoP model in C57BL/6 mice using a battery of tests. Male and female mouse pups were injected with pro-inflammatory cytokine IL-1β twice daily between P1 and P5 to induce EoP associated with systemic inflammation[5]. This model induced inflammatory microglia activity in the brain at P3 with increased gene expression of *Ptgs2* (p = .0008)*, IL-1β* (p = .0025), *Arg1* (p < .0001)*, Lgals3* (p = .0024)*, IL1rn* (p = .0037), and *IL4ra* (p = .0003) in IL-1β- versus saline-injected pups (Fig 1a,b). Following IL-1β injections, pups exhibited significantly reduced body from P2 and peaking at P5 (p < .0001; Fig. 1c–e). Such difference no longer existed at juvenile stage (P28). The IL-1β model was associated with a behavioral phenotype of reduced sociability and reduced motor learning at adult age. Unlike control mice, which prefer social interactions, IL-1β mice had no preference for the social stimulus *versus* the object in the 3-chamber test at P56 (p = .28) (Fig 1f,g). The Barnes maze was used to test motor learning and cognitive flexibility at P90. Mice can have different searching strategies to find the escape box, which reflect different levels of spatial learning[18] (Fig 1h). IL-1β and saline mice showed a significantly different distribution of search strategies on reversal training day 1 (p = .0062) and day 3 (p < .0001), where IL-1β mice demonstrated less use of the direct search (most efficient strategy) compared to saline mice (p = .023) (Fig 1i). The search latency nor the number of errors were altered by IL-1β exposure. These data illustrate the inflammatory profile of the IL-1β model of EoP, associated with subsequent sociability and spatial learning deficits both in in male and female mice. Males and females showed comparable effects of IL-1β on P3 microgliosis and long-term cognitive assessments (Supplementary Figure S1).

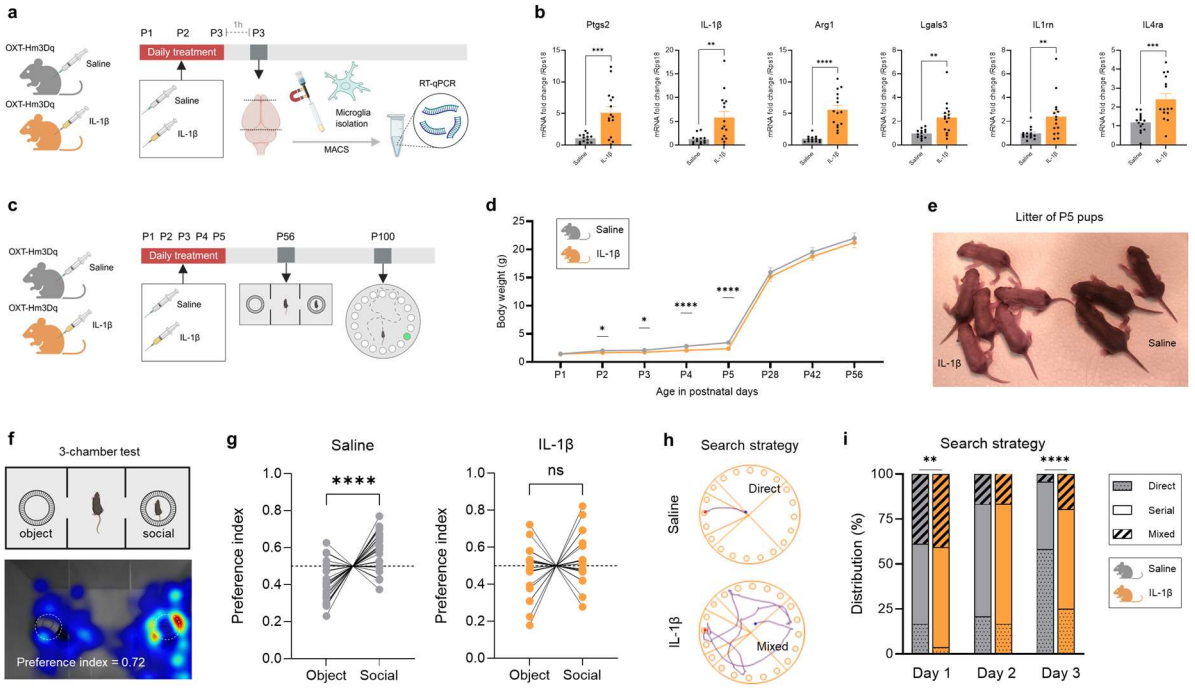

Fig. 1: Neonatal interleukin-1-beta exposure to C57BL/6 mouse pups causes systemic inflammation and long-term behavioral impairments associated with Encephalopathy of Prematurity. a) Schematic showing experimental timeline of RT-qPCR from magnetically sorted microglia from P3 brains, after P1-P3 injection with IL-1β (orange) or saline (gray) substance. **b)** RT-qPCR quantification revealed an increase in inflammatory cytokine expression in microglia from IL-1β compared to saline brains (Ptgs2: p = .0008, IL-1β: p = .0025, Arg1: p < .0001, Lgals3: p = .0024, IL1rn: p = .0037, IL4ra: p = .0003). **c)** Schematic of experimental timeline of behavioral assessment after P1-P5 injection with IL-1β or saline. **d)** Body growth was reduced in IL-1β compared to saline pups between P2 and P5 (p < .0001). This difference was rescued from P28 onwards. **e)** Representative image showing decreased body growth at P5 of IL-1β injected pups versus saline-injected littermates. **f)** Schematic representation of the 3-chamber test at P56 and representative behavior of social preference demonstrated by a saline mouse. **g)** Saline mice showed a clear preference for the social stimulus *vs.* the object during the 3-chamber test (p = .0021). IL-1β mice did not have a preference for the social stimulus, reflecting impaired social behavior. **h)** Representative examples of escape-box (target) search behavior during the P90 Barnes maze test for spatial learning. Example of direct search strategy (top) as used predominantly by saline mice at Day 3, and example of mixed search strategy (bottom), used mostly by the IL-1β mice at Day 3. **i)** Quantification of target search strategy during the Barnes maze reversal phase training days showed different distribution of search strategies in IL-1β mice compared to saline, at Day 1 (p = .0062) and Day 3 (p < .0001): IL-1β mice used less direct search than saline mice (p = .023). RT-qPCR = real-time quantitative polymerase chain reaction; IL-1β = interleukin-1 beta. Statistical differences were assessed in **(b)** with a Student's t test for normal distributions and a Mann-Whitney test for non-normal

distributions, in **(d)** with a repeated-measures ANOVA of age*treatment with Šídák's post-hoc, in **(g)** with a Paired t-test, and in **(i)** with a chi-square test of contingency, and 2-way ANOVA with Šídák's post-hoc. *$p < .05$, **$p < .01$, ***$p < .0005$, ****$p < .0001$. In **(b)** Saline: n = 6-8, IL-1β: n = 6-7. In **(d)** Saline: n = 19, IL-1β: n = 14. In **(g)** Saline: n = 30, IL-1β: n = 22. In **(i)** Saline: n = 12, IL-1β: n = 9. Bar graphs represent Mean ± SEM. Each data point represents an individual sample.

2.2 Neonatal oxytocin release reverses increased microglia density induced by systemic IL-1β exposure

In this study, Cre-dependent Designer Receptors Exclusively Activated by Designer Drugs (DREADD) methodology[19] was used to induce endogenous oxytocin release in neonatal mice under clozapine-n-oxide (CNO) control, causing membrane depolarization of oxytocinergic neurons following injection (as previously shown by our group[20]). This study included 3 experimental groups: pups injected with NaCl ("saline"), pups injected with IL-1β ("IL-1β"), and pups injected with a mix of IL-1β and oxytocin-activating CNO substance ("IL-1β+OXT"). CNO showed no side-effects on readouts of this study (Supplementary Figure S2).

We assessed microgliosis at P3 by quantifying the expression of Iba1 by immunohistochemistry in the cortex and corpus callosum (CC) (Fig 2a). IL-1β pups showed an increase of microglial density of Iba1+ cells compared to saline pups, in both the cortex and CC (Fig 2b,c). Oxytocin release reduced the microglia density back to saline-equivalent levels in the CC and had a trend to decrease in the cortex (p = .06) (Fig 2b,c). We further assessed potential sex effects of IL-1β exposure and oxytocin release on P3 microgliosis. Both sexes showed a similar increase in microglia density after IL-1β exposure (Fig 2e,f), however oxytocin release reduced microglia density only in IL-1β females, but not in IL-1β males (Fig 2e,f).

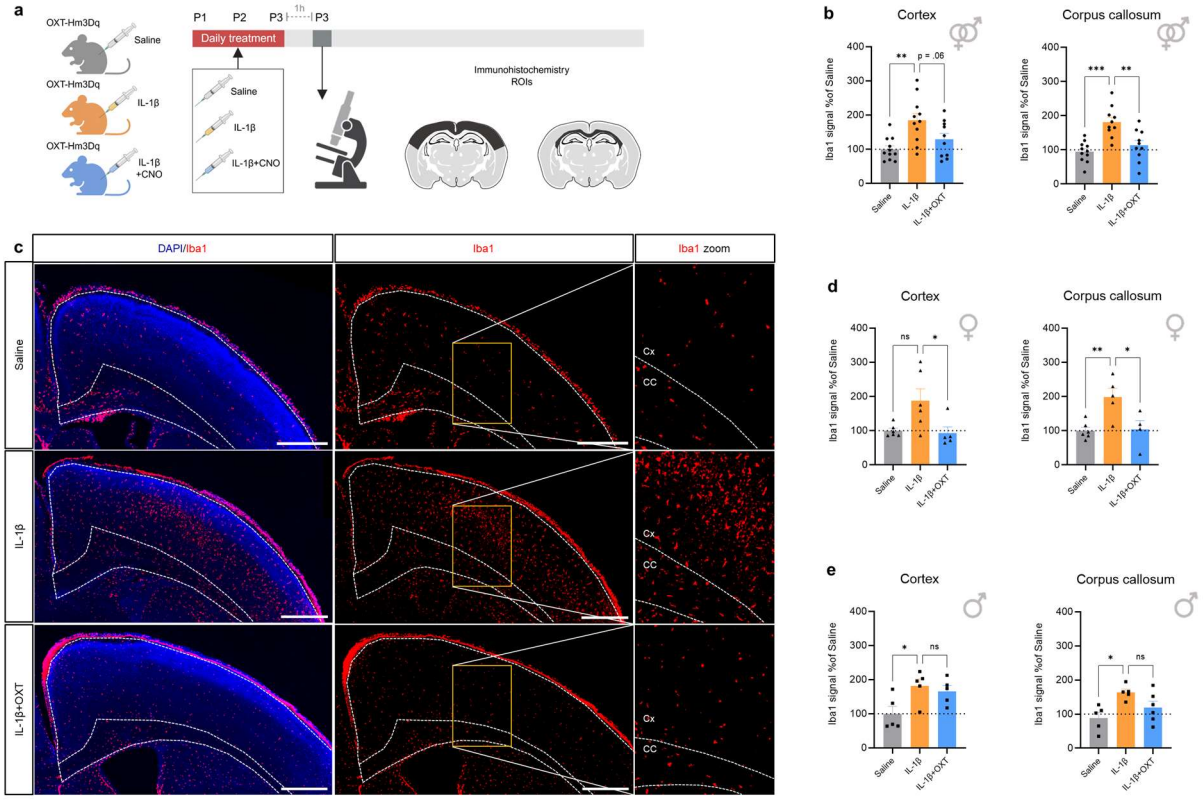

Fig. 2: Oxytocin reduces microglia reactivity induced by systemic inflammation. **a)** Experimental timeline of Iba1 immunohistochemistry on P3 brains with ROI indication (black), after P1-P3 injection with Saline (gray), IL-1β (orange), or IL-1β mixed with OXT-increasing CNO (blue; "IL-1β+OXT" group) in OXT-Hm3Dq DREADD pups. **b)** Iba1^{+} microglia cell density relative to the Saline control group (dotted line; 100%) revealed an increase in IL-1β exposed pups compared to healthy controls in the cortex (p = .002) and corpus callosum (p = .0001). This increase was reversed in IL-1β+OXT compared to untreated IL-1β pups, significantly in the corpus callosum (p = .002) and with a trend in the cortex (p = .057). **c)** Representative micrographs of microglia (Iba1^{+}; red) in the cortex and corpus callosum in Saline, IL-1β and IL-1β+OXT treatment groups at P3. Scale bar = 200 µm. ROIs delineated with dotted lines. **d,e)** Assessment of sex*treatment interaction effect for microglia density in the cortex and corpus callosum revealed therapeutic effects of OXT release on IL-1β microglia phenotype in females (cortex: p = .026; corpus callosum: p = .022) **(d)** but not in males **(e)**. ROI = region of interest; IL-1β = interleukin-1 beta; OXT = oxytocin; CNO = clozapine-n-oxide. Statistical differences were assessed with One-way ANOVA's with Tukey's post-hoc test for normally distributed data and with Kruskal-Wallis test with Dunn's post-hoc for non-normal data distribution. *p < .05, **p < .01, ***p < .0005. Saline: n = 11 (6 females), IL-1β: n = 11 (6 females), IL-1β+OXT: n = 10 (5 females). Bar graphs represent Mean ± SEM. Each data point represents an individual sample.

2.3 Oxytocin release changes microglia transcriptome in mice subjected to systemic inflammation

Next, we performed RNA sequencing on P3 sorted microglia (Fig 3a). Microglial cells were extracted from P3 brains and Expression Weighted Cell-type Enrichment analysis of the top 250 expressed genes in the transcriptomic dataset confirmed a significant enrichment of specifically microglia cells (Fig 3b). 16'038 microglia genes were sequenced and assessed with differential gene expression analysis. IL-1β exposure affected the expression of 4'230 genes in P3 microglia compared to saline (Fig 3c) and segregated the transcriptome of IL-1β samples from healthy controls in the unsupervised heatmap analysis (Fig 3d). Microglia from IL-1β pups demonstrated a pro-inflammatory transcriptomic profile compared to saline pups (Fig 3e) with upregulated cytokines, and signaling pathways such as interleukin and interferon, TNF and NF kappa B. Concurrently, IL-1β microglia showed a downregulation of gene pathways involved in brain development, neurogenesis and neuron migration, axon guidance, oligodendrocyte differentiation and synapse organization (Fig 3e). Downregulated signaling pathways in IL-1β microglia included Wnt, Notch and P13K-Akt signaling, which are involved in microglia-mediated oligodendrocyte maturation[21]. Notably, oxytocin signaling was also downregulated in IL-1β microglia compared to saline.

Females and males showed similar changes in gene expression after IL-1β exposure: 2681 differentially expressed genes (DEGs) were shared between females and males, compared to 799 unique DEGs in females (77% DEGs overlap with males) and 1529 unique DEGs in males (64% DEGs overlap with females) (Fig 3f). Compared to their sex-matched controls, IL-1β females and males both showed increased gene expression of inflammatory and immune pathways, and a downregulation of pathways associated with brain development and cell adhesion (Fig 3g-j). We observed subtle sex effects when cross-examining the DEGs and performing GSEA analysis on the unique DEGs *per* sex (Supplementary Figure S3). DEGs induced by IL-1β that were found in females and not in males were enriched for inflammatory pathways. Downregulated DEGs unique to female IL-1β microglia involved pathways of neural development, and cognitive processes such as memory, learning and behavior. In

IL-1β males, the unique DEG signature included an upregulation of inflammatory and apoptotic processes, and a collection of cytoplasmic and ribosomal translation pathways. The downregulation of transcription processes and Wnt signaling was exclusive in males. Despite these subtle differences, our data suggests that IL-1β exposure induces a largely similar transcriptomic response in P3 microglia between males and females.

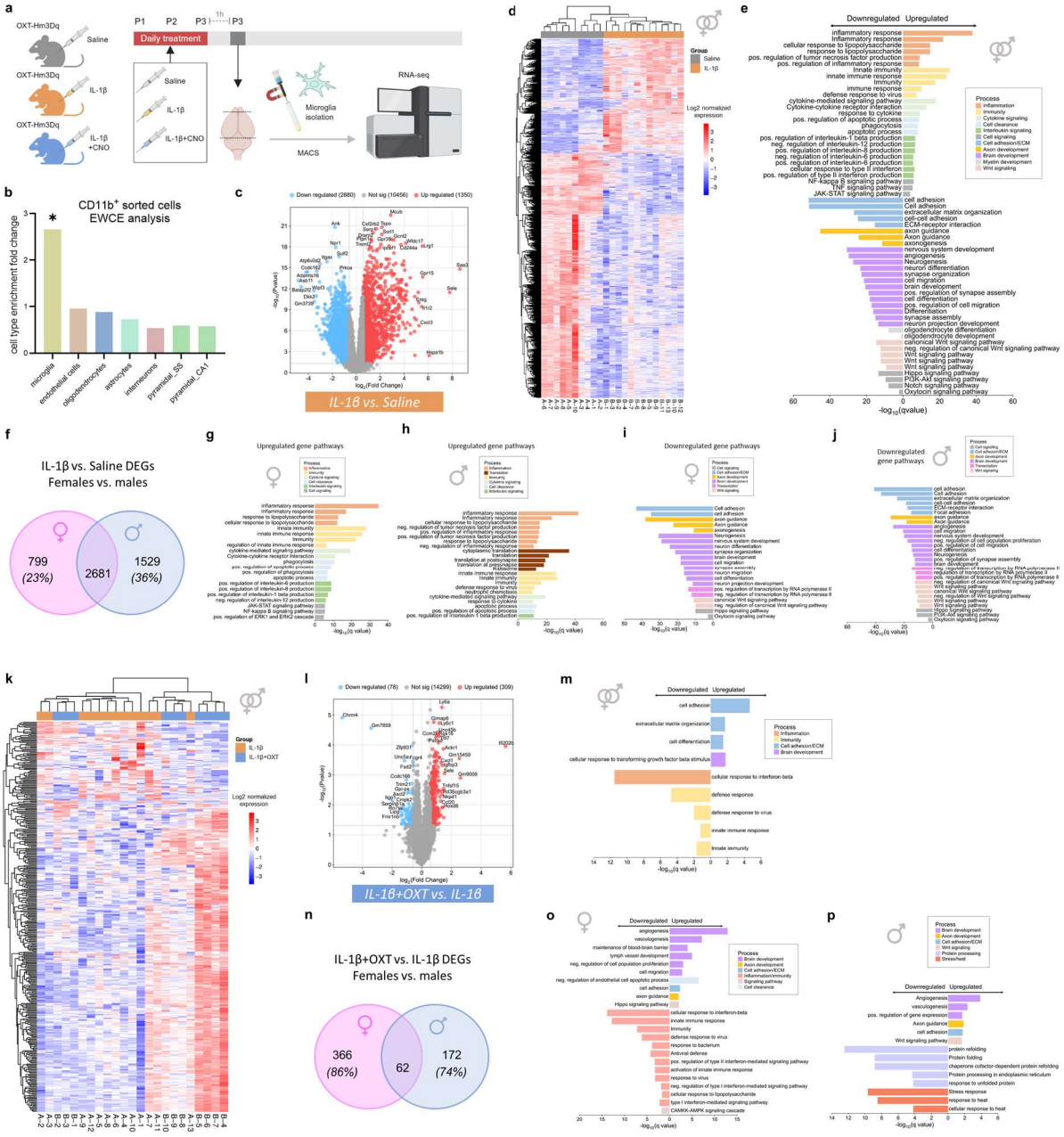

Fig. 3: Oxytocin release changes microglia transcriptome in P3 mice subjected to systemic inflammation. a) Graphical timeline of bulk RNA sequencing experiment of magnetically sorted microglia from P3 brains. Before sacrifice at P3, OXT-Hm3Dq DREADD pups received daily injections

between P1 and P3, the compound depending on treatment group: Saline (gray), IL-1β (orange) or IL-1β mixed with OXT-increasing CNO (blue; "IL-1β+OXT" group). **b)** Bar graph demonstrating results from Expression-Weighted Celltype Enrichment analysis of the top 250 expressed genes, confirming that the dataset was only enriched with microglia cells. **c)** Volcano plot showing 4'230 differentially expressed genes (DEGs) between microglia from P3 IL-1β and Saline pups, including 1'350 upregulated (red) and 2'880 downregulated (blue) genes. **d)** Unsupervised heatmap analysis based on top deregulated genes shows allocation of the IL-1β and Saline samples into their respective experimental groups. **e)** Bar graph representing gene set enrichment analysis (GSEA) results in IL-1β microglia compared to saline microglia, revealing an abundant upregulation of inflammation- and immune-related pathways, and a downregulation of gene pathways involved in cell adhesion, general brain development, oligodendrocyte and axon development, as well as oxytocin signaling. **f)** Venn diagram showing shared and unique DEGs for female and male sex-matched IL-1β versus Saline comparison. 23% of the DEGs in females, and 36% of the DEGs in males, were unique for their respective sex. **g-j)** Bar graph showing GSEA results of IL-1β versus saline microglia in females **(g,i)** and males **(h,j)**. The upregulated **(g,h)** and downregulated **(i,j)** gene pathways in IL-1β microglia compared to saline controls were largely similar between sexes. **k)** Unsupervised heatmap analysis of IL-1β and IL-1β+OXT samples showing mostly separation between experimental groups based on microglia transcriptome. **l)** Volcano plot of the 387 DEGs between microglia from IL-1β+OXT vs IL-1β pups, including 309 upregulated (red) and 78 downregulated (blue) genes. **m)** Bar graph of GSEA results between IL-1β+OXT and IL-1β pups, revealing that OXT reduces gene expression of inflammation and immune pathways, and increases gene expression of cell adhesion and brain development processes in P3 microglia. **n)** Venn diagram showing sex-specific DEGs of microglia transcriptome between IL-1β+OXT and IL-1β pups, where 86% of all DEGs in females were unique (not shared with males), compared to 74% of unique DEGs in males. **o,p)** IL-1β+OXT vs IL-1β GSEA comparison in females **(o)** and males **(p)** revealed sex-specific effects of OXT release on P3 microglia transcriptome in IL-1β, where females show a downregulation of immune and inflammation pathways **(o)**, and males downregulate microglial expression of protein folding **(p)**. Both sexes showed a moderate upregulation of brain development gene expression. IL-1β = interleukin-1 beta; CNO = clozapine-n-oxide; OXT = oxytocin. Saline: n = 10 (5 females), IL-1β: n = 13 (6 females), IL-1β+OXT: n = 10 (5 females). Microglia bulk RNA seq analysis was performed with fold change > 1.5 and FDR-corrected $p < .05$ thresholds. In **(e,g-j,l,m,o,p)** enrichment is represented as the negative log of the q value. Upregulated pathways are positioned on the right side of the y-axis, downregulated pathways on the left side. Bar graphs are sorted on q value, per overlapping cellular process.

Oxytocin treatment changed the microglia transcriptome in brains from P3 IL-1β exposed pups, affecting the expression of 387 genes compared to untreated IL-1β microglia (Fig 3k,l). IL-1β+OXT microglia showed a downregulation of gene pathways involved in inflammation and immune processes compared to untreated IL-1β, emphasizing anti-inflammatory effects of oxytocin release. Upregulated DEGs were enriched for cell adhesion and extracellular matrix gene pathways. When comparing sexes, we observed a distinct effect of oxytocin release on microglia sorted from males and females. Oxytocin affected 428 genes in female IL-1β pups, and 234 genes in males, with only 62 DEGs in common between sexes (Fig 3n). While oxytocin treatment induced a downregulation of inflammation pathways in females (Fig 3o), it did not change pathways related to inflammation in males. Oxytocin-treated IL-1β males showed only a downregulation of pathways involved in protein folding and response to stress/heat (Fig 3p). Females and males both showed an upregulation of microglia gene pathways involved in cell adhesion and brain development processes, including axon guidance, again with greater effects in females (Fig 3o,p). Furthermore, oxytocin upregulated different signaling pathways in males and females. Female IL-1β microglia showed enrichment of the Hippo signaling pathway, and male IL-1β microglia had increased Wnt signaling expression, upon oxytocin treatment (Fig 3o,p). The oxytocin release thereby directly reversed two pathways that were depleted in IL-1β (*versus* saline) in a sex-dependent manner. These data emphasize potential sex differences for the effects of oxytocin treatment on pro-inflammatory microglia.

Finally, we assessed oxytocin's effects on healthy control microglia. In microglia from P3 saline pups, oxytocin release changed the expression of 724 genes and induced an upregulation of gene pathways involved in several brain development processes, including neurogenesis and migration, synapse organization, axon guidance and axonogenesis (Supplementary Figure S4). This suggests that oxytocin stimulates microglia-mediated brain development functions in homeostatic conditions.

2.4 Neonatal oxytocin rescues early-life social behavior deficits induced by systemic inflammation

Preterm infants exposed to systemic inflammation show increased risk of behavioral issues in infancy and adulthood, including impaired social abilities[22]. To assess early-life sociability, we subjected the newborn mice to a battery of social tests at P6 and P14 (Fig 4a). Isolation-induced ultrasound vocalizations (USVs) were recorded at P6, and classified into 11 USV categories with VocalMat[23] (Fig 4b). The distribution of USV categories at P6 was significantly different between experimental groups (Fig 4c,d) (p = .0017). Compared to healthy controls, IL-1β pups showed increased use of *short*, *down*, and *flat* USV categories, and decreased use of *chevron*, *step-up*, *2-steps*, and *complex* USV categories (Fig 4e). Oxytocin treatment reversed most of these alterations and shifted the USV category profile back to healthy control-levels (Fig 4c). Compared to untreated IL-1β, oxytocin-treated IL-1β pups showed a reduced proportion of *flat* USVs, and an increased proportion of *step-up*, *2-step*, and *complex* USVs (Fig 4e). From the 11 USV categories, oxytocin treatment had the most effect on complex USV categories (Fig 4f). USV vocalization rate was not different between experimental groups (Fig 4g).

We found moderate sex effects in the vocalization profile (Fig 4h,i). IL-1β exposure caused more changes to the USV profile in male pups than in females compared to saline: 8/11 USV categories were affected in males, versus 3/11 in females. For female pups, no differences were found between saline and IL-1β+OXT treatment groups, for any USV category (Fig 4h). In contrast, males showed a significant difference between saline and IL-1β+OXT groups for *short*, *chevron* (p = .08), *flat*, and *two-step* USV categories (Fig 4i).

Next, we performed the homing test at P14, which is an indicator of early-life sociability and attachment[24]. While saline-injected mice showed strong preference for their home-cage nest compared to nest material from an unfamiliar cage (Mean preference index: 0.77), IL-1β injected juveniles showed a significant decrease in this preference (p = .0002, Fig 4j). Oxytocin-treated IL-1β group demonstrated a rescued preference for the home-cage nest area, with a preference index significantly higher from the untreated IL-1β group (p = .0188). There was an interaction between sex x treatment on homing test sociability (p = .0237) (Fig 4k,l). Oxytocin treatment rescued nest

preference behavior in females IL-1β mice (p = .0015), but did not significantly affected male IL-1β juveniles (Fig 4k). Similar to previous reports[25], oxytocin exposure did not alter P6 and P14 sociability readouts in control animals (Supplementary Figure S5).

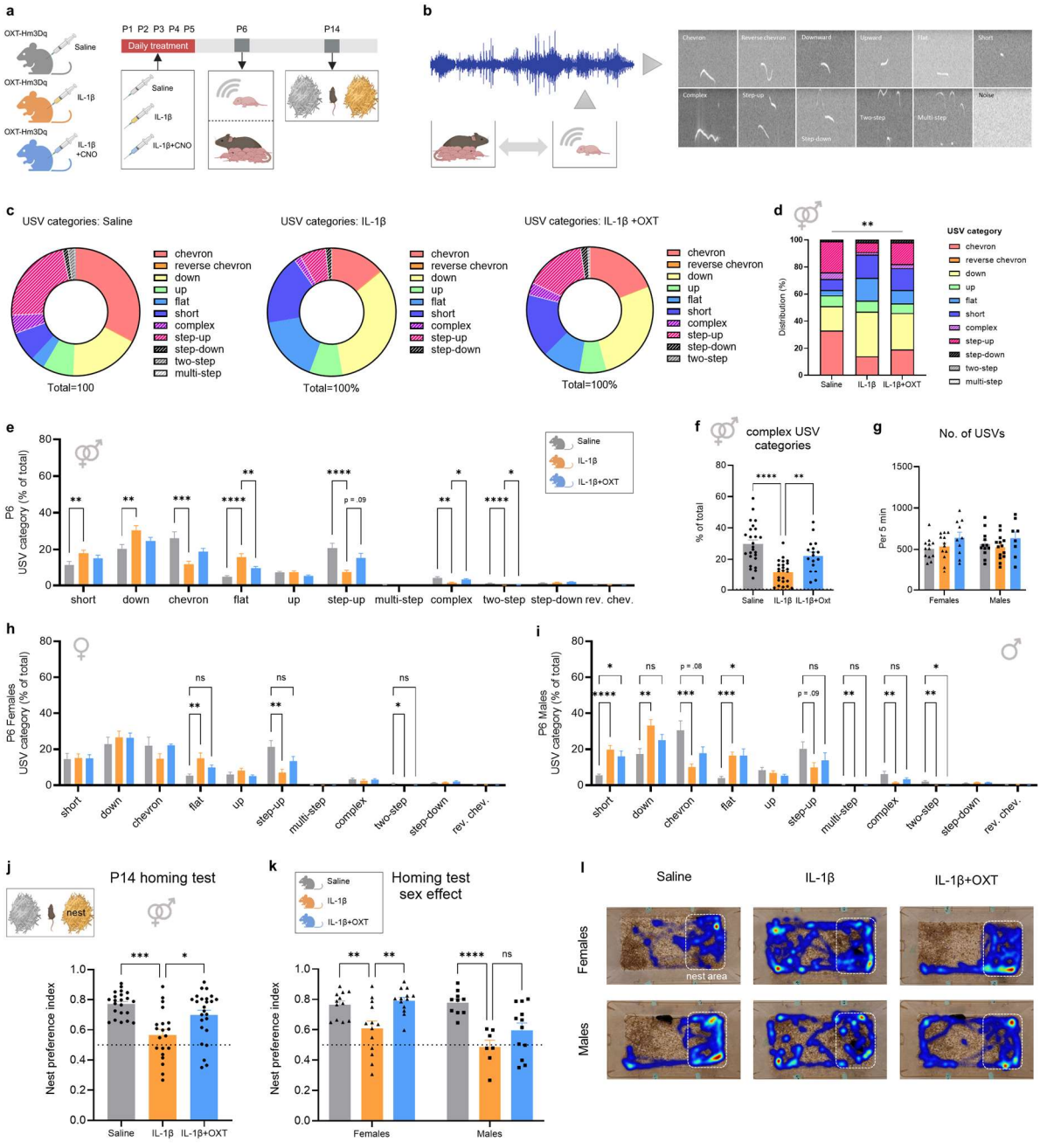

Fig. 4: Oxytocin rescues early-life sociability deficits induced by systemic inflammation. a) OXT-Hm3Dq DREADD pups received daily injections between P1 and P5, the compound depending on treatment group: Saline (gray), IL-1β (orange) or IL-1β mixed with OXT-increasing CNO (blue; "IL-1β+OXT" group). Graphical timeline showing the socio-behavioral test battery including P6 isolation-

induced ultrasound vocalization (USV) analysis and P14 homing test assessment. **b)** Graphical representation of the automatic classification of single USVs from pup sound recordings into 11 categories using VocalMat (Fonseca et al., 2021). **c)** Pie chart showing average USV category proportions for saline (left), IL-1β (middle) and IL-1β+OXT (right) groups. Complex USV categories (*complex, step-up, step-down, two-step, multi-step*) are highlighted with a striped fill pattern. **d)** Bar graph showing distinct average USV category distribution between experimental groups (p = .002). **e)** Quantification of the proportion of USV categories between experimental groups. **f)** Quantification of proportion complex USVs emitted between experimental groups showed decrease in IL-1β pups (vs. Saline: $p < .0001$) and a rescue after OXT treatment (vs. IL-1β: p = .007). **g)** Vocalization degree (number of USVs in 5 minutes) was not different between experimental groups or sexes. **h,i)** The proportion of USV categories per treatment group, separated for females **(h)** and males **(i)**. **j)** Graphical representation of homing test, and quantification of nest preference index per treatment group, showing a decrease in IL-1β (vs. Saline: p = .0002), and a reversal after OXT treatment (vs. IL-1β: p = .019) **k)** Nest preference index showed an interaction between sex and treatment (p = .024). **l)** Representative images showing homing test behavior between treatment groups and sex. For visualization purposes, all nest areas are positioned on the right outer zone of the testing arena (white box). OXT = oxytocin; IL-1β = interleukin-1 beta; CNO = clozapine-n-oxide. Statistical differences were assessed with One-way ANOVA with Tukey's post-hoc for normally distributed data, and with Kruskal-Wallis test with Dunn's post-hoc for non-normally distributed data. In **(d)** USV distribution was assessed between groups with a chi-square test. *$p < .05$, **$p < .01$, ***$p < .0005$, ****$p < .0001$. *In* **(c-i)** Saline: n = 25 (13 females), IL-1β: n = 25 (12 females), IL-1β+OXT: n = 18 (10 females). In **(j,k)** Saline: n = 22 (12 females), IL-1β: n = 20 (13 females), IL-1β+OXT: n = 25 (13 females). Bar graphs represent Mean ± SEM. Each data point corresponds to one animal. In **(b)**, sound wave image acquired with license from Creative Commons Attribution-NonCommercial 4.0 International (adapted).

2.5 Neonatal oxytocin prevents long-term brain microstructural damage induced by systemic inflammation

Next, we assessed brain tissue microstructure at P28 with ex-vivo MRI-DTI (Fig 5a). Microstructural features of white and gray matter regions were assessed with the NODDI (neurite orientation dispersion and density imaging) pipeline[26] (Fig 5b). IL-1β-treated mice showed an increase in

orientation dispersion index (ODI) compared to saline-treated mice in the external capsule (p = .028) (Fig 5c), and the region between CC and external capsule (p = .004) (Fig 5d), reflecting reduced local coherence of axon orientation. Oxytocin treatment restored the ODI in the external capsule to saline-equivalent levels (difference with IL-1β: p = .036). A similar trend was found in the region between the corpus callosum and external capsule (difference with IL-1β: p = .07), demonstrating similar axon coherence for saline mice and mice exposed to IL-1β and oxytocin (Fig 5b,c).

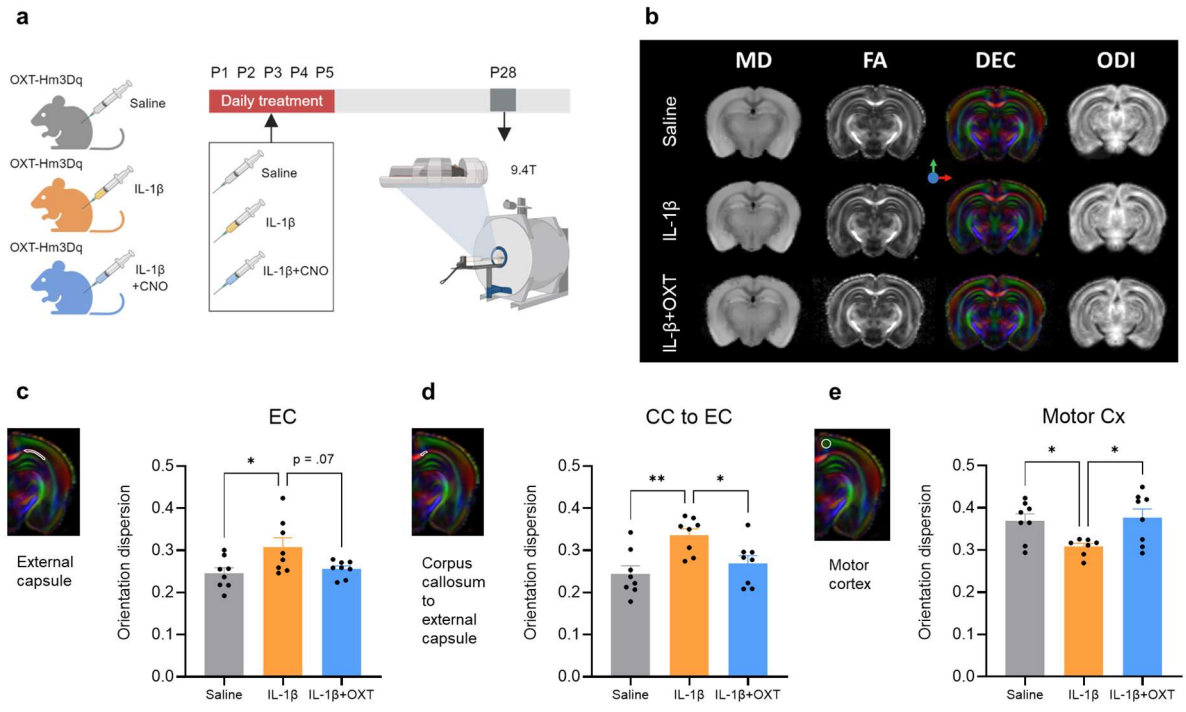

Fig. 5: Oxytocin reverses long-term white and gray matter microstructure deficiencies induced by systemic inflammation. **a)** graphical timeline showing P28 ex-vivo MRI assessment with a 9.4 Tesla scanner, after P1-P5 injections with Saline (gray), IL-1β (orange) or IL-1β mixed with OXT-increasing CNO (blue; "IL-1β+OXT" group) compounds in OXT-Hm3Dq DREADD pups. **b)** Representative MRI sections of Saline (top), IL-1β (middle) and IL-1β+OXT mice (bottom) showing MD, FA, DEC, and ODI signals in the ROIs. The DEC signal is color-coded by the direction of the first eigenvector (ε1), reflecting the anterior-posterior axis (green); the left-right axis (red), and inferior-superior axis (blue). **c-e)** Orientation dispersion index (ODI) as a measure of neurite coherence of EC **(c)**, CC to EC **(d)** and motor cortex **(e)** ROIs, showing increased dispersion in IL-1β mice versus saline mice for the EC (p = .028) and

CC to EC (p = .004) ROIs, and decreased dispersion in the motor cortex. OXT treatment reverses this alteration in IL-1β mice (EC: p = .036; CC to EC: p = .07; motor cortex: p = .027), to saline-equivalent levels. IL-1β = interleukin-1 beta; OXT = oxytocin; CNO = clozapine-n-oxide; EC = external capsule; CC = corpus callosum; MD = medial diffusivity; FA = fractional anisotropy; DEC = direction encoded color. Statistical differences were assessed with One-way ANOVA with Tukey's post-hoc. *p < .05, **p < .01. Saline: n = 8 (4 females), IL-1β: n = 8 (5 females), IL-1β+OXT: n = 8 (5 females). Bar graphs represent Mean ± SEM. Each data point corresponds to one animal.

Saline mice demonstrated typical incoherent neurite orientation in the motor cortex, with higher cortical ODI levels (mean = 0.37) than the EC (mean = 0.25) and CC to EC (mean = 0.24) white matter regions (reflecting the more widespread *cortical* network of axons and dendrites in control animals[27]). IL-1β exposure caused a significant reduction of ODI in the motor cortex (p = .048) (Fig 5e). This was rescued by oxytocin treatment (p = .027), with IL-1β+OXT mice demonstrating saline-like gray matter neurite orientation in the motor cortex (Fig 5e). No other effects on brain microstructure were found. While, no interaction between sex and treatment group was found, females showed a slightly higher overall axon dispersion in white matter regions compared to males (Supplementary Fig S6).

3. Discussion

In this study, we show that chemogenetic activation of oxytocinergic neurons is protective against the neural correlates of EoP in mice. The IL-1β model of EoP is based on systemic inflammation mimicking frequent events associated with delivery in preterm human infants, as well as postnatal complications, including early and late-onset sepsis [3,11]. Here, we replicated for the first time in C57BL/6 mice most of the EoP features previously reported in OF1 mice[6,28–30] including a pro-inflammatory reaction in P3 microglia, deficits in microstructural brain development, and impaired long-term social and cognitive behavior. Increased oxytocin release dampened early neuroinflammatory microglia reactivity, improved long-term white and gray matter microstructure, and rescued sociability deficits following IL-1β systemic injection. This neuroprotective effect of endogenous oxytocin sex-dependent, showing enhanced reduction of microgliosis and improved rescue of social behavior in females than in males.

Increased oxytocin release via chemogenetic stimulation reduced inflammation and immune gene expression in reactive microglia induced by systemic inflammation. These anti-inflammatory functions

of oxytocin are in line but dramatically extent knowledge from existing studies[7,12,31]. Here, we provide novel insights regarding the effect of endogenous oxytocin release without any pharmacological intervention. Microglia are actively involved in the maturation and growth of the developing brain[32] and restoration of their homeostatic functions logically improves neural outcomes. Indeed, oxytocin release rescued the impairments to neurite organization in corpus callosum regions in IL-1β-exposed mice. This suggests that oligodendrocytes are a key target of oxytocin effect on white matter structure. Our P1-P5 treatment window overlaps with a period when immature oligodendrocytes peak in proliferation in mice[5,33]. Developing oligodendrocytes express a high amount of cytokine receptors, making them particularly sensitive to inflammatory cytokines circulating in the brain[34,35]. In EoP, the pro-inflammatory cytokines and free radicals cause blockade in oligodendrocyte maturation, resulting in myelination impairments long-term[5,36]. Oxytocin release reduced microglia pro-inflammatory gene pathways, and promoted a shift to an anti-inflammatory phenotype. This shift was associated with improved oligodendrocyte development in vitro[37], and an in-vivo[38]. Moreover, oxytocin restored typical Wnt signaling in microglia after IL-1β exposure. This pathway is key in oligodendrocyte maturation and in human preterm infants, where genetic variation in Wnt pathway genes predicts white matter structural integrity[6]. White matter damage and immaturity account for a major part of the symptomology of EoP, and predict long-term socio-cognitive functioning[39]. Hence, our data support neuroprotective effects of oxytocin on long-term white matter microstructure after systemic inflammation, plausibly associated with improved oligodendrocyte development through the modulation of microglial functions. This change in oligodendrocyte trajectory would explain how the short neonatal treatment window was sufficient to exert effects that are sustained long after the treatment is discontinued.

EoP is characterized by an increased risk of behavioral problems, including impaired social communication at 2 years old[39]. Here, we assessed early-life sociability with exploration of isolation-induced ultrasound vocalization (USV) profiling. Automated classification algorithms have revealed developmental patterns of mouse USVs, where USVs become increasingly more complex with age[40].

This makes mouse USVs not only reflect sociability but also provide a window into development. Previous work demonstrated that the EoP model induced by systemic IL-1β alters the mean frequency of USVs in P2 pups[41]. The current work extends this by reporting a substantial change in USV category profile for the EoP model, with IL-1β exposed pups emitting increased proportions of basic USV categories at the expense of complex USV categories. Complex USVs represent a developmental tool for pups to distinguish themselves from their littermate's calls, in order to induce enhanced maternal care[40,42]. The lower use of complex USVs in IL-1β pups is suggested to reflect delayed social development[40], and has been similarly described for other perinatal injury models[43]. This profile was not associated with a change in degree of vocalization, which implies that the decrease in complex USVs is not a consequence of 'lack of practice', but rather due to innate changes caused by inflammation itself. Neonatal oxytocin release restored the vocalization profile in IL-1β exposed pups, with its biggest effects on increasing the proportion of complex USVs emitted (*step-up*, *complex*, *two-step* USVs). A preclinical study modeling autism in mice likewise found mostly effects on complex USVs after acute oxytocin administration at P11[44]. The emphasis on complex USVs suggests that oxytocin reverses the developmental delay in social communication in IL-1β mouse pups[40]. The restoration of vocalization behavior by oxytocin could be associated with improved activity of associated brain regions like amygdala, hypothalamus and hippocampus, which are regions highly enriched for oxytocin receptors (Mouse Protein Atlas[45]; proteinatlas.org), and identified as key regulating regions for isolation-induced USV with whole-brain mapping[46]. Moreover, restoration of typical vocalization induced by oxytocin release could also constitute improved social development through restored maternal attachment. This is supported by a study where intranasal oxytocin administration to autism-model pups rescued typical pup-retrieval behavior by dams[47].

Sexual dimorphism is a notable variable in (pre)clinical research[48,49]. The majority of preclinical studies of EoP focus on males[5,6,29], as boys have poorer outcomes after most types of perinatal brain injury[11,50]. To accommodate the increasing ethical need for more inclusive research, however, this study included both sexes and emphasized sex-specific analysis of EoP and oxytocin treatment. Sex is thought to alter

the injury response in models of EoP, driven by distinct responses of early-life microglia to inflammation[50]. Our study describes a moderate sex effect regarding the consequences of systemic inflammation, where males were more severely affected than females, as expected[50]. However, this sex effect was mostly restricted to the behavioral outcomes of EoP. In contrast, the sex effects of IL-1β exposure on microglial transcriptome were limited to subtle differences relating to specific microglial signaling pathways (Wnt pathway in males, and JNK pathway in females). The premise that males and females have different microglial responses to inflammatory challenges is based largely on transcriptomic studies[51,52]. However, Hanamsagar and colleagues[51] report a "developmental delay" of male microglia versus female microglia, which was found at P60 only, while no transcriptomic differences were found for E18, P4 and P14 microglia[51]. Similarly, Hammond and colleagues[52] report 'virtually no differences' between male and female microglia, assessed at E14.5 and P4/5 with single-cell transcriptomics. The sex-specific effects in microgliosis after inflammation could rather be due to differences in cell proliferation and morphology, with males showing more microglia than females early in development (around P4), depending on brain region[53,54]. Hence, more research is needed to elucidate this paradigm. Our data also evidence a robust sex-specific response to neonatal oxytocin release, where females showed more prominent anti-inflammatory and neuroprotective benefits. This is potentially associated with sex differences in the early-life oxytocin system in mice. First, females express Oxt mRNA earlier in development – at E16.5 versus P2 for males[16]. Second, the amount of Oxt and Oxt receptor mRNA expressed just before birth and in the first postnatal days is higher in females than males[16]. These differences underlie the sex-specific developmental trajectory of the young brain, and mimic the differences in adult oxytocin systems where females show higher oxytocin activity, including more oxytocin neurons, immuno-reactive axons and peptide expression[55–57] – although contradicting reports also exist[58,59]. Differences in innate oxytocin signaling could underly the different therapeutic profile of oxytocin release we found in females and males – a notion that is supported by clinical trials in autism spectrum disorder, where treatment efficacy is associated with inter-personal variance in oxytocin receptor expression[60]. These sex-specific effects are important to consider in

further assessment of neonatal EoP, and limiting preclinical studies to male mice is likely to overlook therapeutic mechanisms in females[48].

Early interventions in neonatal care units– such as Kangaroo mother care or developmental care – are well established, and show positive effects on brain development that lasts through adulthood[61]. While some preliminary evidence suggested oxytocin as a putative biological mediator, the characteristics of the underlying mechanism of these interventions have long remained elusive. Here, we link the biological release of oxytocin to improved brain development after neuroinflammation associated with preterm birth via the modulation of microglia phenotypes. Neonatal oxytocin treatment demonstrated long-lasting effects on the developing brain, and thus suggests a re-shaping of brain circuitry – as oxytocin did in a mouse model of autism[62]. A previous report demonstrated anti-inflammatory effects of oxytocin agonist on microglia in a model of IUGR, a pharmacological strategy not applicable for clinical translation. Methodological properties of current study could benefit from more translational potential as DREADD technology mimics natural elevation in humans. Also, they underline for the first-time sex differences in the effect of oxytocin on EoP associated with systemic inflammation. Oxytocin-elevating therapy in the clinic is regarded as general improving for child development, but with unclear biological rationale. We show that oxytocin release has a similar general positive effect on brain development by increasing expression of gene pathways in microglia that were involved in many aspects of brain development (axons, synapse, neurons, genesis, migration, differentiation). So even in a non-inflammatory milieu, microglia could be the connecting factor in the general improving effects of oxytocin on child development.

In conclusion, this study shows that increased endogenous oxytocin release is a promising protectant for the neural correlates of EoP. Oxytocin reduces the reactive pro-inflammatory phenotype of microglial cells, and restores typical development of brain microstructure and social behavior. As such, this study describes a biological basis for the clinical association between oxytocin-increasing

interventions and improved brain development, and it strengthens oxytocinergic activity as a potent non-pharmacological therapeutic strategy for preterm neonates.

4. Materials and methods

1 Animals and breeding strategy

Cre-dependent Hm3Dq-DREADD (Designer Receptors Exclusively Activated by Designer Drugs) mice (B6N;129-Tg(CAG-CHRM3*,-mCitrine)1Ute/J[19], Jackson stock #026220) were crossed with Oxytocin-Ires-Cre mice (B6;129S-Oxttm1.1(cre)Dolsn/J, Jackson stock #024234) to create Oxt-Hm3Dq mice (B6;129S-Oxt-Cre;R26-LSL-hM3Dq-DREADD), which express the excitatory Hm3Dq-DREADD under the oxytocin promotor gene. This genetic profile enables temporally increased neuronal firing of endogenous oxytocin neurons upon administration of clozapine-N oxide solution (Enzo Life, BML-NS-105-0025).

Pups were genotyped at P9 from toe clipping using specific primers by classical PCR as described (Zhu et al, 2017 August 01; Wu Z et al, 2012 September 18). In accordance with the breeding considerations of the Jackson laboratory, double homozygous males (Hm3Dq ki/ki Oxt-Cre ki/ki) were mated with homozygous females for Hm3Dq and heterozygous for the oxytocin-Cre transgene (Hm3Dq ki/ki; Oxt-Cre +/ki). Oxt-Hm3Dq animals were then intercrossed in order to produce both batches for breeder renewal and experimental cohorts. Every experimental litter was subjected to 2 different treatment groups. Each experimented included at least 5 different litters. Male and female pups were included in this study.

In the SOPF area, mice were housed in IVC-filtered top cages, with animal density depending on cage size, in accordance with Swiss regulations (Type II L cages, Allentown). Room temperature and hygrometry were maintained between 20-24°C and between 30% and 70% respectively. The light cycle in the room was programmed on a 12/12h day/night basis. Animals received *ad libitum* extruded

irradiated diets (ref. 150, SAFE) and 0.22 µ filtered and chlorinated tap water. Cage enrichment consisted of autoclaved bedding (Aspen Tapvei), nest and mouse house. Daily inspection of animals, husbandry conditions, functioning of the apparatus and cleaning of cages was ensured by the animal caretakers. Protocols for the use of animals have been approved by the Ethical Committee for Animal Experiments of the University of Geneva and the Veterinary Office of Geneva. The animal facility of the UNIGE Faculty of Medicine is approved by the General Direction on Health of Geneva and meets all the requirements defined by Swiss regulations and laws.

2 Pharmacological treatments

Pregnant dams were monitored two times per day to determine the exact day of delivery (P0). Newborn pups were injected intraperitoneally with either saline, Il1beta or Il1beta + CNO solution from P1 to P3 or P5 – depending on experiments – twice daily at 8 am and 4 pm (+/- 30 min). During the injection phase, pups were weighed daily to adjust the injection volume. To avoid irritation, pups were injected on both sides of the abdomen, usually the right side in the morning and the contralateral side in the afternoon using a Hamilton syringe of 50 µl (Hamilton #80501). When all the pups from a litter had been injected, they were gently soaked in the bedding from their home cage, and placed in the nest next to the mother. All pups were injected by the same experienced researcher to ensure consistency.

2.1 Encephalopathy of Prematurity injury induced by IL-1β injections

The EoP model of systemic IL-1β injections was induced between P1-P5, corresponding to 23-36 weeks of gestation in humans that defines preterm age[63]. We adapted an existing model in different mouse strain[5,6,64] to our C57BL/6 strain. IL-1β (15 µg/ml) was injected intraperitoneally (i.p.) at weight-adjusted volume. Pups were injected with IL-1β twice daily. Pups from control group were injected with NaCl (0.9%).

2.2 Oxytocinergic neuron activity induced by CNO injections

Mice of the IL-1β+oxytocin treatment group received Clozapine-N oxide (CNO) injections to activate the excitatory DREADDs on oxytocin neurons, which causes a temporary increase in endogenous neuronal oxytocin firing (as previously validated by our group[20]). CNO was injected i.p. at a concentration of 10mg/kg at weight-adjusted volume. CNO substance was co-injected with IL-1β to reduce the number of injections to the pups. Pups from the IL-1β+OXT treatment group received CNO+IL-1β injections in the morning, and only Il-1β in the afternoon (based on previous work showing adequate oxytocin functionality with one-daily oxytocin activation[7]). Pups from untreated IL-1β group were injected twice daily with IL-1β.

This study had 3 experimental groups: NaCl injected mice ("Saline mice"), IL-1β injected mice ("IL-1β mice"), and IL-1β-injected mice, co-injected with oxytocin-increasing CNO substance ("IL-1β+OXT mice").

3 P3 Microglia immunohistology

P3 animals were anesthetized with i.p. injections of pentobarbital (150 mg/kg), confirmed by the loss of the toe-pinch reflex, and perfused with PBS and 4% paraformaldehyde (PFA) in PBS1x. Brains were post-fixated overnight in 4% PFA, and embedded in 15% sucrose (morning) and 30% sucrose (afternoon) solution the following day. Brains were snap-frozen in isopentane at -45°C and stored at -20°C until cutting. Brains were cut with a cryostat into free-floating coronal sections of 50 µm and stored in PBS+0.3%Azide solution.

3.1 Immunofluorescence

Free-floating brain sections were blocked with 0.2%TritonX + 10% normal goat serum in PBS1x for 1 hour. After a 5 min wash in PBS1x, sections were incubated overnight with rabbit anti-Iba1 (1:1000; Fujifilm Wako 019-19741) in 3% normal goat serum+PBS1x at 4°C. Following a 3x10 min wash in PBS1x, sections were incubated with goat anti rabbit 594 (1:500, Abcam ab150080) in 0.2%TritonX+10% normal goat serum in PBS1x for 1 hour 30 minutes. After a final wash in PBS1x, sections were mounted

and coverslipped on microscopy slides (ThermoFisher) with flouromount medium that includes DAPI (Abcam ab104139). Slides were stored at 4°C.

3.2 Image acquisition and analysis

Brain sections were imaged with a ZEISS Axioscan.Z1 (Zeiss, Oberkochen, Germany) at 10x. Image analysis was performed with ImageJ/FIJI. Microglia density was quantified as Iba1 immunofluorescence signal density from cortex and corpus callosum ROIs. Signal was corrected for background fluorescence per ROI, per sample. 2 micrographs were averaged per sample – 1 at bregma level lateral ventricles (Allen brain atlas slide 50-55), 1 at level of hippocampus (Allen brain atlas slide 70-75). Signal density was normalized on Saline group, and reported as Iba1 signal intensity % of Saline.

4 P3 Microglia RNA sequencing.

4.1 MACS sorting of Cd11b microglia

Microglia were isolated from P3 pup brains with MACS® magnetic cell sorting technology (Miltenyi Biotech) as described previously[65]. In brief, P3 pups were anesthetized using i.p. pentobarbital (150 mg/kg) and transcardially perfused with PBS1x to remove macrophages. Brains were dissected, the olfactory bulb and cerebellum removed, and the remaining cerebrum was selected for tissue dissociation using the MACS® neural dissociation kit (Miltenyi Biotech). Microglia cells were isolated from brain homogenates via incubation with magnetic anti-mouse CD11b microbeads (Miltenyi Biotech). Isolated microglia were collected using the MultiMACS® cell separator apparatus (Miltenyi Biotech) and stored at -80°C.

4.2 P3 microglia real-time qPCR

For validation of the IL-1β model, RNA was extracted from P3 MACS-sorted microglia using the Nucleospin RNA Plus XS extraction kit (Macherey-Nagel). RNA quantity was measured with Nanodrop 2000 and was normalized across samples. RNA was subjected to reverse transcriptase using the MLV-RT kit (Promega; M1701). Real-time quantitative transcription polymerase chain reaction (RT-qPCR)

was performed in duplicates with PowerUp™ SYBR™ Green Master Mix (ThermoFischer) for 40 cycles with a 2-step program (15 sec of denaturation at 95°C and 1 min of annealing/extension at 60°C). mRNA amplification values were normalized on Rps18 housekeeping gene and calculated as mRNA fold change measures normalized on the Saline group following the ΔΔCt analysis method. Gene expression of a selection of pro-inflammatory, anti-inflammatory and immune-regulatory cytokines was assessed, based on previous findings[6]. Primers were designed with Primer-BLAST[66]. Primer sequences are given in Supplementary Table S1.

4.3 P3 Microglia bulk RNA sequencing

Microglia RNA sequencing was performed at the iGE3 Genomics Platform of the University of Geneva (https://ige3.genomics.unige.ch). RNA was extracted from P3 sorted microglia using the Nucleospin RNA Plus XS extraction kit (Macherey-Nagel). RNA quantification was performed with a Qubit fluorometer (ThermoFisher Scientific) and RNA integrity assessed with a Bioanalyzer (Agilent Technologies). The microglial RNA was sequenced in bulk in two batches, with Illumina HiSeq 4000 and Illumina NovaSeq 6000 next-generation sequencer. The batches had equal distribution of sex and experimental group, and batch effect was corrected for in downstream analysis. Quality control was performed with FastQC (v.0.1.1.9), and the reads were mapped to the reference mouse genome (Ensembl/GRCm39) using STAR aligner (v.2.7.10b).

MACS cell sorting purity was assessed with Expression Weighted Celltype Enrichment analysis[67] for all major neural cell types, based on log normalized expression of top 250 expressed genes in the control group. The analysis was run with default parameters, with the number of repetitions for bootstrap enrichment set to 10.000. Statistical significance was set at $p < .05$.

Differential gene expression (DEG) analysis was performed with edgeR (v.3.42.4). Lowly expressed genes (< 10 raw counts) were filtered out, and gene expression was normalized according to the library size and RNA composition. Differentially expressed genes were estimated using a quasi-likelihood (QL) F-test with rigorous type I error rate control. Corrections for multiple testing were performed with

False Discovery Rate (FDR) and the Benjamini & Hochberg correction (BH). Significant genes were filtered on cut-off values of ≥ 1.5 fold-change and $p < .05$. DEG analysis was performed for the comparisons IL-1β versus Saline, and IL-1β+OXT versus IL-1β, for sexes combined and females and males separately. Unidentified DEGs were excluded from the results.

Gene set enrichment analysis on differentially expressed genes was performed using DAVID Functional Annotation Tool (DAVID Knowledgebase v2024q1, National Institutes of Health). For the IL-1β vs. saline sex effect assessment, additional GSEA was performed on the unique DEGs for females and males, respectively, which were identified by cross-referencing the DEGs from sex-matched analysis (IL-1β males *vs*. saline males, and IL-1β females *vs.* saline females), and removing the shared genes. For all GSEA analyses, the upregulated DEGs were analyzed separately from the downregulated DEGs. Databases of biological processes and KEGG pathways were investigated. Pathways with an FDR value of < .05 were considered.

5 ex-vivo MRI

At P28, mice were were anesthetized with i.p. injections of pentobarbital (150 mg/kg), confirmed with the toe-pinch reflex, and transcardially perfused with PBS and 4% paraformaldehyde (PFA) in PBS1x. Brains were kept in PFA overnight, then changed and kept in PBS1x for 6 weeks until scanning.

MR experiments were performed on an actively-shielded 9.4T/31cm magnet (Agilent) equipped with 12-cm gradient coils (400mT/m, 120µs) with a 2.5 mm diameter birdcage coil. A multi-b-value shell protocol was acquired based on a spin-echo sequence with a matrix size of 64×64 on a FOV of 10×14 mm^2. 12 slices of 0.6 mm thickness were acquired contiguously in the axial plane with TE/TR = 42/2000 ms and 5 averages. 96 diffusion weighted images were acquired, 15 of them as b_0 reference images and 81 separated in 3 shells (δ/Δ=5.5/30 ms) with the following distribution (non-collinear and uniformly distributed in each shell): 21 directions with a b-value of 1750 s/mm^2, 30 directions with a b-value of 3400 s/mm^2 and 30 directions with a b-value of 5100 s/mm^2. The total acquisition time was 15h per brain. Acquired data were fitted using DTI-TK for DTI and the NODDI toolbox[26] for NODDI. As

brains were scanned ex-vivo, a supplementary compartment to model stationary water (i.e. without diffusion) trapped in the structures following death and fixation was added to the conventional NODDI model (isotropic restricted water compartment). The diffusion tensor (DT) was spatially normalized to the study-specific DT template using DTI-TK[68]. The regions of interest (ROI) were manually delineated on direction encoded color maps and mean values of DTI derived parameters (Mean, Axial and Radial Diffusivities (MD, AD and RD) as well as Fractional Anisotropy (FA)) and NODDI estimates (intra-neurite volume fraction (fin), isotropic volume fraction (fiso) as well as Orientation Dispersion Index (ODI)) were calculated and averaged on the 6 following regions assessed: motor cortex (MCx) and somatosensory cortex (SCx) for grey matter; corpus callosum (CC), external capsule (EC) and the region between the CC and EC (CC to EC) for white matter.

6 Behavioral assessments

6.1 P6 Ultrasound vocalization

At P6, ultrasound vocalizations (USVs) were recorded from isolated pups as a readout of early-life sociability and vocal development[40]. Individual pups were fetched from the home-cage and placed in a holding cage with clean bedding, 10 cm under an ultrasonic microphone (Ultramic384; Dodotronic UM384BLE). Vocalizations from isolated pups were recorded for 5 minutes, after which the pup was put in a holding cage containing home-cage bedding and one of the dams. USVs were recorded using Audacity® software (version 3.4.2.) and sampled with a rate of 2000000 Hz. Sound files were analyzed with VocalMat[23], which automatically detects and categorizes each USV into one of 11 different USV classes. Readouts included number of USVs and the distribution of different USV categories vocalized.

6.2 P14 Homing test

At P14, pups were subjected to the homing test, to assess early-life sociability based on maternal scent recognition. The test was performed as previously described[20]. Briefly, a 32x16 cm cage was divided into 2 outer zones of 12 cm. The middle zone (8 cm) contained fresh bedding, one zone on the far side contained bedding from the pup's home-cage nest, and the other far-side zone contained bedding

from an unfamiliar nest with pups. A pup was allowed free exploration for 3 minutes. Readouts were time spent in the home-cage versus unfamiliar bedding area, converted to a preference index for the home-cage area. Cage orientation was changed between trials and bedding from all 3 zones was refreshed between every trial to equalize odor strength between samples.

6.3 P56 Three-chamber test

For validation of the IL-1β model, saline and IL-1β injected pups were subjected as P45 adults to the 3-chamber test of sociability. The test was conducted as described previously[20]. In brief, after a 10-minute habituation phase, mice were allowed free exploration for 5 minutes in an arena with 3 connecting chambers, where one outer chamber included an empty mesh-bar enclosure, and the other outer chamber included an enclosure containing a one-week younger unfamiliar mouse. Data was analyzed as time spent in proximity of 2 cm from both enclosures (nose tracking), and converted into a preference index score for the social stimulus (mouse enclosure) versus the object (empty enclosure).

6.4 P90 Barnes maze

For validation of the IL-1β model, saline and IL-1β injected pups were subjected at P90 to the Barnes maze test of spatial learning and cognitive flexibility. The protocol was adapted from Gawel et al 2019[18] and Van Steenwinckel et al 2019[6]. Briefly, a circular arena of 91.5 cm diameter containing 20 holes was placed 90 cm above the ground, with 1 hole containing an escape box underneath (“target hole”). Four symbols of similar size (circle, square, triangle and cross) were printed black on white paper and hung at the four walls surrounding the arena, at the same distance and height, to act as extra-maze spatial cues[18].

Four days of acquisition were held. Day 1 was commenced with a shaping trial, where the mouse was gently guided towards the target hole and allowed to stay inside for 2 minutes. Then, the acquisition trials started, where 3 minutes of free exploration was allowed. If the mouse did not find the target hole on time, it was guided to the target hole and allowed to stay for 1 minute. Acquisition days consisted of 4 trials per day, with 15 minutes inter-trial-interval. Between trials, mice were kept in a

holding cage with fresh bedding. On day 5, a probe trial was held where the escape box was removed and the mouse was allowed free exploration for 90 seconds. On day 15, this probe trial was repeated, to now test long-term spatial memory.

In the reversal learning phase, the position of the escape box was moved 180° from its previous location. Reversal acquisition days consisted of 3 days with 4 trials of maximum 3 minutes per trial. On reversal acquisition day 4, a reversal probe trial was held where the escape box was removed and the mouse was allowed free exploration for 90 seconds.

We analyzed latency to escape ("primary latency") and number of errors ("primary errors"; i.e., head pokes in non-target holes) for the acquisition trials, and time spent and distance traveled in the target area (defined as the target hole + 2 adjacent holes) for the probe trials. In addition, we assessed search strategy, which reflects if the animal actually uses spatial strategy to resolve the maze (reviewed in Gawel et al., 2019[18]). Three different search strategies were scored: 1) Direct search: animals move directly to the target hole or 1–2 adjacent hole(s) before visiting the target. 2) Serial search: animals visit serially the adjacent holes in a clockwise or counter clockwise manner. 3) Mixed search: animals searching the holes cross the maze through its center or investigate the holes in unorganized fashion Search strategy was manually scored by the same researcher for consistency, who was blinded to experimental conditions. Search strategy distribution per day was analyzed with chi-square test of contingency (two-tailed, alpha at .05).

7 Statistical analysis

Statistical analysis was performed with Graphpad/Prism version 10.4.0 for Windows (GraphPad Software, Boston, Massachusetts USA, www.graphpad.com). All data was checked for outliers with the ROUT method (Q = 0.1%), and tested for normality using Kolmogorov-Smirnov test ($\alpha = .05$). The *n* reported in each figure legend represents sample size after outlier removal. Sample size differentiation into females and males is reported for sex-specific analyses. Comparisons between 2 groups were performed with Student's t test (normal data distribution) or a Mann-Whitney U test (non-normal data

distribution). Analysis between all 3 experimental groups was performed with a One-way ANOVA test with Tukey's post-hoc (normal data distribution) or Kruskal-Wallis test with Dunn's post-hoc (non-normal data distribution). Body growth was measured with a repeated-measures ANOVA with Šídák's post-hoc test. Preference index from the 3-chamber test was assessed with a paired t test. The alpha was set at 0.05, and tested two-tailed. Unless specified otherwise, bar graphs show Mean + SEM values. Statistical trends were identified as *p* values between 0.05 and 0.10. Non-significant post-hoc comparisons are not shown in the graphs. Every data point represents an individual sample in the graphs.

5. References

1. Ohuma, E. O. *et al.* National, regional, and global estimates of preterm birth in 2020, with trends from 2010: a systematic analysis. *Lancet* **402**, 1261–1271 (2023).
2. Volpe, J. J. Brain injury in premature infants: a complex amalgam of destructive and developmental disturbances. *Lancet Neurol* **8**, 110–124 (2009).
3. Gressens, P. Chapter 17 - Inflammation and the Newborn Brain. in *Volpe's Neurology of the Newborn (Seventh Edition)* (ed. Volpe, J. J.) 494-505.e4 (Elsevier, St. Louis (MO), 2025). doi:10.1016/B978-0-443-10513-5.00017-6.
4. Buser, J. R. *et al.* Arrested preoligodendrocyte maturation contributes to myelination failure in premature infants. *Annals of Neurology* **71**, 93–109 (2012).
5. Favrais, G. *et al.* Systemic inflammation disrupts the developmental program of white matter. *Ann Neurol* **70**, 550–565 (2011).
6. Van Steenwinckel, J. *et al.* Decreased microglial Wnt/β-catenin signalling drives microglial pro-inflammatory activation in the developing brain. *Brain* **142**, 3806–3833 (2019).
7. Mairesse, J. *et al.* Oxytocin receptor agonist reduces perinatal brain damage by targeting microglia. *Glia* **67**, 345–359 (2019).

8. Zhang, W. *et al.* Microglia-associated neuroinflammation is a potential therapeutic target for ischemic stroke. *Neural Regen Res* **16**, 6–11 (2020).
9. Cikla, U. *et al.* Suppression of microglia activation after hypoxia-ischemia results in age-dependent improvements in neurologic injury. *J Neuroimmunol* **291**, 18–27 (2016).
10. Izzy, S. *et al.* Nasal anti-CD3 monoclonal antibody ameliorates traumatic brain injury, enhances microglial phagocytosis and reduces neuroinflammation via IL-10-dependent Treg–microglia crosstalk. *Nat Neurosci* **28**, 499–516 (2025).
11. Van Steenwinckel, J. *et al.* Key roles of glial cells in the encephalopathy of prematurity. *Glia* **72**, 475–503 (2024).
12. Knoop, M. *et al.* The Role of Oxytocin in Abnormal Brain Development: Effect on Glial Cells and Neuroinflammation. *Cells* **11**, 3899 (2022).
13. Pavlyshyn, H., Sarapuk, I., Horishna, I., Slyva, V. & Skubenko, N. Skin-to-skin contact to support preterm infants and reduce NICU-related stress. *Int J Dev Neurosci* **82**, 639–645 (2022).
14. Wang, Y., Zhao, T., Zhang, Y., Li, S. & Cong, X. Positive Effects of Kangaroo Mother Care on Long-Term Breastfeeding Rates, Growth, and Neurodevelopment in Preterm Infants. *Breastfeed Med* **16**, 282–291 (2021).
15. Yue, W., Han, X., Luo, J., Zeng, Z. & Yang, M. Effect of music therapy on preterm infants in neonatal intensive care unit: Systematic review and meta-analysis of randomized controlled trials. *J Adv Nurs* **77**, 635–652 (2021).
16. Tamborski, S., Mintz, E. M. & Caldwell, H. K. Sex Differences in the Embryonic Development of the Central Oxytocin System in Mice. *Journal of Neuroendocrinology* **28**, (2016).
17. Rosenkrantz, T. S., Hussain, Z. & Fitch, R. H. Sex Differences in Brain Injury and Repair in Newborn Infants: Clinical Evidence and Biological Mechanisms. *Front Pediatr* **7**, 211 (2019).
18. Gawel, K., Gibula, E., Marszalek-Grabska, M., Filarowska, J. & Kotlinska, J. H. Assessment of spatial learning and memory in the Barnes maze task in rodents-methodological consideration. *Naunyn Schmiedebergs Arch Pharmacol* **392**, 1–18 (2019).

19. Zhu, H. *et al.* Cre dependent DREADD (Designer Receptors Exclusively Activated by Designer Drugs) mice. *Genesis (New York, N.Y. : 2000)* **54**, 439 (2016).

20. Knoop, M. *et al.* Oxytocin release modulates acute neuroinflammation and improves brain development after pediatric traumatic brain injury. 2025.06.02.652172 Preprint at https://doi.org/10.1101/2025.06.02.652172 (2025).

21. van Tilborg, E. *et al.* Impaired oligodendrocyte maturation in preterm infants: Potential therapeutic targets. *Progress in Neurobiology* **136**, 28–49 (2016).

22. Fitzallen, G. C., Taylor, H. G. & Bora, S. What Do We Know About the Preterm Behavioral Phenotype? A Narrative Review. *Front. Psychiatry* **11**, (2020).

23. Fonseca, A. H., Santana, G. M., Bosque Ortiz, G. M., Bampi, S. & Dietrich, M. O. Analysis of ultrasonic vocalizations from mice using computer vision and machine learning. *eLife* **10**, e59161 (2021).

24. Scattoni, M. L., Puopolo, M., Calamandrei, G. & Ricceri, L. Basal forebrain cholinergic lesions in 7-day-old rats alter ultrasound vocalisations and homing behaviour. *Behavioural Brain Research* **161**, 169–172 (2005).

25. Tsuji, C., Fujisaku, T. & Tsuji, T. Oxytocin ameliorates maternal separation-induced ultrasonic vocalisation calls in mouse pups prenatally exposed to valproic acid. *J Neuroendocrinol* **32**, e12850 (2020).

26. Zhang, H., Schneider, T., Wheeler-Kingshott, C. A. & Alexander, D. C. NODDI: practical in vivo neurite orientation dispersion and density imaging of the human brain. *Neuroimage* **61**, 1000–1016 (2012).

27. Fukutomi, H. *et al.* Neurite imaging reveals microstructural variations in human cerebral cortical gray matter. *Neuroimage* **182**, 488–499 (2018).

28. Krishnan, M. L. *et al.* Integrative genomics of microglia implicates DLG4 (PSD95) in the white matter development of preterm infants. *Nat Commun* **8**, 428 (2017).

29. Dufour, A. *et al.* Neonatal inflammation impairs developmentally-associated microglia and promotes a highly reactive microglial subset. *Brain Behav Immun* **123**, 466–482 (2025).

30. Klein, L. *et al.* A unique cerebellar pattern of microglia activation in a mouse model of encephalopathy of prematurity. *Glia* **70**, 1699–1719 (2022).

31. Sünnetçi, E., Solmaz, V. & Erbaş, O. Chronic Oxytocin treatment has long lasting therapeutic potential in a rat model of neonatal hypercapnic-hypoxia injury, through enhanced GABAergic signaling and by reducing hippocampal gliosis with its anti-inflammatory feature. *Peptides* **135**, 170398 (2021).

32. Thion, M. S., Ginhoux, F. & Garel, S. Microglia and early brain development: An intimate journey. *Science* **362**, 185–189 (2018).

33. Salmaso, N., Jablonska, B., Scafidi, J., Vaccarino, F. M. & Gallo, V. Neurobiology of premature brain injury. *Nature neuroscience* **17**, 341–346 (2014).

34. Goldstein, E. Z., Church, J. S., Hesp, Z. C., Popovich, P. G. & McTigue, D. M. A silver lining of neuroinflammation: Beneficial effects on myelination. *Experimental Neurology* **283**, 550–559 (2016).

35. Vaes, J. E. G. *et al.* The impact of trophic and immunomodulatory factors on oligodendrocyte maturation: Potential treatments for encephalopathy of prematurity. *Glia* **69**, 1311–1340 (2021).

36. Rideau Batista Novais, A. *et al.* Transcriptomic regulations in oligodendroglial and microglial cells related to brain damage following fetal growth restriction. *Glia* **64**, 2306–2320 (2016).

37. Miron, V. E. *et al.* M2 microglia and macrophages drive oligodendrocyte differentiation during CNS remyelination. *Nat Neurosci* **16**, 1211–1218 (2013).

38. Chhor, V. *et al.* Characterization of phenotype markers and neuronotoxic potential of polarised primary microglia in vitro. *Brain Behav Immun* **32**, 70–85 (2013).

39. Dubner, S. E., Rose, J., Bruckert, L., Feldman, H. M. & Travis, K. E. Neonatal white matter tract microstructure and 2-year language outcomes after preterm birth. *Neuroimage Clin* **28**, 102446 (2020).

40. Grimsley, J. M. S., Monaghan, J. J. M. & Wenstrup, J. J. Development of Social Vocalizations in Mice. *PLOS ONE* **6**, e17460 (2011).

41. Morin, C. *et al.* C-section and systemic inflammation synergize to disrupt the neonatal gut microbiota and brain development in a model of prematurity. *Brain, Behavior, and Immunity* **123**, 824–837 (2025).

42. Smith, J. C. Responses of adult mice to models of infant calls. *Journal of Comparative and Physiological Psychology* **90**, 1105–1115 (1976).

43. Hermans, E. C., de Theije, C. G. M., Nijboer, C. H. & Achterberg, E. J. M. Ultrasonic vocalization emission is altered following neonatal hypoxic-ischemic brain injury in mice. *Behavioural Brain Research* **471**, 115113 (2024).

44. Tsuji, T. *et al.* Oxytocin administration modulates the *complex* type of ultrasonic vocalisation of mice pups prenatally exposed to valproic acid. *Neuroscience Letters* **758**, 135985 (2021).

45. Sjöstedt, E. *et al.* An atlas of the protein-coding genes in the human, pig, and mouse brain. *Science* **367**, eaay5947 (2020).

46. Mai, L., Inada, H. & Osumi, N. Whole-brain mapping of neuronal activity evoked by maternal separation in neonatal mice: An association with ultrasound vocalization. *Neuropsychopharmacology Reports* **43**, 239–248 (2023).

47. Da Prato, L. C. *et al.* Early life oxytocin treatment improves thermo-sensory reactivity and maternal behavior in neonates lacking the autism-associated gene Magel2. *Neuropsychopharmacol.* **47**, 1901–1912 (2022).

48. Karp, N. A. *et al.* Prevalence of sexual dimorphism in mammalian phenotypic traits. *Nat Commun* **8**, 15475 (2017).

49. Flanagan, K. L. Sexual dimorphism in biomedical research: a call to analyse by sex. *Transactions of The Royal Society of Tropical Medicine and Hygiene* **108**, 385–387 (2014).

50. Kelly, L. A., Branagan, A., Semova, G. & Molloy, E. J. Sex differences in neonatal brain injury and inflammation. *Front. Immunol.* **14**, (2023).

51. Hanamsagar, R. *et al.* Generation of a microglial developmental index in mice and in humans reveals a sex difference in maturation and immune reactivity. *Glia* **65**, 1504–1520 (2017).

52. Hammond, T. R. *et al.* Single-Cell RNA Sequencing of Microglia throughout the Mouse Lifespan and in the Injured Brain Reveals Complex Cell-State Changes. *Immunity* **50**, 253-271.e6 (2019).

53. Schwarz, J. M., Sholar, P. W. & Bilbo, S. D. Sex differences in microglial colonization of the developing rat brain. *Journal of Neurochemistry* **120**, 948–963 (2012).

54. Han, J., Fan, Y., Zhou, K., Blomgren, K. & Harris, R. A. Uncovering sex differences of rodent microglia. *Journal of Neuroinflammation* **18**, 74 (2021).

55. Kramer, K. M., Cushing, B. S., Carter, C. S., Wu, J. & Ottinger, M. A. Sex and species differences in plasma oxytocin using an enzyme immunoassay. *Can. J. Zool.* **82**, 1194–1200 (2004).

56. Carter, C. S. Sex differences in oxytocin and vasopressin: implications for autism spectrum disorders? *Behav Brain Res* **176**, 170–186 (2007).

57. Häussler, H. U., Jirikowski, G. F. & Caldwell, J. D. Sex differences among oxytocin-immunoreactive neuronal systems in the mouse hypothalamus. *J Chem Neuroanat* **3**, 271–276 (1990).

58. Dumais, K. M., Bredewold, R., Mayer, T. E. & Veenema, A. H. Sex differences in oxytocin receptor binding in forebrain regions: correlations with social interest in brain region- and sex- specific ways. *Horm Behav* **64**, 693–701 (2013).

59. Bale, T. L. & Dorsa, D. M. Sex differences in and effects of estrogen on oxytocin receptor messenger ribonucleic acid expression in the ventromedial hypothalamus. *Endocrinology* **136**, 27–32 (1995).

60. Watanabe, T. *et al.* Oxytocin receptor gene variations predict neural and behavioral response to oxytocin in autism. *Social Cognitive and Affective Neuroscience* **12**, 496–506 (2017).

61. Charpak, N. *et al.* Kangaroo mother care had a protective effect on the volume of brain structures in young adults born preterm. *Acta Paediatr* **111**, 1004–1014 (2022).

62. Bertoni, A. *et al.* Oxytocin administration in neonates shapes hippocampal circuitry and restores social behavior in a mouse model of autism. *Mol Psychiatry* **26**, 7582–7595 (2021).

63. Craig, A. *et al.* Quantitative analysis of perinatal rodent oligodendrocyte lineage progression and its correlation with human. *Exp Neurol* **181**, 231–240 (2003).

64. Favrais, G., Schwendimann, L., Gressens, P. & Lelièvre, V. Cyclooxygenase-2 mediates the sensitizing effects of systemic IL-1-beta on excitotoxic brain lesions in newborn mice. *Neurobiology of Disease* **25**, 496–505 (2007).

65. Bokobza, C. *et al.* Magnetic Isolation of Microglial Cells from Neonate Mouse for Primary Cell Cultures. *JoVE* 62964 (2022) doi:10.3791/62964.

66. Ye, J. *et al.* Primer-BLAST: A tool to design target-specific primers for polymerase chain reaction. *BMC Bioinformatics* **13**, 134 (2012).

67. Skene, N. G. & Grant, S. G. N. Identification of Vulnerable Cell Types in Major Brain Disorders Using Single Cell Transcriptomes and Expression Weighted Cell Type Enrichment. *Front. Neurosci.* **10**, (2016).

68. Zhang, H., Yushkevich, P. A., Alexander, D. C. & Gee, J. C. Deformable registration of diffusion tensor MR images with explicit orientation optimization. *Med Image Anal* **10**, 764–785 (2006).

69. Tang, D. *et al.* SRplot: A free online platform for data visualization and graphing. *PLoS One* **18**, e0294236 (2023).

6. Acknowledgements

This study was funded by the Swiss National Science Foundation (no. 197462). Author ST was supported by Swiss National Science Foundation no. 223414. Figures were made with BioRender (https://www.biorender.com/). Figure 3 was made with SRplot[69].

7. Author information

7.1 Authors and affiliations

Department of Child Growth and Development, Faculty of Medicine, University of Geneva, 1205 Geneva, Switzerland: Marit Knoop, Ece Trak, Marie-Laure Possovre, Yohan van de Looij, Gabriel Schirmbeck, Eduardo Sanches, Olivier Baud

Center for Biomedical Imaging (CIBM), Animal Imaging Technology Section, Ecole Polytechnique Fédérale de Lausanne (EPFL), Lausanne, Switzerland: Yohan van de Looij

Department of Psychiatry, University Hospital of Geneva and University of Geneva, 1205 Geneva, Switzerland: Stergios Tsartsalis

PROTECT, Inserm U1141, Université Paris Diderot, Paris, France : Julien Pansiot

Division of Neonatology and Pediatric Intensive Care, Children's University Hospital of Geneva, 1205 Geneva, Switzerland: Olivier Baud

Department of Neonatal Medicine, FHU Prem'Impact, Cochin-Port Royal Hospital, Assistance Publique-Hôpitaux de, Paris Cité University , 75014, Paris, France : Olivier Baud

Obstetric, Perinatal, Paediatric and Life Course Epidemiology Team (OPPaLE), Center for Research in Epidemiology and StatisticS (CRESS), Alimentation Et L'Environnement (INRAe), Institut National Pour La Santé Et La Recherche Médicale (INSERM; French Institute for Health and Medical Research), Institut National de Recherche Pour L'Agriculture, Paris Cité University, Paris, France: Olivier Baud

7.2 Author contributions

MK developed experimental methods, performed data collection and analysis, and wrote the manuscript. MLP developed experimental methods and performed supplementary data collection and analysis. ET performed data collection and analysis. YL performed and analyzed the MRI imaging experiment. ST contributed to data analysis of the RNA Seq experiment. GS and ES contributed to development of experimental methods and to data collection. All authors edited the manuscript. OB acquired funding and supervised the project.

7.3 Corresponding author

Correspondence is invited to Olivier Baud (olivier.baud@aphp.fr)

Neonatal oxytocin release mitigates neuroinflammation and rescues neural correlates of encephalopathy of prematurity

Marit Knoop, Marie-Laure Possovre, Ece Trak, Yohan van de Looij, Eduardo Sanches, Stergios Tsartsalis, Julien Pansiot, Gabriel Schirmbeck and Olivier Baud.

Supplementary Figures

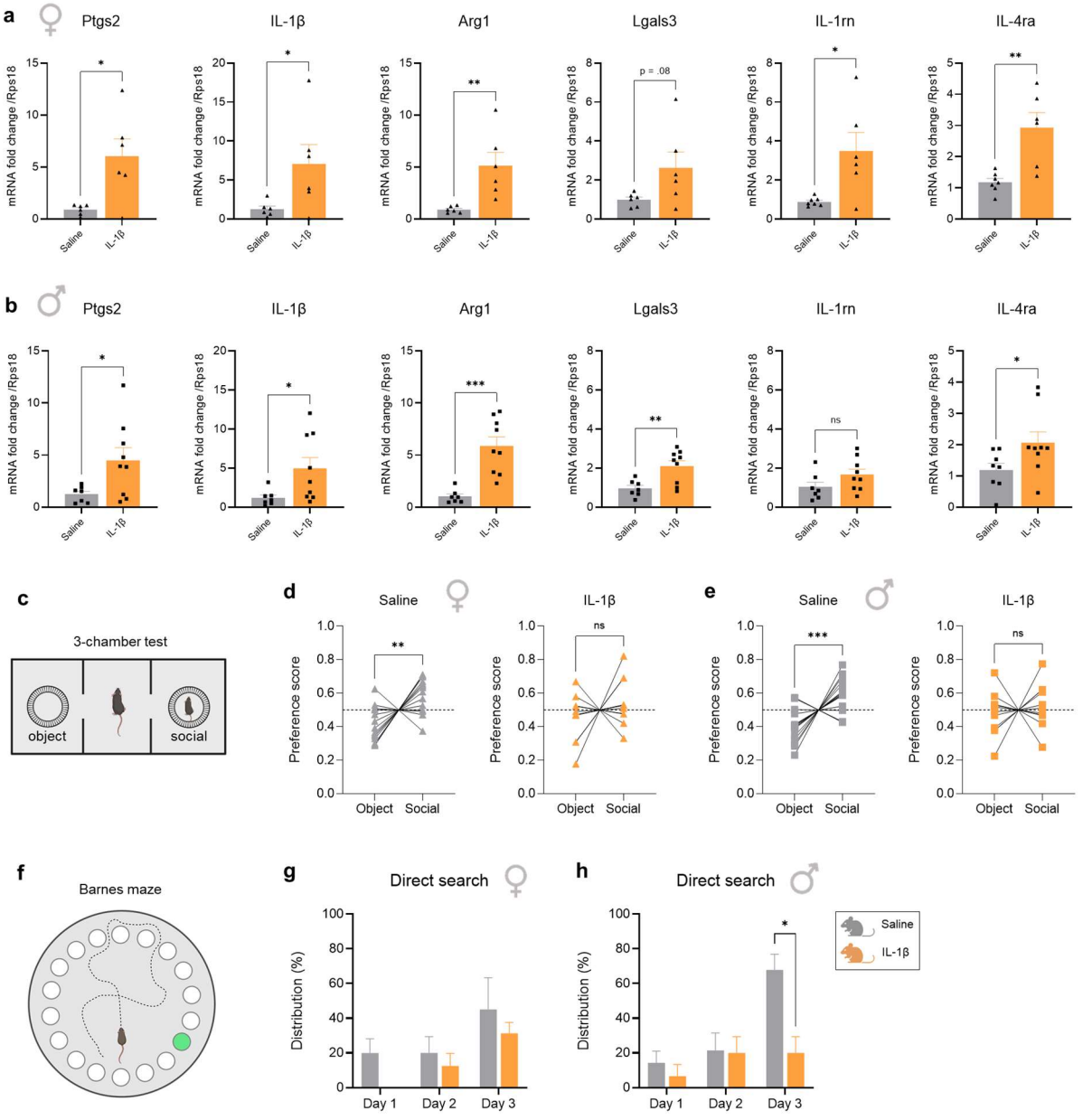

Fig S1: Sex-dependent effects of neonatal interleukin-1 beta injection on acute microglia reactivity and long-term behavioral outcomes. Mouse pups were injected with saline or IL-1β solution (see Fig 1). **a,b)** Cytokine expression of sorted microglia from P3 brains was similar between females **(a)** and males **(b)**. **c)** Schematic of P56 3-chamber test and the social preference trial. **d,e)** Preference scores for the social stimulus versus the object for Saline (gray) and IL-1β-injected mice (orange). No difference between females **(d)** and males **(e)** were found for loss of social preference in the IL-1β group. **f)** Schematic of the P90 Barnes maze. **g,h)** Search strategy during reversal training trials was assessed, and the proportion direct search utilized showed an interaction effect of Training day * sex: females were unaffected by IL-1β treatment **(g)**, but IL-1β injection in males caused a reduction in proportion direct search used, compared to healthy controls **(h)**. IL-1β = interleukin-1 beta. Statistical

analysis was performed with Student's t-test or Mann-Whitney test for non-normally distributed data **(a,b)**, with Paired t-test or Wilcoxon matched-pairs signed rank test for non-normally distributed data **(d,e)**, and with Two-way ANOVA with Šídák's post-hoc **(h,i)**. *p < .05, **p < .01, ***p < .0005, ****p < .0001. In **(a)** Saline: n = 6/7, IL-1β: n = 6. In **(b)** Saline: n = 7/8, IL-1β: n = 9. In **(d)** Saline: n = 14, IL-1β: n = 11. In **(e)** Saline: n = 16, IL-1β: n = 11. In **(g)** Saline: n = 5, IL-1β: n = 4. In **(h)** Saline: n = 7, IL-1β: n = 5. Bar graphs represent Mean ± SEM. Each data point represents an individual sample.

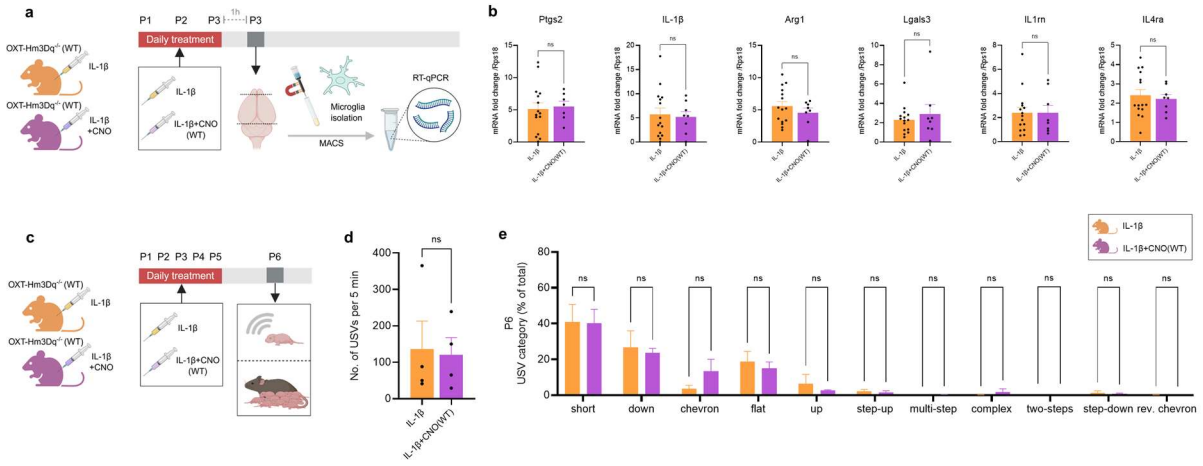

Fig. S2: Clozapine-n-oxide (CNO) does not affect microglial reactivity and social impairment induced by systemic inflammation in DREADD wild-type mice. OXT-Hm3Dq (-/-) wild-type (WT) pups were injected with IL-1β (orange), or IL-1β mixed with CNO substance ("IL-1β+CNO(WT)" group; purple). **a)** After P1-P3 injections, microglia cells were sorted from P3 brains and gene expression was assessed with RT-qPCR analysis of a battery of inflammatory cytokines, normalized on Saline control group. **b)** Inflammatory cytokine expression showed no effects of CNO on microglial reactivity in WT mice exposed to IL-1β. **c)** Next, we assessed side-effects of CNO on social behavior after systemic inflammation. IL-1β (orange) and IL-1β+CNO(WT) pups (purple) were injected between P1 and P5, and subjected to isolation-induced ultrasound vocalization (USV) recording at P6. **d,e)** WT pups did not show a difference in vocalization rate **(d)** or USV category distribution **(e)** when injected with IL-1β+CNO *vs*. only IL-1β. Together, the data shows CNO did not mediate the effects of IL-1β exposure on early-life microglial reactivity or social behavior, which supports that the effects of CNO found in OXT-Hm3Dq experimental mice are attributable to increased oxytocin and not to the CNO *per se*. OXT = oxytocin; WT = wild type; CNO = clozapine-n-oxide; IL-1β = interleukin-1 beta. Statistical analysis was performed with Student's t tests or Mann-Whitney test for non-normal data distribution. **p* < .05, ***p* < .01, ****p* < .0005, *****p* < .0001. In **(b)** IL-1β: *n* = 15, IL-1β +CNO(WT): *n* = 4-8. In **(d,e)** IL-1β: *n* = 4, IL-1β+CNO(WT): *n* = 4. Bar graphs represent Mean ± SEM. Each data point represents an individual sample.

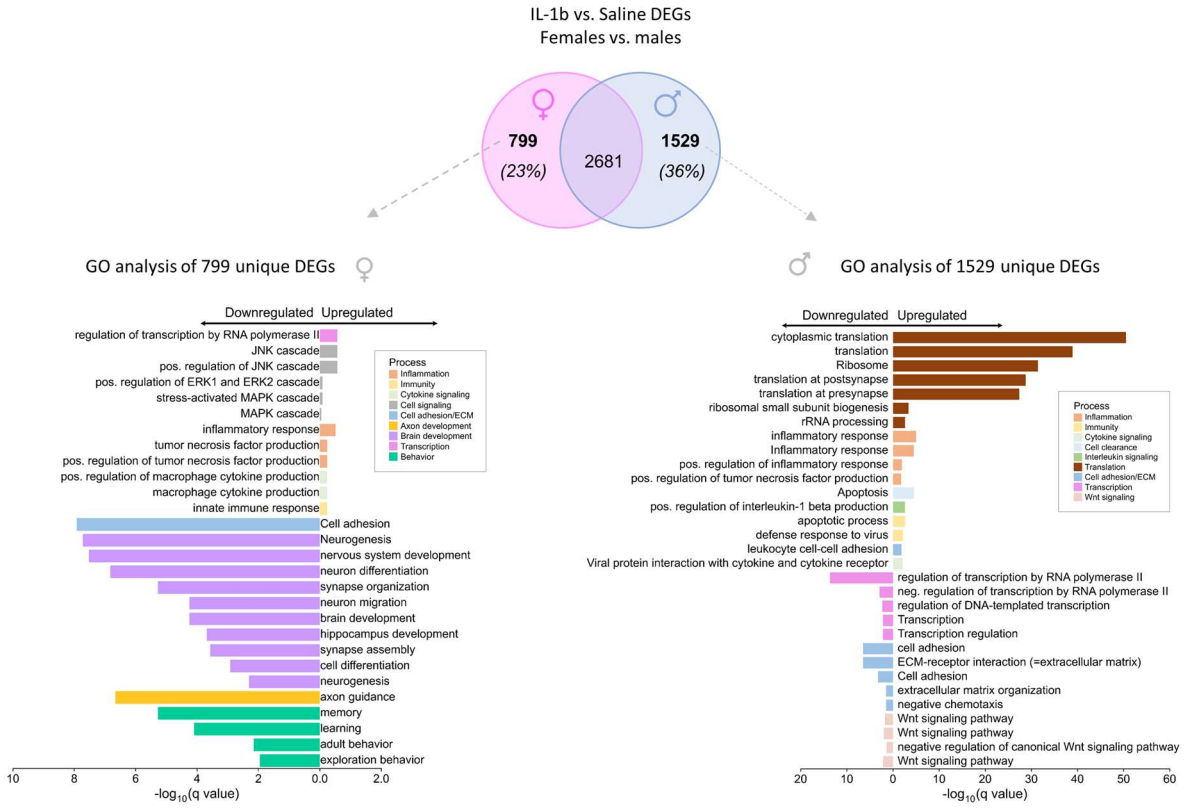

Fig. S3: GSEA analysis of unique sex-matched differentially expressed genes in microglia after IL-1β exposure. Gene set enrichment (GSEA) analysis of unique DEGs for IL-1β vs. saline microglia per sex (i.e., microglial genes that were not differentially expressed in IL-1β vs. saline pups of the other sex). Females showed 799 unique DEGs in IL-1β vs. saline (left), and males had 1529 unique DEGs (right). Unique DEGs for IL-1β females showed downregulation of brain development pathways as well as behavioral processes. Unique DEGs for IL-1β males showed upregulation of translational processes, and the downregulation of transcription processes, as well as downregulation of Wnt signaling. IL-1β = interleukin-1 beta; DEG = differentially expressed gene; GSEA = gene set enrichment analysis. Saline: *n* = 10 (5 females), IL-1β: *n* = 13 (6 females). GSEA analysis was performed with fold change > 1.5 and FDR-corrected $p < .05$ thresholds. Enrichment is represented as the negative log of the q value. Upregulated pathways are positioned on the right side of the y-axis, downregulated pathways on the left side. Bar graphs are sorted on q value, per overlapping cellular process.

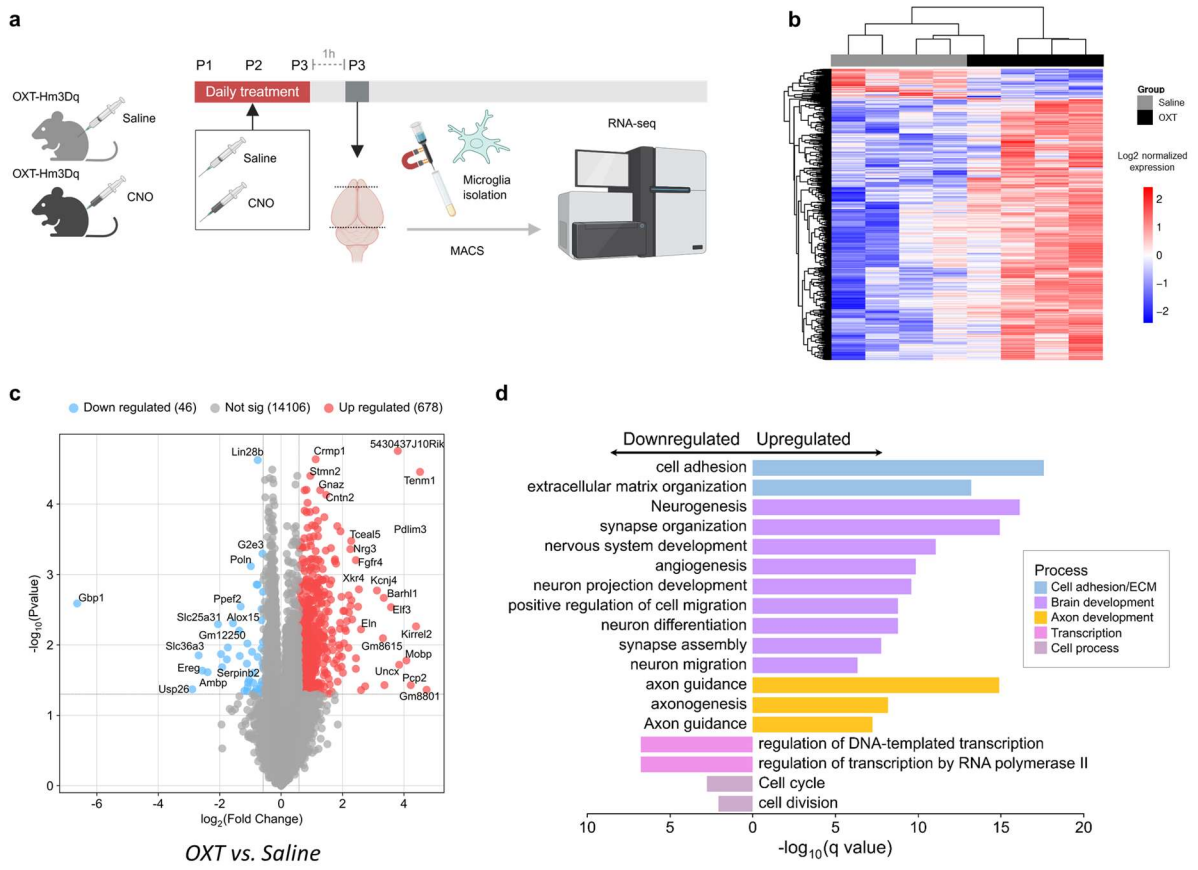

Fig. S4: Oxytocin release increases gene expression of brain development pathways in control microglia. a) OXT-Hm3Dq DREADD pups were injected with saline (gray) or OXT-increasing CNO substance ("OXT" group; black) between P1 and P3. At P3, microglia were sorted from pup brains, and bulk-sequenced to assess the effect of oxytocin release on gene expression of control microglia. **b)** Unsupervised heatmap analysis showed segregation and overlap between samples from Saline and OXT groups based on top gene expression. **c)** Volcano plot of the 724 differentially expressed genes in microglia from animals exposed to OXT release (CNO) *vs.* saline at P3, including 46 downregulated genes (in blue) and 678 upregulated genes (in red). **d)** Bar graph showing significantly enriched gene sets between OXT and saline microglia. OXT increased gene expression of cell adhesion, brain development and axon development pathways while reduced genes related to RNA transcription and cellular processes. The data suggests general stimulating effects of oxytocin on microglial support of brain development in P3 mice. OXT = oxytocin; CNO = clozapine-n-oxide. Saline: n = 4 (2 females), OXT: n = 4 (2 females). Microglia bulk RNA seq analysis was performed with fold change > 1.5 and FDR-corrected p < .05 thresholds. In **(d)** enrichment is represented as the negative log of the q value. Upregulated pathways are positioned on the right side of the y-axis, downregulated pathways on the left side. Bar graphs are sorted on q value, per overlapping cellular process.

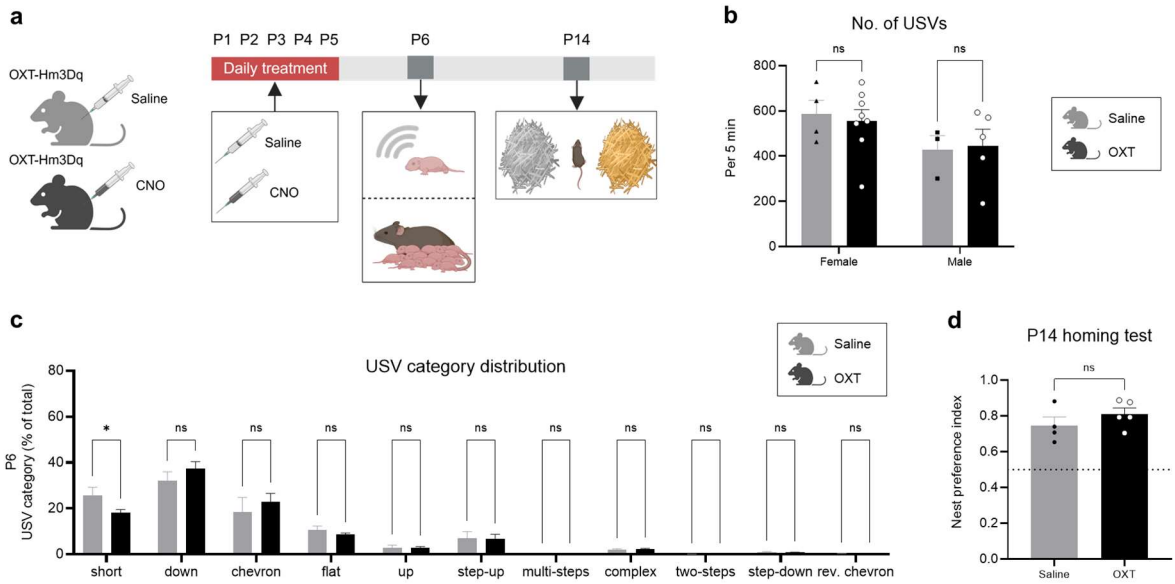

Fig. S5: Oxytocin release does not have sustained effects on social behavior in control animals. a) To assess the baseline effect of oxytocin release on sociability in control animals, we injected OXT-Hm3Dq DREADD pups with saline (gray bars) or OXT-increasing CNO substance ("OXT" group; in black) between P1 and P5. Sociability was assessed with P6 ultrasound vocalization (USV) analysis and P14 homing test assessment. **b)** Quantification of vocalization rate showed no effect of OXT on control animals, in neither females nor males. **c)** USV category distribution was largely unaffected by OXT release, except for a reduction in the proportion of *short* USVs emitted. **d)** Nest preference during the P14 homing test was unaffected by OXT release. These data suggest that P1-P5 increased oxytocinergic neuronal activity does not have sustained effects on sociability readouts at P6 and P14. In **(b,c)** Saline: *n* = 7 (3 females), OXT: *n* = 13 (8 females). In **(d)** Saline: *n* = 4, OXT: *n* = 5. Statistical analysis performed with Student's t- test (normal data distribution). Bar graphs represent Mean ± SEM. Each data point represents an individual sample.

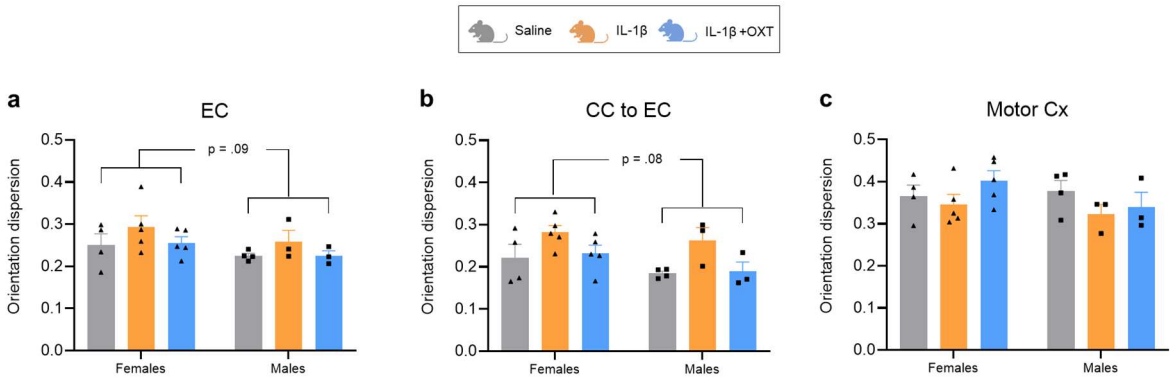

Fig S6: Sexual dimorphism in white matter axon dispersion in P28 mice. **a,b)** Sex-specific analysis of P28 *ex-vivo* diffusion tensor MRI revealed an overall increase in orientation dispersion in white matter regions for females compared to males. **c)** Orientation dispersion in the motor cortex was similar between sexes. No interaction effect between sex and treatment was found. Statistical differences were assessed with Two-way ANOVA with Šídák's post-hoc. Saline: n = 8 (4 females), IL-1β: n = 8 (5 females), IL-1β+OXT: n = 8 (5 females). Bar graphs represent Mean ± SEM. Each data point corresponds to one animal.

Appendix D

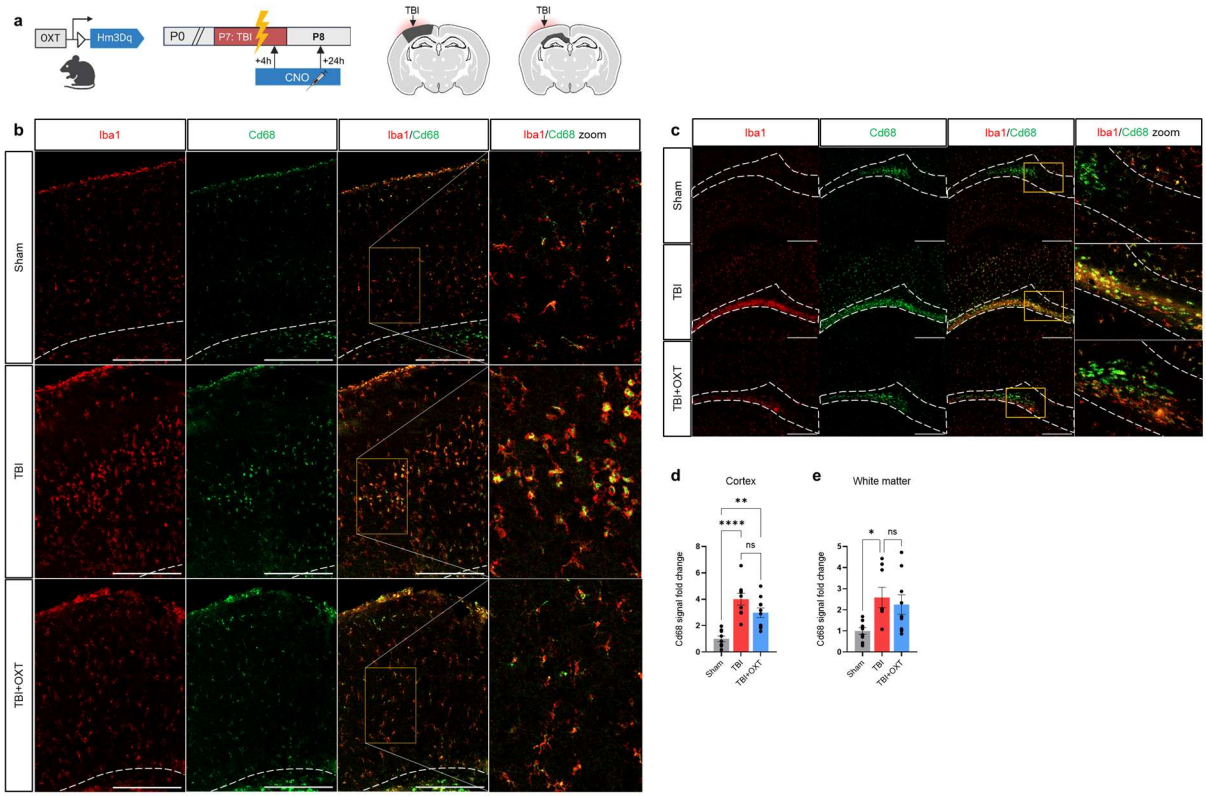

Immunohistochemistry of CD68^{+} phagocytic activity 24h after TBI. **a)** Experimental timeline and ipsilateral ROI indication. **b,c)** Representative micrographs of Iba1 (red) and Cd68 (green) signal in cortex **(b)**, and white matter **(c)** ROIs in Sham, TBI and TBI+OXT groups 24h post-TBI (P8), as a representation of phagocytic compartment size in microglia. Scale bar = 200 µm. **d,e)** Quantification of Cd68 signal fold change showed that TBI increased the phagocytic compartment in microglia compared to sham, at the injury site **(d)** and in the proximate white matter **(e)**. Oxytocin treatment had no effect on Cd68 density. TBI = traumatic brain injury. CNO = clozapine n-oxide. Statistical differences were assessed with One-way ANOVA with Tukey's post-hoc analysis. ****$p < .0001$, **$p < .01$, *$p < .05$. Bar graphs represent Mean ± SEM. Each data point represents an individual sample.